Astrophysics and Space Science Library 441

Ivan I. Shevchenko

The Lidov-Kozai Effect – Applications in Exoplanet Research and Dynamical Astronomy

ASSL

Springer

The Lidov-Kozai Effect – Applications in Exoplanet Research and Dynamical Astronomy

Astrophysics and Space Science Library

Ivan I. Shevchenko

The Lidov-Kozai Effect – Applications in Exoplanet Research and Dynamical Astronomy

Springer

Ivan I. Shevchenko
Pulkovo Observatory of the Russian
Academy of Sciences
St. Petersburg, Russia

ISSN 0067-0057 ISSN 2214-7985 (electronic)
Astrophysics and Space Science Library
ISBN 978-3-319-43520-6 ISBN 978-3-319-43522-0 (eBook)
DOI 10.1007/978-3-319-43522-0

Library of Congress Control Number: 2016951301

Cover illustration: An exoplanet seen from its moon (artist's impression). Credit: IAU/L. Calçada

Printed on acid-free paper

This Springer imprint is published by Springer Nature
The registered company is Springer International Publishing AG Switzerland

Preface

> Up to now, it nearly makes me laugh and cry of rapture when I recall this result.
>
> Vladimir Beletsky, *Six Dozens (Memoirs)*

The Lidov-Kozai effect (LKE), as any other basic astrophysical phenomena, has several "faces", or manifestations. The most familiar face, granted in Wikipedia, is the phenomenon of coupled periodic variations (which can be very large) of the inclination and eccentricity of an orbiting body, which (the variations) may take place in the presence of an inclined-enough perturber.

A face, less familiar to the general audience, but physically the generic one, is the so-called phenomenon of ω-*libration*; i.e., libration of the *argument of pericenter* of an orbiting body, when an inclined-enough perturber is present. In fact, the ω-libration is at the core of the LKE: it is just a large-amplitude ω-libration that entails the mentioned coupled variations in inclination and eccentricity.

Another concept, frequently present in the modern astrophysical literature, is the LKE as a valuable tool to explain various merger events. Indeed, if it is "necessary to merge" any gravitating binary (say a binary consisting of two ordinary stars, or black holes, or asteroids, or a star and a "hot Jupiter," or a planet and an artificial satellite, etc.) into a single object, the LKE is commonly the first one in the queue of possible explaining mechanisms that come to mind of an astrophysicist. This is just because it is rapid and no dissipation is needed—only the presence of a perturber. This third face revealed itself already in the pioneering works of Lidov (who outlined a condition for a merger of a satellite with the Earth, in particular the Moon with the Earth), and since then it has been becoming only more and more attractive for researchers.

To date, the LKE, in all of these faces, has been verified to be important in the dynamics of a lot of kinds of astrophysical objects. Historically the applications started with satellites and asteroids; now they comprise comets, trans-Neptunian objects, exoplanets, multiple stars, and many others. Perhaps, of most interest for the astronomical and astrophysical community at present is its relevance for many exoplanetary systems.

Recent years witnessed major advancements in the theory of LKE. In particular, another face of the LKE emerged: the so-called *flip* (orbit turnover) phenomenon.

It would be no exaggeration to say that at present the Lidov-Kozai effect becomes one of the most studied astrophysical effects; this is manifested, in particular, in a

sharp rise of citations of the pioneer articles of Lidov and Kozai during recent years (see Fig. 1).

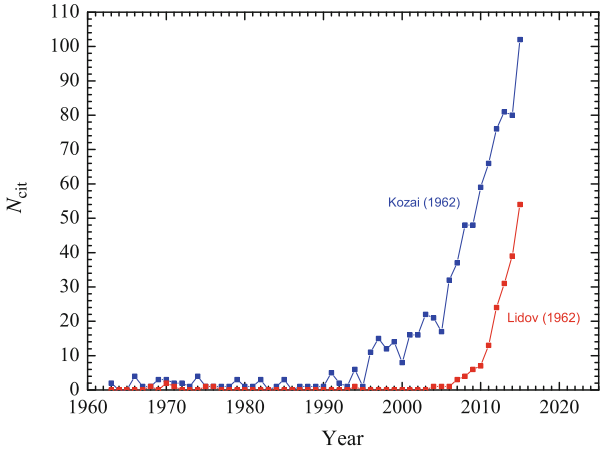

Fig. 1 The per-year number of citations of the pioneer articles of Lidov and Kozai, as a function of time, up to year 2015 inclusive (The citation data of the NASA ADS database have been used to construct the diagram)

The topics, covered in this book, include: historical background for appearance of works by Lidov and Kozai in the beginning of the 1960s (*Luna*-3, etc.); modern secular theories and integrable approximations in celestial mechanics; an overview of classical works on the Lidov-Kozai effect; modern advancements and generalizations in the Lidov-Kozai theory, in particular in the framework of noncircular and nonrestricted problems; the Lidov-Kozai mechanism explaining the observed orbital configurations of irregular satellites, explaining comets-sungrazers, and explaining the observed dynamical patterns in the asteroid and Kuiper belts; the role of the Lidov-Kozai mechanism (in particular the Lidov-Kozai migration) in sculpting exoplanetary systems; applications in stellar dynamics, such as scenarios for formation of close binary stars; and explanations for highly eccentric stellar orbits in the Galactic center.

The initial aim of this book was to provide the most full coverage of the effect's theory and applications. However, due to a large amount of the published and newly appearing advancements, it is practically impossible to fulfill this aim in detail. Therefore, apart from the provided bibliography, for further reading on the subject, I would recommend the material on the Lidov-Kozai effect in asteroidal dynamics, presented in Sects. 8.2 and 11.2.2 of the book *Modern Celestial Mechanics* by A. Morbidelli (2002), and the material on the LKE in exoplanetary dynamics presented in Sects. 7 and 8 of the review "The Long-Term Dynamical Evolution of Planetary Systems" by M. B. Davies et al. (2014).

The presented book is self-contained: only basic knowledge in mathematics and mechanics is required for understanding the material, if read from the beginning. I hope that the book can be helpful for a researcher working in astrophysics, celestial mechanics, stellar dynamics, theoretical mechanics, and space mission design, at any level (researcher, graduate student, undergraduate student), depending on the interests of the reader.

I am most grateful to Vladislav Sidorenko, Konstantin Kholshevnikov, Mikhail Vashkovyak, and Alessandro Morbidelli for valuable remarks and comments. I am especially thankful to Vladislav Sidorenko for providing rare bibliographic materials on the subject.

Saint Petersburg, Russia Ivan I. Shevchenko
2016

Contents

Chapter 1
Dynamical Essence and Historical Background

Shortly after the first space launches Mikhail Lidov and Yoshihide Kozai independently discovered that under certain conditions both the eccentricity and the inclination of a natural or artificial celestial body can undergo large coupled periodic changes (Kozai 1962; Lidov 1961, 1962, 1963a). This result immediately attracted the attention of researchers in Celestial Mechanics due to a dramatic contrast with the previous studies of secular effects. The latter were mainly based on the assumption that the motion is near-circular and near-planar. Being reasonable for the planets, this assumption was too restrictive for the analytical investigation of the secular effects in the dynamics of asteroids and artificial satellites.

One of the most paradoxical phenomena arising due to the Lidov-Kozai effect is the falling of artificial satellites onto the Earth due to the increase of eccentricities of their orbits under the perturbations from the Moon and Sun (the semimajor axis being constant).

The first instance of such a falling was demonstrated by the Soviet space probe *Luna*-3. This probe was designed for taking photo images of the back side of the Moon. It was launched initially in an orbit with the perigee outside (of course) the upper boundary of the Earth's atmosphere. After the mission was successfully accomplished, and the probe made several orbits around the Earth, the secular rise in the eccentricity resulted in a decrease of the perigee (because the semimajor axis is conserved). So, after eleven orbital revolutions *Luna*-3 entered the atmosphere of the Earth.

Currently the Lidov-Kozai effect can be characterized as ubiquitous to be met throughout modern Celestial Mechanics and Astrophysics. It manifests itself not only in the dynamics of satellites and asteroids, as considered originally in the works of Lidov and Kozai, but also in the motion of classes of comets, Kuiper belt objects, components of multiple stars, extrasolar planets and many other astrophysical objects.

I. I. Shevchenko, *The Lidov-Kozai Effect – Applications in Exoplanet Research and Dynamical Astronomy*, Astrophysics and Space Science Library 441,
DOI 10.1007/978-3-319-43522-0_1

Let us consider the LKE's basic dynamical manifestations, i.e., its observable essence. To be able to do this, one should first recall the notion of the Keplerian orbital elements.

1.1 The Keplerian Orbital Elements

The Keplerian orbital elements are defined and discussed in detail in numerous books; in particular, see Danby (1962), Murray and Dermott (1999), and Morbidelli (2002). Here we provide a brief synopsis.

In the two-body problem, the Keplerian orbital elements are used to characterize the form and orientation of the secondary's orbit around the primary, and the position of the secondary in its orbit, if the primary is chosen as the origin of the coordinate frame. As well, in the *barycentric* coordinate frame,[1] they are used to characterize the form and orientation of both orbits around the system's center of mass, and the position of the bodies in their orbits.

We consider merely the case of elliptic orbits. As illustrated in Fig. 1.1, the size and form of an ellipse is completely determined by a set of two parameters: the *semimajor axis* a and the *eccentricity* e; or by any pair of their algebraic derivatives, say *semimajor axis* a and semiminor axis b, or *pericentric distance* $q = a(1 - e)$ and *apocentric distance* $Q = a(1 + e)$, etc.

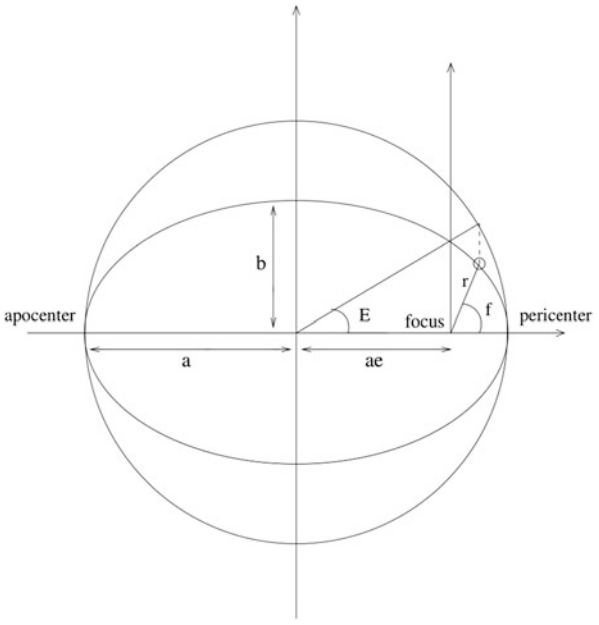

Fig. 1.1 Keplerian elements a, e and E of the planar elliptic orbital motion (Figure 1.1 from Morbidelli (2002). With permission from Academic Books)

[1] The frame referred to the center of mass of the system.

The orbital point closest to the primary is called the *pericenter*; and the farthest one the *apocenter*. The *pericentric distance* q (the distance between the pericenter and the primary) and the *apocentric distance* Q (the distance between the apocenter and the primary) are given by

$$q = a(1-e), \quad Q = a(1+e). \tag{1.1}$$

If the primary is the Sun, then the pericenter and apocenter are called *perihelion* and *aphelion*; if the primary is the Earth, they are called *perigee* and *apogee*; if the primary is a star, they are called *periastron* and *apoastron*. Generally, they are also called *periapse* and *apoapse*, and the line connecting them the *apsidal line*.

To locate the secondary in the orbit, let us first introduce a Cartesian frame (x, y); see Fig. 1.1. Axis x is directed to the pericenter, and axis y completes the orthogonal frame; the frame origin is at the ellipse's focus where the primary resides. A polar frame (r, f) is also naturally defined: the angle f, called the *true anomaly*, determines the angular position of the secondary in the orbit, and r its distance from the primary.

The Cartesian coordinates of the secondary are given by the formulas

$$x = a(\cos E - e)\ , \quad y = a(1-e^2)^{1/2} \sin E, \tag{1.2}$$

and the polar coordinates by the formulas

$$r = a(1 - e\cos E)\ , \quad \cos f = \frac{\cos E - e}{1 - e\cos E}\ , \quad \sin f = \frac{(1-e^2)^{1/2}\sin E}{1 - e\cos E}\ , \tag{1.3}$$

where the *eccentric anomaly* E is the angle between the directions (as seen from the ellipse's center) to the pericenter and to the point of vertical projection of the body's position onto the circle tangent to the ellipse at the pericenter and apocenter, as shown in Fig. 1.1.

The eccentric anomaly E is given implicitly by the so-called *Kepler equation*:

$$E - e\sin E = n(t - t_0), \tag{1.4}$$

where n is the *mean motion* (the mean orbital frequency):

$$n = (\mathcal{G}(m_0 + m_1))^{1/2} a^{-3/2}; \tag{1.5}$$

$\mathcal{G}$ is the gravitational constant, m_0 and m_1 are the masses of the primary and the secondary; t is time, t_0 is the *epoch* (time instant) of the pericenter transit. The Kepler equation can be solved with respect to E numerically (e.g., by iterations).

The orbital period is given by

$$T = \frac{2\pi}{n}, \tag{1.6}$$

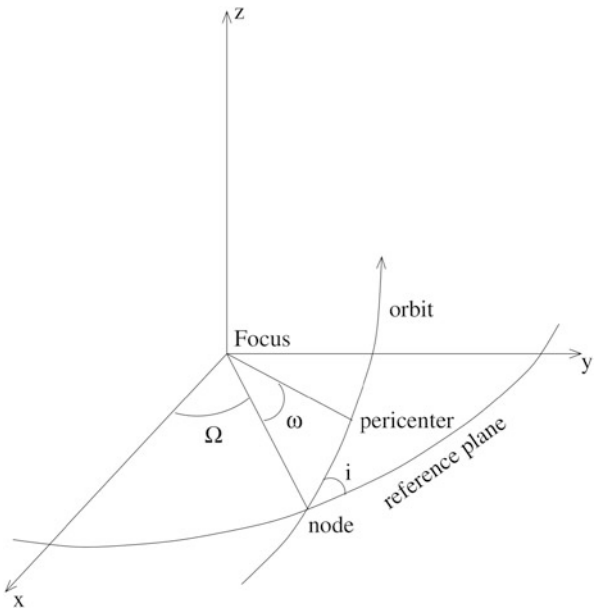

Fig. 1.2 Keplerian elements i, Ω and ω of the spatial orbital motion (Figure 1.2 from Morbidelli 2002. With permission from Academic Books)

and the angle called *mean anomaly* is defined by the formula

$$M = n(t - t_0). \tag{1.7}$$

Apart from f, E, and M, three more angles are needed to define the ellipse's orientation in 3D space. Let (x, y, z) be a Cartesian frame with the origin at the ellipse's focus where the primary resides, as shown in Fig. 1.2. The inclination i is defined as the angle between the orbital plane and the plane (x, y). This plane is arbitrary, but, in applications, it is usually chosen to coincide with some physically or dynamically distinguished plane, say, the plane of the Earth's equator, or, the ecliptic plane.

An inclined orbit ($i \neq 0$) intersects the (x, y) plane at two points, called the *nodes*: the *ascending* and *descending* ones, at which the body moves from the negative to positive values of z, and vice versa, respectively. The angular position of the ascending node with respect to axis x is designated by Ω; this angle is called the *longitude of ascending node*.[2]

The *argument of pericenter* ω is the angular position of the pericenter with respect to the "primary—ascending node" direction. Thus, it is defined with respect to a movable direction in space. Instead of ω, it is often convenient to use a *dogleg*

[2]Note that all *longitudes* are defined with respect to immovable coordinate axes.

angle[3] ϖ, called the *longitude of pericenter* and defined by the formula

$$\varpi = \Omega + \omega, \tag{1.8}$$

though Ω and ω belong to different, generally intersecting planes. Note that symbol ϖ is *not* letter ω "with tilde", as one may wrongly suppose, but it is a rare version of letter π, called *curly* π.

If retrograde orbits are also considered, the longitude of pericenter is defined by the generalized formula

$$\varpi = \Omega + \operatorname{sign}(\cos i)\,\omega. \tag{1.9}$$

Another important angle it the *mean longitude*, defined as

$$\lambda = \varpi + M. \tag{1.10}$$

Often it is designated also as l.

1.2 The "omega-libration"

A manifestation of the LKE most familiar to the research community consists in coupled periodic variations (which can be very large) of the inclination and eccentricity of an orbiting body, which (the variations) may take place in the presence of an inclined-enough perturber.

A manifestation of the LKE, less familiar to the general audience, but physically the generic one, is the so-called phenomenon of *ω-libration*; i.e., libration of the argument of pericenter of an orbiting body, when an inclined-enough perturber is present. In fact, the ω-libration is at the core of the LKE: it is just a large-amplitude ω-libration that entails the mentioned coupled variations in inclination and eccentricity. This will be proved later on, when we shall analyze *averaged* equations of motion.

As follows from Equation (1.8), $\omega = \varpi - \Omega$. Therefore, one may interpret the libration of ω as a 1:1 resonance between the variations of ϖ and Ω. Note that angles ϖ and Ω are dynamically much more meaningful and "physical" (though ϖ is a dogleg angle) than ω, because they are measured with respect to an immovable axis.

In such a way, we are brought to the notion of the *LK-resonance*. Of course, not any libration can be attributed to a resonant phenomenon, because the libration/circulation state of an angle may depend on the choice of a coordinate system

[3] This strange terminology arises from the fact that ϖ is a sum of two angles in two planes generally intersecting with each other, see Fig. 1.2.

(in particular, its origin). Further on in this book we shall discuss the problem whether the LK-resonance is indeed a resonance, as understood generally in nonlinear dynamics, and what is its place in the general typology of resonances.

1.3 The Breakthrough Premises

Until the beginning of the Space era, the studies of secular effects in celestial mechanics were mostly based on the assumption that the motion is near-circular and near-planar. The theory of secular motions of the Solar system planets, developed by Lagrange and Laplace, was based just on these assumptions. This was dictated merely by the necessities of theoretical astronomy of that time.

On the other hand, prominent astronomical objects in orbits highly-inclined with respect to the ecliptic plane were well-known already two centuries ago. For example, Pallas, the second discovered (in 1802) asteroid, has inclination $i \approx 35^\circ$ (for more details on its orbit see Table 7.1). A number of prominent comets are highly-inclined (see Table 6.1). However, the astronomers were reluctant to build theories of the long-term motion of such objects, and this is comprehensible, taking in account their unimportance for any applications at that time. There was a lot of more interesting problems looking much more actual. At that time, in the field of studies of minor bodies, only short-term ephemerides were of interest. (An example from our times: who cares at present where is *Luna*-1, launched in a heliocentric orbit in 1959, and called a man-made "tenth" planet? Of course, this remark does not mean that a study of the long-term motion of *Luna*-1 may lead to a theoretical breakthrough.)

The long-term stability of the planetary motion in the Solar system looked to be a much more actual problem. And the corresponding theory, the theory of the secular motion of planets, was constructed by Lagrange and Laplace already at the end of the eighteenth century. According to this theory, appropriate for the low-eccentric and low-inclined bodies, such as the Solar system planets, the secular frequencies of the longitudes ϖ and Ω of the perturbed bodies (e.g., Mercury, Venus, Earth, Mars, Saturn, Uranus, and Neptune, perturbed mostly by Jupiter) in a frame associated with the Laplace invariable plane are approximately equal in modulus but opposite in sign (see Table 7.1 in Morbidelli 2002); thus, the Lagrange–Laplace theory, valid in a limited domain of initial conditions, provided no ground to suspect the existence of such a phenomenon as ω-libration. This explains why the discovery by Lidov and Kozai was so unexpected.

Being reasonable for planets, the requirement for the motion to be close-to-circular and close-to-planar is too restrictive to allow for a complete analytical investigation of the secular effects in the dynamics of artificial satellites, as well as in the dynamics of asteroids and comets.

Only in the middle of the twentieth century a few studies concerning abstract problems on the existence of integrals in the non-planar problem appeared (see Moiseev 1945a,b, and references therein).

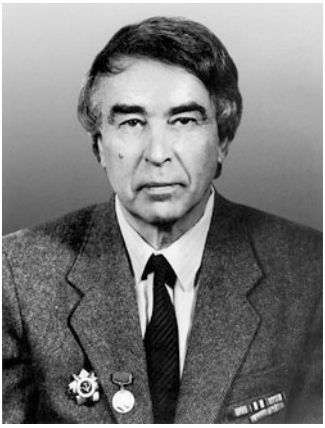

Fig. 1.3 Mikhail L'vovich Lidov (1926–1993) (Photo from Lidov 2010)

Fig. 1.4 Yoshihide Kozai (1928–), lecturing at the conference "Asteroids, Comets, Meteors 2012" (Photo from the website of ACM 2012)

There is no doubt that the Lidov-Kozai theory emerged as a theoretical response to the necessities of the Space era. Lidov's classical work was published in 1961, four years after Sputnik, and it is a sublimation of a large work dedicated to the theory of spaceflight. Moreover, there is no doubt that the inspiration of Kozai's (1962) work, though devoted to asteroids, stems from the same origin. Indeed, Kozai refers in his paper mostly to works on satellite dynamics, and, in particular, to Lidov's report at the IUTAM Symposium (Paris, May 1962), where Lidov's theory was presented.[4]

The theoretical discoveries by Mikhail Lidov and Yoshihide Kozai (see portraits in Figs. 1.3 and 1.4) immediately attracted the attention of researchers in Celestial Mechanics, first of all due to the dramatic contrast with the previous studies of secular effects.

To provide a most vivid and graphical illustration for the new theory, Lidov (1963b) calculated the orbital evolution of a "polar Moon". He showed that in some

[4]Lidov himself did not attend the Symposium; his report was delivered by Albert Molchanov. The report was published in 1963 (Lidov 1963c).

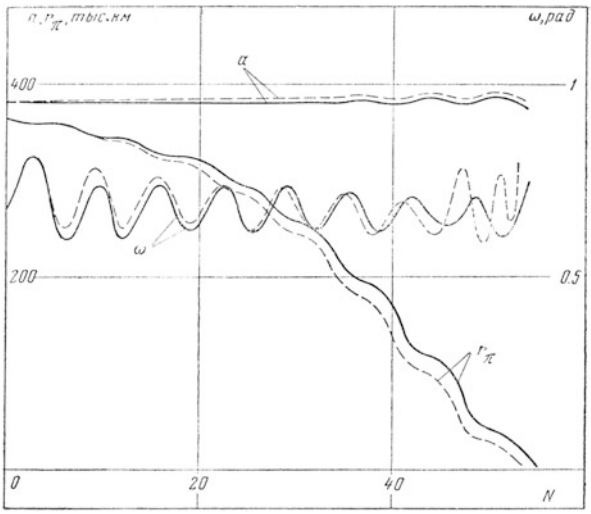

Fig. 1.5 The orbital evolution of a "polar Moon". The time dependence of the semimajor axis a, perigee distance r_π (in thousands of kilometres), and argument of perigee ω (in radians) is shown. The time N is measured in orbital periods of the "polar Moon" (Figure 7 from Lidov 1963b)

Fig. 1.6 A cartoon by I.V.Novozhilov "Lidov drops the Moon on the Earth" (A figure from Beletsky 1972)

∼50 orbital revolutions such a Moon would fall on the Earth (see Fig. 1.5). Thus, an explanation was given why the orbit of the real Moon is far from being highly inclined. Beletsky (1972) recollects that the result was first met by colleagues with a distrust (as physically unexpected for a non-dissipative system), but then applauded; see the cartoon "Lidov drops the Moon on the Earth" in Fig. 1.6.

1.4 From *Luna*-3 to Modern Space Missions

The first instance of a "man-made LKE" was demonstrated by the Soviet space probe *Luna*-3. This probe was designed to obtain photo images of the back side of the Moon. It was launched initially in an orbit with the perigee outside (of course) the upper boundary of the Earth's atmosphere, and the apogee enclosing the Moon; see the orbital scheme in Fig. 1.7.

The probe transferred first photos of the dark side of the Moon, and the achievement was applauded all over the world. This was a contribution to Astrophysics. In what concerns Celestial Mechanics, *Luna*-3 was the first ever space mission exploiting a *gravity assist*. The assist was necessary on the following reason. At a first glance, it may seem that the best scheme for the flight would be an elongated ellipse, encompassing (at the apocenter) the Moon. However, a probe in such an orbit would return to the perigee following a route over the southern hemisphere of the Earth. (Note that the probe's trajectory was strongly inclined to

Fig. 1.7 A Soviet postal stamp dedicated to the *Luna*-3 mission in 1959. The mission orbital scheme is presented

the Moon's orbital plane; the scheme in Fig. 1.7 does not catch this fact.) In such a route, it would be impossible to transmit messages with the processed images to radio receivers on the territory of the Soviet Union (in the northern hemisphere). Therefore, the initial branch of the actual orbit was designed to "dive" under the Moon, so that the Moon's gravity would assist to direct the returning probe over the Earth's northern hemisphere, as needed (Raushenbakh and Ovchinnikov 1997). This was the first *gravitational manoeuvre* in the history of spaceflights.

Yet another significant achievement of the *Luna*-3 mission, from the viewpoint of astrodynamics, was a realization of the probe's active orientation. Without fixing the orientation, it would be impossible to obtain the photos. This accomplishment was also the first one in the world's history.

Most of the Moon images were successfully transmitted to the Earth, when the probe was on its way back. After the mission was over, the probe continued to move in a highly-eccentric highly-inclined orbit. The secular rise of the eccentricity (in "exchange" with the inclination, the semimajor axis being conserved), due to the LKE, inevitably decreased the pericentric distance. After eleven orbital revolutions, taking in sum about a half-year, *Luna*-3 entered the atmosphere of the Earth in April, 1960. This fact was noted by Lidov in the beginning of his pioneer paper (Lidov 1961). Thus the fate of *Luna*-3 inspired one of the most fruitful studies in celestial mechanics of the twentieth century.

An interested reader, using formulas presented further in this book, may try to calculate a theoretical timescale for the secular decrease of the pericentric distance, from the initial one to that corresponding to the downfall. The initial values of the pericentric distance and the eccentricity of the orbit of *Luna*-3 were $q \approx 40{,}600$ km and $e \approx 0.84$, whereas the orbital plane of the probe was almost orthogonal to that of the Moon. The orbital period was $\approx$15 d.

One can conclude that, apart from performing a gravitational manoeuvre, an accomplishment of active orientation, and—most notably for mass media—obtaining the Moon's dark side photos (all this was done for the first time in the world's history), the fourth great feat of *Luna*-3 mission in 1959 was a "man-made" demonstration of the LKE. However, this is not duely acknowledged up to now.

It is pertinent to recall that Mikhail Lidov was a laureate of the *Lenin prize*, one of the highest state rewards in the Soviet Union, granted for major achievements in science and culture. (The Lenin prize medal, side by side with decorations of the Second world war veteran, can be seen in the portrait in Fig. 1.3.) The prize was awarded for the orbital design of the first space missions, *Luna*-3 among them.

In our times, taking into account the LKE while planning and designing space missions is no less important than it was in 1959. A spectacular example is provided by Fig. 1.8, where the long-term evolution of the perigee distances of *Prognoz*, *Interbol*, and *Spektr-R* satellites is plotted. The Figure provides a clear-cut illustration how it is vital for the working schedule of a satellite mission to fit

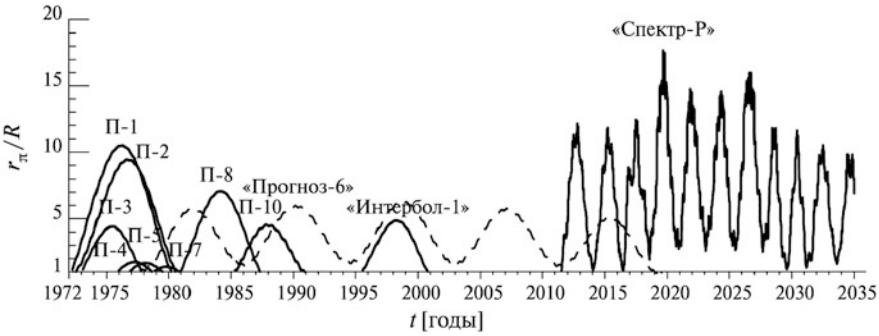

Fig. 1.8 The long-term evolution of the perigee distance (in units of the Earth radius) for *Prognoz*, *Interbol*, and *Spektr-R* satellites; the time is in years (Figure 15 from Prokhorenko 2015. With permission from the Institute of Space Research of the Russian Academy of Sciences)

the time limits (set by the LKE) for the *ballistic existence* of the satellite, if no orbit correction is planned. In case of the *Spektr-R* mission, a timely-accomplished orbital correction allowed one to prolong the mission considerably; for more details see a review by Prokhorenko (2015).

Chapter 2
Averaging and Normalization in Celestial Mechanics

Near-integrable Hamiltonian systems (i.e., the systems composed by an integrable part and a small perturbation) are a common model currently used to study the dynamics of celestial bodies. This is the study of such systems that Poincaré called the "general problem of dynamics" (Poincaré 1899). Usually the so-called *perturbation approach* is used to transfer the perturbation to higher orders of the Hamiltonian expansion, by means of a canonical transformation close to identity. Then, neglecting the remainder, one can use the truncated Hamiltonian for the analysis of the effects characterizing the system dynamics over long time intervals. Since in Celestial Mechanics these effects are called secular, the construction of a suitable transformation can be interpreted as a development of a secular theory of the dynamical phenomena under consideration.

In this book, mostly the restricted three-body problem (R3BP) is considered, in which a massless particle moves under gravitational attraction of two bodies (the primaries),[1] orbiting around their barycenter. There are several cases when the motion of the massless particle (the tertiary) can be treated as a slightly perturbed Keplerian motion: (1) the distance between the tertiary and one of the primaries is always much less than the distance between the primaries; (2) the distance between the tertiary and the primaries' barycenter is always much greater than the distance between the primaries; (3) the mass of the primary is much greater than the mass of the secondary.

To write down the Hamiltonian of R3BP in the form convenient for application of the perturbation technique, one needs to introduce the *Delaunay variables*. Then the Hamiltonian becomes a sum of an integrable part, corresponding to the Keplerian

[1] The three bodies are called the primary, the secondary, and the tertiary in accord (usually) with the hierarchy of their masses. However, other ways of enumeration are also possible, e.g., according to the hierarchy of the geometric configuration. This is usually clear from the context. The two "primaries" comprise the primary and the secondary.

I. I. Shevchenko, *The Lidov-Kozai Effect – Applications in Exoplanet Research and Dynamical Astronomy*, Astrophysics and Space Science Library 441,
DOI 10.1007/978-3-319-43522-0_2

motion, and a small perturbation. A consequent formal *averaging* of the perturbation over the *fast variables* allows one to construct a first-order theory describing the secular effect in the particle dynamics outside resonances with the primaries.

Basic concepts of the perturbation approach in Hamiltonian dynamics are discussed in many monographs and reviews; see, in particular, Poincaré (1899, 1905), Murray and Dermott (1999), Morbidelli (2002), Arnold et al. (2006), and Ferraz-Mello (2007). These sources are used for the material presentation in this section.

2.1 The Hamiltonian Formalism

In the subsequent analytical treatments, we usually use the equations of motion in the Hamiltonian formulation. Therefore, let us recall how basic problems of celestial mechanics can be expressed in the Hamiltonian "language".

A first-order system of $2n$ ordinary differential equations (ODEs)[2]

$$\frac{\mathrm{d}\mathbf{x}}{\mathrm{d}t} = \mathbf{F}(\mathbf{x}) \tag{2.1}$$

(where $\mathbf{x}$ is a vector variable, $\mathbf{F}(\mathbf{x})$ an arbitrary vector function) is said to have a Hamiltonian form, if there exists a scalar function $\mathcal{H}(\mathbf{x})$, called the *Hamiltonian*, such that the system can be represented in the form

$$\frac{\mathrm{d}p_i}{\mathrm{d}t} = -\frac{\partial \mathcal{H}(\mathbf{x})}{\partial q_i}\,, \quad \frac{\mathrm{d}q_i}{\mathrm{d}t} = +\frac{\partial \mathcal{H}(\mathbf{x})}{\partial p_i}\,, \quad (i = 1, \ldots, n)\,, \tag{2.2}$$

or, equivalently, in the vector form,

$$\dot{\mathbf{p}} = -\nabla_{\mathbf{q}} \mathcal{H}(\mathbf{x})\,, \quad \dot{\mathbf{q}} = +\nabla_{\mathbf{p}} \mathcal{H}(\mathbf{x})\,, \tag{2.3}$$

where $\mathbf{x} = (\mathbf{q}, \mathbf{p}) = (q_1, \ldots, q_n, p_1, \ldots, p_n)$; t is an independent variable (time). The variables $q_1, \ldots, q_n$ and $p_1, \ldots, p_n$ are called the canonical *coordinates* and *momenta* of the system, respectively; n is called the *number of degrees of freedom* of the system. The *canonical variables* $\mathbf{q}$ and $\mathbf{p}$ are called to be *conjugate* to each other.

The advantage of the Hamiltonian formalism is that it allows one to perform all analytic operations with the scalar Hamiltonian function, instead of analyzing the whole set of equations of motion. Many equations in mechanics (including celestial mechanics) and physics can be set in Hamiltonian form. In particular, the equations of motion in a potential $U(\mathbf{r})$ (where $\mathbf{r} \equiv (x, y, z)$ is the position vector of a particle

[2]Note that in this book all vector quantities are set in bold font.

in a Cartesian frame), namely,

$$\frac{\mathrm{d}^2\mathbf{r}}{\mathrm{d}t^2} = -\nabla_{\mathbf{r}}\, U(\mathbf{r}), \tag{2.4}$$

where the gradient operator $\nabla_{\mathbf{r}} \equiv \left(\frac{\partial}{\partial x}, \frac{\partial}{\partial y}, \frac{\partial}{\partial z}\right)$, can be written down in form (2.2), setting

$$\mathbf{q} = \mathbf{r}, \quad \mathbf{p} = \frac{\mathrm{d}\mathbf{r}}{\mathrm{d}t}, \quad \mathcal{H} = \frac{\|\mathbf{p}\|^2}{2} + U(\mathbf{q}). \tag{2.5}$$

2.2 The Two-Body Problem in a Hamiltonian Form

Consider first a Hamiltonian formulation of the two-body problem. Recall that, in this problem, two point masses m_0 and m_1 move under mutual gravitational attraction. The Newtonian equations of motion in an orthogonal frame are given by

$$\frac{\mathrm{d}^2\mathbf{u}_0}{\mathrm{d}t^2} = \frac{\mathcal{G}m_1}{\|\mathbf{u}_1 - \mathbf{u}_0\|^3}(\mathbf{u}_1 - \mathbf{u}_0)\,, \quad \frac{\mathrm{d}^2\mathbf{u}_1}{\mathrm{d}t^2} = \frac{\mathcal{G}m_0}{\|\mathbf{u}_0 - \mathbf{u}_1\|^3}(\mathbf{u}_0 - \mathbf{u}_1)\,, \tag{2.6}$$

where $\mathbf{u}_0$ and $\mathbf{u}_1$ are the bodies' positions in an inertial frame, $\mathcal{G}$ is the gravitational constant; $\|\mathbf{x}\| \equiv (x_1^2 + x_2^2 + x_3^2)^{1/2}$ is the length (norm) of vector $\mathbf{x}$ (see, e.g., Szebehely 1967).

If a frame is centered on the center of mass of the system, then the frame is called *barycentric*. Such a frame is inertial. If a frame is centered on the primary, it is called *heliocentric*, or *geocentric*, or *selenocentric*, etc., depending on the primary body. Such a frame is non-inertial. The relative position of bodies is $\mathbf{r} = \mathbf{u}_1 - \mathbf{u}_0$; the barycenter is located at $\mathbf{s} = (m_0\mathbf{u}_0 + m_1\mathbf{u}_1)/(m_0 + m_1)$.

Thus, $\mathbf{r}$ is the position vector of m_1 with respect to m_0, and $\mathbf{s}$ is the absolute position vector of the barycenter. From Equations (2.6) one has

$$\frac{\mathrm{d}^2\mathbf{r}}{\mathrm{d}t^2} = -\frac{\mathcal{G}(m_0 + m_1)}{\|\mathbf{r}\|^3}\mathbf{r}\,, \tag{2.7}$$

$$\frac{\mathrm{d}^2\mathbf{s}}{\mathrm{d}t^2} = 0\,. \tag{2.8}$$

Equation (2.7) describes the relative motion of bodies, and equation (2.8) means simply that the barycenter moves inertially.

Equations (2.7) are straightforwardly reducible to a Hamiltonian form with the Hamiltonian

$$\mathcal{H}_{\text{Kepler}} = \frac{\|\mathbf{p}\|^2}{2} - \frac{\mathcal{G}(m_0 + m_1)}{\|\mathbf{q}\|}, \tag{2.9}$$

where canonical coordinates $\mathbf{q}$ are the Cartesian primary-centric coordinates, and canonical momenta $\mathbf{p} \equiv \frac{\mathrm{d}\mathbf{q}}{\mathrm{d}t}$.

The Hamiltonian equations of motion are

$$\dot{\mathbf{q}} = +\nabla_{\mathbf{p}}\mathcal{H}_{\text{Kepler}}, \qquad \dot{\mathbf{p}} = -\nabla_{\mathbf{q}}\mathcal{H}_{\text{Kepler}}, \tag{2.10}$$

where the gradient operators

$$\nabla_{\mathbf{p}} \equiv \left(\frac{\partial}{\partial p_x}, \frac{\partial}{\partial p_y}, \frac{\partial}{\partial p_z}\right), \qquad \nabla_{\mathbf{q}} \equiv \left(\frac{\partial}{\partial x}, \frac{\partial}{\partial y}, \frac{\partial}{\partial z}\right). \tag{2.11}$$

The Hamiltonian $\mathcal{H}_{\text{Kepler}}$ is nothing but the total energy of the system, equal to the sum of its kinetic and potential energies. It does not depend on time explicitly; such types of Hamiltonian systems are called *autonomous*. It is easy to show that, for such systems, $\mathcal{H}$ is conserved.

2.3 An *N*-Body Problem in a Hamiltonian Form

Consider the motion of a massless particle in the gravitation field of the Sun and N planets; thus, there are N perturbers. This is a restricted many-body problem (strictly speaking, a restricted $N + 2$-body problem, because the total number of bodies is equal to $N + 2$). If the perturbers are set to move in fixed orbits, the Newtonian equations of the particle's motion, written down in a primary-centric (heliocentric) Cartesian frame, are given by

$$\frac{\mathrm{d}^2\mathbf{r}}{\mathrm{d}t^2} = -\frac{\mathcal{G}m_0}{\|\mathbf{r}\|^3}\mathbf{r} + \sum_{i=1}^{N} \mathcal{G}m_i \left(\frac{\mathbf{r}_i - \mathbf{r}}{\|\mathbf{r}_i - \mathbf{r}\|^3} - \frac{\mathbf{r}_i}{\|\mathbf{r}_i\|^3}\right) \tag{2.12}$$

(see, e.g., Morbidelli 2002; Murray and Dermott 1999), where $\mathbf{r}$ and $\mathbf{r}_i$ ($i = 1, \ldots, N$) are the primary-centric positions of the particle and N gravitating perturbers (with masses m_i), respectively. Note that the first term in the parentheses (under the sum) corresponds to an obvious *direct* perturbation from planet m_i, and the second term to a less obvious *indirect* perturbation from the same planet. The *indirect* perturbation arises due to the gravitational effect of the planet on the Sun, implying a shift in the position of the system's center of mass.

The right-hand side of Equations (2.12) is representable as $-\nabla_{\mathbf{r}} U(\mathbf{r})$ with

$$U(\mathbf{r}) = -\frac{\mathcal{G}m_0}{\|\mathbf{r}\|} - \mathcal{G}\sum_{i=1}^{N} m_i \left(\frac{1}{\|\mathbf{r} - \mathbf{r}_i\|} - \frac{\mathbf{r}\cdot\mathbf{r}_i}{\|\mathbf{r}_i\|^3} \right) , \tag{2.13}$$

where $\mathbf{r}\cdot\mathbf{r}_i$ is the scalar product of $\mathbf{r}$ and $\mathbf{r}_i$. Consequently, in accord with Equation (2.4), the system's Hamiltonian is written as

$$\mathcal{H} = \frac{\|\mathbf{p}\|^2}{2} - \frac{\mathcal{G}m_0}{\|\mathbf{q}\|} - \mathcal{G}\sum_{i=1}^{N} m_i \left(\frac{1}{\|\mathbf{q} - \mathbf{r}_i\|} - \frac{\mathbf{q}\cdot\mathbf{r}_i}{\|\mathbf{r}_i\|^3} \right) , \tag{2.14}$$

where the canonical conjugate variables are coordinates $\mathbf{q} \equiv \mathbf{r}$ and momenta $\mathbf{p} \equiv \frac{\mathrm{d}\mathbf{q}}{\mathrm{d}t}$.

According to formula (2.14), $\mathcal{H} = \mathcal{H}_0 + \mathcal{H}_1$, where $\mathcal{H}_0 = \frac{\|\mathbf{p}\|^2}{2} - \frac{\mathcal{G}m_0}{\|\mathbf{q}\|}$ coincides with Hamiltonian (2.9) of the two-body problem if one sets m_1 to zero, and term $\mathcal{H}_1$ can be regarded as a perturbation to the two-body problem. With respect to $\mathcal{H}_0$, the relative strength of the perturbation is of the order of ratio of the perturbers' mass to that of the primary.

Here the perturbers are assumed to move in fixed (unperturbed) orbits, i.e., the $\mathbf{r}_i(t)$ are given functions. Thus, $\mathcal{H} = \mathcal{H}(\mathbf{p}, \mathbf{q}, t)$. As it depends explicitly on time, the system is *non-autonomous*.

2.4 The Delaunay Variables

It is often desirable in celestial mechanics to work in canonical variables that are straightforwardly expressible through *osculating*[3] Keplerian orbital elements. (Definitions of the Keplerian orbital elements are given in Sect. 1.1. The Keplerian elements in the two-body problem do not form themselves a canonical set, as it is easy to check.)

What is more, it is often desirable to work with variables that are straightforwardly connected to basic dynamical quantities, such as energy and angular momentum; in order that one could expect the corresponding variables to be approximately conserved when the motion is "perturbed".

A set of such useful canonical variables, which is most popular now, was introduced by Delaunay. In the two-body problem, the *Delaunay variables* are

[3] Approximating the orbital motion of a body at a given instant in a best way (in some sense; see, e.g., Murray and Dermott 1999).

defined as

$$\begin{array}{lll} L = [\mathcal{G}(m_0+m_1)a]^{1/2}, & l = M, \\ G = L(1-e^2)^{1/2}, & g = \omega, \\ H = G\cos i, & h = \Omega, \end{array} \tag{2.15}$$

where L and l, G and g, H and h form three pairs of conjugate *"action-angle" variables*. In what concerns *actions* L, G, and H, the first of them, L, is a function of sole a (semimajor axis) and thus can be expressed through the total energy; G is the module of the reduced (per unit of mass) angular momentum; and H is the reduced angular momentum vector's vertical component. Indeed, the reduced angular momentum of the system is $\mathbf{r} \times \mathrm{d}\mathbf{r}/\mathrm{d}t$. Its norm G and its projection H on the vertical axis z are given by

$$G = [\mathcal{G}(m_0+m_1)a(1-e^2)]^{1/2}, \quad H = G\cos i\,. \tag{2.16}$$

Thus, the *actions* are all conserved in the two-body problem. The conjugate *angles* l, g, and h are just the mean anomaly M, argument of pericenter ω, and longitude of ascending node Ω, respectively. In the two-body problem, g and h are also constants of motion, and l circulates with a constant frequency (the mean motion n).

The angles l, g, and h are poorly defined at the inclinations or eccentricities close to zero; the *modified Delaunay variables*, given by

$$\begin{array}{lll} \Lambda = L = [\mathcal{G}(m_0+m_1)a]^{1/2}, & \lambda = l+g+h = M+\varpi, \\ P = L-G = L[1-(1-e^2)^{1/2}], & p = -g-h = -\varpi, \\ Q = G-H = 2G\sin^2\frac{i}{2}, & q = -h = -\Omega, \end{array} \tag{2.17}$$

evade this disadvantage (e.g., Morbidelli 2002).

When expressed in the Delaunay variables (2.15), the Hamiltonian of the two-body problem is given by

$$\mathcal{H}_{\mathrm{Kepler}} = -\frac{\mathcal{G}^2(m_0+m_1)^2}{2L^2} = -\frac{\mathcal{G}(m_0+m_1)}{2a}. \tag{2.18}$$

As immediately follows from the corresponding Hamiltonian equations of motion, the variables g, h, L, G, and H are conserved. In what concerns l, it varies according to the equation

$$\frac{\mathrm{d}l}{\mathrm{d}t} = +\frac{\partial \mathcal{H}_{\mathrm{Kepler}}}{\partial L} = \frac{\mathcal{G}^2(m_0+m_1)^2}{L^3}. \tag{2.19}$$

2.5 Near-Integrable Systems

If a Hamiltonian function depends merely on canonical momenta, i.e.,

$$\mathcal{H}(\mathbf{p}, \mathbf{q}) = \mathcal{H}(\mathbf{p}), \tag{2.20}$$

then the system is integrable and the trajectories are given by simple formulas, namely,

$$\mathbf{p} = \text{ const}, \quad \mathbf{q} = \boldsymbol{\omega}_0 t + \mathbf{q}_{(t=0)}, \tag{2.21}$$

where $\boldsymbol{\omega}_0 = \nabla_{\mathbf{p}} \mathcal{H}$.

If a Hamiltonian system is near-integrable, i.e., close (in the sense of a small parameter) to the integrable one, given by Equation (2.20), this means (by definition) that it can be represented in the form

$$\mathcal{H}(\mathbf{p}, \mathbf{q}) = \mathcal{H}_0(\mathbf{p}) + \epsilon \mathcal{H}_1(\mathbf{p}, \mathbf{q}) \,, \tag{2.22}$$

where ϵ is the small unitless parameter, $\epsilon \ll 1$.

Assume also that $\nabla_{\mathbf{p}} \mathcal{H}_0 \sim \nabla_{\mathbf{p}} \mathcal{H}_1$ by the order of magnitude. Under such conditions, one can treat $\mathcal{H}_0$ as a so-called *integrable approximation*, and $\mathcal{H}_1$ as a *perturbation* (Arnold et al. 2002, 2006; Morbidelli 2002). Therefore, system (2.22) is called *near-integrable*. Of course, any system that is reducible by a canonical transformation to form (2.22) is also near-integrable.

The solution of a system with Hamiltonian $\mathcal{H}_0$ approximates the solution of the perturbed system *with accuracy* $\sim \epsilon^{\alpha}$, where $\alpha \leq 1$ is some constant whose value depends on the system properties and initial conditions (see Arnold et al. 2002, 2006). This means that the divergence of the approximate solution from the exact one is of the order ϵ^{α} on the unit interval of time. Conversely, on the time interval equal to $\epsilon^{-\alpha}$, the divergence is of order of unity. Therefore, on a long-enough timescale the integrable approximation, given by $\mathcal{H}_0$, fails. Then, to describe the motion correctly, one must take into account the perturbation. *Perturbation theories* and corresponding *perturbative approaches* allow one to do this analytically, or to diminish the amount of the corresponding numerical work substantially.

The Hamiltonians of the restricted and planetary problems both are reducible to form (2.22), where ϵ is of the order of the perturbers' mass. In case of the Solar system, $\epsilon \sim 10^{-3}$, because the ratio of masses of Jupiter and Sun is $\approx 1/1047$. Similar small perturbations are characteristic for many satellite and exoplanetary systems. That is why the perturbative approach is often so useful and fruitful, allowing one to provide an analytical description to many complicated dynamical phenomena.

One of the basic tasks of the perturbative approaches consists in elimination of dependences of a Hamiltonian on *fast* variables, by means of a canonical transformation. As soon as they are eliminated, they become *cyclic* (by definition), and the

conjugate transformed momenta become constant, to the order of transformation. In fact, if all momenta of the system are constant, the solution of the transformed system is given by formulas (2.21), and the solution of the original system can be found by substituting the inverse transformation of variables into these formulas. In celestial mechanics, the role of the fast variables is usually played by the mean longitudes or anomalies. The procedure of elimination of a fast variable is called *averaging* of the system in this variable.

The notion of averaging is related to a (superior) notion of *normalization*. The normalization procedure consists in reducing the Hamiltonian to some "simple" form; e.g., to the *Birkhoff normal form*, in which all dependences on the canonical angles are eliminated in all orders of the Hamiltonian expansion in powers of a small parameter.

To keep the system Hamiltonian, the *normalizing transformation* must be canonical. Usually it is required to find: the normal form of the Hamiltonian up to a specified order; the generating function of the normalizing transformation; the formulae of direct and inverse transformations of the canonical variables. In all applications to the three-body problem, the procedure implies cumbersome analytical calculations. That is why the normalization is often accomplished by means of computer algebra.

2.6 The von Zeipel Method

Among the methods used for averaging and normalization in celestial mechanics, the von Zeipel method (von Zeipel 1916)[4] and the Hori–Deprit method (Deprit 1969; Hori 1966) are most popular. Though less convenient algorithmically, the first of them is an older one and it is analytically straightforward, that is why we describe it first. What is more, it was just the von Zeipel method that was mostly used by researchers for the averaging purposes in developments of the Lidov-Kozai theory.

In fact, the "von Zeipel method" was introduced by Poincaré (1899), who called it the "Lindstedt method". Von Zeipel used it extensively in studies in celestial mechanics, that is why the method is usually called now after his name. The method is described in a number of monographs, in particular, in Giacaglia (1972), Hagihara (1972), Kholshevnikov (1985), Zhuravlev and Klimov (1988), and Marchal (1990). Here we give a brief synopsis, based mostly on reviews in Giacaglia (1972), Zhuravlev and Klimov (1988), and Morbidelli (2002). The designations are generally such as adopted in Morbidelli (2002).

As a first step, any perturbative treatment of a near-integrable Hamiltonian system aims to find a *close-to-identity* canonical transformation

$$\mathbf{p} = \mathbf{p}^1 + \epsilon \mathbf{f}_1(\mathbf{p}^1, \mathbf{q}^1) , \quad \mathbf{q} = \mathbf{q}^1 + \epsilon \mathbf{g}_1(\mathbf{p}^1, \mathbf{q}^1) , \tag{2.23}$$

[4] The method was originally introduced by Poincaré (1899).

that allows one to transform Hamiltonian (2.22) to

$$\mathcal{K}(\mathbf{p}^1, \mathbf{q}^1) = \mathcal{H}_0(\mathbf{p}^1) + \epsilon\mathcal{K}_1(\mathbf{p}^1) + \epsilon^2\mathcal{K}_2(\mathbf{p}^1, \mathbf{q}^1) \,, \tag{2.24}$$

where $\mathcal{K}_1$ is nothing but the term $\mathcal{H}_1$ averaged over the angles $\mathbf{q}$, and $\mathcal{K}_2$ is a new function of the order not greater than $\mathcal{H}_1$. The Hamiltonian $\mathcal{H}_0 + \epsilon\mathcal{K}_1$ provides an *integrable approximation* (of order ϵ^2) of the original dynamical system.

To achieve a higher level of approximation of the motion, one can iterate, looking at each consecutive step for the canonical transformation

$$\mathbf{p}^{r-1} = \mathbf{p}^r + \epsilon^r \mathbf{f}_r(\mathbf{p}^r, \mathbf{q}^r) \,, \quad \mathbf{q}^{r-1} = \mathbf{q}^r + \epsilon^r \mathbf{g}_r(\mathbf{p}^r, \mathbf{q}^r) \,, \tag{2.25}$$

such that the Hamiltonian obtains the *Birkhoff normal form*

$$\mathcal{K}(\mathbf{p}^r) = \mathcal{H}_0(\mathbf{p}^r) + \epsilon\mathcal{K}_1(\mathbf{p}^r) + \cdots + \epsilon^r\mathcal{K}_r(\mathbf{p}^r) + O(\epsilon^{r+1}) \,. \tag{2.26}$$

Thus, at any consecutive step r of the procedure (at any consecutive order r in ϵ), the system's approximation is integrable, and the solution is given by

$$\mathbf{p}^r = \text{const}, \quad \mathbf{q}^r = \boldsymbol{\omega}^r t + \mathbf{q}^r_{(t=0)} \,, \tag{2.27}$$

where

$$\boldsymbol{\omega}^r = \nabla_{\mathbf{p}^r}[\mathcal{H}_0(\mathbf{p}^r) + \epsilon\mathcal{K}_1(\mathbf{p}^r) + \cdots + \epsilon^r\mathcal{K}_r(\mathbf{p}^r)] \,. \tag{2.28}$$

Constructing the inverse composition of all iterated transformations of the variables, one obtains the solution in the original variables $\mathbf{p}$ and $\mathbf{q}$.

Let us see how these perturbation techniques are realized in the von Zeipel algorithm. Consider Hamiltonian system (2.3) with Hamiltonian (2.22), i.e., a near-integrable original system. Our aim is to transform its Hamiltonian to normal form (2.26). To distinguish the transformed canonical variables and Hamiltonian from the original ones, we designate them by $\mathbf{P}$, $\mathbf{Q}$, and $\mathcal{K}$:

$$\mathcal{K}(\mathbf{P}) = \mathcal{K}_0(\mathbf{P}) + \epsilon\mathcal{K}_1(\mathbf{P}) + \cdots + \epsilon^r\mathcal{K}_r(\mathbf{P}) + O(\epsilon^{r+1}) \,. \tag{2.29}$$

To the second order in ϵ, the sought Hamiltonian is

$$\mathcal{K}(\mathbf{P}) = \mathcal{K}_0(\mathbf{P}) + \epsilon\mathcal{K}_1(\mathbf{P}) + \epsilon^2\mathcal{K}_2(\mathbf{P}) \,. \tag{2.30}$$

In the von Zeipel algorithm, the normalizing canonical transformation is determined by a *generating function* $\mathcal{S}(\mathbf{q}, \mathbf{P}, \epsilon)$:

$$\mathbf{p} = \nabla_{\mathbf{q}}\mathcal{S}(\mathbf{q}, \mathbf{P}, \epsilon) \,, \quad \mathbf{Q} = \nabla_{\mathbf{P}}\mathcal{S}(\mathbf{q}, \mathbf{P}, \epsilon) \,, \tag{2.31}$$

which is sought in the form of a power series in ϵ:

$$\mathcal{S}(\mathbf{q},\mathbf{P},\epsilon) = \mathbf{q}\cdot\mathbf{P} + \epsilon\mathcal{S}_1(\mathbf{q},\mathbf{P}) + \epsilon^2\mathcal{S}_2(\mathbf{q},\mathbf{P}) + \dots \ . \tag{2.32}$$

As needed, the generated transformation is close to identity; at $\epsilon = 0$ it is strictly identical: $\mathbf{p} = \mathbf{P}$, $\mathbf{q} = \mathbf{Q}$.

Evidently, the generating function must satisfy the equation

$$\mathcal{H}(\mathbf{q}, \nabla_{\mathbf{q}}\mathcal{S}, \epsilon) = \mathcal{K}(\mathbf{P}) = \text{const} \ . \tag{2.33}$$

Expanding $\mathcal{H}$, $\mathcal{S}$, and $\mathcal{K}$ in power series in ϵ, one has at each consequent order (0, 1, 2, ...) of ϵ:

$$\mathcal{H}_0(\mathbf{P}) = \mathcal{K}_0(\mathbf{P}) \ , \tag{2.34}$$

$$\nabla_{\mathbf{p}}\mathcal{H}_0\cdot\nabla_{\mathbf{q}}\mathcal{S}_1 + \mathcal{H}_1(\mathbf{q}, \nabla_{\mathbf{q}}\mathcal{S}_0) = \mathcal{K}_1(\mathbf{P}) \ , \tag{2.35}$$

$$\nabla_{\mathbf{p}}\mathcal{H}_0\cdot\nabla_{\mathbf{q}}\mathcal{S}_2 + \nabla_{\mathbf{p}}\mathcal{H}_1\cdot\nabla_{\mathbf{q}}\mathcal{S}_1 + \frac{1}{2}\sum_{i,\,j}\frac{\partial^2\mathcal{H}_0}{\partial p_i\partial p_j}\frac{\partial\mathcal{S}_1}{\partial q_i}\frac{\partial\mathcal{S}_1}{\partial q_j} + \mathcal{H}_2(\mathbf{q}, \nabla_{\mathbf{q}}\mathcal{S}_0) = \mathcal{K}_2(\mathbf{P}) \ , \tag{2.36}$$

$$\dots \ ,$$

where $1 \le i \le n$, $1 \le j \le n$ (and n is the number of degrees of freedom). Substituting $\nabla_{\mathbf{q}}\mathcal{S}_0 = \mathbf{P}$ and $\nabla_{\mathbf{p}}\mathcal{H}_0 = \mathcal{K}(\mathbf{P})$, we arrive at a sequence of linear equations in partial derivatives. Starting with order one in ϵ, this sequence is given by

$$\mathcal{K}(\mathbf{P})\cdot\nabla_{\mathbf{q}}\mathcal{S}_1 + \mathcal{H}_1(\mathbf{q},\mathbf{P}) = \mathcal{K}_1(\mathbf{P}) \ , \tag{2.37}$$

$$\mathcal{K}(\mathbf{P})\cdot\nabla_{\mathbf{q}}\mathcal{S}_2 + \mathcal{F}_2(\mathbf{q},\mathbf{P},\nabla_{\mathbf{q}}\mathcal{S}_1) = \mathcal{K}_2(\mathbf{P}) \ , \tag{2.38}$$

$$\mathcal{K}(\mathbf{P})\cdot\nabla_{\mathbf{q}}\mathcal{S}_3 + \mathcal{F}_3(\mathbf{q},\mathbf{P},\nabla_{\mathbf{q}}\mathcal{S}_1,\nabla_{\mathbf{q}}\mathcal{S}_2) = \mathcal{K}_3(\mathbf{P}) \ , \tag{2.39}$$

$$\dots \ .$$

Taking into account that the original Hamiltonian is periodic in angles $\mathbf{q}$, it is straightforward to choose $\mathcal{K}_1(\mathbf{P})$ equal to $\mathcal{H}_1(\mathbf{q},\mathbf{P})$ averaged over $\mathbf{q}$: $\mathcal{K}_1(\mathbf{P}) = \bar{\mathcal{H}}_1(\mathbf{P})$. Then, one has an equation for $\mathcal{S}_1$:

$$\mathcal{K}(\mathbf{P})\cdot\nabla_{\mathbf{q}}\mathcal{S}_1(\mathbf{q},\mathbf{P}) = \bar{\mathcal{H}}_1(\mathbf{P}) - \mathcal{H}_1(\mathbf{q},\mathbf{P}) \ . \tag{2.40}$$

This equation can be solved with respect to $\mathcal{S}_1$ by expanding $\mathcal{H}_1(\mathbf{q},\mathbf{P})$ in the Fourier series in $\mathbf{q}$ (recall that $\mathcal{H}_1(\mathbf{q},\mathbf{P})$ is periodic in $\mathbf{q}$), and seeking for $\mathcal{S}_1$ also in the form of a Fourier series. (Such a procedure is described in the next section for an analogous situation.)

Substituting the determined $\mathcal{S}_1$ and $\mathcal{K}_2(\mathbf{P}) = \bar{\mathcal{F}}_2(\mathbf{P})$ in Equation (2.38), one arrives at an equation for $\mathcal{S}_2(\mathbf{q}, \mathbf{P})$:

$$\boldsymbol{\omega}(\mathbf{P}) \cdot \nabla_{\mathbf{q}} \mathcal{S}_2(\mathbf{q}, \mathbf{P}) = \bar{\mathcal{F}}_2(\mathbf{P}) - \mathcal{F}_2(\mathbf{q}, \mathbf{P}, \nabla_{\mathbf{q}} \mathcal{S}_1) \,. \tag{2.41}$$

This equation is analogous to (2.40) and is solved in the same manner.

At each higher consecutive order in ϵ, the step algorithm is completely analogous. This is how the von Zeipel algorithm can be summarized.

Note that since the original system is generally non-integrable, the obtained regular solution is strictly *formal*, i.e., the series representing the solution are not obliged to converge. To obtain a solution closest to the true one, the iterations should be terminated at some optimum order r, depending on the system itself and on the value of ϵ.

2.7 The Hori–Deprit Method

At present, the most popular perturbative approach is one based on methods proposed by Hori (1966) and Deprit (1969). They employ the Lie perturbation techniques. This approach provides a number of advantages; in particular, the normalizing transformation is canonical by construction.

In the von Zeipel method, the generating function depends on "old" coordinate and "new" momentum variables. The absence of mixture of similar kind represents one of the principal advantages of the Hori–Deprit method over the von Zeipel method. What is more, the crucial advantage of the Hori–Deprit method consists in its practical recursiveness: it is based on recurrent explicit formulas, which reduce the normalization in every successive order to a standard mathematical procedure.

Let $\mathbf{q}$ and $\mathbf{p}$ be conjugate canonical coordinates and momenta, and $f(\mathbf{p}, \mathbf{q})$ and $g(\mathbf{p}, \mathbf{q})$ are some functions of them; then the Poisson bracket of f and g is defined as

$$\{f, g\} = \nabla_{\mathbf{q}} f \cdot \nabla_{\mathbf{p}} g - \nabla_{\mathbf{p}} f \cdot \nabla_{\mathbf{q}} g = \sum_{i=1}^{n} \frac{\partial f}{\partial q_i} \frac{\partial g}{\partial p_i} - \frac{\partial f}{\partial p_i} \frac{\partial g}{\partial q_i} \,, \tag{2.42}$$

where n is the number of degrees of freedom.

For an arbitrary function $f = f(\mathbf{p}, \mathbf{q})$, where $\mathbf{p}$ and $\mathbf{q}$ are the solutions of a Hamiltonian system with a Hamiltonian $\mathcal{S}$, one has

$$\frac{\mathrm{d}f}{\mathrm{d}t} = \nabla_{\mathbf{q}} f \cdot \dot{\mathbf{q}} + \nabla_{\mathbf{p}} f \cdot \dot{\mathbf{p}} = \{f, \mathcal{S}\} \,. \tag{2.43}$$

Let us expand f in a power series of t in the neighbourhood of $t = 0$:

$$f(t) = f(0) + \sum_{k=1}^{\infty} \frac{t^k}{k!} \cdot \frac{\mathrm{d}^k f}{\mathrm{d}t^k}\bigg|_{t=0} , \tag{2.44}$$

where $f(0) \equiv f(\mathbf{p}(0), \mathbf{q}(0))$ and $\frac{\mathrm{d}^k f}{\mathrm{d}t^k}\Big|_{t=0} \equiv \frac{\mathrm{d}^k f}{\mathrm{d}t^k}(\mathbf{p}(0), \mathbf{q}(0))$. Noting that

$$\frac{\mathrm{d}f}{\mathrm{d}t} = \{f, \mathcal{S}\} , \quad \frac{\mathrm{d}^2 f}{\mathrm{d}t^2} = \left\{ \frac{\mathrm{d}f}{\mathrm{d}t}, \mathcal{S} \right\} = \{\{f, \mathcal{S}\}, \mathcal{S}\} , \quad \ldots , \tag{2.45}$$

and defining the *Lie operators* D^k with generator $\mathcal{S}$ by the recurrent relation

$$D^k f = D(D^{k-1} f) , \quad \text{where } Df = D^1 f = \{f, \mathcal{S}\} , \tag{2.46}$$

one can express $f(t)$ as

$$f(t) = f(0) + \sum_{k=1}^{\infty} \frac{t^k}{k!} \cdot D^k f\big|_{t=0} , \tag{2.47}$$

Series (2.47) is called the *Lie series* of a function f along the flow $\mathcal{S}$. Expansion (2.47) can be interpreted as an operator applied to f. As such, it is henceforth designated $L^t_{\mathcal{S}} f$.

Recall that a transformation of variables is called canonical, if it preserves the Hamiltonian form of equations. It is straightforward to verify (see Morbidelli 2002) that a transformation $(\mathbf{p}, \mathbf{q}) \to (\mathbf{P}, \mathbf{Q})$ of the form

$$\mathbf{p} = \mathbf{P} + \int_0^{\epsilon} \dot{\mathbf{P}} \mathrm{d}t = L^{\epsilon}_{\mathcal{S}} \mathbf{P} , \quad \mathbf{q} = \mathbf{Q} + \int_0^{\epsilon} \dot{\mathbf{Q}} \mathrm{d}t = L^{\epsilon}_{\mathcal{S}} \mathbf{Q} , \tag{2.48}$$

is canonical, if there exists a function $\mathcal{S}(\mathbf{P}, \mathbf{Q}, \epsilon)$ such that $\dot{\mathbf{P}}$ and $\dot{\mathbf{Q}}$ satisfy Hamiltonian equations

$$\dot{\mathbf{P}} = -\partial \mathcal{S} / \partial \mathbf{Q} , \quad \dot{\mathbf{Q}} = \partial \mathcal{S} / \partial \mathbf{P} . \tag{2.49}$$

Function $\mathcal{S}(\mathbf{P}, \mathbf{Q}, \epsilon)$ (where ϵ is a parameter) is called the *generating Hamiltonian* or the *generating function*.

Equations (2.48) represent an outcome of a canonical transformation (defined by the Hamiltonian flow with Hamiltonian $\mathcal{S}$), taken at a "time moment" ϵ. The *Lie perturbation techniques* are based on the transform representation (2.48).

Consider the normalizing transformation in the first order of ϵ. Thus, we define $\mathbf{p}^1 \equiv \mathbf{P}$, $\mathbf{q}^1 \equiv \mathbf{Q}$. As in case of any Lie series of a function, one has for the Hamiltonian:

$$\mathcal{K} = L^{\epsilon}_{\mathcal{S}} \mathcal{H} . \tag{2.50}$$

We seek for a generating function $\mathcal{S}$ such that the Hamiltonian (2.22) is transformed to the Birkhoff normal form in the first order of ϵ, i.e., the dependence on angles is eliminated in the first order.

According to (2.47), to the second order in ϵ, one has

$$\mathcal{K} = \mathcal{H}_0 + \epsilon\mathcal{H}_1 + \epsilon\{\mathcal{H}_0, \mathcal{S}\} + \epsilon^2\{\mathcal{H}_1, \mathcal{S}\} + \frac{\epsilon^2}{2}\{\{\mathcal{H}_0, \mathcal{S}\}, \mathcal{S}\} + O(\epsilon^3)\ . \tag{2.51}$$

It is implied that $\mathcal{H}_0$, $\mathcal{K}$, and $\mathcal{S}$ are all functions of $\mathbf{p}^1$, $\mathbf{q}^1$. Picking out the terms of the first order in ϵ, we equate them to a function of momenta only:

$$\mathcal{H}_1 + \{\mathcal{H}_0, \mathcal{S}\} = \bar{\mathcal{H}}_1\ . \tag{2.52}$$

The generating function $\mathcal{S}(\mathbf{p}^1, \mathbf{q}^1)$ can be found from this equation, the $\bar{\mathcal{H}}_1$ function being subject to the mentioned restriction (the dependence merely on $\mathbf{p}^1$). This equation, called the *homologic equation*, is nothing but a linear equation in partial derivatives, and it is easily solvable. It is sufficient to find any particular solution of this equation.

As described in Morbidelli (2002), the solution can be obtained in the following way. Since $\mathcal{H}$ is periodic in angles $\mathbf{q}^1$, one may expand $\mathcal{H}_1$ in the Fourier series:

$$\mathcal{H}_1(\mathbf{p}^1, \mathbf{q}^1) = \sum_{\mathbf{k}\in\mathbf{Z}^n} c_{\mathbf{k}}(\mathbf{p}^1) \exp\left(\iota\mathbf{k}\cdot\mathbf{q}^1\right)\ , \tag{2.53}$$

where $\iota = \sqrt{-1}$.

The solution of Equation (2.52) is sought also as the Fourier series

$$\mathcal{S}(\mathbf{p}^1, \mathbf{q}^1) = \sum_{\mathbf{k}\in\mathbf{Z}^n} d_{\mathbf{k}}(\mathbf{p}^1) \exp\left(\iota\mathbf{k}\cdot\mathbf{q}^1\right)\ ; \tag{2.54}$$

immediately one has

$$\{\mathcal{H}_0, \mathcal{S}\} = -\iota \sum_{\mathbf{k}\in\mathbf{Z}^n} d_{\mathbf{k}}(\mathbf{p}^1)\mathbf{k}\cdot\boldsymbol{\omega}_0(\mathbf{p}^1) \exp\left(\iota\mathbf{k}\cdot\mathbf{q}^1\right)\ , \tag{2.55}$$

where $\boldsymbol{\omega}_0 = \nabla_{\mathbf{p}^1}\mathcal{H}_0$; and the coefficients of the generating function (2.54) are determined as

$$d_{\mathbf{0}} = 0\ , \quad d_{\mathbf{k}}(\mathbf{p}^1) = -\iota\frac{c_{\mathbf{k}}(\mathbf{p}^1)}{\mathbf{k}\cdot\boldsymbol{\omega}_0(\mathbf{p}^1)} \tag{2.56}$$

at all non-zero $\mathbf{k}$. Besides,

$$\bar{\mathcal{H}}_1(\mathbf{p}^1) = c_0(\mathbf{p}^1)\ . \tag{2.57}$$

In the higher orders in ϵ, the procedure can be accomplished recursively; at each order, an analogous homologic equation is defined and solved (see Giacaglia 1972; Zhuravlev and Klimov 1988). The described procedure is called non-resonant, as it is implied that, in the course of normalization, one does not encounter zero resonant combinations in the denominators in Equations (2.56). For algorithms tackling the resonant situations, see the aforementioned monographs.

By means of the described algorithm the components of the generating function and the normalized Hamiltonian can be successively found, up to the required order of normalization. As a result we obtain the normalized Hamiltonian and the generating function of the normalizing transformation.

The canonical variables which the obtained generating function depends upon are not mixed. This circumstance allows one to calculate the normalizing transformation of the canonical variables as the Lie transformation with the generator equal to the newly found generating function $\mathcal{S}$. This transformation is given by the formulas

$$\mathbf{p} = \mathbf{P} + \sum_{k=1}^{\infty} \frac{\epsilon^k}{k!} D^k \mathbf{P}\Big|_{\epsilon=0} , \quad \mathbf{q} = \mathbf{Q} + \sum_{k=1}^{\infty} \frac{\epsilon^k}{k!} D^k \mathbf{Q}\Big|_{\epsilon=0} . \tag{2.58}$$

Variables $\mathbf{Q}$ and $\mathbf{P}$ represent the new canonical coordinates and momenta. The inverse transformation is the Lie transformation with the generator $(-S)$:

$$\mathbf{P} = \mathbf{p} + \sum_{k=1}^{\infty} \frac{(-\epsilon)^k}{k!} D^k \mathbf{p}\Big|_{\epsilon=0} , \quad \mathbf{Q} = \mathbf{q} + \sum_{k=1}^{\infty} \frac{(-\epsilon)^k}{k!} D^k \mathbf{q}\Big|_{\epsilon=0} . \tag{2.59}$$

When calculating the transformations of the canonical variables in practice, it is sufficient to leave the terms up to the order $M-1$ inclusive in the right-hand parts of the formulas, where M is the final order of normalization. Such length of expansions is sufficient to transform the Hamiltonian to the normal form of the given order, or, in the case of inverse transformation, to the initial form.

Chapter 3
Classical Results

This chapter is devoted to classical results, mostly presented in the pioneer works by Mikhail Lidov and Yoshihide Kozai. To start with, we derive the secular Lidov-Kozai Hamiltonian (the LK Hamiltonian) for the circular R3BP, where the averaged perturbation is approximated by the quadrupole term of the Hamiltonian expansion in the ratio of semimajor axes of the test particle (tertiary) and the gravitating binary. Since there is only one angular variable remaining in the LK Hamiltonian (the argument of pericenter), the corresponding motion equations can be solved by quadrature. The fact that the second angle (the longitude of the ascending node) is missing is a lucky fortuitous property of the problem.

Kozai proposed a convenient technique to analyze the qualitative properties of these secular effects: he constructed phase portraits, characterizing the secular evolution of the eccentricity and the argument of pericenter for various initial conditions. Taking into account that the corresponding phase trajectories lie on the level curves of the LK Hamiltonian, the trajectories can be drawn without integration of the motion equations. The topology of the phase portraits depends essentially on the norm of the vertical component of the tertiary's orbital angular momentum. At its certain value, a bifurcation occurs: whereas for the norm's greater values the argument of pericenter always circulates, for its smaller values an equilibrium point appears, accompanied with the trajectories (around the point), corresponding to libration of the argument of pericenter. This libration island is nothing but the famous *Lidov-Kozai resonance*.

The integration of the averaged motion equations by quadrature requires application of elliptic functions. Already in 1962 Kozai demonstrated how this could be done (Kozai 1962), but only quite a considerable time later on his ideas were realized by Lidov's disciple Mikhail Vashkovyak (1999) and Kinoshita and Nakai (1999, 2007).

I. I. Shevchenko, *The Lidov-Kozai Effect – Applications in Exoplanet Research and Dynamical Astronomy*, Astrophysics and Space Science Library 441,
DOI 10.1007/978-3-319-43522-0_3

To complete our review of the classical results, we discuss how the LKE can be suppressed in various dynamical situations. Indeed, if an additional perturbation dominates over the LK-term in the Hamiltonian of the motion, then the LKE may disappear (Lidov 1963b; Morbidelli 2002). In particular, such a suppression explains the stable existence of the *regular* satellites of Uranus. In their case, the suppression "agent" is the satellites' orbital precession forced by the Uranus oblateness and the moons' mutual perturbations.

3.1 A Single-Averaged R3BP

As an example of a secular theory, we consider Moiseev's scheme of averaging of the R3BP. The reason is that this scheme is useful for our further analysis, as it has a direct relation to the LK scheme. Indeed, a double-averaging is utilized in the LK scheme, thus involving the single-averaging as an ingredient of the whole procedure.

In the single-averaged R3BP, the perturbing function is averaged over one variable (that with the largest frequency of variation), namely, the mean anomaly of the satellite. As soon as a perturber is in an outer orbit, the satellite's mean anomaly is "faster" than that of the perturber. In the Hill approximation, only the lowest order term in the ratio of the semimajor axes of the satellite and the perturber is taken into account in the perturbing function. This averaging scheme was introduced by Moiseev (1945a,b).[1]

Moiseev (1945a,b) deduced equations of motion in the single-averaged problem and found two integrals of the motion. Contrary to the double-averaged case (considered in this book later on), there is no third integral here; thus, the problem is not integrable in the spatial case (when the system has three degrees of freedom).

Based on Moiseev's averaging scheme, Vashkovyak (2005) derived explicit equations of motion in the single-averaged R3BP, in the Hill approximation. Here we reproduce these equations in convenient notations, and, following Vashkovyak (2005), delineate the conditions for their applicability.

Consider the motion of a planetary satellite perturbed by a distant external body (e.g., the Sun). The perturbing body is assumed to move in a circular orbit of radius $a_{\rm pert}$. The planetocentric Keplerian orbital elements of the satellite, i.e., the semimajor axis, eccentricity, inclination, argument of pericenter, longitude of ascending node, and mean anomaly, are denoted, as usually, by a, e, i, ω, Ω, and M, respectively. The angles are referred to the plane of motion of the perturbing body and to a fixed arbitrary direction in this plane.

[1] Nikolay Dmitrievich Moiseev (1902–1955), a professor of the Moscow University, was the founder of the Moscow school of celestial mechanics. The mentioned papers were typeset in 1941, but, due to calamities of the war, the publication was delayed until 1945.

The Keplerian mean motion of the satellite is $n = (\mathcal{G}m)^{1/2}/a^{3/2}$, and that of the perturbing body is $n_{\rm pert} = [\mathcal{G}(m_0 + m_{\rm pert})]^{1/2}/a_{\rm pert}^{3/2}$. Following Vashkovyak (2005), we introduce a dimensionless parameter of the problem, $\nu = n_{\rm pert}/(n\beta)$, where $\beta = 3m_{\rm pert}a^3/(16m_0a_{\rm pert}^3)$. $\mathcal{G}$ is the gravitational constant, m_0 and $m_{\rm pert}$ are the masses of the primary (planet) and the perturbing body, respectively. If $m_0/m_{\rm pert} \ll 1$, then $n_{\rm pert}^2 \approx \mathcal{G}m_{\rm pert}/a_{\rm pert}^3$, $\beta \approx 3n_{\rm pert}^2/(16n^2)$, and $\nu \approx 16n/(3n_{\rm pert})$.

The unitless "time" is defined as

$$\tau = \beta n(t - t_0), \tag{3.1}$$

where t_0 is the initial time.

The mean longitude of the perturbing body is given by

$$\lambda_{\rm pert} = \lambda_{\rm pert}|_{t=t_0} + n_{\rm pert}(t - t_0) = \lambda_{\rm pert}|_{\tau=0} + \nu\tau. \tag{3.2}$$

The longitude of ascending node of the satellite's orbit, Ω, is present in the averaged perturbing function R only in combination with the mean longitude of the perturbing body, $\lambda_{\rm pert}$.[2] Denoting

$$\Upsilon = \Omega - \lambda_{\rm pert}|_{\tau=0} - \nu\tau, \tag{3.3}$$

let us average the perturbing function $\mathcal{R}$ (corresponding to the third term in expression (2.14); see also Murray and Dermott 1999) over the mean anomaly of the satellite:

$$\mathcal{V} = \frac{1}{2\pi}\int_0^{2\pi} \mathcal{R}\,{\rm d}M. \tag{3.4}$$

Here the perturbing function is normalized by factor $\mathcal{G}m\beta/a$. Taking the integral in the quadrupole (Hill) approximation, one has

$$\mathcal{V} = \mathcal{V}_{\rm H} + O(a/a_{\rm pert})^3, \tag{3.5}$$

where

$$\begin{aligned}\mathcal{V}_{\rm H} = {} & \frac{4}{3} + 2(e^2 - \sin^2 i) + e^2\sin^2 i(5\cos 2\omega - 3) - 10e^2\cos i\sin 2\omega\sin 2\Upsilon + \\ & + [2\sin^2 i + 10e^2\cos 2\omega + e^2\sin^2 i(3 - 5\cos 2\omega)]\cos 2\Upsilon\end{aligned} \tag{3.6}$$

[2]This follows from the so-called D'Alembert rules, specifying which combinations of angles can be present in the Fourier expansions of perturbing functions. The formulation of the D'Alembert rules is given in section 1.9.3 in Morbidelli (2002).

(Vashkovyak 2005). The equations of motion are easily derivable, as soon as a perturbing function is given (see Murray and Dermott 1999). In accord with expression (3.6), the secular equations for the single-averaged Hill problem are given by

$$\frac{\mathrm{d}a}{\mathrm{d}\tau} = 0, \tag{3.7}$$

$$\frac{\mathrm{d}e}{\mathrm{d}\tau} = 10e(1-e^2)^{1/2}[\sin^2 i \sin 2\omega + (2-\sin^2 i)\sin 2\omega \cos 2\Upsilon + 2\cos i \cos 2\omega \sin 2\Upsilon], \tag{3.8}$$

$$\frac{\mathrm{d}i}{\mathrm{d}\tau} = -2\sin i\,(1-e^2)^{-1/2}\{5e^2 \cos i \sin 2\omega(1-\cos 2\Upsilon) - \\ -[2+e^2(3+5\cos 2\omega)]\sin 2\Upsilon\}, \tag{3.9}$$

$$\frac{\mathrm{d}\omega}{\mathrm{d}\tau} = 2(1-e^2)^{-1/2} \times \\ \times\{4+e^2-5\sin^2 i + 5(\sin^2 i - e^2)\cos 2\omega + 5(e^2-2)\cos i \sin 2\omega \sin 2\Upsilon + \\ +[5(2-e^2-\sin^2 i)\cos 2\omega - 2 - 3e^2 + 5\sin^2 i]\cos 2\Upsilon\}, \tag{3.10}$$

$$\frac{\mathrm{d}\Upsilon}{\mathrm{d}\tau} = -\nu - 2(1-e^2)^{-1/2}\{[2+e^2(3-5\cos 2\omega)]\cos i\,(1-\cos 2\Upsilon) - 5e^2 \sin 2\omega \sin 2\Upsilon\}. \tag{3.11}$$

Moiseev (1945b) found out that the secular system in this problem has two integrals:

$$a = \text{const}, \tag{3.12}$$

$$\mathcal{V} + \nu(1-e^2)^{1/2}\cos i = \text{const}. \tag{3.13}$$

In the Hill approximation, $\mathcal{V} = \mathcal{V}_\mathrm{H}$, where $\mathcal{V}_\mathrm{H}$ is given by formula (3.6).

Vashkovyak (2005) formulated conditions for the applicability of the secular equations to describe the long-term motion of natural satellites of planets in the Solar system. Let us enumerate them. Recall first of all that the radius of a planet's Hill sphere a_H, in units of the semimajor axis of a perturbing body, a_pert, is given by

$$a_\mathrm{H}/a_\mathrm{pert} = \left[3\left(1+\frac{m_\mathrm{pert}}{m_0}\right)\right]^{-1/3}. \tag{3.14}$$

Then, the semimajor axis of a satellite's orbit, a, in units of $a_{\rm H}$, is equal to

$$\frac{a}{a_{\rm H}} = 4\left[\frac{4}{3\nu^2}\left(1+\frac{m_0}{m_{\rm pert}}\right)^2\right]^{1/3} \approx 2^{8/3}3^{-1/3}\nu^{-2/3} \approx 4.40\nu^{-2/3}. \tag{3.15}$$

The planetocentric orbit of a satellite should lie within the Hill sphere. This implies the inequality $a(1+e) \lesssim a_{\rm H}$. Therefore, an allowed lower limit for ν is given by $\nu_{\rm min} \approx 9.24$ at $e = 0$, and by $\nu_{\rm min} \approx 26.1$ at $e = 1$.

Vashkovyak (2005) compared these theoretical bounds with the values of ν observed for the real planetary satellites in the Solar system. For the real satellites (including the irregular most distant satellites of the giant planets), the ratio of mean motions, $n_{\rm pert}/n$, does not exceed ≈ 0.16; therefore, one has $\nu \approx 16n/(3n_{\rm pert}) \gtrsim 33$, and the theoretical condition for $\nu_{\rm min}$ is thus satisfied.

3.2 The Double-Averaged R3BP

The first secular theory in celestial mechanics was constructed by Lagrange and Laplace: they built an analytical theory describing the long-term averaged behaviour of the Solar system planets. However, this theory was limited to the case of small mass parameters and small planetary eccentricities and inclinations; besides, resonances were assumed to be absent. Brown (1936) applied techniques of canonical transformations to describe the long-term averaged behaviour of stellar triple systems; in particular, he obtained the Hamiltonian in the quadrupole approximation. Three integrals in the double-averaged circular R3BP were found by Moiseev (1945a,b).

3.2.1 The Lidov-Kozai Hamiltonian

In this subsection, we derive the secular Lidov-Kozai Hamiltonian (the LK Hamiltonian) for the circular R3BP, where the averaged perturbation is approximated by the quadrupole term of the Hamiltonian expansion in the ratio of semimajor axes of the test particle (tertiary) and the gravitating binary. Since there is only one angular variable that remains in the LK Hamiltonian (the argument of pericenter), the corresponding motion equations can be solved by quadrature.

In the *restricted* version of the N-body problem, one of the bodies (called the *test particle* or simply the *particle*) is massless in the sense that it gravitates only passively: the particle's motion is affected by the gravity of all other bodies, but the particle's gravity does not affect the motion of other bodies. The orbits of the massive bodies are assumed to be known. According to expression (2.14), the

Hamiltonian is given by

$$\mathcal{H} = \mathcal{H}_{\text{Kepler}} + \mathcal{H}_{\text{interaction}} \tag{3.16}$$

(Malhotra 2012; Murray and Dermott 1999), where the *Keplerian Hamiltonian* is

$$\mathcal{H}_{\text{Kepler}} = -\frac{\mathcal{G}m_0}{2a} \tag{3.17}$$

(where a is the semimajor axis of the particle's orbit around primary m_0), and the *interaction Hamiltonian* is

$$\mathcal{H}_{\text{interaction}} = -\sum_{i=1}^{N} \mathcal{G}m_i \left[\frac{1}{\|\mathbf{r} - \mathbf{r}_i\|} - \frac{(\mathbf{r} - \mathbf{r}_0) \cdot (\mathbf{r}_i - \mathbf{r}_0)}{\|\mathbf{r}_i - \mathbf{r}_0\|^3} \right], \tag{3.18}$$

where $\mathbf{r}$ is the position vector of the test particle.

In the R3BP, the interaction Hamiltonian reduces to

$$\mathcal{H}_{\text{interaction}} = -\mathcal{G}m_1 \left[\frac{1}{\|\mathbf{r} - \mathbf{r}_1\|} - \frac{(\mathbf{r} - \mathbf{r}_0) \cdot (\mathbf{r}_1 - \mathbf{r}_0)}{\|\mathbf{r}_1 - \mathbf{r}_0\|^3} \right]. \tag{3.19}$$

Let us derive the Lidov-Kozai Hamiltonian in the R3BP, taking expression (3.19) as a starting point. For this purpose, we follow an approach by Malhotra (2012).

As there remains only one perturber, further on we designate m_1 as m_{pert}. Thus, the masses of the primary and the perturber are designated by m_0 and m_{pert}; the radius of perturber's circular orbit by a_{pert}; the semimajor axis of particle's orbit by a. It is assumed that $a \ll a_{\text{pert}}$.

Setting $\mathbf{r}_0 = 0$, we rewrite Equation (3.19) in the form

$$\mathcal{H}_{\text{interaction}} = -\mathcal{G}m_{\text{pert}} \left(\frac{1}{\|\mathbf{r} - \mathbf{r}_{\text{pert}}\|} - \frac{\mathbf{r} \cdot \mathbf{r}_{\text{pert}}}{\|\mathbf{r}_{\text{pert}}\|^3} \right), \tag{3.20}$$

where $\mathbf{r}$ and $\mathbf{r}_{\text{pert}}$ are the *astrocentric* position vectors of the particle and the perturber, respectively.

After expanding Equation (3.20) in power series of ratios $\|\mathbf{r}\| / \|\mathbf{r}_{\text{pert}}\|$ up to the second order, the double-averaging over the angles (both the mean longitude of the perturber and the mean longitude of the particle) is performed. In the process, the variables are transformed to the osculating orbital elements. (The perturber's orbital plane is chosen to be the reference plane, with respect to which the particle's inclination is measured.)

The averaging can be performed either by straightforward integration over the angles (see, e.g. Broucke 2003), or by application of the normalization methods described in Sects. 2.6 and 2.7, e.g., the von Zeipel method, as accomplished by

Kozai (1962). To the given (quadrupole) order of the perturbation theory, the resulting double-averaged Hamiltonian will be the same, whatever approach is chosen, and is given by

$$\langle \mathcal{H}_{\text{interaction}} \rangle \simeq -\frac{\mathcal{G}m_{\text{pert}}a^2}{8a_{\text{pert}}^3}\left[2+3e^2-3(1-e^2+5e^2\sin^2\omega)\sin^2 i\right], \tag{3.21}$$

where ω is the particle's argument of pericenter. Of course, all the orbital elements of the particle's orbit in this formula are the transformed (*averaged*) ones (though the notations are the same as for the original osculating elements).

From expression (3.21), it immediately follows that there exist three independent integrals of motion. First of all, the Hamiltonian $\langle \mathcal{H}_{\text{interaction}} \rangle$ is time independent; thus, it is an integral. Besides, $\langle \mathcal{H}_{\text{interaction}} \rangle$ is independent of the mean longitude l and the longitude of ascending node Ω; therefore, the conjugate Delaunay momenta $L = [\mathcal{G}(m_0 + m_{\text{pert}})a]^{1/2}$ and $H = L(1-e^2)^{1/2}\cos i$ (see definitions (2.15)) are also integrals. We find that our three-degree-of-freedom averaged system has three integrals and thus is completely integrable.

Note that the Delaunay momentum $G = L(1-e^2)^{1/2}$ is not conserved; thus, the eccentricity varies secularly, and so does the inclination; these variations are coupled due to the conservation of H.

The three integrals can be rewritten in the classical form:

$$c_0 \equiv a = \text{const}, \tag{3.22}$$

$$c_1 \equiv (1-e^2)\cos^2 i = \text{const}, \tag{3.23}$$

$$c_2 \equiv e^2\left(\frac{2}{5}-\sin^2 i\sin^2\omega\right) = \text{const} \tag{3.24}$$

(Kozai 1962; Lidov 1961). The expression for c_2 is derived from the equalities $\langle \mathcal{H}_{\text{interaction}} \rangle = \text{const}$ and $H = \text{const}$.

Expressed in terms of the Delaunay variables (see Sect. 2.4), the Hamiltonian $\langle \mathcal{H}_{\text{interaction}} \rangle$ takes the form

$$\langle \mathcal{H}_{\text{interaction}} \rangle = -\frac{\mathcal{G}m_{\text{pert}}a^2}{8a_{\text{pert}}^3}\left[5+3\frac{H^2}{L^2}-6\frac{G^2}{L^2}-15\left(1-\frac{G^2}{L^2}-\frac{H^2}{G^2}+\frac{H^2}{L^2}\right)\sin^2\omega\right]. \tag{3.25}$$

This is the *Lidov-Kozai Hamiltonian*, expressed explicitly in canonical variables (Malhotra 2012). (In literature on the subject, it is more customary to find the Hamiltonian expressed in orbital elements, as presented in Equation (3.21); then, to derive the corresponding equations of motion one must rewrite the Hamiltonian in canonical variables first.)

The corresponding Hamiltonian equations are given by

$$\dot{G} = -\frac{\partial \mathcal{H}}{\partial \omega} = -\frac{15\mathcal{G}m_{\text{pert}}a^2}{8a_{\text{pert}}^3} e^2 \sin^2 i \sin 2\omega \,, \tag{3.26}$$

$$\dot{\omega} = \frac{\partial \mathcal{H}}{\partial G} = \frac{3\mathcal{G}m_{\text{pert}}a^2}{4a_{\text{pert}}^3 G} \left[2\frac{G^2}{L^2} + 5\left(\frac{H^2}{G^2} - \frac{G^2}{L^2} \right) \sin^2 \omega \right], \tag{3.27}$$

$$\dot{\Omega} = \frac{\partial \mathcal{H}}{\partial H} = -\frac{3\mathcal{G}m_{\text{pert}}a^2}{4a_{\text{pert}}^3} \frac{H}{L^2} \left[1 - 5\left(1 - \frac{L^2}{G^2} \right) \sin^2 \omega \right]. \tag{3.28}$$

The exact LK-resonance takes place, if $\dot{\omega} = 0$. From Equation (3.27) it follows that, apart from some limiting situations, the condition is satisfied at $\omega = \pm\pi/2$ and $G = (5H^2L^2/3)^{1/4}$. Thus, the LK-resonance center is situated at $\omega = \pm\pi/2$, $e = [1-(5c_1/3)^{1/2}]^{1/2}$, $i = \arccos(3c_1/5)^{1/4}$. This stationary solution exists if $c_1 \leq 3/5$. Accordingly, the *critical inclination*, above which the LK-resonance exists, is given by $i_{\text{crit}} \approx 39.2°$.

3.2.2 Equations and Constants of Motion

We still consider the motion of a massless particle in the framework of the R3BP. The perturber's orbit is set to be circular of radius a_{pert}; its plane defines the reference plane. Let us write down the particle's equations of secular motion in the Keplerian elements (a, e, i, ω, Ω). Though designated in the same way as the ordinary osculating Keplerian elements, it is implied that they are *mean*, representing the time averages on the timescales of the orbital periods of the particle and the perturber.

In the double-averaged Equations (3.26), (3.27) and (3.28), one may transform the Delaunay variables to the Keplerian elements, and, thus, obtain the equations of motion in the elements. Alternatively, averaging Equations (3.7), (3.8), (3.9), (3.10) and (3.11) with respect to the perturber's mean anomaly (see Broucke 2003; Lidov 1961), and returning to non-normalized time t, one gets the same resulting equations:

$$\frac{\mathrm{d}a}{\mathrm{d}t} = 0, \tag{3.29}$$

$$\frac{\mathrm{d}e}{\mathrm{d}t} = \frac{15}{8} \frac{n_{\text{pert}}^2}{n} e(1-e^2)^{1/2} \sin^2 i \sin 2\omega, \tag{3.30}$$

$$\frac{\mathrm{d}i}{\mathrm{d}t} = -\frac{15}{16} \frac{n_{\text{pert}}^2}{n} e^2(1-e^2)^{-1/2} \sin 2i \sin 2\omega, \tag{3.31}$$

$$\frac{\mathrm{d}\omega}{\mathrm{d}t} = \frac{3}{8}\frac{n_{\mathrm{pert}}^2}{n}(1-e^2)^{-1/2}[(5\cos^2 i - 1 + e^2) + 5(1-e^2-\cos^2 i)\cos\omega], \tag{3.32}$$

$$\frac{\mathrm{d}\Omega}{\mathrm{d}t} = \frac{3}{8}\frac{n_{\mathrm{pert}}^2}{n}\cos i(1-e^2)^{-1/2}[5e^2\cos 2\omega - 3e^2 - 2], \tag{3.33}$$

where n_{pert} is the mean motion of the perturbing body.

These equations of motion in the elements are nothing but the Lagrange equations (see Murray and Dermott 1999) defined by the double-averaged perturbing function. The equations of motion in the elements $(a, e, i, \omega, \Omega)$ in the double-averaged R3BP are considered in a number of papers; see, e.g., Innanen et al. (1997), Carruba et al. (2002), and Tamayo et al. (2013). Corrections to the first two papers are given in Carruba et al. (2003).

The single-averaged problem (described by Equations (3.7), (3.8), (3.9), (3.10) and (3.11)) has a *cylindrical symmetry* with respect to the z axis: the perturber's mean anomaly M_{pert} is present in the equations only through the difference $D = \Omega - M_{\mathrm{pert}}$. This entails the absence of Ω in the right-hand sides of the equations in the double-averaged problem; this absence is obvious in Equations (3.29), (3.30), (3.31), (3.32) and (3.33). The mean anomaly M is also eliminated from the right-hand sides, due to the averaging. Only three elements (e, i, and ω) remain present.

We see that equations (3.30), (3.31), and (3.32) form a self-contained closed system of equations, the semimajor axis a being constant. Once they are solved, the longitude of the ascending node Ω can be immediately found from Equation (3.33).

Though the mean anomaly M is averaged out, an equation for the mean anomaly at epoch M_0 is still warranted. It is given by

$$\frac{\mathrm{d}M_0}{\mathrm{d}t} = -\frac{1}{8}\mathcal{G}m_{\mathrm{pert}}\frac{n_{\mathrm{pert}}^2}{n}[(3e^2+7)(3\cos^2 i - 1) + 15(1+e^2)\sin^2 i\cos^2\omega]. \tag{3.34}$$

It can be used to define an approximate mean anomaly, $M = M_0 + nt$, if needed. The formula for M is so simple only because $a = \text{const}$ and $n = \text{const}$ here. Note that the semimajor axis a is constant both in the single-averaged and double-averaged problems.

Equations (3.30)–(3.31) give an integral:

$$c_1 = (1-e^2)\cos^2 i, \tag{3.35}$$

which is essentially the z component of the angular momentum squared. Obviously, $0 \le c_1 \le 1$. Besides, the constancy of (3.35) means that (1) the secular variations of e and i are coupled in anti-phase if $0 \le i \le \pi/2$ (in particular, if i decreases tending to zero, $i \to 0$, then e increases, $e \to (1-c_1)^{1/2}$), and (2) the variations of e and i are coupled in phase if $\pi/2 \le i \le \pi$ (in particular, if i increases tending to π, $i \to \pi$, then e increases as well, $e \to (1-c_1)^{1/2}$).

The averaged perturbing function (or, the averaged interaction potential, see Equation (3.21)) is constant, because it does not contain time explicitly. Simplifying Equation (3.21) by using Equation (3.35), one has one more non-trivial integral:

$$c_2 = e^2 \left(\frac{2}{5} - \sin^2 i \sin^2 \omega \right). \tag{3.36}$$

Quite obviously, $-3/5 \le c_2 \le -2/5$ (because $0 \le (\sin i \sin \omega)^2 \le 1$).

The conserved semimajor axis a, integral c_1, and integral c_2 form a set of three integrals of the double-averaged problem; thus, this averaged problem, which has three degrees of freedom, is completely integrable.

Recall that the single-averaged problem is non-integrable (as discussed in Sect. 3.1), as the original non-averaged one.

3.2.3 *Classification of Orbits*

A straightforward analysis of analytical expressions for c_1 and c_2, performed by Lidov (1961), allowed him to locate the domains of possible motion in the (c_1, c_2) plane.

In Fig. 3.1, it is the "triangle" ABEDA. The classification of dynamical regimes, according to location in this triangle in the (c_1, c_2) plane, is discussed in a number of works, in particular, see Lidov (1961) and Broucke (2003).

Inside the triangle, the vertical line $c_2 = 0$ separates two basic types of motion: (1) at $c_2 < 0$ the orbits have the argument of pericenter librating; (2) at $c_2 > 0$ the

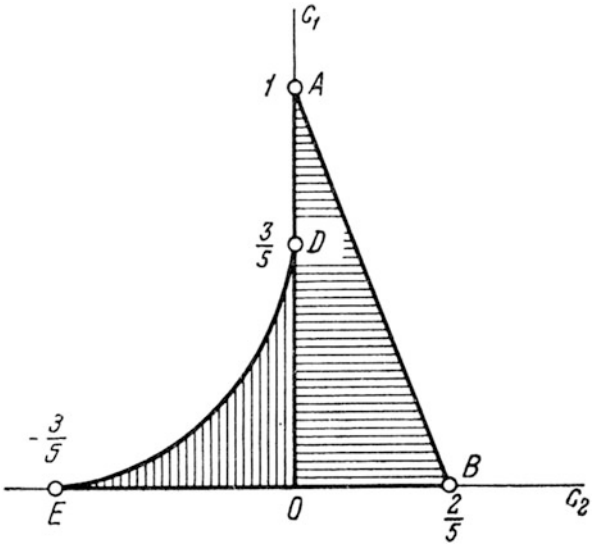

Fig. 3.1 The domains of possible values of constants c_1 and c_2 (Figure 1 from Lidov 1961)

orbits have the argument of pericenter circulating.[3] In case (1), the libration of ω takes place around either $\pi/2$ or $3\pi/2$. The librating orbits exist only if $0 \le c_1 \le 3/5$. In case (2), the circulating orbits exist in the whole interval $0 \le c_1 \le 1$.

The triangular region ABEDA in Fig. 3.1 has three corners (A, B, E) and two other important boundary points more (D and 0, i.e., the zero point). The corner points A, B, and E have the following dynamical meaning.

Point A ($c_1 = 1$, $c_2 = 0$) corresponds to the circular equatorial orbit ($e = 0$, $\sin i = 0$).

Point B ($c_1 = 0$, $c_2 = \frac{2}{5}$) corresponds to the rectilinear orbits ($e = 1$) with an arbitrary inclination and $\sin\omega = 0$.

Point E ($c_1 = 0$, $c_2 = -\frac{3}{5}$) corresponds to the polar orbits ($\cos i = 0$) with an arbitrary eccentricity and ω such that $e^2(5\sin^2\omega - 2) = 3$. At $e = 1$ one has a rectilinear orbit with $\sin\omega = \pm 1$.

The points D and 0 have the following dynamical meaning.

Point D ($c_1 = \frac{3}{5}$, $c_2 = 0$) corresponds to the circular ($e = 0$) orbits with a *critical inclination*. The critical inclination is defined by the equation $\cos^2 i = \frac{3}{5}$; therefore, $i_{\text{crit}} \approx 39.23°$.[4] The point D is a bifurcation point (that is why the inclination is called critical): on decreasing the values of c_1, the orbits with librating pericenter (those with $c_2 < 0$) emerge just at this point, at $c_1 = \frac{3}{5}$. In other words, the *LK-resonance* becomes possible.

Point 0 ($c_1 = c_2 = 0$) corresponds to the orbits of the following three kinds:

1. circular ($e = 0$) polar ($\cos i = 0$) orbits with arbitrary ω;
2. elliptic (e arbitrary) polar ($\cos i = 0$) orbits with $\sin^2\omega = \frac{2}{5}$;
3. inclined (i arbitrary) rectilinear ($e = 1$) orbits with $\sin^2 i \sin^2\omega = \frac{2}{5}$.

The boundary segments AB, BE, ED, and DA of the triangle ABEDA have the following dynamical meaning.

Segment AB corresponds to the orbits such that $2c_1 + 5c_2 = 2$. Taking c_1 and c_2 from Equations (3.35) and (3.36), one has

$$(5e^2\sin^2\omega + 2 - 2e^2)\sin^2 i = 0. \tag{3.37}$$

The first factor is zero only at point B, where $e = 1$ and $\sin\omega = 0$ simultaneously. Thus, apart from point B, the whole segment is defined by the second factor in Equation (3.37), which is zero at the inclinations $i = 0$ and $i = \pi$. The corresponding orbits are the equatorial planar orbits, with eccentricity $e = (1 - c_1)^{1/2}$; these orbits are precessing, namely, ω increases.

[3] The vertical line $c_2 = 0$ is analogous, in such a way, to the separatrix of the nonlinear mathematical pendulum: it separates the regimes of librations and circulations of an angle.

[4] Note that this value is the critical inclination in the considered model. If the problem is non-hierarchical (say, as in a real asteroid–Jupiter–Sun system), or the body which the particle orbits is oblate (say, as in a real satellite–planet–Sun system), the critical inclinations would be different.

Interval BE corresponds to the orbits such that $c_1 = 0$. This condition corresponds either to the polar ($\cos i = 0$) or to the rectilinear ($e = 1$) orbits.

Curve ED corresponds to the orbits such that the elements e and i are constant.[5] The constant values are related by the equation $e^2 = 1 - \frac{5}{2}\cos^2 i$; whereas $\omega = \pm\pi/2$. These equilibrium solutions correspond to the centers of the LK-resonance.

Interval DA ($c_2 = 0$, $3/5 < c_1 < 1$) corresponds to the orbits such that $e = 0$, i.e., to the circular orbits.

Interval 0D ($c_2 = 0$, $c_1 < 3/5$) corresponds to the separatrix solutions,[6] separating the domains of librating and circulating arguments of pericenter. On the separatrices, the eccentricity e tends either to zero or away from it. For these orbits, the relation $\sin^2 i \sin^2 \omega = \frac{2}{5}$ holds.

The orbits inclined above the critical value $i_{\rm crit} = \arccos(3/5)^{1/2}$ may suffer large eccentricity variations, especially large if an orbit is close to the separatrix of the LK-resonance. The reason is that the LK-resonance is present in the phase space if $i > i_{\rm crit}$. In case of the 90°-inclination the eccentricity always tends to unity, no matter what is its initial value; thus, the pericentric distance tends to zero, and such (polar) orbits are practically short-lived.

What is more, the value $\arccos(3/5)^{1/2} \approx 39°$ for the critical inclination $i_{\rm crit}$ is valid only in the limit $a/a_{\rm pert} \to 0$ (where a and $a_{\rm pert}$ are the semimajor axes of the particle and the perturber, respectively). As soon as, in any real problem, $a/a_{\rm pert}$ is not zero, $i_{\rm crit}$ is less than the classical value. The critical inclination diminishes with increasing $a/a_{\rm pert}$. This was shown already by Kozai (1962) both numerically and analytically: e.g., if $a/a_{\rm pert} = 0.5$ then $i_{\rm crit} \approx 32°$, as follows from figure 1 in Kozai (1962).

If $c_1 = (1-e^2)^{1/2}\cos i$ is close to unity, the particle's eccentricity and inclination suffer only small variations. Large variations become possible only if $c_1 < 3/5$, because the LK-resonance is then possible.

If the system is in LK-resonance, the secular e and i vary periodically; the maximum eccentricity is achieved at $i = 0$, and the maximum inclination at $e = 0$. The maximum values of eccentricity and inclination obtainable during these variations depend on the value of c_1. For instance, $e_{\rm max} = 0.87$, 0.98, and $i_{\rm max} = 60°$, 78°, if $c_1 = 0.5$, 0.2, respectively (Kozai 2012). For the main-belt asteroids, the periods of such variations are typically of the order of a few thousand years; on this reason, the secular variations cannot be detected directly for this kind of objects; they are studied numerically (by numerical integrations) and analytically.

[5] Note that when we speak here on the constancy of any element, the long-term (average) behaviour in the double-averaged problem is implied. In the single-averaged problem (and, of course, in the original non-averaged problem), the solution oscillates around the mean values given by the solution of the double-averaged problem.

[6] The analogous well-known separatrix of the mathematical pendulum is illustrated in Fig. 4.5.

3.2.4 The Lidov-Kozai Diagrams

Using the LK integrals c_1 and c_2, one can visualize patterns of the secular dynamics by constructing suitable diagrams, representing contour plots of the solutions (level curves of the Hamiltonian). Examples of such diagrams were provided already by Kozai (1962) and Lidov (1963b).

In particular, Kozai (1962) proposed a convenient technique to analyze the qualitative properties of the secular effects: he constructed phase portraits, characterizing the secular evolution of the eccentricity and the argument of pericenter for various initial conditions. Taking into account that the corresponding phase trajectories lie on the level curves of the LK-Hamiltonian, the trajectories can be drawn without integration of the motion equations. The topology of the phase portraits depends essentially on the norm of the vertical component of the particle's orbital angular momentum.

As we know already from the preceding subsection, at its certain value, a bifurcation occurs: whereas for the norm's greater values the argument of pericenter always circulates, for its smaller values an equilibrium point appears, accompanied with the trajectories (around the point), corresponding to libration of the argument of pericenter. This libration island is nothing but the famous *Lidov-Kozai resonance*.

The level curves in the (ω, e) plane are constructed using the relation

$$c_2(\omega, e, c_1) = e^2 \left[\frac{2}{5} - \left(1 - \frac{c_1}{1-e^2}\right) \sin^2 \omega \right] = \text{const}, \tag{3.38}$$

easily derivable from expressions (3.35) and (3.36). Solving the equation $c_2(\omega, e, c_1) = \text{const}$ on a set of various values of constant c_2 (subject to the inequality $-3/5 \leq c_2 \leq -2/5$), one can visualize the global dynamical behaviour of the system by constructing the corresponding curves in the (ω, e) plane, for one and the same value of c_1.

Using such plots, Kozai (1962) represented graphically the secular dynamics of two asteroids, (1036) Ganymed and (1373) Cincinnati. Ganymed is a NEO (Near-Earth Object) belonging to the Amor group, and Cincinnati is an outer main-belt asteroid. Orbital data for them are presented in Table 7.1; note high values of the inclination and eccentricity. According to the contour plots built by Kozai, (1373) Cincinnati is inside the LK-resonance, whereas (1036) Ganymed is not.

A vivid example (a strictly model one) of a pronounced LK-resonant pattern in the (ω, x) plane, where $x = 1 - e^2$, is given in Fig. 3.2, for $c_1 = (1 - e^2)\cos^2 i = 0.25$. Such contour plots are extensively used now in studies of various astrophysical systems, in particular, in exoplanetary studies. In Fig. 3.3, the contour plot for the same value of c_1 as in Fig. 3.2 is shown as built by Holman et al. (1997) to describe possible secular dynamics of an exoplanet orbiting one of the components of the double star 16 Cyg AB. In Fig. 3.3, a curve given by a direct numerical integration of the non-averaged equations of motion is superimposed on the contour plot. The initial conditions for this integration were chosen to be near the separatrix of the

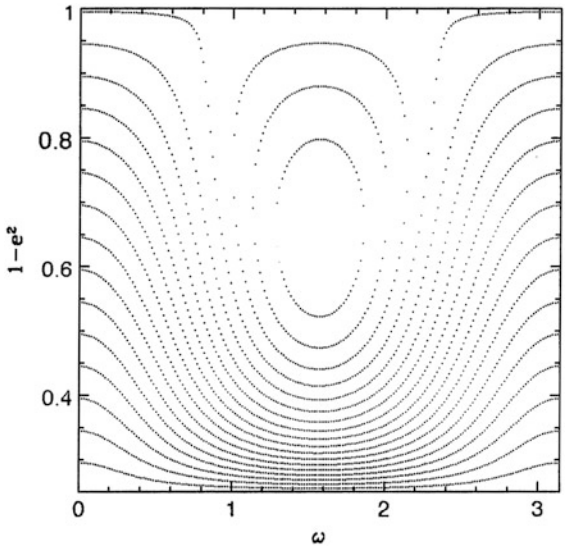

Fig. 3.2 Integral curves at $c_1 = 0.25$ (Figure 3 from Malhotra (2012). With permission from UNESCO-Encyclopedia of Life Support Systems (EOLSS). ©UNESCO-Encyclopedia of Life Support Systems (EOLSS))

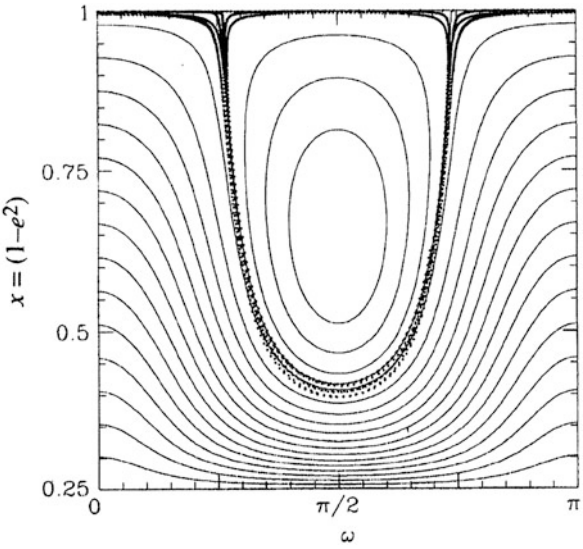

Fig. 3.3 Integral curves at $c_1 = 0.25$, with the chaotic separatrix superimposed; see text for details (Figure 3 from Holman et al. (1997). With permission from Nature Publishing Group)

LK-resonance; therefore, the motion is chaotic and the resulting curve on the graph is irregular. Details on the possible dynamics of planet 16 Cyg Bb are given in Sect. 8.3.

Sometimes, instead of using the Cartesian frame (ω, e) (or, say, (ω, x)), it is more convenient to present the level curves in the polar coordinates, e (or x) as the radial one, and ω as the angular one, thus setting $e\cos\omega$ and $e\sin\omega$ as the Cartesian axes (see, e.g., Broucke 2003; Prokhorenko 2002a,b). We will provide examples of such diagrams further on, when discussing applications.

3.2.5 *The Solution in the Jacobi Elliptic Functions*

The integration of the averaged equations of motion by quadrature requires application of elliptic functions. Already in 1962 Kozai demonstrated that the solution could be found via Weierstrass elliptic functions. In 1968, a partial solution for all required elements except Ω, i.e., for elements e, i, and ω (with the initial condition $\omega_0 = 0, \pm\pi/2$), was explicitly expressed in the Jacobi elliptic functions by Lidov's disciple Yu. F. Gordeeva (1968). The task was completed by Vashkovyak (1999) and Kinoshita and Nakai (1999, 2007), who gave the full explicit elegant solution in the Jacobi elliptic functions.

In this section, we describe how this general solution is obtained, according to Kinoshita and Nakai (2007). This general solution is valid for any initial values of the eccentricity, inclination, and argument of pericenter of the perturbed particle.

In terms of the Delaunay variables (2.15), the averaged Hamiltonian, as we know from Sect. 3.2.1, is a function of three Delaunay momenta and only one angle, ω:

$$\mathcal{H} = \mathcal{H}(L, G, H, \omega), \tag{3.39}$$

see Equation (3.25). Momenta L and H are constant, but G is not. Integral (3.23) has the form

$$c_1 = (H/L)^2 = (1 - e^2)\cos^2 i. \tag{3.40}$$

In what follows, it is used as a parameter. The non-indexed elements a, e, etc., refer to the test particle, as usual.

Kinoshita and Nakai (2007) take the averaged Hamiltonian in the form

$$\mathcal{H} = \beta[(2 + 3e^2)(3\cos^2 i - 1) + 15e^2 \sin^2 i \cos 2\omega], \tag{3.41}$$

where

$$\beta = \frac{m_{\text{pert}}}{16(m_0 + m_{\text{pert}})} n_{\text{pert}}^2 a_{\text{pert}}^2 (1 - e_{\text{pert}}^2)^{-3/2}, \tag{3.42}$$

m_0 and m_{pert} are the masses of the primary and the perturber, a_{pert} and e_{pert} are the semimajor axis and the eccentricity of the perturber, n_{pert} is its mean motion.

Integral (3.24) has the form

$$c_2 = e^2 \left(\frac{2}{5} - \sin^2 i \sin^2 \omega \right). \tag{3.43}$$

On the separatrix, $c_2 = 0$ and $\mathcal{H} = \mathcal{H}(e = 0) = 2\beta(3c_1 - 1)$. As explained in Sect. 3.2.3, the motion is libration or circulation according to the values of c_1 and c_2: if $c_1 > 3/5$, then the motion is circulation; if $c_1 < 3/5$ and $c_2 < 0$, then the motion is libration; if $c_1 < 3/5$ and $c_2 > 0$, then the motion is circulation.

Hamiltonian (3.41) is equivalent to Hamiltonian (3.21), except for the constant coefficient β, in which a dependence on the possible (small) eccentricity of the perturber is taken into account. Therefore, this Hamiltonian is valid, in some approximation, in the elliptic R3BP.[7] The remainder that is ignored in Hamiltonian (3.41) is of the order (in the ratio to the main term) $\sim e e_{\rm pert} a/a_{\rm pert}$, if $e_{\rm pert} \neq 0$, or $\sim (a/a_{\rm pert})^2$, if $e_{\rm pert} = 0$.

The equations for the variables $x \equiv 1 - e^2$ and ω are defined by Hamiltonian (3.41). They are given by

$$\frac{{\rm d}\sqrt{x}}{{\rm d}t} = \frac{15}{8}(x-1)\sin^2 i \sin 2\omega, \tag{3.44}$$

$$\frac{{\rm d}\omega}{{\rm d}t} = -\frac{3}{8}x^{-1/2}\left[x - 5\cos^2 i - 5(x - \cos^2 i)\cos 2\omega\right], \tag{3.45}$$

where the original system's time τ has been normalized, making it unitless: $t = \gamma\tau$,

$$\gamma = \frac{m_{\rm pert}}{(m_0 + m_{\rm pert})}\frac{n_{\rm pert}^2}{n}(1 - e_{\rm pert}^2)^{-3/2}. \tag{3.46}$$

The solution can be found by expressing ω through c_1 and x using the energy constant (3.41), and then substituting the obtained expression for ω in Equation (3.44); thus, Equation (3.44) is reduced to

$$\frac{{\rm d}x}{{\rm d}t} = -3^{3/2}2^{-1/2}\left[(x - x_1)(x - x_2)(x - x_3)\right]^{1/2}, \tag{3.47}$$

where

$$x_1 = \frac{\alpha}{6} - \frac{1}{6}(\alpha^2 - 60c_1), \tag{3.48}$$

$$x_2 = \frac{\alpha}{6} + \frac{1}{6}(\alpha^2 - 60c_1), \tag{3.49}$$

[7] Note that the weakly elliptic R3BP was considered already in the pioneering work by Lidov (1961).

$$x_3 = \frac{1}{4}\left[5 + 5c_1 - \frac{5c_1}{x_0} - x_0 - 5(1-x_0)\left(1 - \frac{c_1}{x_0}\right)\cos 2\omega_0\right], \tag{3.50}$$

$$\alpha = \frac{1}{2}\left[5 + 5c_1 + \frac{5c_1}{x_0} + x_0 + 5(1-x_0)\left(1 - \frac{c_1}{x_0}\right)\cos 2\omega_0\right], \tag{3.51}$$

where $x_0 = 1-e_0^2$; $c_1 = (1-e_0^2)\cos^2 i_0$; the zero subscripts designate that the initial value of a variable is taken: e_0, i_0, and ω_0 are the initial values of the eccentricity, inclination, and argument of pericenter.

Once a solution for x is found, that for ω is given by

$$\sin^2\omega = \frac{2x(x_3 - x)}{5(1-x)(x-c_1)} \tag{3.52}$$

or

$$\cos^2\omega = \frac{3(x_2 - x)(x-x_1)}{5(1-x)(x-c_1)}. \tag{3.53}$$

Defining the quantities

$$x_{\min} = \min\{x_1, x_2, x_3\}, \tag{3.54}$$

$$x_{\text{med}} = \text{med}\{x_1, x_2, x_3\}, \tag{3.55}$$

$$x_{\max} = \max\{x_1, x_2, x_3\} \tag{3.56}$$

(as in Gordeeva 1968), one can write down an explicit formula for x, following from Equation (3.47) by definition of the Jacobi elliptic function cn:

$$x = x_{\text{med}} + (x_{\min} - x_{\text{med}})\,\text{cn}^2\theta, \tag{3.57}$$

where

$$\theta = \frac{2}{\pi}\left(f_\omega t + \omega_0 + \frac{\pi}{2}\right)K(k), \tag{3.58}$$

$$f_\omega = \frac{3^{3/2}\pi}{2^{5/2}K(k)}(x_{\max} - x_{\min})^{1/2}\gamma. \tag{3.59}$$

Here $K(k)$ is the complete elliptic integral of the first kind:

$$K(k) = \int_0^{\pi/2} \frac{\mathrm{d}\theta}{(1 - k^2\sin^2\theta)^{1/2}}, \tag{3.60}$$

and modulus k is given by

$$k^2 = \frac{x_{\text{med}} - x_{\text{min}}}{x_{\text{max}} - x_{\text{min}}}. \tag{3.61}$$

From the solution, the minimum and maximum values of the eccentricity can be determined, which correspond, respectively, to the maximum and minimum values of the inclination. These extrema are given by

$$e_{\text{min}} = (1 - x_{\text{med}})^{1/2}, \quad e_{\text{max}} = (1 - x_{\text{min}})^{1/2}, \tag{3.62}$$

$$i_{\text{min}} = \arccos(c_1/x_{\text{min}})^{1/2}, \quad i_{\text{max}} = \arccos(c_1/x_{\text{med}})^{1/2}. \tag{3.63}$$

The elements e, i, and ω vary with the periods

$$P_e = \frac{\pi}{f_\omega}, \quad P_i = \frac{\pi}{f_\omega}, \quad P_\omega = \frac{2\pi}{f_\omega}, \tag{3.64}$$

where f_ω is given by formula (3.59).

These are nothing but the *periods of LK-oscillations*.

The equation for the longitude of the ascending node is given by a Hamilton's equation, defined by Hamiltonian (3.41) expressed through the Delaunay variables. The resulting equation is analogous to Equation (3.28), and has the form

$$\frac{\mathrm{d}\Omega}{\mathrm{d}t} = \frac{3}{4}\gamma c_1^{1/2}\left(1 - 2\frac{x_3 - c_1}{x - c_1}\right), \tag{3.65}$$

Its solution can be directly expressed through complete and incomplete elliptic integrals of the first and third kinds (Vashkovyak 1999), or it can be found in the form of a Fourier expansion (Kinoshita and Nakai 1999). In the latter approach, one has

$$\Omega = f_\Omega t + \Omega_0 + \sum_{m=1}^{\infty} b_m \sin 2m\omega, \tag{3.66}$$

where

$$f_\Omega = \frac{3}{4}\gamma c_1^{1/2}\left(1 - 2\frac{x_3 - c_1}{x_{\text{max}} - c_1}\right) - \varepsilon\Lambda_0(\xi, k) f_\omega, \tag{3.67}$$

and

$$\Lambda_0(\xi, k) = \frac{2}{\pi}(EF(\xi, k') + KE(\xi, k') - KF(\xi, k')) \tag{3.68}$$

is the Heuman Lambda function; $F(\xi, k')$ is the incomplete elliptic integral of the first kind; E and $E(\xi, k')$ are, respectively, the complete and incomplete elliptic integral of the second kind; $k' = \left(1 - k^2\right)^{1/2}$, and

$$\sin \xi = \left(\frac{x_{\max} - x_{\min}}{x_{\max} - c_1} \right)^{1/2}. \tag{3.69}$$

The quantity ε is given by

$$\varepsilon = \begin{cases} 1, & \text{if } 0 < i < \frac{\pi}{2}, \\ -1, & \text{if } \frac{\pi}{2} < i < \pi. \end{cases} \tag{3.70}$$

The Fourier coefficients are given by

$$b_m = -\frac{2(-q)^m}{m(1 - q^{2m})} \sinh \frac{m\pi F(\xi, k')}{K}, \tag{3.71}$$

where the Jacobi nome, according to Abramowitz and Stegun (1970), is given by

$$q = \exp\left(-\pi \frac{K'(k)}{K(k)} \right), \tag{3.72}$$

$$K'(k) = \int_0^{\pi/2} \frac{\mathrm{d}\theta}{[1 - (1 - k^2) \sin^2 \theta]^{1/2}}. \tag{3.73}$$

The period of LK-oscillations of the argument of ascending node is given by

$$P_\Omega = \frac{2\pi}{f_\Omega}, \tag{3.74}$$

where f_Ω is given by formula (3.67).

This completes the analytical solution in the version of Kinoshita and Nakai (2007).

Kinoshita and Nakai (2007) checked its accuracy by a comparison with direct numerical integrations of the original non-averaged equations of motion in the elliptic R3BP. The integrations were performed for an asteroid and a planetary satellite, namely, a main-belt asteroid (3040) Kozai and an irregular Neptunian satellite Laomedeia NXII. (3040) Kozai orbits the Sun and is perturbed mostly by Jupiter, whereas Laomedeia orbits Neptune and is perturbed mostly by the Sun.

Orbital data on (3040) Kozai and Laomedeia are given in Tables 7.1 and 5.4, respectively. (3040) Kozai is a main-belt asteroid with the current orbital elements $a = 1.84$ AU, $e = 0.20$, $i = 47°$. Laomedeia, also called Neptune XII or S/2002 N3, is a prograde irregular satellite of Neptune with $a = 24$ mln km, $e = 0.40$, $i = 34°$. Thus, the orbits of both objects are strongly inclined with respect to the reference

planes, defined by the orbital planes of the perturbers. (In fact, the reference planes, from which the inclinations are measured, are approximately the ecliptic plane in both cases.)

As follows from both the analytical and numerical solutions, (3040) Kozai resides in LK-resonance (ω librates), and Laomedeia does not (ω circulates), though it is close to LK-resonance.

The osculating elements were used in both integrations, but the results were averaged to provide a better comparison with the analytical solution. Nevertheless, in both cases, the averaging-out of the short-periodic terms induced differences between the osculating and mean elements, thus causing inevitable differences between the analytical and numerical solutions. This factor dominated the (small) inaccuracy of the analytical solution in case of Laomedeia.

In case of (3040) Kozai, another circumstance produced a greater inaccuracy. Indeed, the ratio of the semimajor axes of the asteroid and the perturber are not at all small for (3040) Kozai: $a/a_{\text{Jupiter}} \simeq 0.35$, and on this reason the neglected terms in the perturbing function are not small enough. Therefore, the analytical solution is not so much accurate, as in case of Laomedeia. For Laomedeia, the ratio of the semimajor axes of the satellite and the perturber is ≈ 70 times less; therefore, the neglected terms are indeed small.

Despite these inevitable consequences of approximation, the analytical solution provides a rather good qualitative description of the dynamical behaviour for both (3040) Kozai and Laomedeia.

3.3 LKE-Preventing Phenomena

Let us discuss how the LKE can be suppressed in various dynamical situations. Indeed, if an additional perturbation dominates over the LK-term in the Hamiltonian of the motion, then the LKE may disappear (Lidov 1963b; Morbidelli 2002).

Such suppression explains, e.g., the stable existence of the *regular* Uranian satellites, considered already in 1963 by Lidov (1963b). The suppression "agent" here is the satellites' orbital precession forced by the Uranus oblateness and the moons' mutual perturbations.

The LKE suppression phenomena may have various origins. An example is presented by the stability of our Solar system notwithstanding the *Galactic tide*. Indeed, the planetary orbits in the Solar system are subject to long-term perturbations due to the Galactic tide; and, being inclined by $\sim 60^\circ$ with respect to the Galactic plane, the Solar system might seem to be vulnerable to destabilization by the LKE. In reality, luckily for us, the LKE is suppressed by the precession of the planetary orbits due to their mutual perturbations. Only at the distance of about a hundred thousand AU (the radius of the Oort cloud) from the Sun the LKE becomes operational (Matese and Whitman 1992; Morbidelli 2002).

Another vivid example is provided by the fact that in some compact binaries, subject to a perturbation from a distant companion star, the LKE-suppressing mechanism is due to the relativistic precession of the inner binary (Fabrycky and Tremaine 2007).

Thus, an assessment of the LKE effectiveness in real celestial-mechanical systems often needs taking into account possible interfering perturbations, – sometimes rather weak, because the LKE acts on long timescales.

To assess the LKE effectiveness analytically, the most easy way is to compare the timescale of the LKE in a given problem with the period of the orbital precession caused by a suppressing mechanism that may be in action. There is a number of suppressing mechanisms. The most ubiquitous are: (1) gravitational perturbations from other (than the secondary) bodies orbiting the primary; (2) primary's or tertiary's non-sphericity implying non-zero quadrupole moments; (3) general relativity. The second one subdivides in two important factors: (2*a*) oblateness of the primary's figure, due to rotation; (2*b*) tidal interaction between the primary and the tertiary, implying deformations of their figures. Historically, it is just case 2*a* that was first recovered as a mechanism suppressing the LKE (Lidov 1963b).

Of course, all the suppressing mechanisms may act in concert. Generally, the perturbations are small, that is why the total rate of precession of the line of apsides (the total rate of change of the longitude of pericenter) can be written as a linear sum:

$$\dot{\varpi}_{\rm sum} = \dot{\varpi}_{(1)} + \dot{\varpi}_{(2a)} + \dot{\varpi}_{(2b)} + \dot{\varpi}_{(3)}. \tag{3.75}$$

An analogous formula can be written for the total rate of change of the longitude of ascending node. For our purposes (comparison of the precession rates) it is enough to consider the rates of change of the longitude of pericenter.

3.3.1 Perturbations by Additional Orbiting Bodies

Suppose one has a system demonstrating the LKE; then, if an additional orbiting body with non-zero mass is introduced in the system, the precession caused by the perturbation from the introduced body may suppress the otherwise present LKE. The suppression of this kind is possible in N-body systems with $N \geq 4$.

A famous example of the orbital precession caused by orbiting bodies is given by the orbital precession of Mercury. The rate of Mercury's apsidal precession due to the perturbations from all other planets is equal to $532''$ per century; the general relativity adds $43''$ per century, whereas the Solar oblateness and tidal effects are negligible (see, e.g. Clemence 1947). Thus, in Mercury's precession, the contribution of the planetary perturbations is the dominant one.

The basic expressions describing the secular evolution in the circumbinary and circumcomponent planar cases are given in Chap. 8. The formula for the precession

rate is individual in each of these two cases. It is given by

$$\dot{\varpi} = \frac{3\pi}{2} \frac{m_0 m_1}{(m_0 + m_1)^{3/2}} \frac{a_\mathrm{b}^2}{a^{7/2}} \left(1 + \frac{3}{2} e_\mathrm{b}^2\right) \tag{3.76}$$

in the circumbinary case (here the barycentric frame is adopted), and by

$$\dot{\varpi} = \frac{3\pi}{2} \frac{m_1}{m_0^{1/2}} \frac{a^{3/2}}{a_\mathrm{b}^3} \left(1 - e_\mathrm{b}^2\right)^{-3/2} \tag{3.77}$$

in the circumcomponent case (here an astrocentric frame is adopted); m_0 and m_1 are the masses of the binary components (we set $m_0 \geq m_1$), a_b is the binary semimajor axis, e_b is the binary eccentricity, a is the semimajor axis of the particle's orbit. The masses are measured in Solar units, distances in astronomical units (AU), and time in years. Thus, the gravitational constant $\mathcal{G}$ is equal to $4\pi^2$. The formulas are derived in the hierarchical setting of the restricted three-body problem.

Formula (3.77) can be applied to estimate the rate of Mercury's precession caused by other planets; it provides rather good results for each planet contribution (which are listed, e.g., in Clemence 1947), except for the contribution of Venus, because the configuration Sun–Mercury–Venus is rather far from hierarchical.

3.3.2 *Primary's Oblateness*

Let us consider the orbital precession of a satellite orbiting an oblate massive central body (a planet). In our analysis we follow an approach adopted by Roy (1988) and Murray and Dermott (1999). First of all, let us introduce orthogonal and spherical coordinate frames for a satellite of a planet, as depicted in Fig. 3.4: x, y, z are the Cartesian coordinates; r, λ, φ are the spherical coordinates: satellite's radial distance, longitude, and latitude, respectively.

The axisymmetric gravitational potential of a non-spherical body (a primary) is given by the expression

$$\mathcal{V} = -\frac{\mathcal{G} m_\mathrm{p}}{r} \left[1 - \sum_{i=2}^{\infty} J_i \left(\frac{R_\mathrm{p}}{r}\right)^i P_i(\sin\varphi)\right], \tag{3.78}$$

where $\mathcal{G}$ is the gravitational constant, m_p and R_p are the mass and mean radius of the planet, P_i are the Legendre polynomials of degree i, J_i are the so-called zonal harmonics, which characterize the oblateness. The quantities J_i are unitless. Odd harmonics J_{2j+1} ($j = 1, 2, \ldots$) are generally small for planets (though the Earth has $J_3 \approx 1.5 J_4$). The first two even harmonics J_2 and J_4, measured for the planets of our Solar system, are listed in Table 5.1.

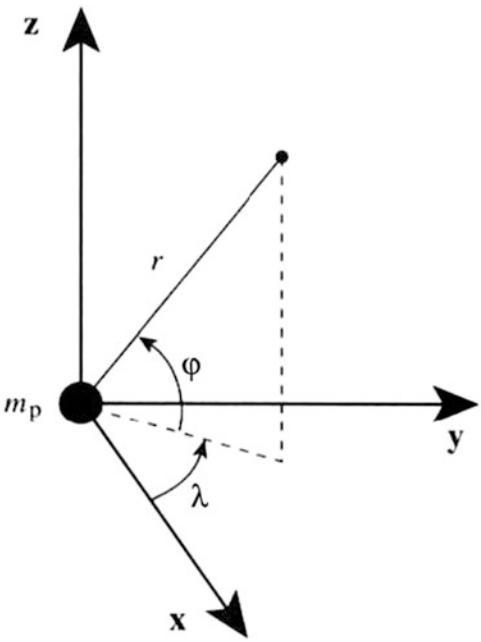

Fig. 3.4 The Cartesian and spherical coordinate frames for a planetary satellite: x, y, z are the Cartesian coordinates, and r, λ, φ are the radial distance, longitude, and latitude of the satellite (Figure 6.6 from Murray and Dermott (1999). With permission from Cambridge University Press)

For a satellite moving in an orbit with semimajor axis a around a spherical central body ($J_i = 0, i = 2, 3, \ldots$), potential (3.78) reduces to the potential of a gravitating point, and the mean motion is given by the expression $n_0 = (\mathcal{G}m_\mathrm{p}/a^3)^{1/2}$, following from Kepler's third law. For a satellite moving around a planet with $J_2 \neq 0$ (an oblate planet), the mean motion is given by

$$n = n_0 \left[1 + \frac{3}{2} J_2 \left(\frac{R_\mathrm{p}}{a} \right)^2 \right]^{1/2} \tag{3.79}$$

(Murray and Dermott 1999). Thus, generally, $n > n_0$ for a fixed a.

Let us adopt an approximate expression for the perturbing function, truncated at the lowest order of expansion in R_p/r:

$$\mathcal{R} = -\frac{\mathcal{G}m_\mathrm{p}}{r} \cdot J_2 \left(\frac{R_\mathrm{p}}{r} \right)^2 P_2(\sin\varphi), \tag{3.80}$$

where

$$P_2(\sin\varphi) = \frac{1}{2}(3\sin^2\varphi - 1). \tag{3.81}$$

Considering Fig. 3.4, one has

$$\begin{pmatrix} x \\ y \\ z \end{pmatrix} = r \begin{pmatrix} \cos\Omega\cos(\omega+f) - \sin\Omega\sin(\omega+f)\cos i \\ \sin\Omega\cos(\omega+f) + \cos\Omega\sin(\omega+f)\cos i \\ \sin(\omega+f)\sin i \end{pmatrix}, \tag{3.82}$$

where i is the inclination, f is the true anomaly, and ω is the argument of pericenter. Therefore, the latitude φ is given by the equation

$$\sin\varphi = \sin i \sin(f+\omega). \tag{3.83}$$

Then, one can (1) substitute $r = a(1-e^2)/(1+e\cos f)$ in $\mathcal{R}$, given by expression (3.80); (2) represent $\sin f$ and $\cos f$ as the power series in the mean anomaly M; and, finally, (3) average $\mathcal{R}$ over M ($0 \le M \le 2\pi$). This gives the averaged $\mathcal{R}$, up to the second order in e and $\sin i$ and in the lowest order of expansion in R_p/a:

$$\langle\mathcal{R}\rangle = \frac{3}{4} J_2 R_\mathrm{p}^2 n^2 (e^2 - \sin^2 i). \tag{3.84}$$

Taking the Lagrange planetary equations (provided, e.g., in Subbotin 1968, or Murray and Dermott 1999) for the longitude of pericenter ϖ and for the longitude of ascending node Ω, and using formula (3.84) for the perturbing function and formula (3.79), one has finally in the lowest order of expansion in R_p/a:

$$\dot{\varpi} = \frac{3}{2} J_2 n_0 \left(\frac{R_\mathrm{p}}{a}\right)^2, \tag{3.85}$$

$$\dot{\Omega} = -\frac{3}{2} J_2 n_0 \left(\frac{R_\mathrm{p}}{a}\right)^2. \tag{3.86}$$

We see that $\dot{\varpi} = -\dot{\Omega}$ in this approximation.

3.3.3 *Tides*

The tidal phenomena are important in tight astrophysical binaries, such as tight binary stars, binary asteroids, star–planet systems, first of all the systems with "hot Jupiters". For the tight stellar binaries also a mutual mass transport may play a significant role, apart from the tidal deformations. For a star–planet system, a general picture of the tidal precession is given by Ragozzine and Wolf (2009), for a binary asteroid by Perets and Naoz (2009) and Fang and Margot (2012). An introduction to the celestial-mechanical theory of tides, including definitions of the

effective dissipation parameter Q, the Love number, etc., can be found in Murray and Dermott (1999). The tidal precession is a complex phenomenon, that is why we consider only basic results here, appropriate for exoplanetary applications discussed in the book further on.

In a star–planet system, the tidal bulge raised on the planet is always aligned almost exactly towards the star: the lag angle $\sim 1/Q$, where the effective dissipation parameter $Q \gg 1$ (e.g., for the giant planets one has $Q \gtrsim 10^5$). On the other hand, the height of the bulge strongly varies with the "star–planet" distance, sharply falling with increasing the distance. This inhibits any description based on a single constant value of the J_2 harmonic. For the tidal bulge raised on the star, the situation is the same; however, the bulge on the planet is most important for the precession. Taking into account the dependence of the bulge size on the "star–planet" distance allows one to estimate the tidal precession rate with a satisfactory accuracy (Ragozzine and Wolf 2009; Sterne 1939).

According to Sterne (1939) and Eggleton and Kiseleva-Eggleton (2001), the rate of the apsidal precession due to the tidal bulges, raised on both the primary and the secondary ("star" and "planet"), is given by

$$\dot{\varpi}_{\rm tidal} = \dot{\varpi}_{\rm tidal,\,0} + \dot{\varpi}_{\rm tidal,\,1} =$$

$$= \frac{15}{2} k_{2,0} \left(\frac{R_0}{a}\right)^5 \frac{m_1}{m_0} f(e) n + \frac{15}{2} k_{2,1} \left(\frac{R_1}{a}\right)^5 \frac{m_0}{m_1} f(e) n, \tag{3.87}$$

where

$$f(e) = (1-e^2)^{-5} \left(1 + \frac{3}{2}e^2 + \frac{1}{8}e^4\right) \approx 1 + \frac{13}{2}e^2 + \frac{181}{8}e^4 + \ldots. \tag{3.88}$$

The subscripts 0 and 1 refer to the primary and the secondary, respectively; m, R, and k_2, are the masses, mean radii, and Love numbers of the bodies; n, a, and e are, respectively, the mean motion, size and eccentricity of the binary.

The Love number k_2 is a unitless quantity that characterizes an effect of an applied potential on the gravity field of the planetary interiors. It can be calculated, given the interior density distribution (e.g. Sterne 1939). If the density rises towards the center, i.e., the mass is concentrated to the core, then the k_2 values are small ($k_2 \ll 1$). In this case, the gravity field is mostly unaffected by the masses located closer to the surface of the object. This is typical for the stars: e.g., the Solar-type stars have $k_2 \sim 0.03$ (Claret 1995).

Planets, especially rocky planets, are different in this respect: their gravity fields are strongly affected by the distortions of mass distributions near their surfaces. The weaker the object is condensed towards its center, the greater is its k_2. A spherical object with uniform density has $k_2 = 3/2$; this is the maximum value for the Love number. The gas giants Jupiter and Saturn have $k_2 \simeq 0.49$ and 0.32, respectively, indicating the presence of relatively massive cores.

The size of the tidal bulge is directly proportional to the mass of the body that raises the tide, and the tide on the planet is dominant in determining the precession rate. The ratio of the rates induced by the secondary and the primary is given by the formula

$$\frac{\dot{\varpi}_{\mathrm{tidal},\,1}}{\dot{\varpi}_{\mathrm{tidal},0}} = \frac{k_{2,\,1}}{k_{2,0}} \left(\frac{R_1}{R_0}\right)^5 \left(\frac{m_0}{m_1}\right)^2. \tag{3.89}$$

For a typical "star–planet" system this ratio is estimated to be $\simeq 100$ (Ragozzine and Wolf 2009).

3.3.4 General Relativity

Einstein's explanation of the "anomalous" precession of the pericenter of Mercury's orbit was one of the major successes of the theory of general relativity. As in the case with Mercury, general relativity can contribute much to the apsidal precession of exoplanets, because many of them (especially, the "hot Jupiters") move in tight orbits. The rate of the relativistic precession (in radians per planetary orbital revolution) is directly proportional to the ratio of the gravitational radius R_{g} of the parent star and the pericentric distance q of the planetary orbit. Einstein's formula for the apsidal precession rate is

$$\dot{\varpi}_{\mathrm{GR}} = \frac{6\pi\mathcal{G}m_0}{c^2 a(1-e^2)} = \frac{6\pi R_{\mathrm{g}}}{a(1-e^2)} = \frac{6\pi R_{\mathrm{g}}}{q(1+e)}, \tag{3.90}$$

where $\mathcal{G}$ is the gravitational constant, m_0 and $R_{\mathrm{g}} = \mathcal{G}m_0 c^{-2}$ are the mass and the gravitational radius of the body around which the particle orbits, c is the speed of light, e is the eccentricity of the planetary orbit (see, e.g. Clemence 1947).

As follows from Equation (3.90), the smaller is the pericentric distance $q = a(1-e)$, the more rapid is the precession. For "hot Jupiters", $\dot{\varpi}_{\mathrm{GR}}$ can reach rather large values, exceeding the value for Mercury by orders of magnitude.

The rate of Mercury's apsidal precession due to the perturbations from all other planets is equal to $532''$ per century; the general relativity adds $43''$ per century (see, e.g. Clemence 1947). The planetary contributions to the orbital precession of Mercury (the exact values, as cited in Clemence (1947), and the values given by Heppenheimer's formula (3.77)) are listed in Table 3.1. Note that the only serious differences of the analytical estimates from the exact numerical ones take place for Venus and Earth, because the hierarchical approximation, in which formula (3.77) is valid, breaks down for them.

Table 3.1 Contributions to the advance of the perihelion of Mercury, in arcseconds per century

Planet	Exact value (Clemence 1947)	Value given by Eq. (3.77)
Venus	277.86 ± 0.68	151.42
Earth	90.04 ± 0.08	70.34
Mars	2.54	2.164
Jupiter	158.58	159.27
Saturn	7.30 ± 0.01	7.707
Uranus	0.141	0.1455
Neptune	0.042	0.0446

3.3.5 The Orbital Precession in Total

The four giant planets of our Solar system rotate very fast, all of them have periods of axial rotation of the order of 10 h. On this reason their figures are significantly oblate, especially in the cases of Jupiter and Saturn; see Table 5.1. The rotational oblateness of the planets dominates over other effects determining the apsidal precession of the satellites of these planets.

The "hot Jupiters", apart from the fact that they move close to their parent stars, have another serious distinction from the giant planets of our Solar system: their axial rotation is drastically slower. At close distances to the parent stars, the tidal slowing-down of the rotation leads to its synchronization with the orbital motion. In the synchronous state, one and the same side of a planet is exposed to the parent star, analogously to the synchronous state of the Moon with respect to the Earth. (Note that the tidal effect sharply rises with decreasing the orbital semimajor axis.) Thus, the rotational oblateness of the parent planets contributes little to the total apsidal precession of such planets. Instead, the tides dominate over all other contributions. *Very hot Jupiters* (the giant exoplanets with semimajor axes $a \lesssim 0.025\,\mathrm{AU} \sim 6$ stellar radii) are expected to have the tides on the planets that induce the orbital precession with the rate up to $\approx 20°$ per year, as in the case of WASP-12b (Ragozzine and Wolf 2009).

For the hot Jupiters, the general relativity is the second most important contribution to the apsidal precession. Generally, it evokes the precession by an order of magnitude slower than that evoked by the planetary tidal bulge (Ragozzine and Wolf 2009).

If the contributions to the total precession rate are all small, the total rate can be calculated as a linear sum of the individual contributions, see Equation (3.75). Comparing the period of the total precessional effect with the period of LK-oscillations, one can judge whether the LKE is suppressed or not.

3.4 Critical Radii

Studying the motion of Jovian satellites, already in 1805 Laplace realized that the choice of a convenient reference plane for defining the orbital inclination of a satellite depends on the size of its orbit (Laplace 1805): near the planet, where perturbations caused by the planet's oblateness dominate, it is pertinent to measure the inclinations with respect to the planet's equatorial plane, whereas far from the planet, where Solar perturbations dominate,—with respect to the planet's ecliptic plane. In intermediate situations, the reference plane is defined as the plane orthogonal to the axis of precession of a satellite's orbit (e.g., Tremaine et al. 2009). Indeed, if a satellite has the orbital semimajor axis large enough, the precession of its orbit is mostly controlled by the Sun; conversely, if the orbit size is small, it is controlled by the parent planet's oblateness.

Thus, for the planetary satellites in the low orbits where the perturbations caused by the host planet's oblateness dominate, the Laplace plane is approximately the planet's equatorial plane; for the planetary satellites in the high orbits where the Solar perturbations dominate, the Laplace plane is approximately the planet's ecliptic plane. The transition between these two limits takes place at a radial distance from the planet known as the *Laplace radius*:

$$r_{\mathrm{L}} = \left[J_2 \frac{m_{\mathrm{p}}}{m_{\mathrm{Sun}}} R_{\mathrm{p}}^2 a_{\mathrm{p}}^3 \left(1 - e_{\mathrm{p}}^2\right)^{3/2} \right]^{1/5} \tag{3.91}$$

(Goldreich 1966; Tamayo et al. 2013; Tremaine et al. 2009), where m_{p} and m_{Sun} are the masses of the planet and the Sun, R_{p}, J_2, a_{p}, and e_{p} are the planet's mean radius, second zonal harmonic coefficient, orbital semimajor axis and eccentricity, respectively.

In fact, as follows from its definition, the Laplace radius plays the role of the *critical radius* above which the LKE becomes operational. The notion of critical radius is easily generalized to the cases of other possible perturbations. Indeed, the period of precession induced by any of the known LKE-preventing mechanisms (considered in the preceding section) increases with the distance from the system center (because the cause of precession becomes farther from the particle), whereas the period of LK-oscillations, on the contrary, diminishes (because the perturber becomes closer). Therefore, in each case, a distance from the center exists where the periods become equal. This is just the *critical radius*, above which the LKE becomes operational.

Formula (3.59) gives the exact frequency of LK-oscillations. An approximate frequency is given by the constant factor of Equation (3.32). Equating the LK-frequency sequentially to the frequencies of precession induced by the primary's non-sphericity, tides, or general relativity, one gets equations defining the critical

radius $a = a_{\rm crit}$ in each case:

$$\dot{\omega}_{\rm LK}(a) \approx \dot{\omega}_{\rm obl}(a), \tag{3.92}$$

$$\dot{\omega}_{\rm LK}(a) \approx \dot{\omega}_{\rm tidal}(a), \tag{3.93}$$

$$\dot{\omega}_{\rm LK}(a) \approx \dot{\omega}_{\rm GR}(a). \tag{3.94}$$

Based on Equation (3.92), formula (3.91) can be derived by retaining the leading terms in formulas (3.85) and (3.86), calculating the difference $\dot{\omega} = \dot{\varpi} - \dot{\Omega}$, and equating $\dot{\omega}$ to the LK-frequency, given by Equation (3.32). The same result is achieved by equating $\dot{\varpi}$ to that given by formula (3.77) (note that the unit system should be adjusted in the latter case).

Equations (3.93) and (3.94) define the critical radii for the cases of tidal and general-relativistic perturbations, respectively. To obtain explicit relations, the frequencies given by formulas (3.87) and (3.90) should be substituted in the right-hand sides of the equations.

Apart from the listed perturbations, the LKE can be quenched by perturbations from inner (with respect to the test particle) bodies orbiting the primary. Their effect can be incorporated in formula (3.91) by modifying the value of J_2:

$$J_2' = J_2 + \frac{1}{2R_{\rm p}^2} \sum_{i=1}^{n} \frac{m_i}{m_{\rm p}} a_i^2, \tag{3.95}$$

and by substituting J_2' instead of J_2 in formula (3.91) (Tremaine et al. 2009). Here it is supposed that n satellites move in circular equatorial orbits around the planet; their orbits are much smaller in size than that of the test particle. The physical sense of the formula is that the perturbing satellites are "spread" by averaging along the orbits, thus enhancing the physical oblateness of the central body.

Finishing this Chapter, let us consider a remarkable example of a system where the LKE is suppressed *twice*. This is the satellite system of Pluto. In fact, Pluto and Charon form a central binary of this system: the mass ratio of Charon and Pluto is rather large, $m_1/m_0 = 0.12$. The inclination of the binary's plane, with respect to the plane of the binary's orbit around the Sun, is equal to 119°; therefore, the question immediately arises: why the system is not destabilized by the LKE induced by the Sun? Or, maybe, we observe it in the process of destabilization?

The answer is that the binary's orbital precession induced by the Pluto–Charon tidal interaction dominates over the secular motions induced by the LKE; thus, the LKE is quenched (Michaely et al. 2015). Then, another question is immediate: what about other satellites, Styx, Nix, Kerberos and Hydra, which move in wider orbits coplanar with the central binary? For them, the tidal effect is negligible, because it sharply diminishes with increasing the distance from the system's center. The answer, in its turn, is that the LKE-quenching precession is still induced for them, but by another mechanism,—that conditioned by the non-point-mass gravitational potential of the central binary Pluto–Charon.

In the presence of a central binary, the critical orbital radius above which a satellite cannot survive, due to the LKE, can be calculated by means of formula (3.91), where J_2' is substituted instead of J_2. In formula (3.95), the original J_2 is set to zero, and it is enough to take only Charon in account, i.e., $n = 1$. On similar grounds, Michaely et al. (2015) derived the following formula, which allows one to estimate the critical semimajor axis $a_{\rm crit}$ in such systems:

$$a_{\rm crit} = \left[\frac{3m_1 m_2 \left(1 - e_1^2\right)^{3/2}}{8m_0(m_1 + m_2)\left(1 - e^2\right)^{3/2}} \left(5\cos^2 i - 1\right) \right]^{1/5} \left(a_1^3 a_2^2\right)^{1/5} , \tag{3.96}$$

where m_0 is the mass of the perturber, and $m_1 \geq m_2$ are the two masses comprising the binary orbiting the perturber; a_1 and a_2 are the semimajor axes of the "large" and "small" binaries, respectively (the large binary is formed by the perturber and the barycenter of the small binary); e_1 is the eccentricity of the large binary. The small binary is assumed to be circular, i.e., $e_2 = 0$. The semimajor axis and eccentricity of an outer massless satellite of the small binary are designated by a and e; and i is the inclination of the satellite's orbit with respect to the orbital plane of the small binary. It is assumed that the inclination of the small binary with respect to the large binary is high enough, so that the LK-resonance is potentially present.

In the Sun-perturbed Pluto–Charon system, m_0, m_1, and m_2 are, respectively, the masses of the Sun, Pluto, and Charon; a_1 and a_2 are, respectively, the semimajor axis of Pluto's orbit around the Sun and the semimajor axis of the Pluto–Charon binary; e_1 is the eccentricity of Pluto's orbit around the Sun; and $e_2 = 0$ (the Pluto–Charon binary is almost circular). Substituting the values of all these quantities in formula (3.96), one finds $a_{\rm crit} = 0.004\,\text{AU}$. As Michaely et al. (2015) found out, all satellites of the Pluto–Charon binary lie well within this limit; the most distant one, Hydra, follows an orbit whose size is by an order of magnitude less than $a_{\rm crit}$. On the other hand, the value of $a_{\rm crit}$ is still much smaller than the Hill radius of the Pluto–Charon system.

Chapter 4
The Theory Advances

. . . the integrability of the non-restricted problem under consideration is, in a way, a happy coincidence.

Lidov and Ziglin (1976)

Since the time when the Lidov-Kozai effect was discovered, a substantial and steady progress in the analytical theory of this secular effect has been observed. This Chapter is an attempt to describe the progress of the LKE concept.

First of all, let us enumerate integrable cases of the double-averaged restricted three-body problem, mostly following a classification by Vashkovyak (1984). Recall that the double-averaged elliptic R3BP has basically two integrals: the semimajor axis a of the particle and the double-averaged perturbing function $\mathcal{V}(a, e, i, \omega, \Omega)$. Seven cases are distinguishable, where an additional integral exists, rendering the problem integrable:

1. The *circular* R3BP, known to be integrable since the works by Moiseev (1945a,b). When the perturber's eccentricity $e_{\rm pert} = 0$, the third integral in form (3.23) exists.
2. The *rectilinear* R3BP ($e_{\rm pert} = 1$) is integrable, because the third integral in form (3.23) can also be obtained, upon choosing a suitable reference frame (Vashkovyak 1984).
3. The *planar elliptic* R3BP. If $\sin i = 0$, then the existence of two basic integrals $a = \text{const}$ and $\mathcal{V}(a, e, i, \omega, \Omega) = \text{const}$ is sufficient to render the problem integrable (Aksenov 1979a,b; Vashkovyak 1982).
4. The *close-to-coorbital* particle–perturber configuration of the R3BP ($a \approx a_{\rm pert}$, $e \approx 0$, $\sin i \approx 0$), considered in Lidov and Ziglin (1974).
5. The *orthogonal apsidal orbits* of the spatial elliptic R3BP ($i = \pi/2$, $\sin \Omega = 0$). In this case, $i = \text{const}$ and $\Omega = \text{const}$ (Vashkovyak 1984).
6. The *Hill problem*, in which the size of the particle's orbit is much smaller than the size of the perturber's orbit. The third integral in form (3.23) exists, as first revealed by Lidov (1961).

I. I. Shevchenko, *The Lidov-Kozai Effect – Applications in Exoplanet Research and Dynamical Astronomy*, Astrophysics and Space Science Library 441,
DOI 10.1007/978-3-319-43522-0_4

7. The *inverse Hill problem*—the case opposite to case (6), namely, the size of the particle's orbit is much greater than the size of the perturber's orbit. This case corresponds to the *circumbinary* motion of the particle. The third integral has form $e = 0$ (Ziglin 1975).

Unlike cases (1)–(5), cases (6) and (7) are limit cases, as the integrability takes place in the limits $a/a_{\rm pert} \to 0$ and $a/a_{\rm pert} \to \infty$, respectively.

4.1 LKE in the Non-hierarchical Circular R3BP

Already in 1962, Kozai, using a numerical approach, calculated critical inclinations in the circular R3BP (Kozai 1962). It turned out that the critical inclination monotonously decreases with increasing the ratio $\alpha = a/a_{\rm pert}$ of the semimajor axes of the particle and the perturber. For example, at $\alpha = 0.5$ the critical inclination is equal to only $\approx 32°$, and it formally drops to zero at $\alpha \approx 0.88$. Recall that at $\alpha = 0$ it is equal to $\approx 39°$.

The critical inclinations for both inner and outer variants of the problem (i.e., for a perturbed particle either in inner or outer orbits with respect to a perturber) in the whole possible range of α ($0 < \alpha < \infty$) were calculated by Krasinsky (1972, 1974), who used a special representation of the perturbing function. The importance of the LKE at any α, in the dynamics of short-period comets and similar highly-eccentric objects, in presence of several perturbers, was revealed in a numerical study by Kozai (1979). The numerical integration was accomplished taking into account four giant planets as perturbers, the α parameter for the objects studied thus taking values in broad ranges.

A complete theory of the LKE at any α in the framework of the circular R3BP was developed by Vashkovyak (1981a). When there is no restriction on the ratio of the semimajor axes of the body and perturber, serious analytical difficulties for application of the averaging procedure appear due to possible crossings of orbits. Detailed studies of these difficulties and the ways to overcome them were performed by Lidov and Ziglin (1974), Vashkovyak (1981b), and Gronchi and Milani (1998, 1999).

In the works by Quinn et al. (1990) (on the quasi-parabolic comets arriving from the Oort cloud), Bailey et al. (1992) (on the LKE-maintained production of most of the sungrazing comets), and Thomas and Morbidelli (1996) (on the long-period comets) the basic inferences of Kozai (1979) were confirmed and the numerical-experimental techniques raised to a new level.

A semi-analytical approach was proposed by Thomas and Morbidelli (1996) to describe the LKE in the motion of long-period comets in the outer Solar system in presence of several perturbers (the giant planets). In their scheme, the averaging of the Hamiltonian is performed numerically, using the Gauss–Kronrod algorithm, suitable to deal with singular functions. This is necessary to allow for planet-crossings, though the double integral in the averaging procedure is

always well-defined (see notes below). By constructing semi-analytical contour-level diagrams in the planes "$e \sin\omega$–$e\cos\omega$" and "ω–X",[1] where $X = (1-e^2)^{1/2}$, Thomas and Morbidelli (1996) were able to describe the LKE-associated global secular dynamics in the outer Solar system, thus demonstrating that the structure of the phase space in presence of several perturbers is considerably modified, first of all due to possibilities of crossings between the cometary and planetary orbits. The location, emergence and death of the ω-libration islands, governed by the behaviour of the curves of node-crossings of the orbits of planets, were described; the Thomas–Morbidelli diagrams are reviewed in more detail below in Chap. 7.

In the outer Solar system (the case of inner perturbers), as certified by the theory of Thomas and Morbidelli (1996), the particle's argument of perihelion ω may librate not only when the initial inclination is high, but also when it is quite moderate. At small inclinations, ω may librate around stable equilibria located at $\omega = 0°$ and $\omega = 180°$. If one increases the initial inclination, at $i \sim 30°$ these equilibria loose stability, and the classical equilibria emerge at $\omega = 90°$ and $\omega = 270°$.

In the main belt of asteroids, the LKE pumps the eccentricity of highly-inclined objects to values at which they become planet-crossing, and this leads to their close encounters with planets. Thus, the LKE causes the main belt depletion at high inclinations. In the Kuiper belt, on the contrary, quite a number of objects are observed to be at high inclinations. This is because the LK-mechanism (due to the presence of inner perturbers) in this region does not pump eccentricities to planet-crossing values, if the initial eccentricities are small or moderate, at any inclinations (Thomas and Morbidelli 1996). On this reason, the inclined close-to-circular and moderately elongated orbits are not destabilized.

A similar LK-mechanism (with inner perturbers) affects the motion of a minor body in the inner Solar system, if the body moves in a moderately inclined orbit slightly exterior to the orbit of Venus or the Earth (Michel and Thomas 1996). Indeed, if the body's inclination is not high enough, then the perturbations from Venus or the Earth dominate over the Jovian perturbations, and, thus, the LK-dynamics is similar to that present in the Kuiper belt. Conversely, at high enough inclinations, the Jovian perturbations dominate over the perturbations from Venus and the Earth, and the LK-dynamics is similar to that in the main belt. As demonstrated by Michel and Thomas (1996), the LKE may serve as a mechanism for the temporary protection from close encounters with perturbing planets.

A close encounter of an asteroid with a planet corresponds to a mathematical singularity in the equations of motion, where zeros ($\mathbf{r} - \mathbf{r}_i = 0$) appear in denominators. This makes analytical averaging impossible. However, Gronchi and Milani (1998, 1999) demonstrated that the averaging integrals of the Hamiltonian remain well-defined. Therefore, the numerical averaging can be used to describe the secular dynamics, even when crossings of the planetary orbits are possible.

[1] The choice of the "ω–X" plane is especially appropriate for studies of a highly-eccentric motion; see Sects. 6.2 and 7.3.

Gronchi and Milani (1999) identified regular islands of LK-libration for *Centaurs* (the objects intermediate, in the orbit size, between the main-belt asteroids and the TNOs) in the LK-diagrams; the islands are defined by the curves of node-crossings of the planetary orbits. Inside the islands the Centaurs are protected from encounters with the planets.

More applications of the LKE theory in the dynamics of asteroids, TNOs, and Centaurs are discussed in Chap. 7.

4.2 LKE in Presence of Mean Motion Resonances

The role of *mean motion resonances* in the dynamics of asteroids became evident already in the nineteenth century, since the discovery of the *Kirkwood gaps* in the asteroid belt (Kirkwood 1867). The gaps correspond to simple rational commensurabilities between the orbital periods of Jupiter and asteroids, such as 3/1, 4/1, 7/3, etc. The consequent discovery of Trojans (the asteroids in 1/1 resonance with Jupiter) and Hildas (the asteroids in 3/2 resonance with Jupiter) showed that resonances may as well correspond to stable asteroidal groups, in contrast to the unstable objects in the Kirkwood gaps. However, notwithstanding the instability, some asteroids were identified to move inside the gaps.

Resonance signifies that a *resonant* (also named *critical*) angle, or argument, is in libration. For a *mean motion resonance*, the resonant argument is defined as a linear combination (with integer coefficients) of mean longitudes and other angular elements of the orbital motion of two (or more) gravitating bodies. These combinations are not arbitrary, but are subject to restrictions imposed by the D'Alembert rules. The formulation of the D'Alembert rules is given in section 1.9.3 in Morbidelli (2002); in a general setting, functions with the D'Alembert properties (characteristics) and their transformations are considered in Kholshevnikov (1997, 2001) and Ferraz-Mello (2007).

The classical averaging procedure that was used to derive the LKE solution fails in presence of a mean motion resonance, because one more (apart from the argument of pericenter) *slow* angle appears, namely, the resonant argument corresponding to the resonance. This is the main difficulty with applying perturbation methods in presence of a resonance.

Giacaglia (1968, 1969) adapted the von Zeipel method (described here in Sect. 2.6) to analyze the secular motion of a particle (asteroid) in mean motion resonances with an outer perturber (Jupiter), in the framework of the circular R3BP. The perturber's mass was assumed to be much smaller than that of the primary. Giacaglia (1969) showed that two classical integrals of motion (the semimajor axis a and $c_1 = (1 - e^2)\cos^2 i$, see Equation (3.23)) remain valid in the resonant case, if the motion takes place at the resonance center. If the amplitude of libration is small, these two integrals can be used as approximations.

In 1985, Kozai developed a simpler semi-analytical approach to deal with the secular dynamics of asteroids in mean motion resonances (Kozai 1985). For the sake of analytical simplicity, he assumed that an asteroid is in *exact* mean motion resonance, i.e., the amplitude of resonant librations is zero; the object is at the resonance center. (However, all major perturbing planets were taken into account, assumed to move in circular coplanar orbits.) Using this approach, Kozai performed a survey (on the subject of possible LK-oscillations) of the main-belt asteroids, known to year 1985 to reside in 1/1, 4/3, 3/2, 2/1, and 3/1 mean motion resonances with Jupiter. Only a few objects were found to be in ω-libration. In particular, no such Jovian Trojan (1/1 resonance) was identified, though Jovian Trojans are numerous and highly-inclined. Only in the 3/1 resonance three ω-librators were found; these are (292) Ludovica, (329) Svea, and (1379) Lomonosowa (see Table 7.1). Thus, it was shown that the LKE in presence of mean motion resonances exists in the motion of real bodies.

Perhaps the most famous case when the LKE interacts with a low-order mean motion resonance is the case of a "former planet", the Kuiper belt object Pluto (Williams and Benson 1971). It is well known that it resides in the 2/3 mean motion resonance with Neptune. The presence of this resonance results, in particular, in that the LKE becomes operational at low eccentricities, thus making Pluto an ω-librator and maintaining its survivability, though the pericentric distance of Pluto is smaller than the radius of Neptune's orbit (see Sect. 7.4.1 for details).

A number of asteroids residing both in the LK-resonance and in other secular or mean-motion resonances were identified by Michel and Thomas (1996). For example, (1981) Midas is locked both in the LK-resonance and in the ν_{16} secular resonance (the resonant argument for the ν_{16} resonance is defined as $\Omega - \Omega_6$, where Ω and Ω_6 are the longitudes of ascending nodes of an asteroid and Saturn, respectively).

In more detail, the LKE in presence of mean motion and secular resonances will be considered in Chap. 7, in application to the dynamics of asteroids and TNOs.

4.3 The "eccentric LK-mechanism"

In the circular R3BP, as follows from formula (3.23) for the c_1 integral of motion, the sign of $\cos i$ is conserved, whatever parameters and initial conditions of the motion are. In other words, a prograde orbit ($0 \leq i < \pi/2$) cannot become retrograde ($\pi/2 < i \leq \pi$), and vice versa.

In the elliptic R3BP, such transitions are prohibited only in the *quadrupole model* (the simplest one), in which the Hamiltonian expansion is truncated at the second order of the ratio of the semimajor axes of the particle and the perturber, i.e., in the *quadrupole approximation*. However, if higher-order terms are taken into account, the prograde-retrograde (and vice versa) transitions, called *orbital flips* (flips from prograde to retrograde motion or vice versa), become possible, already in the *octupole approximation*. The flips arise due to the so-called *eccentric*

LK-mechanism, discovered by Naoz et al. (2011) and Katz et al. (2011) by considering an advanced approximation of the Lidov-Kozai Hamiltonian based on retaining the octupole terms.

Let us underline that the double-averaged elliptic R3BP in the octupole and higher approximations is non-integrable, because the particle's longitude of the ascending node is no more absent in the Hamiltonian and, therefore, the vertical component of the particle's angular momentum is not conserved.

The mechanism of Naoz et al. (2011) and Katz et al. (2011) corresponds to the octupole-order regime with "low-eccentricity, high-inclination" initial conditions for the orbital flips. It turns out that this mechanism is not the only one that provides flips. Li et al. (2014b) pointed out the possibility of flips in another octupole-order regime with "high-eccentricity, low-inclination" initial conditions; in this latter case, the flip takes place as the orbital plane turns over its major axis.

We will consider these theories and their applications to exoplanetary dynamics in Chap. 8. Before doing this, it is pertinent to consider the LKE in a more general framework, namely, in the framework of the double-averaged *general* (or, *non-restricted*) 3BP. In the general problem, all three masses are non-zero.

4.4 The Stellar Three-Body Problem in Octupole Approximation

With a purpose to describe the secular evolution of triple stellar systems, the Lidov-Kozai theory was generalized to the case of the general 3BP already in the 1960s and 1970s of the twentieth century (Harrington 1968, 1969; Lidov and Ziglin 1976). As Harrington (1968) showed, the double-averaged Hill approximation of the stellar problem (a strongly hierarchical three-body system) is integrable. A qualitative analysis of the secular evolution in the stellar problem was undertaken by Lidov and Ziglin (1976). Phase portraits presented in their paper clearly demonstrate the LKE features.

The secular motion in the general 3BP was studied by Harrington (1968, 1969), Lidov and Ziglin (1976), Ferrer and Osácar (1994), and other authors. The analytical studies concentrated on the *inner* case, in which the dynamics of the inner binary is investigated. In the quadrupole approximation, Lidov and Ziglin (1976) and Ferrer and Osácar (1994) considered the motion of the inner binary and performed a complete classification of the orbits and bifurcations. Note that Ferrer and Osácar (1994) used the Hori–Deprit method to normalize the Hamiltonian; this method is described in Sect. 2.7. Other authors mostly preferred the von Zeipel method, which is more widespread, due to historical reasons, but technically less convenient.

In this section, we consider the hierarchical stellar three-body problem: three material points of non-zero masses move in orbits such that the distance between two of them is always much less than the distance separating any of these two points from the third one.

4.4.1 Triple Stars in the Galaxy

Triple stellar systems are ubiquitous in the Galaxy. As a rough estimate, a third of all binaries have one or even more gravitationally bound companions; about 10 % of all binaries with the primary of Solar type belong to triples, while more than 60 % of all Solar-type stars in the Galaxy are in binaries (Duquennoy and Mayor 1991; Tokovinin 1997). What is more, obviously there is an observational bias against identification of secondaries and a much greater observational bias against identification of distant tertiaries (in hierarchical systems); therefore, the actual percentages of binaries and triples are even greater.

Especially representative and important are triples in dense stellar clusters (and, most prominently, in the cores of globular clusters) on evident dynamical reasons: primordial binaries permanently interact to form triples, short-lived or long-lived (McMillan et al. 1991).

As follows from observations, the tighter is a binary, the greater is the chance that it has a third companion; thus, almost all *tight binaries* are, in fact, members of systems of multiplicity greater than two. (For rigourous statistical results see Duquennoy and Mayor 1991; Riddle et al. 2015; Tokovinin 2014; Tokovinin et al. 2006.) This might be a manifestation of the LKE: the efficiency of tides in the inner binary is very sensitive to secular LK-variations of pericentric distances, due to perturbations from the outer companion; thus, such LK-variations may lead to substantial shrinking of the inner binary (see Mazeh and Shaham 1979).

On the other hand, all existing criteria for the stability of gravitating triples certify that a triple is stable only if the third body's orbit is wider enough than the inner binary (more exactly, the third body's pericenter must be greater enough than the apocenter of the second body); see, e.g., Mardling and Aarseth (2001). Therefore, the observed triples are all *hierarchical*: the inner binary is much smaller than the outer one.

Note that long-lived non-hierarchical *choreographies* are, in principle, theoretically possible (Chenciner and Montgomery 2000; Šuvakov et al. 2013), but an exceptional fine-tuning of the initial conditions is required for such systems to appear in reality; in any case, they have never been yet observed.

4.4.2 The Hierarchical Stellar Three-Body Problem in Historical Perspective

A classical secular theory describing the long-term motion of planets in the Solar system was developed by Lagrange and Laplace in the eighteenth century. This theory is perfectly presented in the monographs by Brouwer and Clemence (1961) and Murray and Dermott (1999). As soon as the ratios of semimajor axes of the Solar system planets cannot be regarded as "small", the theory does not use the assumption of small values of $\alpha = a_1/a_2$ (the ratio of the semimajor axes of the

perturbed body and the perturber), and is valid in all orders in α. On the other hand, its validity is limited to the low-eccentric and low-inclined (with respect to the invariable plane) orbits around a dominating mass (as in the Solar system).

In such a setting, the N-body problem is called the *planetary* N-body problem; and, in particular, at $N = 3$, it is called the *planetary* 3BP, as distinctive from the *restricted* 3BP. Of course, any secular theory for a general 3BP in the limit of small eccentricities and inclinations must provide the results identical to the results of the Lagrange–Laplace classical secular theory for the planetary 3BP.

Harrington (1968, 1969), using the von Zeipel method, deduced a quadrupole-order approximation (i.e., retaining the terms up to the second order inclusive in α) of the averaged Hamiltonian in the Delaunay variables for the *hierarchical* triples with arbitrary masses, arbitrary initial eccentricities of the inner and outer binaries and arbitrary initial orientations of the orbits. The derived expression turned out to be similar to that found by Kozai (1962) in the same approximation in the restricted 3BP.

Lidov and Ziglin (1976) investigated the double-averaged general 3BP in the same (quadrupole-order) approximation and provided a classification of orbits over the full intervals of mass ratios and initial values of eccentricities and inclinations. Lidov and Ziglin (1976) called the integrability of the problem in the given approximation a "happy coincidence", because a particular angle variable (the argument of pericenter of the distant perturber) is cyclic (does not appear) in this approximation. However, it is present in the higher approximations, and the integrability fails.

Soderhjelm (1984) performed averaging of the Hamiltonian up to the octupole order (i.e., retaining the terms up to the third inclusive in α), but merely in the planar problem (in which the orbital planes of the inner and outer binaries are assumed to be coplanar). He showed that the octupole terms dominated over the quadrupole ones. Therefore, the quadrupole approximation is completely inadequate in such a case.

Marchal (1990), using averaging by the von Zeipel method, obtained the octupole-order Hamiltonian in the spatial setting of the problem. Krymolowski and Mazeh (1999), using the same method, deduced the octupole-order Hamiltonian, including additionally all terms of order $\alpha^{7/2}$, arising in the process of normalization of the Hamiltonian. Marchal (1990) kept some of these terms.

A straightforward derivation of the equations of motion in the double-averaged stellar problem was given in the octupole approximations by Ford et al. (2000) and Naoz et al. (2013a), among others. These equations are applicable in broad ranges of parameters' values and initial conditions, in particular, (1) at almost all values of the mass ratios that allow for a stable hierarchical configuration and (2) at any relative initial inclination of the third body's orbit with respect to the inner binary.

Naoz et al. (2013a) revisited the Hamiltonian formulation of the stellar problem and demonstrated how the elimination of nodes[2] in the Hamiltonian formulation

[2]By the *elimination of nodes* one implies the elimination of Delaunay variables H_i and h_i ($i = 1, 2$) in the Hamiltonian, see Jefferys and Moser (1966); H_i and h_i are defined by Equations (2.15).

of the stellar problem should be performed correctly, providing the correct form of differential equations for the secular evolution of inclinations with respect to the invariable plane.

Note that the conservation of semimajor axes is an immediate consequence of performing the double-averaging in the angles l_1 and l_2 (thus they are eliminated from the Hamiltonian and become cyclic). To prove that the semimajor axes are indeed conserved, one has to justify the averaging, but this procedure is merely heuristic. In fact, it is easy to provide examples (in the framework of the R3BP with a test particle in an outer orbit), in which the particle's semimajor axis is not conserved secularly. If moving in an orbit eccentric enough, the particle can be ejected from the system due to a chaotic diffusion (caused by the overlap of integer mean motion resonances of the particle with the central binary) in both eccentricity and semimajor axis; close encounters with the inner binary are not necessary for the disintegration of the triple (see Shevchenko 2015).

Generally, recall that there is only one non-trivial integral in the non-averaged general 3BP: the Jacobi integral, implying that the variations of the energy of the "binaries" are coupled with variations in the vertical components of their angular momenta.

4.4.3 Equations of Motion in the Jacobi Frame

Consider the motion of a hierarchical triple in the framework of the general 3BP, i.e., all three components of the triple, including the smallest one, have non-zero masses.

In contrast with the astrocentric coordinates, the so-called Jacobi coordinates allow one to represent the Hamiltonian of any system of $N + 1$ gravitating points in a rather simple way, as a sum of N two-body Keplerian Hamiltonians plus perturbations. Therefore, hereafter we use the Jacobi frame. A detailed presentation of a few-body Hamiltonian in the Jacobi frame is given, e.g., in Murray and Dermott (1999) and Malhotra (2012); only a brief outline is given here.

The Jacobi frame is introduced recursively: the coordinates of the ith body are defined with respect to the center of mass of the system of bodies $0, 1, 2, \ldots, i-1$. Thus, the coordinates of a secondary (mass m_1) are defined with respect to the primary (to the center of mass of a system consisting of a sole mass m_0); the coordinates of a third body are defined with respect to the center of mass of the primary and secondary; and so on.

Consider N massive bodies orbiting a primary (mass m_0). By $\mathbf{r}_i$ ($i = 0, 1, \ldots N$) we denote the inertial coordinates of the primary and the bodies; the partial mass $M_i \equiv \sum_{j=0}^{i} m_j$; the full mass of the system is $M_N = M_{i=N}$. The Jacobi coordinates

are defined by the recursive relations

$$\tilde{\mathbf{r}}_0 = \frac{1}{M_N}\sum_{j=0}^{N} m_j \mathbf{r}_j, \tag{4.1}$$

$$\tilde{\mathbf{r}}_{i+1} = \mathbf{r}_{i+1} - \mathbf{R}_i, \quad \mathbf{R}_i = \frac{1}{M_i}\sum_{j=0}^{i} m_j \mathbf{r}_j. \tag{4.2}$$

Thus, the motion of body $i+1$ is referred to a frame centered on a center of mass of the "preceding" i-body subsystem.

In a Hamiltonian formulation, the canonical momenta conjugate to $\tilde{\mathbf{r}}_i$ are

$$\tilde{\mathbf{p}}_i = \tilde{m}_i \frac{\mathrm{d}\tilde{\mathbf{r}}_i}{\mathrm{d}t}, \tag{4.3}$$

where

$$\tilde{m}_i = \frac{m_i M_{i-1}}{M_i}; \tag{4.4}$$

and the Hamiltonian is given by

$$\mathcal{H} = \frac{\tilde{p}_0^2}{2M_N} + \sum_{i=1}^{N} \frac{\tilde{p}_i^2}{2\tilde{m}_i} - \sum_{i=1}^{N} \frac{\mathcal{G} m_0 m_i}{\|\mathbf{r}_{i0}\|} - \sum_{0<i<j} \frac{\mathcal{G} m_i m_j}{\|\mathbf{r}_{ij}\|}, \tag{4.5}$$

where $\mathbf{r}_{i0} = \mathbf{r}_i - \mathbf{r}_0$, $\mathbf{r}_{ij} = \mathbf{r}_i - \mathbf{r}_j$.

The momentum $\tilde{\mathbf{p}}_0$ of the system's barycenter is constant; therefore, the first term in Equation (4.5) can be omitted. Then, Equation (4.5) can represented as a sum of N Keplerian Hamiltonians, $\mathcal{H}^{(i)}_{\text{Kepler}}$, and a perturbation, $\mathcal{H}_{\text{interaction}}$:

$$\mathcal{H} = \sum_{i=1}^{N} \mathcal{H}^{(i)}_{\text{Kepler}} + \mathcal{H}_{\text{interaction}}, \tag{4.6}$$

where

$$\mathcal{H}^{(i)}_{\text{Kepler}} = \frac{\tilde{p}_i^2}{2\tilde{m}_i} - \frac{\mathcal{G} m_0 m_i}{\|\tilde{\mathbf{r}}_i\|}, \tag{4.7}$$

$$\mathcal{H}_{\text{interaction}} = -\sum_{0<i<j} \frac{\mathcal{G} m_i m_j}{\|\mathbf{r}_{ij}\|} + \sum_{i=1}^{N} \left(\frac{\mathcal{G} m_0 m_i}{\|\tilde{\mathbf{r}}_i\|} - \frac{\mathcal{G} m_0 m_i}{\|\mathbf{r}_{i0}\|} \right). \tag{4.8}$$

4.4.4 The Octupole Hamiltonian of the Stellar Problem

In this subsection, we derive the equations of secular motion in the averaged hierarchical general 3BP in the *octupole approximation* using classical perturbation techniques. This derivation was performed first by Marchal (1990), followed by the works by Krymolowski and Mazeh (1999), Ford et al. (2000), and Naoz et al. (2013a), featuring various aspects of the problem. Our description is based on these sources, mostly on the works by Ford et al. (2000) and Naoz et al. (2013a).

First of all note that in real triple stellar systems, the long-term orbital behaviour is influenced by tides, effects of general relativity (if the central binary is tight), and stellar evolution (stellar mass loss and/or transfer). Hereafter we assume that these factors are absent; in other words, their timescales are much greater than the timescale of the pure secular dynamics.

A hierarchical triple is naturally decomposed into the inner binary (formed by two central masses m_0 and m_1) and an "outer binary" (formed by the outer mass m_2 and the center of mass of the inner binary, as if the two central masses were concentrated to a single point), as described in Sect. 4.4.3.

Note that, apart from this subscript system adopted in this book for the mass designations, hereafter we use subscripts "1" and "2" to distinguish between the orbital elements of the inner and outer binaries, respectively.

It should be emphasized that the numbering of the bodies reflect merely the hierarchy of the geometrical configuration of the triple. The masses are arbitrary. Thus, the derived equations of motion are valid for any mass ratios, as long as the system maintains a hierarchical configuration.

Such a decomposition is naturally described in the Jacobi frame, described in Sect. 4.4.3. Here it is illustrated in Fig. 4.1, where vector $\mathbf{r_1}$ is the position vector of m_1 with respect to m_0, and $\mathbf{r_2}$ is the position vector of m_2 with respect to the barycenter of the inner binary. In the Jacobi frame, the Hamiltonian of the triple system is given by a sum of two "Keplerian terms" and an "interaction term", see Equation (4.6).

The hierarchical constitution of a triple implies that any close approaches and encounters are absent; therefore, a perturbation theory, with the small parameter α equal to the ratio of semimajor axes of the outer body and the central binary, can be built. Hamiltonian (4.6) can be rendered the form (Harrington 1968, 1969):

$$\mathcal{H} = \frac{\mathcal{G}m_0m_1}{2a_1} + \frac{\mathcal{G}(m_0+m_1)m_2}{2a_2} + \frac{\mathcal{G}}{a_2}\sum_{j=2}^{\infty}\alpha^j M_j \left(\frac{r_1}{a_1}\right)^j \left(\frac{a_2}{r_2}\right)^{j+1} P_j(\cos\Phi), \qquad (4.9)$$

where $\mathcal{G}$ is the gravitational constant,

$$M_j = m_0m_1m_2\frac{[m_0^{j-1} - (-m_1)^{j-1}]}{(m_0+m_1)^j}, \qquad (4.10)$$

Φ is the angle between vectors $\mathbf{r}_1$ and $\mathbf{r}_2$ (see Fig. 4.1), $P_j(\cos\Phi)$ are the Legendre polynomials in $\cos\Phi$. If $m_0 \sim m_1$ (the case of the central binary of comparable

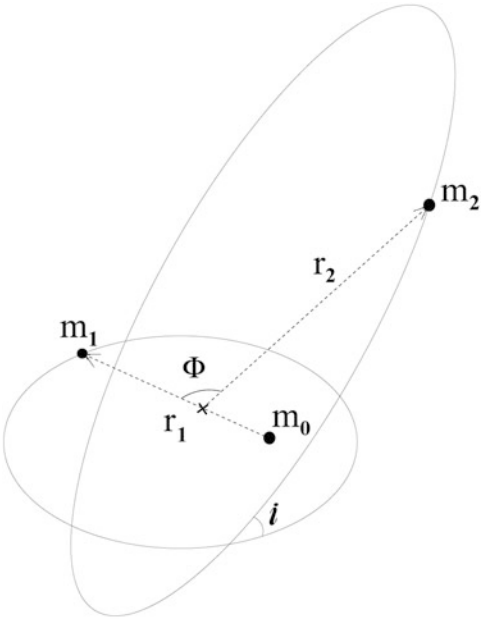

Fig. 4.1 The hierarchical triple system in the Jacobi frame (Figure 1 from Ford et al. (2000). Copyright AAS. Reproduced with permission)

masses), the terms with odd j in Hamiltonian (4.9) are relatively unimportant; in case of exact equality $m_0 = m_1$ they even vanish, as follows from formula (4.10).

In formula (4.9), the interaction term is presented in the form of a multipole expansion. Henceforth, we retain only the quadrupole terms (those with $j = 2$) and the octupole terms (those with $j = 3$); i.e., the Taylor series in α is truncated at the third order, the fourth and higher orders are ignored. Accordingly, the Hamiltonian containing the terms of the multipole expansion up to $j = 2$ inclusive is called *quadrupole*, and that containing the terms up to $j = 3$ inclusive is called *octupole*.

Let a_1 and a_2 be the osculating semimajor axes of the inner and outer binaries. The parameter $\alpha = a_1/a_2 < 1$ will serve as a small parameter of the perturbation theory. This will be justified later on by the fact that a_1 and a_2 are conserved secularly; thus, α is a constant of the secular motion.

Let e_1, e_2 and i_1, i_2 be the osculating eccentricities and inclinations of the inner and outer binaries. The Delaunay variables are defined by formulas (2.15). Thus, the set of angles is: l_1 and l_2 are the mean anomalies, g_1 and g_2 are the arguments of pericenters, h_1 and h_2 are the longitudes of ascending nodes; numbered "1" and "2" for the inner binary and the outer binary cases, respectively. The canonical momenta, conjugate to these angles, are given by

$$L_1 = \frac{m_0 m_1}{m_0 + m_1}[\mathcal{G}(m_0 + m_1)a_1]^{1/2}, \tag{4.11}$$

$$L_2 = \frac{m_2(m_0 + m_1)}{m_0 + m_1 + m_2}[\mathcal{G}(m_0 + m_1 + m_2)a_2]^{1/2}, \tag{4.12}$$

$$G_1 = L_1(1 - e_1^2)^{1/2}, \tag{4.13}$$

$$G_2 = L_2(1 - e_2^2)^{1/2}, \tag{4.14}$$

$$H_1 = G_1 \cos i_1, \tag{4.15}$$

$$H_2 = G_2 \cos i_2. \tag{4.16}$$

Canonical momenta G_1 and G_2 are nothing but the modules of the angular momenta of the inner and outer binaries, respectively, in the Jacobi frame. The *invariable plane* of the triple system is defined as the plane orthogonal to the vector of the total angular momentum of the triple, see Fig. 4.2. Let the z-axis be the direction of the total angular momentum. Therefore, H_1 and H_2 are the z-components of the angular momenta of the inner and outer binaries, as illustrated in Fig. 4.2.

In the Delaunay variables, the Hamiltonian equations of motion are given by

$$\frac{\mathrm{d}L_k}{\mathrm{d}t} = \frac{\partial \mathcal{H}}{\partial l_k}, \qquad \frac{\mathrm{d}l_k}{\mathrm{d}t} = -\frac{\partial \mathcal{H}}{\partial L_k}, \tag{4.17}$$

$$\frac{\mathrm{d}G_k}{\mathrm{d}t} = \frac{\partial \mathcal{H}}{\partial g_k}, \qquad \frac{\mathrm{d}g_k}{\mathrm{d}t} = -\frac{\partial \mathcal{H}}{\partial G_k}, \tag{4.18}$$

$$\frac{\mathrm{d}H_k}{\mathrm{d}t} = \frac{\partial \mathcal{H}}{\partial h_k}, \qquad \frac{\mathrm{d}h_k}{\mathrm{d}t} = -\frac{\partial \mathcal{H}}{\partial H_k}, \tag{4.19}$$

where $k = 1, 2$.

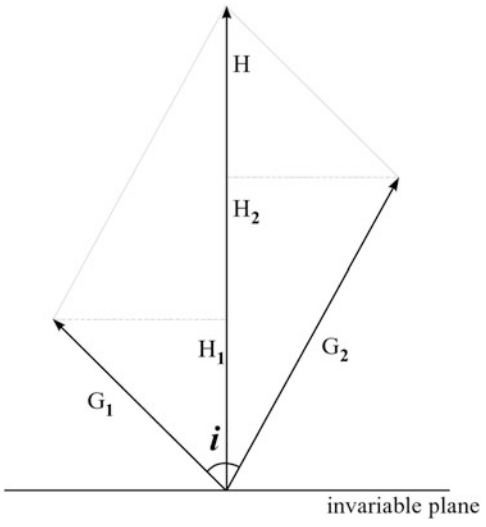

Fig. 4.2 Canonical variables G_1, G_2, H_1, H_2, and the total angular momentum vector **H** (Figure 2 from Ford et al. (2000). Copyright AAS. Reproduced with permission)

At this step, the theorem of *elimination of nodes* (Jefferys and Moser 1966) can be applied to reduce the system's number of degrees of freedom from six to four. However, this should be done with a certain care, as the canonical equations resulting from the averaged Hamiltonian are not valid for the whole set of canonical variables: they do not describe the evolution of the longitudes of ascending nodes and their conjugate momenta (Naoz et al. (2013a); for more details, see Sect. 4.4.5).

The formal trick of the elimination of nodes is accomplished in the following way. As follows from the system symmetry with respect to rotations about the total angular momentum vector (as soon as the invariable plane is set as the reference plane, see Fig. 4.2), by means of the substitution

$$H_1 = \frac{1}{2H}(H^2 + G_1^2 - G_2^2), \quad H_2 = \frac{1}{2H}(H^2 - G_1^2 + G_2^2), \tag{4.20}$$

the variables H_1 and H_2 are eliminated from the Hamiltonian.

The octupole truncation of Hamiltonian (4.9) can be represented as

$$\begin{aligned}\mathcal{H}_{\rm oct} = & \frac{\beta_0}{2L_1^2} + \frac{\beta_1}{2L_2^2} + 8\beta_2 \frac{L_1^4}{L_2^6}\left(\frac{r_1}{a_1}\right)^2\left(\frac{a_2}{r_2}\right)^3(3\cos^2\Phi - 1) + \\ & + 2\beta_3 \frac{L_1^6}{L_2^8}\left(\frac{r_1}{a_1}\right)^3\left(\frac{a_2}{r_2}\right)^4(5\cos^3\Phi - 3\cos\Phi),\end{aligned} \tag{4.21}$$

where

$$\beta_0 = \mathcal{G}^2\frac{(m_0m_1)^3}{m_0 + m_1}, \tag{4.22}$$

$$\beta_1 = \mathcal{G}^2\frac{(m_0 + m_1)^3m_2^3}{m_0 + m_1 + m_2}, \tag{4.23}$$

$$\beta_2 = \frac{\mathcal{G}^2}{16}\frac{(m_0 + m_1)^7}{(m_0 + m_1 + m_2)^3}\frac{m_2^7}{(m_0m_1)^3}, \tag{4.24}$$

$$\beta_3 = \frac{\mathcal{G}^2}{4}\frac{(m_0 + m_1)^9}{(m_0 + m_1 + m_2)^4}\frac{m_2^9(m_0 - m_1)}{(m_0m_1)^5}. \tag{4.25}$$

Now, using representation (4.21), the Hamiltonian can be normalized in each order of α, by eliminating the short-period terms corresponding to the orbital timescale. For this purpose, the Hori–Deprit method can be used, based on the Lie series techniques, as described in Sect. 2.7. However, in the studies in this field, an older method, namely, the von Zeipel method, was usually used, due to historical reasons. This method is less convenient (the algorithm is technically more complicated) than the Hori–Deprit method; in particular, the generating function is

defined in *mixed* variables, i.e., it is a function of both "old" and "new" variables. However, in the given problem the normalization is accomplished only in two orders of α (namely, α^2 and α^3), therefore, the advantages of the Hori–Deprit method are not decisive.

Harrington (1968, 1969) used the von Zeipel method to obtain the normalized quadrupole Hamiltonian; in this lowest order the normalizing procedure is equivalent to a straightforward double averaging over the short-period angles. Marchal (1990), Krymolowski and Mazeh (1999), and Ford et al. (2000) used the von Zeipel method to obtain the normalized octupole Hamiltonian. Here we omit cumbersome intermediate algebraic manipulations inherent to the normalization procedure and present just the final Hamiltonian. Thus, the normalized octupole Hamiltonian is given by

$$\begin{aligned}\mathcal{H}_{\rm oct} = \; & C_2[(2+3e_1^2)(3\theta^2-1)+15e_1^2(1-\theta^2)\cos 2g_1]+ \\ & + C_3 e_1 e^2[A\cos\varphi + 10\theta(1-\theta^2)(1-e_1^2)\sin g_1 \sin g_2], \end{aligned} \tag{4.26}$$

where

$$\cos\varphi = -\cos g_1 \cos g_2 - \theta \sin g_1 \sin g_2, \tag{4.27}$$

$$C_2 = \frac{\mathcal{G}^2}{16}\frac{(m_0+m_1)^7}{(m_0+m_1+m_2)^3}\frac{m_2^7}{(m_0m_1)^3}\frac{L_1^4}{L_2^3G_2^3}, \tag{4.28}$$

$$C_3 = \frac{15}{16}\frac{\mathcal{G}^2}{4}\frac{(m_0+m_1)^9}{(m_0+m_1+m_2)^4}\frac{m_2^9(m_0-m_1)}{(m_0m_1)^5}\frac{L_1^6}{L_2^3G_2^5}, \tag{4.29}$$

$$A = 4 + 3e_1^2 - \frac{5}{2}(1-\theta^2)(2+5e_1^2-7e_1^2\cos 2g_1), \tag{4.30}$$

$$\theta = \cos(i_1 - i_2) = \frac{1}{2G_1G_2}(H^2 - G_1^2 - G_2^2), \tag{4.31}$$

$$H = |\mathbf{H}|, \quad \mathbf{H} = \mathbf{G}_1 + \mathbf{G}_2 \tag{4.32}$$

(see Fig. 4.2). The value of H is set by initial conditions. Note that the quadrupole Hamiltonian is given by Equation (4.26) with the octupole term (that with factor C_3) omitted.

The angle φ is nothing but the angle between the position vectors of the pericenters of the inner and outer binaries. The angle $i \equiv i_1 - i_2$ is the mutual inclination of the binaries; see Figs. 4.1 and 4.2.

For the sake of technical clarity, the designations of variables in Hamiltonian (4.26) are kept to be the same as original ones, i.e., the original and averaged ("mean") variables are designated by the same symbols. However note that dynamically they are different: the original variables suffer short-period time

oscillations, eliminated in the behaviour of the "mean" variables. The averaged semimajor axes a_1 and a_2 are obviously constant, because the mean anomalies l_1 and l_2, conjugate to L_1 and L_2 have been averaged out, and, therefore, the averaged L_1 and L_2 are constant.

The canonical equations of motion for the "mean" e_i and g_i ($i = 1, 2$) are given by

$$\frac{\mathrm{d}e_1}{\mathrm{d}t} = \frac{\partial e_1}{\partial G_1}\frac{\partial \mathcal{H}_{\mathrm{oct}}}{\partial g_1}, \quad \frac{\mathrm{d}g_1}{\mathrm{d}t} = -\frac{\partial \mathcal{H}_{\mathrm{oct}}}{\partial G_1}, \tag{4.33}$$

$$\frac{\mathrm{d}e_2}{\mathrm{d}t} = \frac{\partial e_2}{\partial G_2}\frac{\partial \mathcal{H}_{\mathrm{oct}}}{\partial g_2}, \quad \frac{\mathrm{d}g_2}{\mathrm{d}t} = -\frac{\partial \mathcal{H}_{\mathrm{oct}}}{\partial G_2}. \tag{4.34}$$

In a final explicit form, obtainable after substituting $\mathcal{H}_{\mathrm{oct}}$ in them, these equations look rather cumbersome; they can be found in Ford et al. (2000) and Naoz et al. (2013a). The equations can be numerically integrated. At each step of a numerical integration, as soon as e_i and g_i are determined, Equation (4.31) allows one to find the inclination i.

According to Naoz et al. (2013a), the secular equations for i_1 and i_2 (the inclinations with respect to the invariable plane) can be written in the form

$$\frac{\mathrm{d}\cos i_1}{\mathrm{d}t} = \frac{1}{G_1}\frac{\mathrm{d}H_1}{\mathrm{d}t} - \frac{1}{G_1}\frac{\mathrm{d}G_1}{\mathrm{d}t}\cos i_1, \tag{4.35}$$

$$\frac{\mathrm{d}\cos i_2}{\mathrm{d}t} = \frac{1}{G_2}\frac{\mathrm{d}H_2}{\mathrm{d}t} - \frac{1}{G_2}\frac{\mathrm{d}G_2}{\mathrm{d}t}\cos i_2, \tag{4.36}$$

where the angular momenta time derivatives are determined from the normalized Hamiltonian.

4.4.5 Technical Dangers of Formal Elimination of Nodes

The procedure of *elimination of nodes* in the equations of motion of the general three-body problem was invented by Carl Jacobi. It is performed in a frame where the total angular momentum vector of the system defines the z-axis (Jefferys and Moser 1966). The plane orthogonal to this vector is called the *invariable plane*. In such a frame, the relation $h_1 = h_2 + \pi$ holds, where h_1 and h_2 are the longitudes of ascending nodes. On the other hand, the longitudes of the ascending nodes enter the original Hamiltonian only in the form of combination $h_1 - h_2$ (due to the D'Alembert rules, see references in Sect. 4.2). It might be tempting to make the substitution $h_1 - h_2 = \pi$ in the Hamiltonian, thus making the both longitudes cyclic; however, such an operation would be inadequate.

The reason is that the substitution $h_1 - h_2 = \pi$ is equivalent to the transformation $h_1 \to \tilde{h}_1 + \pi$, $h_2 \to \tilde{h}_1$, where $\tilde{h}_1$ is a new variable. First of all, this transformation is degenerate ($\mathbb{R}^2 \mapsto \mathbb{R}^1$). Besides, any full transformation of variables containing this one cannot be canonical. Let us write down a necessary and sufficient condition for a transformation to be canonical (Markeev 1990):

$$\mathbf{M}^{\mathrm{T}}\mathbf{J}\mathbf{M} = c\mathbf{J}, \tag{4.37}$$

where $\mathbf{M}$ is the Jacobi matrix of the transformation, $\mathbf{M}^{\mathrm{T}}$ is the transposed $\mathbf{M}$, $\mathbf{J}$ is the symplectic unity matrix, and c is the *valence* of the transformation. The matrices $\mathbf{M}$ and $\mathbf{J}$ are given by

$$\mathbf{M} = \begin{pmatrix} \frac{\partial \mathbf{Q}}{\partial \mathbf{q}} & \frac{\partial \mathbf{Q}}{\partial \mathbf{p}} \\ \frac{\partial \mathbf{P}}{\partial \mathbf{q}} & \frac{\partial \mathbf{P}}{\partial \mathbf{p}} \end{pmatrix}, \quad \mathbf{J} = \begin{pmatrix} \mathbf{0} & \mathbf{E}_n \\ -\mathbf{E}_n & \mathbf{0} \end{pmatrix}, \tag{4.38}$$

where $\mathbf{q}$, $\mathbf{p}$ and $\mathbf{Q}$, $\mathbf{P}$ are the conjugate pairs of old and new variables, respectively; $\mathbf{E}_n$ is the unity matrix $n \times n$, and n is the number of degrees of freedom.

We see that for any transformation containing $q_1 = Q_1 + \pi$ and $q_2 = Q_1$ the matrix $\mathbf{M}$ is obviously degenerate; besides, equality (4.37) cannot be fulfilled for such a matrix, i.e., the transformation is non-canonical. However, after the equations of motion are deduced from the original Hamiltonian, the substitution $h_1 - h_2 = \pi$ is correct to accomplish, of course.

In the Hamiltonian itself, the substitution $h_1 - h_2 = \pi$ can be performed only as a symbolic formal trick, in understanding that the validity of the Hamiltonian in the variables h_1, H_1, h_2, H_2 is corrupted, but it is preserved in other pairs of variables.

Naoz et al. (2013a) pointed out that if the substitution $h_1 - h_2 = \pi$ is made in the Hamiltonian, thus making it independent of the longitudes of ascending nodes, one may be led to a false inference that the z-components of the orbital angular momenta are conserved.[3] In reality, H_1 and H_2 are conserved merely in the *test-particle quadrupole approximation* of the problem. In any problem setting that is more general, one should either use the original correct Hamiltonian to derive the full set of equations of motion, or use complementary relations for the components of angular momenta, in addition to the equations for other "non-corrupted" variables derived from the node-eliminated Hamiltonian.

The octupole-order equations for e_1, e_2, g_1, g_2 are given in Ford et al. (2000); the octupole order equations for $e_1, e_2, g_1, g_2, h_1, h_2, H_1, H_2$ are given in the Appendix B of the article by Naoz et al. (2013a). For the first four variables, the equations are the same in the both sources. Note that in Naoz et al. (2013a) there is a misprint repeated in several places: the expressions $\sin i^2$ and $\cos i^2$, whenever they appear, should be corrected to $\sin^2 i$ and $\cos^2 i$, respectively.

[3] See critics of Kozai's (1962) argumentation and works of other authors in this respect in Naoz et al. (2013a).

One may average the quadrupole Hamiltonian (4.9) over l_1 and l_2 without eliminating nodes. In this way, Naoz et al. (2013a) derived the secular Hamiltonian in the form

$$\begin{aligned}\mathcal{H} = \frac{C_2}{8}\Big\{&(1+3\cos 2i_2)\left[(2+3e_1^2)(1+3\cos 2i_1)+30e_1^2\cos 2g_1\sin^2 i_1\right]+\\&+3\cos 2\Delta h[10e_1^2\cos 2g_1(3+\cos 2i_1)+4(2+3e_1^2)\sin^2 i_1]\sin^2 i_2+\\&+12(2+3e_1^2-5e_1^2\cos 2g_1)\cos\Delta h\sin 2i_1\sin 2i_2+\\&+120e_1^2\sin i_1\sin 2i_2\sin 2g_1\sin\Delta h-\\&-120e_1^2\cos i_1\sin 2i_2\sin 2g_1\sin 2\Delta h\Big\},\end{aligned} \tag{4.39}$$

where $\Delta h = h_1 - h_2$, and C_2 is still given by formula (4.28):

$$C_2 = \frac{\mathcal{G}^2}{16}\frac{(m_0+m_1)^7 m_2^7}{(m_0+m_1+m_2)^3 m_0^3 m_1^3}\frac{L_1^4}{L_2^3 G_2^3}. \tag{4.40}$$

Hamiltonian (4.39) provides correct secular equations for the full set of canonical variables, including h_1, h_2, H_1, H_2.

4.4.6 *Octupole Approximation Versus Quadrupole Approximation: New Behaviours*

For the close-to-coplanar triples and for the triples with low-eccentric inner binaries, the Lidov-Kozai dynamics in the quadrupole approximation is trivial: the arguments of pericenters circulate, the eccentricities and inclinations are quasi-constant. Therefore, higher-order terms dominate in the qualitative real dynamics. Conversely, if the Lidov-Kozai cycle is prominent (e.g., if the inner binary and the outer binary are inclined enough with respect to each other), then the octupole terms can be regarded as a perturbation of the dominating quadrupole-order dynamics.

The quadrupole Hamiltonian is just Hamiltonian (4.26) with the octupole term (that with factor C_3) omitted:

$$\mathcal{H}_{\text{quad}} = C_2[(2+3e_1^2)(3\theta^2-1)+15e_1^2(1-\theta^2)\cos 2g_1]. \tag{4.41}$$

We see that the argument of pericenter g_2 is absent here; therefore, G_2 and e_2 are secular constants, and the form of the perturber's orbit does not change. This is valid only in the quadrupole approximation.

As angle g_2 is cyclic, the system with Hamiltonian (4.41) is integrable (in the given approximation). The eccentricity and the argument of pericenter of the inner

binary are governed by the equations

$$\frac{\mathrm{d}e_1}{\mathrm{d}t} = \frac{C_2}{G_1}(1-e_1^2)\left[30e_1(1-\theta^2)\sin 2g_1\right], \tag{4.42}$$

$$\frac{\mathrm{d}g_1}{\mathrm{d}t} = 6C_2\left\{\frac{1}{G_1}\left[4\theta^2+(5\cos 2g_1-1)(1-e_1^2-\theta^2)\right]+\frac{\theta}{G_2}\left[2+e_1^2(3-5\cos 2g_1)\right]\right\}. \tag{4.43}$$

Ford et al. (2000) demonstrated that, in any simulation aimed to describe real systems, the quadrupole approximation must be used with a great caution, because the octupole-order term may influence the secular dynamics in a *qualitative* way.

This is illustrated in Fig. 4.3, for a system with the following parameters: $m_2 = m_1 = 0.001m_0$, $\alpha = a_2/a_1 = 0.01$; and the initial conditions are: $e_1 = 0.05$, $e_2 = 0.9$, and the relative inclination $i = 70°$. On setting $m_0 = 1M_{\mathrm{Sun}}$ and $a_1 = 1$ AU, the time unit is equal to one year.

In the plot, the time behaviour of the eccentricity of the inner binary is shown as derived from a direct numerical integration of the original 3BP (the dashed line) and from a numerical integration of the equations of motion in the octupole approximation (the solid line). The quadrupole theory predicts a *constant* amplitude of the secular eccentricity oscillations (equal to that of the first oscillation in the time plot). Obviously, this is in sharp contradiction with what we see in the plot: in the real and octupole settings of the problem, the eccentricity suffers long-term amplitude variations, during which it achieves values close to unity. The timescale of these variations is much greater than the LK-oscillation period. A way to estimate this timescale will be considered in the next section.

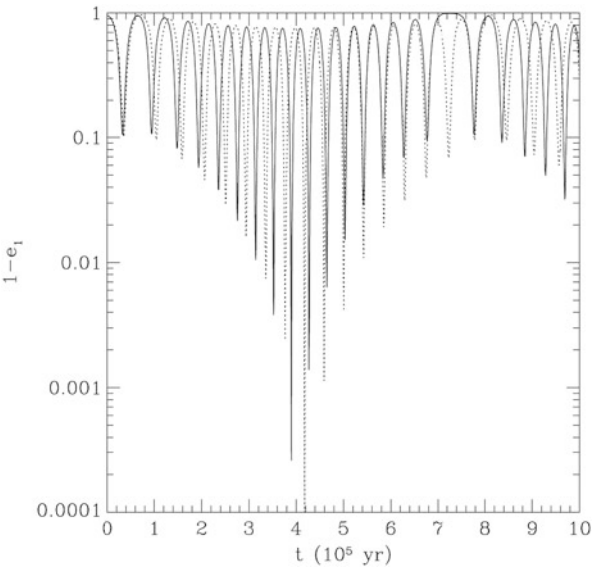

Fig. 4.3 The eccentricity of the inner orbit as a function of time (a typical example), as given by numerical integrations of the octupole-order equations (the *solid curve*) and of the original non-approximated system (the *dashed curve*). See text for the system parameters and initial conditions (Figure 5 from Ford et al. (2000). Copyright AAS. Reproduced with permission)

We see that the difference between the quadrupole and octupole theories is indeed qualitative: such eccentricity bursts may lead to coming into play of the *tidal and general-relativistic* effects (at low pericentric distances), or even to a *catastrophic merger* of the central masses.

An important and striking dynamical phenomenon, that arises if one considers systems more sophisticated that the circular R3BP, is the phenomenon of *orbital flips*. In Sect. 4.3, we have already become acquainted with the *eccentric LK-mechanism* in the elliptic R3BP: Naoz et al. (2011) and Katz et al. (2011) used the integrable LK-Hamiltonian as a starting point for a perturbative approach, and discovered this mechanism, due to which the so-called "flips" (turnovers) of the orbits become possible.

In other words, the eccentric LK-mechanism describes transitions from the prograde orbital motion to the retrograde one and vice versa. On a new theoretical level, in the framework of the general (non-restricted) 3BP, Naoz et al. (2013a) demonstrated that the full Hamiltonian equations in the non-restricted problem allow for a possibility of *periodic transitions* between the prograde and retrograde motion regimes of the inner binary. If the octupole terms are retained and the outer orbit is eccentric, then the inner binary can perform flips between the prograde and retrograde regimes; during such flips, the inner binary stretch to extremely high eccentricities, its semimajor axis being constant.

4.5 Timescales of the LKE

4.5.1 Timescales of the Classical LK-Oscillations

As shown by Malhotra (2012) in the circular R3BP framework, the LKE periodically causes a sharp (exponential) rise of the eccentricity of a test particle; of course, this rise is local in time[4] and its appearance depends on initial conditions. The characteristic timescale for such a rise, in the case of initial small eccentricities and large inclinations, can be represented as a function of the orbital semimajor axis a of the test particle:

$\sim 530a^{-3/2}$ years for a satellite in orbit around the Earth and subject to the Solar perturbation (here a is in units of the Earth radius, $R_{\text{Earth}} \approx 6400$ km),
$\sim 70a^{-3/2}$ years for a satellite in orbit around the Earth and subject to the Lunar perturbation (here a is also in units of the Earth radius),
$\sim 1.3a^{-3/2}$ years for a satellite in orbit around the Moon and subject to the Earth perturbation (here a is in units of the Moon radius, $R_{\text{Moon}} \approx 1700$ km).

[4]Indeed, for a bounded motion, the eccentricity is limited by the value of 1 from above, and any increase decelerates on approaching a maximum.

Of course, these timescale estimates are very approximate and have a limited physical meaning. However, if one compares, e.g., the real lifetime of the space probe *Luna*-3 (≈6 months)[5] with that following from the formula given above for a satellite in orbit around the Earth and subject to the Lunar perturbation (≈3 months), one finds a rather good agreement by the order of magnitude, though the initial eccentricity of the probe was not at all small.

The considered timescale of the exponential jump of the eccentricity is solely illustrative. To provide a rigourous description of the temporal behaviour, one should estimate the period of LK-oscillations. If one wishes to find analytical estimates in the quadrupole approximation, then the double-averaged equations of motion can be used straightforwardly, in the way as Lidov (1961, 1962, 1963a), Kozai (1962), and Gordeeva (1968) did in the framework of the R3BP. Gordeeva (1968) derived explicit exact and simple asymptotic formulas for the period, in dependence on the problem parameters and initial conditions.[6] She derived an explicit formula for the LK-period, expressing it through a complete elliptic integral of the first kind, and revealed an asymptotic logarithmic dependence on the initial data near the separatrix of LK-resonance. What is more, she derived a formula for the timescale of a satellite's *ballistic existence* (i.e., a satellite's existence until it enters the atmosphere); this timescale is expressed through an incomplete elliptic integral of the first kind.

The timescale study, in application to the space mission design, was continued in the works by Prokhorenko (2002a), who studied the solutions obtained by Lidov (1961) for the satellite version of the double-averaged circular R3BP and made a comparative analysis of the secular periods at various values of parameters and initial data; what is more, a comparative analysis of the timescales of the ballistic existence of satellites in highly-eccentric orbits subject to perturbations of outer bodies was performed (Prokhorenko 2002b). These estimates were used in the design of long-lived satellites in highly-elliptical orbits, such as *Spektr-R* astrophysical space mission (Prokhorenko 2002a,b).

Apart from differences in the values of coefficients, the quadrupole secular theory in the non-restricted problem is similar to that in the restricted one; thus, the formula for the period is functionally the same. At the center of LK-resonance, the period of LK-oscillations in the eccentricity and inclination is given by Mazeh and Shaham (1979) and Holman et al. (1997):

$$P_{\mathrm{LK}} \approx P_1 \frac{(m_0 + m_1)}{m_2} \left(\frac{a_2}{a_1}\right)^3 (1 - e_2^2)^{3/2}, \tag{4.44}$$

[5] The LKE in its dynamics was discussed in Chap. 1.

[6] Note that there is a misprint in Gordeeva's (1968) formula (2′): $\beta = 1 - \frac{5}{3}c_2$ should be corrected to $\beta = 1 - \frac{5}{2}c_2$.

where P_1, m_0, m_1, and a_1 are, respectively, the orbital period, masses and semimajor axis of the inner binary; P_2, m_2, and e_2 are, respectively, the orbital period, mass, and eccentricity of the outer perturber.

The period of ω-libration increases with its amplitude, tending to infinity on approaching the separatrix of the LK-resonance (Gordeeva 1968). However, deviation of $P_{\rm LK}$ from its value at the resonance center becomes significant only in a close vicinity to the separatrix; thus, usually, the actual period has the same order of magnitude as that given by formula (4.44), being only somewhat greater.

At the quadrupole order of approximation, the secular system is integrable, and, as it is well-known already starting from the works of Lidov (1961, 1962, 1963a) and Gordeeva (1968), the period of secular motion can be expressed through elliptic integrals.

Let us recall the derivation of the secular variation timescale for the eccentricity and inclination in the test particle limit of the three-body problem, following Gordeeva (1968), Kinoshita and Nakai (2007), and Antognini (2015); see also Sect. 3.2.5. Obviously, the secular period can be expressed as

$$T_{\rm LK} = \oint \frac{{\rm d}t}{{\rm d}x} {\rm d}x, \tag{4.45}$$

where $x \equiv (1-e^2)^{1/2}$, and e is the particle's eccentricity.

Expressing $\cos 2g_1$ and $\sin 2g_1$ in terms of the value of the averaged quadrupole Hamiltonian $\mathcal{H}_{\rm quad}$, given by Equation (4.41), one has

$$\sin 2g_1 = \left\{ 1 - \left[\frac{3x^4 + x^2(\mathcal{H}_{\rm quad} - 9c_1 - 5) + 15c_1}{15(1-x^2)(x^2-c_1)} \right]^2 \right\}^{1/2}, \tag{4.46}$$

where, as usual in this book, $c_1 = (1-e^2)\cos^2 i$; see Equation (3.23). Then, formula (4.45) gives

$$\begin{aligned} T_{\rm LK} &= \frac{L_1}{30 C_2} \oint \frac{x^2}{(1-x^2)(x^2-c_1)} \times \\ &\times \left\{ 1 - \left[\frac{3x^4 + x^2(\mathcal{H}_{\rm quad} - 9c_1 - 5) + 15c_1}{15(1-x^2)(x^2-c_1)} \right]^2 \right\}^{-1/2} {\rm d}x, \end{aligned} \tag{4.47}$$

where C_2 is given by Equation (4.40). The integral can be expressed in terms of incomplete elliptic integrals of the first kind.

Expressing $\mathcal{H}_{\rm quad}$ through c_2 (given by Equation (3.24)), one finds

$$T_{\rm LK} = \frac{L_1}{15 C_2} \int_{x_{\rm min}}^{x_{\rm max}} (1-x^2)^{-1} \left\{ \left(1 - \frac{c_1}{x^2}\right)^2 - \left(\frac{1}{5} - \frac{c_1}{x^2} + \frac{2c_2}{1-x^2} \right)^2 \right\}^{-1/2} {\rm d}x. \tag{4.48}$$

The extrema $x_{\min}$ and $x_{\max}$ can be determined by substituting the corresponding values of g_1 in the quadrupole Hamiltonian, written in the form

$$\mathcal{H}_{\text{quad}} = \frac{1}{x^2}\left[(5-3x^2)(x^2-3c_1) - 15(1-x^2)(x^2-c_1)\cos 2g_1\right]. \tag{4.49}$$

In the case of libration, both extrema occur at $g_1 = \pm\pi/2$; and in the case of rotation the minimum occurs at $g_1 = 0$ and $g_1 = \pm\pi$, and the maximum occurs at $g_1 = \pm\pi/2$. Defining

$$\zeta \equiv 3 + 5c_1 + 5c_2, \tag{4.50}$$

one has

$$x_{\min} = \left\{\frac{1}{6}\left[\zeta - (\zeta^2 - 60c_1)^{1/2}\right]\right\}^{1/2}, \tag{4.51}$$

$$x_{\max} = \left\{\frac{1}{6}\left[\zeta + (\zeta^2 - 60c_1)^{1/2}\right]\right\}^{1/2}, \qquad \text{if } c_2 < 0, \tag{4.52}$$

$$x_{\max} = \left(1 - \frac{5}{2}c_2\right)^{1/2}, \qquad \text{if } c_2 > 0 \tag{4.53}$$

(Antognini 2015; Gordeeva 1968).

Using expression (4.48) with the integration limits (4.51), (4.52) and (4.53) one can calculate numerically T_{LK} for any values of the problem parameters and initial data.

An example of such a calculation is given in Fig. 4.4, where a contour plot of the normalized period $f(c_1, c_2) = 15T_{\text{LK}}C_2L_1^{-1}$ of LK-oscillations is presented. The contour levels correspond to constant values of $f(c_1, c_2)$, indicated in the plot. The period uniformly increases when the (c_1, c_2) values approach the separatrix line $c_2 = 0$ at $0 \le c_1 \le 3/5$, tending to infinity on the separatrix. However, the rise is sharp only in a close vicinity to the separatrix, otherwise the period does not vary much, being by the order of magnitude constant over the most area of the possible values of (c_1, c_2). Besides, one can see that the period is determined mostly by the value of c_2, in comparison with c_1. Similar contour plots are presented in Prokhorenko (2002a, 2015; see Figures 6c and 3 in these two papers, respectively).

4.5.2 Timescales of the Eccentric LK-Mechanism

It is well-known that, in the quadrupole approximation, there is no secular variation of the *amplitude* of the LK-oscillations in eccentricity and inclination. However, in the octupole approximation, the amplitude is typically subject to enormous

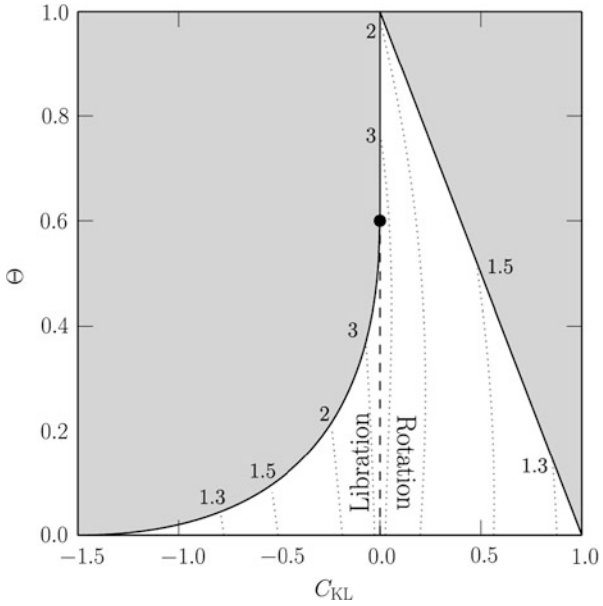

Fig. 4.4 The domains of possible values of constants $C_{\mathrm{KL}} \equiv \frac{5}{2}c_2$ and $\Theta \equiv c_1$ designated as adopted in Antognini (2015). The *dotted lines* are the contour levels of the normalized period of LK-oscillations as given by the integral in formula (4.48). Compare to the diagram in Fig. 3.1 (Figure 1 from Antognini (2015). With permission from Oxford University Press)

long-term variations, as established by Ford et al. (2000), Katz et al. (2011), and Lithwick and Naoz (2011). These variations take place on the timescales much longer than the LK-period. They are illustrated above in Fig. 4.3.

These long-term variations are nothing but a manifestation of the *eccentric LK-mechanism*, called so because the eccentricity oscillations become enormous when the orbital plane of the inner binary is close to the orthogonality with the orbital plane of the perturber. The variations of the mutual inclination, coupled to the eccentricity, may even cause the inner binary to suffer an *orbital flip* from prograde to retrograde motion, or vice versa.

During a flip the pericentric distance can decrease so much that a number of astrophysical phenomena (tides, collisions, mass transfer, effects of general relativity) may come into play. Therefore, the timescale T_{ELK} of the eccentric LK-mechanism is an important quantity that needs to be estimated.

It is much longer than the timescale of the classical LK-oscillations. Katz et al. (2011), Naoz et al. (2013b), and Li et al. (2015) heuristically estimated the timescale as

$$T_{\mathrm{ELK}} \sim T_{\mathrm{LK}} \epsilon_{\mathrm{oct}}^{-1}, \tag{4.54}$$

where

$$\epsilon_{\rm oct} \equiv \frac{e_2}{(1-e_2^2)}\frac{a_1}{a_2}. \tag{4.55}$$

The quantity $\epsilon_{\rm oct}$ represents the ratio of the amplitudes of the octupole and quadrupole terms in the Hamiltonian, thus characterizing the importance of the octupole term.

If the mass parameter $\mu = m_1/(m_0 + m_1)$ of the central binary is not small, a mass factor should be introduced in definition (4.55). This will be done later on in Chap. 8, in formula (8.14). This factor can be important in some situations; in particular, the octupole term vanishes in the limit of an equal-mass inner binary.

Antognini (2015) studied the problem both analytically and numerically and showed that

$$T_{\rm ELK} \sim T_{\rm LK}\epsilon_{\rm oct}^{-1/2}, \tag{4.56}$$

contrary to formula (4.54).

Let us consider in brief how relationship (4.56) is derived. In astronomical and astrophysical systems, the LKE may come into play if the mutual inclination of the "binaries" of the triple is large, as we know. On the other hand, to obtain a large amplitude of the LK-oscillation, one should choose a low initial eccentricity of the inner binary. Therefore, it is actual to be able to estimate the LK-period in the case of the "high inclination, low eccentricity" initial conditions.

The octupole term in the Hamiltonian is dynamically important if the outer orbit is eccentric, as follows from Equation (4.55). That is just why the octupole-term effect is known as the "eccentric LK-mechanism" (ELK).

At the octupole order of approximation, the Hamiltonian contains all slow angles; therefore, the octupole Hamiltonian is not integrable, contrary to the quadrupole one. The quantities c_1 or c_2, given by Equations (3.23) and (3.24), are no more constants of the motion. However, one may assume that, in the octupole approximation, c_1 or c_2 vary only slowly, with a timescale much longer than the ordinary LK-period.

To study the ELK-oscillations, Katz et al. (2011) introduced an approach based on the *Laplace vector* formalism. The Laplace vector (or, the *eccentricity vector*) is defined as $\mathbf{e} = e(\sin i_e \cos\Omega_e, \sin i_e \sin\Omega_e, \cos i_e)$, where i_e and Ω_e are the inclination and longitude of ascending node of the test particle's orbit. The vector $\mathbf{e}$ is directed towards the pericenter of the inner orbit. It is assumed that in the octupole approximation the parameter Ω_e varies only slowly (as c_1 or c_2 do), with the timescale much longer than the ordinary LK-period. Thus, Ω_e, c_1, and c_2 are assumed to be nearly constant over each separate LK-oscillation, but they may vary substantially on much longer timescales. If this condition of approximate constancy is not fulfilled, the ELK-oscillations may acquire non-periodic (in fact, chaotic) character, as shown by Li et al. (2014a).

Katz et al. (2011) averaged the equations of motion over an individual LK-cycle, and thus derived the equations describing the long-term ELK-behaviour in e and c_1:

$$\frac{\mathrm{d}\Omega_e}{\mathrm{d}\tau} = c_1 \frac{6E(m) - 3K(m)}{4K(m)}, \tag{4.57}$$

$$\frac{\mathrm{d}c_1}{\mathrm{d}\tau} = -\frac{15\pi}{128 \cdot 10^{1/2}} \frac{\epsilon_{\mathrm{oct}} c_1^{1/2} \sin\Omega_e}{K(m)} (8 - 55c_2)(6 + 10c_2)^{1/2}, \tag{4.58}$$

where $\tau = t/T_{\mathrm{LK},\, i=90^\circ}$, i.e., τ is time normalized by the period of LK-oscillation with a flip; $K(m)$ and $E(m)$ are the complete elliptic integrals of the first and second kind, respectively, with the parameter (the squared modulus)

$$m(c_2) \equiv \frac{3\left(1 - \frac{5}{2}c_2\right)}{3 + 5c_2}. \tag{4.59}$$

Katz et al. (2011) derived an additional approximate integral of motion, given by

$$\Phi \equiv F(c_2) - \epsilon_{\mathrm{oct}} \cos\Omega_e, \tag{4.60}$$

where

$$F(c_2) \equiv \frac{32 \cdot 3^{1/2}}{\pi} \int_{x(c_2)}^{1} \frac{K(\eta) - 2E(\eta)}{(41\eta - 21)(2\eta + 3)^{1/2}} \mathrm{d}\eta. \tag{4.61}$$

Also the quantity

$$\phi_q \equiv \frac{c_1}{2} + \frac{5}{2}c_2 \tag{4.62}$$

turned out to be a constant of motion. Thus, in the octupole theory, there are three constant parameters, defining the long-term behaviour: ϕ_q, Φ, and ϵ_{oct}. Recall that in the quadrupole theory, there were only two such parameters, c_1 and c_2. Consequently, the secular dynamics in the octupole case is more complicated and rich.

Based on this theory, Antognini (2015) derived an analytical formula for the period of the ELK-oscillations (the period of c_1, c_2, and Ω_e):

$$T_{\mathrm{ELK}} \sim \frac{256 \cdot 10^{1/2}}{15\pi\epsilon_{\mathrm{oct}}^{1/2}} T_{\mathrm{LK},\, i=90^\circ}. \tag{4.63}$$

The timescale for a flip to occur is given by

$$T_{\mathrm{flip}} \sim \frac{T_{\mathrm{ELK}}}{2}, \tag{4.64}$$

because the inner binary suffer two flips during the ELK-cycle.

Formula (4.64) is valid for the octupole-order regime with the "low-eccentricity, high-inclination" initial conditions. As found by Li et al. (2014b), flips are also possible in another octupole-order regime, that with "high-eccentricity, low-inclination" initial conditions. Estimates of the flip timescale in that regime can be found in Li et al. (2014b).

4.6 LKE: Resonance or Not

Several brief definitions of the LKE, pointing out its essence, can be found in the literature. Usually the LKE is characterized as a kind of resonance. According to Malhotra (1998), "the 'Kozai resonance' or the 'Kozai mechanism' after Y. Kozai (1962), is defined by the 1:1 commensurability of the secular precession rates of the perihelion and the orbit normal such that the argument of perihelion is stationary (or librates)."

In another formulation, due to Morbidelli (2002), "the Kozai resonance can be regarded as a 1:1 resonance between the precession frequencies of the longitude of perihelion ϖ and of the longitude of node Ω of the small body. Therefore, the argument of perihelion $g \equiv \varpi - \Omega$ is the critical angle of the resonance."

Kinoshita and Nakai (2007) write: "...if the z-component of the angular momentum of an asteroid disturbed by outer giant planets is small, the argument of the perihelion librates around 90° or 270° and both the eccentricity and the inclination largely change. This phenomenon is called the Kozai mechanism or the Kozai resonance."

According to Malhotra (2012), "The Kozai–Lidov effect ...is a type of secular resonance in which the apsidal and nodal precession rates are equal and of opposite sign, and the orbital eccentricity is excited from small to large values on secular timescales." Moreover, it is "one of the most surprising and non-intuitive resonances in the ...restricted three-body problem".

On the other hand, treating the LKE as resonance was criticized by Arnold et al. (2002, p. 219): "The word 'resonance' is used here [in Arnold's et al. book] due to historical reasons; for sure, there is no any resonance, but regions of libration in the phase portrait ...".

Let us consider whether indeed the LKE is of resonant nature, as understood generally in nonlinear dynamics.

4.6.1 Nonlinear Resonance in the Pendulum Model

Resonance represents the central concept of nonlinear dynamics. Chirikov (1982) defines it in such a way: "Resonance is understood as such situation when some frequencies of a non-perturbed system are close to each other or to frequencies of an external perturbation". How one can be convinced in the existence of resonance

in the motion of any particular celestial bodies? In fact, any observed ratio of frequencies can be approximated by some rational number with any degree of precision; but does resonance actually exist? To solve this problem, a *resonant phase* (named also *resonant* or *critical angle*, or *resonant* or *critical argument*) is defined. This is a linear combination (an algebraic sum) of angular variables of the system with integer coefficients, the choice of which defines the resonant relation between the frequencies. If the amplitude of variation of the resonant phase is limited, i.e., this angle librates, similarly to librations of a pendulum, then the system is in resonance; if it increases or decreases unlimitedly, i.e., rotates, then resonance is absent. The trajectory at the boundary between libration and rotation is the *separatrix*. Thus, the dynamics of a rigid pendulum provides a model of resonance. In a certain sense, this model of resonance is most universal, though other models of resonance exist (Chirikov 1979, 1982).

In celestial mechanics one deals, as a rule, with *nonlinear resonances*: the frequency of the phase oscillations on resonance depends on the amplitude (energy) of the oscillations, as in the pendulum example.[7] In case of linear resonance the frequency does not depend on the amplitude.

A slightest external push of the rigid pendulum, placed near its upper position of equilibrium ($\phi = \pm\pi = \pm 180°$, where ϕ is the pendulum angle measured from the lower position of equilibrium), is capable to change the motion character considerably (e.g., to change oscillation to rotation). This phenomenon is nothing but the so-called *essential dependence on initial conditions*. What would occur, if the pendulum or any other system with a separatrix were subject to a periodic perturbation? The motion near the separatrix in the generic case, i.e., for the majority of the initial conditions and parameter values, becomes most unusual. Now this is well-known, but for the first time a confusing and intricate behaviour of the trajectories close to the *perturbed separatrix* (in the three-body problem) was pointed out in 1899 by Henri Poincaré (1899). However, it was not supposed at that time that the character of this intricate motion is in any sense "random".

In 1959 Chirikov described dynamical chaos in a Hamiltonian system as a phenomenon arising due to *interaction of resonances*. For a criterion of chaos emergence, he proposed a criterion of *resonance overlap* (Chirikov 1959, 1979). Let us give an explaining example. The phase space in case of the non-perturbed rigid pendulum has two dimensions, defined by two variables: the pendulum angle ϕ and the momentum $p = ml\dot{\phi}$, where m is the mass of the pendulum, l is its length, $\dot{\phi}$ is the rate of variation of ϕ. In the well-known *phase portrait* "ϕ–p" of the non-perturbed pendulum (Fig. 4.5), a single domain ("cell") of librations, bound by the non-perturbed separatrix, is present. Thus, the pendulum model of resonance in the non-perturbed case describes a single resonance.

[7]The properties of nonlinear resonance are described in detail in Chirikov's general review (Chirikov 1982), where the fundamental concepts of nonlinear dynamics are explained in most accessible and, at the same time, rigourous way.

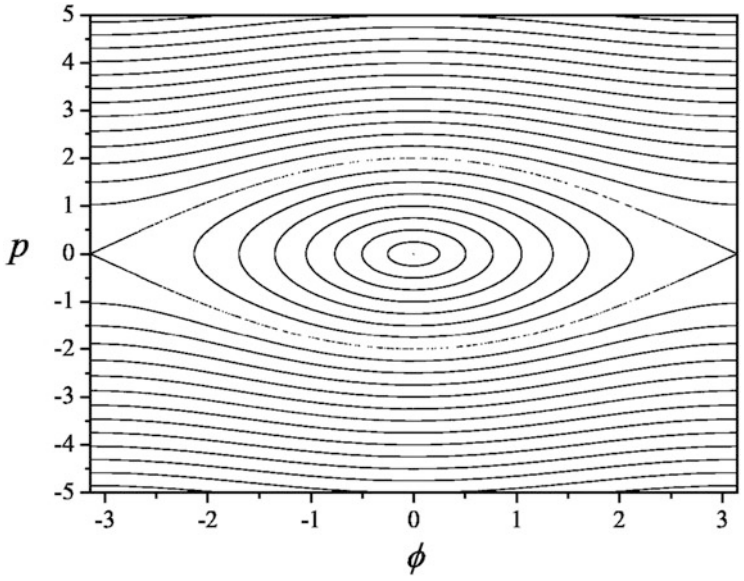

Fig. 4.5 A phase portrait of the non-perturbed pendulum

If one "switches on" a periodic perturbation, e.g., a vibration of the suspension point, then the phase space of this dynamical system is not two-dimensional anymore, and, to represent the global dynamics, one should construct a *phase space section*. It is built as follows: one plots the values of the system variables on the graph not continuously but "stroboscopically", i.e., discretely at constant time intervals equal to the period of perturbation. On the section constructed in this way one discovers not one but three domains of librations—three resonances (Fig. 4.6). If the perturbation frequency is relatively large, the separation of resonances in the momentum is large and they almost do not interact. On reducing the frequency of perturbation, the resonances approach each other and *chaotic layers* widen in the vicinity of the separatrices, where, as it is well visible in Fig. 4.6, the motion is irregular; on reducing further the frequency of perturbation, the layers merge into a single chaotic layer,—a result of the interaction of resonances at their strong mutual approach in the phase space.

In Chirikov's saying, "...the physicist first of all tries to find out which resonances play role in this or that system and how do they interact with each other" (Chirikov 1982). It is just the presence of resonances, often regarded to be the embodiments of order, leads to the unpredictable, chaotic character of the motion. In other words, the presence of resonances in the phase space causes the presence of the chaotic component in this space. However, as we have just seen, for chaos to exist, the presence of not one but two or more resonances in the phase space is required, because their interaction is necessary.

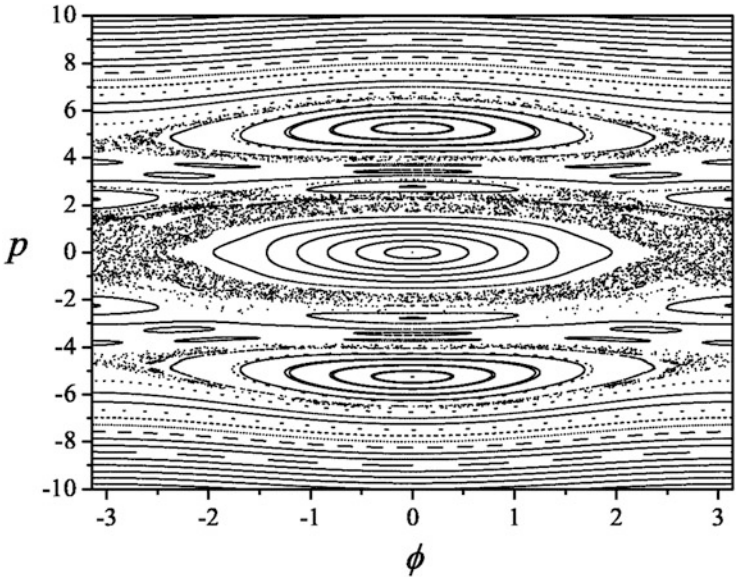

Fig. 4.6 A triplet of interacting resonances at a moderate relative frequency of perturbation (Figure 1 from Shevchenko (2007). With permission from Cambridge University Press)

A perturbed pendulum model of nonlinear resonance is generally described by the Hamiltonian in the form

$$H = \frac{\mathcal{G}p^2}{2} - \mathcal{F}\cos\phi + a\cos(\phi - \tau) + b\cos(\phi + \tau) \tag{4.65}$$

(Chirikov 1979; Lichtenberg and Lieberman 1992; Shevchenko 2000). The first two terms in formula (4.65) represent the Hamiltonian of the unperturbed pendulum; ϕ is the pendulum angle (the resonance phase angle), p is the momentum. The periodic perturbations are represented by the last two terms; τ is the perturbation phase angle: $\tau = \Omega t + \tau_0$, where Ω is the perturbation frequency,[8] and τ_0 is its initial phase. The quantities $\mathcal{F}$, $\mathcal{G}$, a, b are constants. The frequency of small-amplitude oscillations on resonance is $\omega_0 = (\mathcal{F}\mathcal{G})^{1/2}$. The properties of the chaotic layer around the separatrices are mostly defined by the *adiabaticity parameter* $\lambda = \Omega/\omega_0$, which can be also formulated as a measure of the overlapping of resonances.

An example of the phase space section of the Hamiltonian (4.65) at $\tau = 0 \bmod 2\pi$ is shown in Fig. 4.6 ($\Omega = 5$, $\omega_0 = 1$, $a = b$, $a/\mathcal{F} = 0.5$; $\lambda = 5$). This is a chaotic resonance triplet.

[8]Note that the same symbol Ω is used throughout this book to traditionally designate the longitude of ascending node.

4.6.2 The Place of LK-Resonance in the General Typology of Resonances

If expressed in terms of the Delaunay variables explicitly, the Lidov-Kozai Hamiltonian in the circular R3BP has form (3.25). Taking into account that the Delaunay momenta L and H, as well as $c_1 = H^2/L^2$, are constants of motion, it can be rendered the form

$$\mathcal{H}_{\rm LK} = A\left[\frac{3}{2}\frac{G^2}{L^2} + \frac{15}{2}c_1\frac{L^2}{G^2} + \frac{15}{2}\left(1 + c_1 - \frac{G^2}{L^2} - c_1\frac{L^2}{G^2}\right)\cos 2\omega\right], \tag{4.66}$$

where

$$A = -\frac{\mathcal{G}m_{\rm pert}a^2}{8a_{\rm pert}^3},$$

and unimportant constant terms are omitted.

The maximum value of G, as follows from its definition, takes place at $e = 0$, and is equal to L. Let us make a canonical transformation, introducing a new momentum p: $G \to (1-p)L$, $\omega \to \omega$, $\mathcal{H}_{\rm LK} \to -L\mathcal{H}_{\rm LK}$ (recall that L is constant). Thus, the new Hamiltonian

$$\mathcal{H}_{\rm LK} = -\frac{A}{L}\left\{\frac{3}{2}(1-p)^2 + \frac{15}{2}\frac{c_1}{(1-p)^2} + \frac{15}{2}\left[1 + c_1 - (1-p)^2 - \frac{c_1}{(1-p)^2}\right]\cos 2\omega\right\}. \tag{4.67}$$

Expanding $\mathcal{H}_{\rm LK}$ in powers of p up to the second order inclusive, one has

$$\mathcal{H}_{\rm LK} = -\frac{A}{L}\left\{3(5c_1-1)p + \frac{3(1+15c_1)}{2}p^2 + \left[15(1-c_1)p - \frac{15(1+3c_1)}{2}p^2\right]\cos 2\omega\right\}. \tag{4.68}$$

Assuming that the ω-libration island is small (as appropriate if c_1 is in a neighbourhood of 3/5), one can use Hamiltonian (4.68) to approximate the real secular libration.

Indeed, constructing contour plots for Hamiltonian (4.68), one may certify that they are undistinguishable (in representing the libration island) from the corresponding plots for original Hamiltonian (4.67), if $c_1 > 0.5$; for an example of such a comparison see Fig. 4.7.

Thus, we have reduced the LK-Hamiltonian to form (4.68), valid as an approximation if the ω-libration island is small.

In the previous subsection we have considered the pendulum model of resonance. Hamiltonian (4.68) does not fit this model, as it contains a dependence on the momentum in the coefficient of the harmonic term. In this sense, it is reminiscent of the *parametric resonance* model, which was extensively studied, e.g., in the

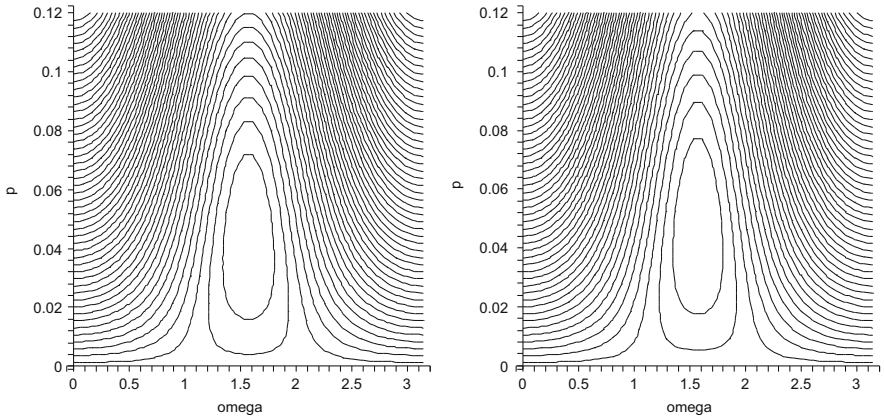

Fig. 4.7 Contour plots for Hamiltonian (4.68) (*left panel*) and Hamiltonian (4.67) (*right panel*), $c_1 = 0.5, A = -L$ (Computed by the author)

theory of accelerators already in the 1950s and 1960s of the twentieth century (see Kolomensky and Lebedev (1966), and references therein). The properties of the parametric resonance are considered in detail in Chirikov (1979). In the parametric resonance model, the dependence on the momentum in the coefficient of the harmonic term is linear.

The parametric resonance model coincides with a particular case of the *second fundamental model* of resonance proposed by Henrard and Lemaître (1983) and Lemaître (1984). (The first one is nothing but the pendulum model.) In a minimal parametrization (by a single parameter α), the second fundamental model has the form

$$\mathcal{H} = \frac{1}{2}p^2 + \alpha p + (2p)^{m/2} \cos m\omega. \tag{4.69}$$

The parametric model corresponds to the *second order resonance* ($m = 2$), in the usual terminology; see Lemaître (1984).

However, in Hamiltonian (4.68), also a quadratic term is present. Shinkin (1995) proposed a *third fundamental model* of resonance, described by the parameterized formula

$$\mathcal{H} = \frac{1}{2}p^2 + \alpha \prod_{i=1}^{4} (p + \beta_i)^{j_i/2} \cos m\omega, \tag{4.70}$$

where the integer numbers $j_1 + j_2 + j_3 + j_4 \leq m$; α and β_i ($i = 1, 2, 3, 4$) are arbitrary parameters (see Breiter 2003; Shinkin 1995). By an appropriate parametrization and a constant shift in p, Hamiltonian (4.68) can be reduced to form (4.70) with $j_1 = j_2 = 1, j_3 = j_4 = 0$.

Another important relevant question is whether the separatrix of LK-resonance is a "real" separatrix, i.e., the motion period on it is infinite, as in the pendulum model considered in the previous subsection. As we know, the argument of pericenter ω may librate or circulate; and these kinds of motions reflect physically different situations. What is more, not only "direct" circulations are possible, but, if one considers also inclinations from $\pi/2$ to π, the "reverse" ones, as in the pendulum model.

Gordeeva (1968) derived an asymptotic formula (Equation (7) in her paper) for the period of LK-librations in the vicinity of the separatrix in the R3BP; the asymptotic (on approaching the separatrix) period is given by

$$T \sim 2 \ln \frac{4}{(1-k^2)^{1/2}}, \tag{4.71}$$

where the modulus k of the complete elliptic integral of the first kind K is defined in Chap. 3. Equation (4.71) describes the asymptotic behaviour of Equation (3.59) at $k \to 1$.

On approaching the separatrix $c_2 = 0$ (see Fig. 3.1), the modulus k tends to unity; therefore, according to formula (4.71), the period tends to infinity; and the separatrix, in this sense, is analogous to the separatrix of the nonlinear pendulum. According to formula (4.71), the asymptotic divergence of the period, on approaching the separatrix, is of logarithmic type; i.e., it is the same as in the pendulum model.

Chapter 5
Understanding Irregular Satellites

Beginning with this Chapter, we start to consider various phenomena due to the LKE in astronomical and astrophysical systems. Historically, the first theoretical works on this mechanism by Lidov (1961) were devoted to planetary satellites, both natural and artificial; that is why we start with an overview of the most pronounced LK-phenomena in the satellite dynamics, namely, with the LKE in the dynamics of irregular satellites of giant planets.

For a planetary satellite, the qualitative LK-mechanism can be described as following: the secular variations in the eccentricity and inclination are coupled,[1] as integral (3.23) certifies, if the R3BP conditions are fulfilled at least approximately. The dynamical cause of the effect lies in the presence of a distant perturber; in the given case, it is the Sun, or some other massive satellite (e.g., the Moon in the Earth–Moon system). Therefore, if a satellite's orbit is inclined initially high enough with respect to the orbital plane of the host planet, the satellite's eccentricity may strongly (depending on initial conditions) oscillate on the secular timescale, and, when the eccentricity is maximum, the pericentric and apocentric distances are, respectively, minimum and maximum. Therefore, at the pericenter, the satellite may be destroyed by planetary tides or may collide with a large regular moon or with the planet itself. On the other hand, at the apocenter, the satellite may leave the planet's *Hill sphere* and escape.

The Hill sphere of a planet engulfs a zone of the planet's gravitational dominance: inside it, the planet's gravity dominates over the Solar perturbations, and the latter cannot enforce the satellites' escape. For example, in the Earth case, the *Hill radius* (radius of the Hill sphere) is about four ($\approx$3.9) times greater than the orbital semimajor axis of the Moon, that is why the Moon is safe with us.

The Hill radius can be estimated by means of an analysis of the locations of the libration points in the three-body problem (see, e.g., Murray and Dermott 1999). In

[1] They are in antiphase, if the inclination $i < \pi/2$, and in phase, if $i > \pi/2$.

I. I. Shevchenko, *The Lidov-Kozai Effect – Applications in Exoplanet Research and Dynamical Astronomy*, Astrophysics and Space Science Library 441,
DOI 10.1007/978-3-319-43522-0_5

a planet–Sun system, if the planet's orbit is circular, the Hill radius is given by

$$R_{\rm H}^{\rm circ} = \left(\frac{m_{\rm p}}{3m_{\rm Sun}}\right)^{1/3} a_{\rm p}, \tag{5.1}$$

where $m_{\rm p}$ and $m_{\rm Sun}$ are the masses of the planet and the Sun, respectively, and $a_{\rm p}$ is the semimajor axis of the planet's orbit.

If the orbit of the secondary (planet) is eccentric, then the radius of the stability zone is approximately equal to $R_{\rm H}^{\rm circ}$ calculated at the secondary's pericenter (Hamilton and Burns 1992):

$$R_{\rm H} \approx \left(\frac{m_{\rm p}}{3m_{\rm Sun}}\right)^{1/3} a_{\rm p}(1-e_{\rm p}), \tag{5.2}$$

where $e_{\rm p}$ is the eccentricity of the secondary. This formula expresses the so-called *Hill sphere at pericenter scaling*.

As established in astronomical observations of satellites of the giant planets (Jupiter, Saturn, Uranus, and Neptune), the satellites with orbits inside ∼0.05 of the Hill radius of the parent planet tend to be in close-to-circular prograde equatorial orbits.[2] These are called "regular" satellites. Conversely, the satellites with orbits outside ∼0.05 of the Hill radius tend to have large eccentricities and inclinations, and many are retrograde. These are called "irregular" satellites.

A more rigourous definition can be adopted: Nesvorný et al. (2003) define an *irregular* as a satellite that has the orbital semimajor axis large enough for the precession of the satellite's orbit to be controlled by the Sun, not by the parent planet's oblateness; i.e., the Solar perturbations dominate over the perturbations caused by the planet's non-sphericity.[3] Thus, a satellite is irregular if its orbital semimajor axis is greater than the *Laplace radius* (defined above in Sect. 3.4, see formula (3.91)), i.e., it satisfies the inequality

$$a \gtrsim r_{\rm L} \approx \left(J_2 R_{\rm p}^2 a_{\rm p}^3 \frac{m_{\rm p}}{m_{\rm Sun}}\right)^{1/5} \tag{5.3}$$

(Burns 1986; Nesvorný et al. 2003), where J_2, $R_{\rm p}$, $a_{\rm p}$, and $m_{\rm p}$ are the planet's parameters: its second zonal harmonic coefficient, mean radius, orbital semimajor axis, mass, respectively; $m_{\rm Sun}$ is the Solar mass.

The Hill and Laplace radii for the Solar system planets are given in Table 5.1. An inspection of this Table testifies that the approximate and rigourous definitions of irregulars are similar indeed: for all giant planets, the value of $r_{\rm L}/r_{\rm H}$ belongs to

[2]The term "prograde" designates the planetocentric motion co-directional with the host planet's heliocentric orbital motion; "retrograde" designates the motion opposite to the prograde one.

[3]Note that the given definitions of an irregular satellite apply only to the satellite systems of Jovian planets; otherwise the Moon should be also called irregular.

Table 5.1 Masses, figures, and critical radii for the Solar system planets

Planet	Mass m_p (10^{27} g)	Mean radius R_p(km)	Obliquity (°)	$J_2 \cdot 10^6$	$J_4 \cdot 10^6$	r_H/R_p	r_L/R_p
Mercury	0.3301	2440	~ 0.1	60	...	90.4	2.66
Venus	4.8673	6052	177.3	4	2	167	2.24
Earth	5.9722	6371	23.45	1083	−2	235	8.41
Mars	0.64169	3390	25.19	1960	−19	320	11.4
Jupiter	1898.1	69,911	3.12	14,696	−587	743	35.4
Saturn	568.32	58,232	26.73	16,291	−915	1080	48.4
Uranus	86.810	25,362	97.86	3343	−29	2680	64.0
Neptune	102.41	24,622	29.56	341	−35	4600	93.2

Notes: Obliquity is the angle between the planet's equatorial and orbital planes; J_2 and J_4 are the second and fourth zonal harmonic coefficients; r_H and r_L are the Hill and Laplace radii. The Table is compiled based on data given in the JPL Database (http://jpl.nasa.gov/), Murray and Dermott (1999), and Tremaine et al. (2009). The values of r_H and r_L for Mercury, Venus, Earth, and Mars are given as calculated by the author. The stated value of r_L for the Earth is formal because the Lunar perturbations are not taken into account

the interval between 0.02 and 0.05. It is interesting that, in case the rocky planets also had irregulars, the approximate definition of irregulars for them would be still valid: as follows from the Table, for Mercury, Earth, and Mars, r_L/r_H is still in the range 0.02–0.05, for Venus it is 0.013. Thus, all planets in the Solar system have similar (by the order of magnitude) values of r_L/r_H. The basic reason is that r_L and r_H depend on the planetary parameters rather weakly.

The irregular satellites are mostly small in size, their diameters $D \sim$ 1–10 km. However, each giant planet has one irregular moon with $D >$ 100 km, these moons are: JVI Himalia, SIX Phoebe, UXVII Sycorax, and NII Nereid. Nereid is the largest one ($D \approx$ 340 km).

The irregulars comprise the majority (in number, but not in mass) of the total satellite population in the Solar system: ∼110 out of the total count of ∼170 (as known in the year of publication of this book).

As we shall see in this Chapter, the orbital distributions of irregulars around parent planets are controlled by the LKE. As established by Carruba et al. (2002) and Nesvorný et al. (2003), the most general property of these distributions is that, due to the LKE, most orbits with $i \sim 90°$ are short-lived, and thus no irregular satellites have inclinations in the range between ∼50° and ∼140°, except two Neptunian moons N9 Halimede and N11 Sao. On the other hand, the secular orbital dynamics of two Saturnian moons S22 Ijiraq and S24 Kiviuq and Jovian moon J34 Euporie is most probably controlled by the LKE.

We consider the irregular satellite systems of Jupiter and Saturn in two separate sections, whereas the satellite systems of Uranus and Neptune are analyzed in a single one, because the two latter systems are mutually similar, though different from the Jovian and Saturnian systems. The major difference is that the non-survivability of orbits due to the LKE occur in the systems of Uranus and Neptune in a narrower inclination range than in the systems of Jupiter and Saturn.

5.1 Irregular Satellites: Origin and Orbits

5.1.1 Where They Came From

While the orbits of regular satellites lie deep inside the Hill spheres of their parent planets, the orbits of irregular satellites occupy substantial fractions of inner space of these spheres. What is more, whereas the orbital architecture of regulars is qualitatively similar to that of the Solar system planets (i.e., the orbits are mostly coplanar and close-to-circular), the orbital distributions of the irregulars are strongly disordered.

That is why the origin of irregular satellites is thought to be very different in comparison with that of regulars. The regulars are supposed to be formed in just the same way as planets, i.e., by means of accretion of solids in protodisks (Stevenson et al. 1986). The origin of irregulars seems to be totally different. Indeed, in contrast to regulars, most of them follow retrograde orbits, and this sole fact certifies that they cannot originate from a single nebula. Besides, their eccentricities and inclinations are too large in general to be an outcome of the standard accretion process in a flattened disk.

Therefore, the irregulars are thought to be minor bodies (e.g., asteroids) captured somehow from heliocentric orbits. They had not formed in vicinities of parent planets, but arrived from other realms of the Solar system. Thus, rigorously speaking, the "parent planet" (around which an irregular orbits) is really not a *parent* one. The capture in the three-body problem (the Sun–planet–asteroid problem, in particular) is a complicated, though a thoroughly studied process; see, e.g., Belbruno (2004). Due to the Hamiltonian nature of the three-body problem, such a capture is reversible, and the captured body is doomed to become free again, sooner or later. To make the capture irreversible, non-Hamiltonian perturbations (e.g., gas drag or light pressure) ought to be active.

Several mechanisms of transformation of a body-intruder into an irregular have been proposed: *collisional scenario* (Colombo and Franklin 1971; Gladman et al. 2001), *pull-down capture* (Heppenheimer and Porco 1977; Saha and Tremaine 1993), and *gas-drag capture* (Pollack et al. 1979, 1991). The collisional scenario postulates a disruption of a parent regular satellite by a body passing in a heliocentric orbit; this explains naturally that irregulars cluster in swarms of bodies with similar orbital elements. In the pull-down capture scenario, a body coorbital with a planet is captured by the planet due to mass growth of the latter, as the planet accretes matter at an early stage of its cosmogonical evolution and its Hill sphere swells. In the gas-drag capture scenario, an outer body enters the planet's gas envelope (also at an early evolutionary stage) and slowly spirals down; when the gas depletes, the orbit "freezes".

5.1.2 *Orbital Distributions*

As established already in the beginning of 2000s, there exists a broad gap in the inclination distribution (with respect to the ecliptic plane) of the known irregular satellites: almost no object has the inclination in the range between $\approx 50°$ and $\approx 140°$; see Fig. 5.1. A plausible explanation of this fact is that orbits with $i \sim 90°$ are subject to destruction due to the LKE (Carruba et al. 2002; Nesvorný et al. 2003).

The LKE can produce this gap in two ways (Carruba et al. 2002): (1) the pericenter distance $q = a(1-e)$ may decrease until the orbit starts to cross the orbits of massive inner regular moons (e.g., the orbit of Callisto in the case of the Jovian system), or even until it falls on the parent planet, i.e., until the equality $q = R_p$ starts to hold, where R_p is the planet's radius; (2) the apocenter distance $Q = a(1 + e)$

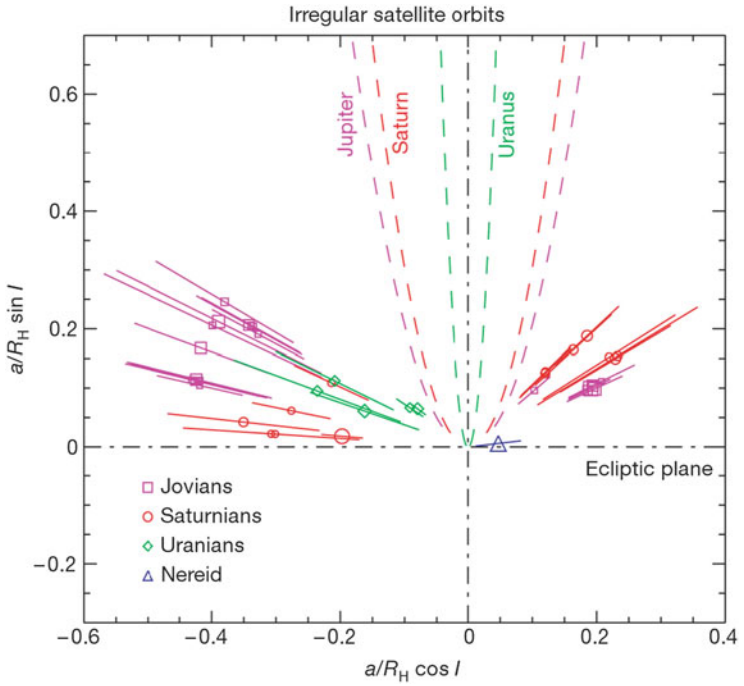

Fig. 5.1 The irregular moons (known up to 2002) of Jupiter, Saturn, Uranus, and Neptune, presented in "polar coordinates": the angular position (with respect to the horizontal axis) of a satellite in the diagram is equal to the satellite's inclination i to the ecliptic plane, and the radial position is equal to the satellite's orbital semimajor axis a in units of the parent planet's Hill radius R_H. The center-pointing straight line intervals represent the pericenter–apocenter variations in the orbital radii. The symbol size characterizes physical sizes of the moons, namely, diameters in the logarithmic scale. The moons on the right side of the diagram are prograde, and those on the left side are retrograde. A broad gap in the inclinations, centered on $i = 90°$, is evident. The *dashed curves* indicate the borders of the regions where any satellite in a close-to-polar orbit is removed by the LKE (Figure 1 from Gladman et al. (2001). With permission from Nature Publishing Group)

may increase up to $Q \sim R_{\rm H}$ (the Hill radius), where Solar perturbations destabilize the orbit.

At present, this cosmogonical process is over: Nesvorný et al. (2003) performed long-term numerical integrations of the orbits of all known (at that time) irregulars, taking into account all relevant perturbations, and showed that the known irregular moons are dynamically long-lived.

5.2 Jovian System

Jupiter has 59 irregulars, among them only 7 prograde (see Table 5.2). They form several swarms consisting of moons with similar orbital elements. For example, the Himalia group comprises five moons with semimajor axes $a \sim 0.2 R_{\rm H}$ (where $R_{\rm H}$ is Jupiter's Hill radius, $R_{\rm H} = 51$ mln km $= 0.34$ AU), eccentricities $e \sim 0.2$, and inclinations $i \sim 30°$ (see Table 5.2). This similarity certifies their common (most probably collisional) origin. The Ananke, Carme, and Pasiphae groups contain moons of smaller physical sizes, but comprise more than a dozen members each.

Note that the inclination values cited in this chapter for irregulars of all planets are all measured with respect to the local *Laplace plane*, defined in Sect. 3.4. Irregulars usually have orbits much greater in size than the *Laplace radius* (also defined in Sect. 3.4; for its specific planetary values see Table 5.1). At such large distances, the Laplace plane coincides approximately with the ecliptic plane.

Carruba et al. (2002) performed massive numerical experiments, integrating orbits of a variety of hypothetical Jovian satellites on a long timescale (10^9 years). It turned out that the LKE due to the Solar perturbations plays the most prominent role in the secular orbital evolution, either driving the pericenters of the satellites with $70° \lesssim i \lesssim 110°$ into the domain of massive regulars (where the satellites are eliminated on the timescale of 10^7–10^9 years, due to collisions or gravitational scattering), or driving the apocenters of the satellites out of the planet's Hill sphere. When one takes into account all relevant perturbations, the gap broadens up to $55° \lesssim i \lesssim 130°$ (from $\sim 70° \lesssim i \lesssim 110°$).

Thus, the LKE has produced a major "footprint" in the global orbital architecture of the Jovian irregulars. What is more, the LKE seems to be still operational in the orbital dynamics of some of them. Namely, the secular dynamics of the Jovian moon J34 Euporie seems to be controlled by the LKE, the pericenter argument ω librating around 90° with the full amplitude of 60°, nearly constant over 10^8 years (Nesvorný et al. 2003).

Besides, according to Carruba et al. (2002), there exists a "stable phase space" with orbits surviving on the timescale of 10 Myr for any moon trapped in the LK-resonance (i.e., a moon with the pericenter locked in libration around $\pm 90°$). It contains $\sim$10 % of all stable orbits, suggesting that at high inclinations there may exist moons that have not yet been discovered.

Based on analytical (in the framework of the double-averaged Hill problem), numerical (direct numerical integrations), and numerical-analytical approaches,

Table 5.2 Irregular moons of Jupiter

Satellite	a (km)	e	i (°)	D (km)
JXVIII Themisto	7,393,216	0.2115	45.762	8
JXIII Leda	11,187,781	0.1673	27.562	16
JVI Himalia	11,451,971	0.1513	30.486	170
JX Lysithea	11,740,560	0.1322	27.006	36
JVII Elara	11,778,034	0.1948	29.691	86
JLIII Dia	12,570,424	0.2058	27.584	4
JXLVI Carpo	17,144,873	0.2735	56.001	3
S/2003 J12	17,739,539	0.4449	142.680	1
JXXXIV Euporie	19,088,434	0.0960	144.694	2
S/2003 J3	19,621,780	0.2507	146.363	2
S/2003 J18	19,812,577	0.1569	147.401	2
S/2011 J1	20,155,290	0.2963	162.8	1
JLII S/2010 J2	20,307,150	0.307	150.4	1
JXLII Thelxinoe	20,453,753	0.2684	151.292	2
JXXXIII Euanthe	20,464,854	0.2000	143.409	3
JXLV Helike	20,540,266	0.1374	154.586	4
JXXXV Orthosie	20,567,971	0.2433	142.366	2
JXXIV Iocaste	20,722,566	0.2874	147.248	5
S/2003 J16	20,743,779	0.3184	150.769	2
JXXVII Praxidike	20,823,948	0.1840	144.205	7
JXXII Harpalyke	21,063,814	0.2440	147.223	4
JXL Mneme	21,129,786	0.3169	149.732	2
JXXX Hermippe	21,182,086	0.2290	151.242	4
JXXIX Thyone	21,405,570	0.2525	147.276	4
JXII Ananke	21,454,952	0.3445	151.564	28
JL Herse	22,134,306	0.2379	162.490	2
JXXXI Aitne	22,285,161	0.3927	165.562	3
JXXXVII Kale	22,409,207	0.2011	165.378	2
JXX Taygete	22,438,648	0.3678	164.890	5
S/2003 J19	22,709,061	0.1961	164.727	2
JXXI Chaldene	22,713,444	0.2916	167.070	4
S/2003 J15	22,720,999	0.0932	141.812	2
S/2003 J10	22,730,813	0.3438	163.813	2
S/2003 J23	22,739,654	0.3930	148.849	2
JXXV Erinome	22,986,266	0.2552	163.737	3
JXLI Aoede	23,044,175	0.6011	160.482	4
JXLIV Kallichore	23,111,823	0.2041	164.605	2
JXXIII Kalyke	23,180,773	0.2139	165.505	5
JXI Carme	23,197,992	0.2342	165.047	46
JXVII Callirrhoe	23,214,986	0.2582	139.849	9
JXXXII Eurydome	23,230,858	0.3769	149.324	3

(continued)

Table 5.2 (continued)

Satellite	a (km)	e	i (°)	D (km)
S/2011 J2	23,329,710	0.3867	151.8	1
JXXXVIII Pasithee	23,307,318	0.3288	165.759	2
JLI S/2010 J1	23,314,335	0.320	163.2	2
JXLIX Kore	23,345,093	0.1951	137.371	2
JXLVIII Cyllene	23,396,269	0.4115	140.148	2
JXLVII Eukelade	23,483,694	0.2828	163.996	4
S/2003 J4	23,570,790	0.3003	147.175	2
JVIII Pasiphae	23,609,042	0.3743	141.803	60
JXXXIX Hegemone	23,702,511	0.4077	152.506	3
JXLIII Arche	23,717,051	0.1492	164.587	3
JXXVI Isonoe	23,800,647	0.1775	165.127	4
S/2003 J9	23,857,808	0.2761	164.980	1
S/2003 J5	23,973,926	0.3070	165.549	4
JIX Sinope	24,057,865	0.2750	153.778	38
JXXXVI Sponde	24,252,627	0.4431	154.372	2
JXXVIII Autonoe	24,264,445	0.3690	151.058	4
JXIX Megaclite	24,687,239	0.3077	150.398	5
S/2003 J2	30,290,846	0.1882	153.521	2

Notes: The Table is compiled based on data given in the JPL Small-Body Database (http://ssd.jpl.nasa.gov/). Real and probable ω-librators are distinguished in bold font

Vashkovyak and Teslenko (2008a) performed a systematic study of the orbital evolution of all irregulars of Jupiter, known up to 2008, and inferred that the Jovian moon J46 Carpo satisfied the Lidov-Kozai *resonance conditions* $c_1 < 3/5$ and $c_2 < 0$ (Vashkovyak 1999, 2005), where the classical integrals

$$c_1 = (1 - e^2)\cos^2 i, \tag{5.4}$$

$$c_2 = e^2\left(\frac{2}{5} - \sin^2 i \sin^2 \omega\right) \tag{5.5}$$

(see Equations (3.23) and (3.24) or (5.4) and (5.5)). In the diagrams "i–ω" and "i–e" (Fig. 5.2), J46 Carpo is clearly identifiable as an ω-librator. Satellites J34 Euporie, J49 Kore, and S/2003 J3 are very close to ω-libration. By means of monitoring the long-term behaviour of the pericenter argument, Vashkovyak and Teslenko (2008a) identified J18 Themisto as another ω-librator.

Using new precise data on initial values of elements, Emelyanov and Vashkovyak (2012) performed direct numerical integrations of non-averaged equations of motion on timescales of several thousand years and showed that J34 Euporie and J46 Carpo were indeed in ω-libration, whereas J18 Themisto and J49 Kore circulated.

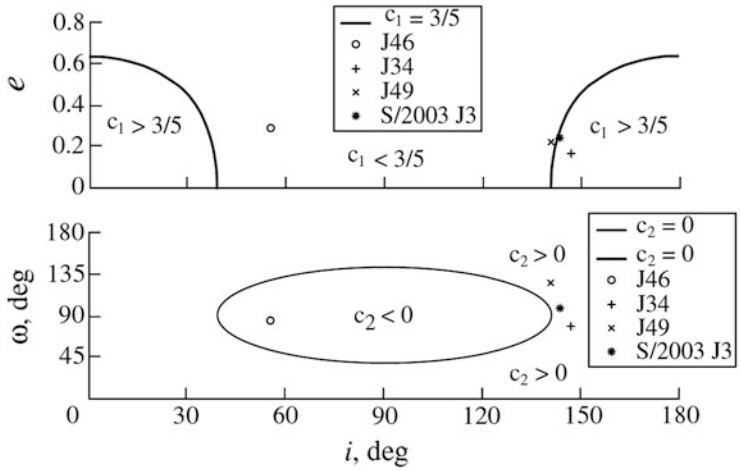

Fig. 5.2 The irregulars of Jupiter in the planes of initial conditions (i_0, e_0) and (i_0, ω_0). The symbols designate moons, and the curves trace constant values of c_1 (in the *upper panel*) and c_2 (in the *lower panel*). Omega-librators are identified (Figure 55 from Vashkovyak and Teslenko (2008a). With permission from Pleiades Publishing Inc)

Thus, at least four Jovian moons reside in LK-resonance or are close to it at present. In Table 5.2, those Jovian satellites that are observed to be in ω-libration, or close to this state, are distinguished in bold font.

5.3 Saturnian System

Saturn has 38 irregulars, among which only 9 are prograde (see Table 5.3). In total, Saturn's irregulars have semimajor axes in the range 0.16–0.36$R_{\rm H}$, where Saturn's Hill radius $R_{\rm H} = 69$ mln km $= 0.46$ AU. The Saturnian irregulars form three swarms of moons with similar orbital elements, namely, the Inuit, Norse, and Gallic groups. Some of them were shown to be remnants (most likely) of larger objects, captured by the planet and then collisionally disrupted (Gladman et al. 2001).

In the framework of the double-averaged Hill problem, Vashkovyak (2001) identified ω-libration in the long-term behaviour of S20 Paaliaq, S22 Ijiraq, S24 Kiviuq, and S29 Siarnaq. However, the phase trajectories of S20 Paaliaq and S29 Siarnaq in the "ω–e" plane were too close to the LK-separatrix (i.e., $c_2 \approx 0$ for them), and in a more precise model of evolution they turned out to circulate (Vashkovyak 2003).

Nesvorný et al. (2003) performed direct numerical integrations of orbits of the Saturnian moons, monitoring the behaviour of various resonance angles allowed by the D'Alembert rules (defined, e.g., in Morbidelli 2002; see also Ferraz-Mello 2007; Kholshevnikov 1997, 2001). The Lidov-Kozai resonance angle (the pericenter

Table 5.3 Irregular moons of Saturn

Satellite	a (km)	e	i (°)	D (km)
SXXIV Kiviuq	11,294,800	0.3288	49.087	16
SXXII Ijiraq	11,355,316	0.3161	50.212	12
SIX Phoebe	12,869,700	0.156242	173.047	213
SXX Paaliaq	15,103,400	0.3631	46.151	22
SXXVII Skathi	15,672,500	0.246	149.084	8
SXXVI Albiorix	16,266,700	0.477	38.042	32
S/2007 S2	16,560,000	0.2418	176.68	6
SXXXVII Bebhionn	17,153,520	0.333	40.484	6
SXXVIII Erriapus	17,236,900	0.4724	38.109	10
SXLVII Skoll	17,473,800	0.418	155.624	6
SXXIX Siarnaq	17,776,600	0.24961	45.798	40
SLII Tarqeq	17,910,600	0.1081	49.904	7
S/2004 S13	18,056,300	0.261	167.379	6
SLI Greip	18,065,700	0.3735	172.666	6
SXLIV Hyrrokkin	18,168,300	0.3604	153.272	8
SL Jarnsaxa	18,556,900	0.1918	162.861	6
SXXI Tarvos	18,562,800	0.5305	34.679	15
SXXV Mundilfari	18,725,800	0.198	169.378	7
S/2006 S1	18,930,200	0.1303	154.232	6
S/2004 S17	19,099,200	0.226	166.881	4
SXXXVIII Bergelmir	19,104,000	0.152	157.384	6
SXXXI Narvi	19,395,200	0.320	137.292	7
SXXIII Suttungr	19,579,000	0.131	174.321	7
SXLIII Hati	19,709,300	0.291	163.131	6
S/2004 S12	19,905,900	0.396	164.042	5
SXL Farbauti	19,984,800	0.209	158.361	5
SXXX Thrymr	20,278,100	0.453	174.524	7
SXXXVI Aegir	20,482,900	0.237	167.425	6
S/2007 S3	20,518,500	0.130	177.22	5
SXXXIX Bestla	20,570,000	0.5145	147.395	7
S/2004 S7	20,576,700	0.5299	165.596	6
S/2006 S3	21,076,300	0.4710	150.817	6
SXLI Fenrir	21,930,644	0.131	162.832	4
SXLVIII Surtur	22,288,916	0.3680	166.918	6
SXLV Kari	22,321,200	0.3405	148.384	7
SXIX Ymir	22,429,673	0.3349	172.143	18
SXLVI Loge	22,984,322	0.1390	166.539	6
SXLII Fornjot	24,504,879	0.186	167.886	6

Note: The Table is compiled based on data given in the JPL Small-Body Database (http://ssd.jpl.nasa.gov/). Real and probable ω-librators are distinguished in bold font

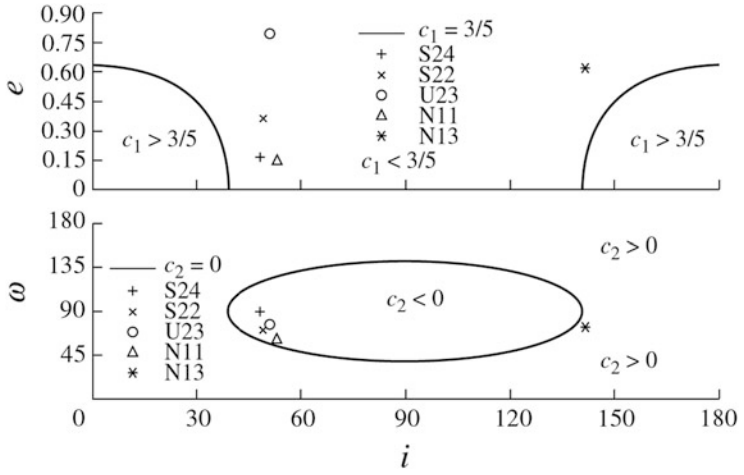

Fig. 5.3 The irregulars of Saturn, Uranus, and Neptune in the planes of initial conditions (i_0, e_0) and (i_0, ω_0). The symbols designate moons, and the curves trace constant values of c_1 (in the *upper panel*) and c_2 (in the *lower panel*). Omega-librators are identified (Figure 53 from Vashkovyak and Teslenko (2008b). With permission from Pleiades Publishing Inc)

argument) was monitored in particular. It was found that the LKE controls the secular orbital dynamics of two Saturnian moons, namely, S22 Ijiraq and S24 Kiviuq: the pericenter argument ω librates in both cases around 90° with the full amplitude of 60°, nearly constant over 10^8 years, certifying that this resonant behaviour is very likely primordial.

Vashkovyak and Teslenko (2008b) integrated numerically the orbits of all irregulars of Saturn, known up to 2008, and confirmed that the moons S22 Ijiraq and S24 Kiviuq satisfied the Lidov-Kozai resonance conditions $c_1 < 3/5$ and $c_2 < 0$ (Equations (3.23) and (3.24) or (5.4) and (5.5)). In the diagrams "i–ω" and "i–e" (Fig. 5.3), the ω-librators are identified. One can see that S20 Paaliaq is close to ω-libration. In Table 5.3, those Saturnian satellites that are observed to be in ω-libration, or close to this state, are distinguished in bold font.

5.4 Uranian and Neptunian Systems

The Uranian and Neptunian systems are mutually similar, but they are not like those described above. The major difference in comparison with the Jovian and Saturnian systems is that the instabilities due to the LKE occur in a narrower inclination range.

Uranus has nine irregulars, all retrograde except one (U23 Margaret, see Table 5.4). Their semimajor axes are in the range 0.06–0.29R_H, where Uranus's Hill radius $R_H = 73$ mln km $= 0.49$ AU. In contrast to the Jovian and Saturnian systems, a large and uniform spread of the moons in the semimajor axis does not

Table 5.4 Irregular moons of Uranus

Satellite	a (km)	e	i (°)	D (km)
UXXII Francisco	4,276,000	0.1459	147.459	22
UXVI Caliban	7,230,000	0.1587	139.885	72
UXX Stephano	8,002,000	0.2292	141.873	32
UXXI Trinculo	8,571,000	0.2200	166.252	18
UXVII Sycorax	12,179,000	0.5224	152.456	150
UXXIII Margaret	14,345,000	0.6608	51.455	20
UXVIII Prospero	16,418,000	0.4448	146.017	50
UXIX Setebos	17,459,000	0.5914	145.883	48
UXXIV Ferdinand	20,900,000	0.3682	167.346	20

Note: The Table is compiled based on data given in the JPL Small-Body Database (http://ssd.jpl.nasa.gov/). Real and probable ω-librators are distinguished in bold font

Table 5.5 Irregular moons of Neptune

Satellite	a (km)	e	i (°)	D (km)
NII Nereid	5,513,818	0.7507	7.090	340
NIX Halimede	16,611,000	0.2646	112.898	62
NXI Sao	22,228,000	0.1365	49.907	44
NXII Laomedeia	23,567,000	0.3969	34.049	42
NX Psamathe	48,096,000	0.3809	137.679	40
NXIII Neso	49,285,000	0.5714	131.265	60

Note: The Table is compiled based on data given in the JPL Small-Body Database (http://ssd.jpl.nasa.gov/). Real and probable ω-librators are distinguished in bold font

allow one to identify any clustering that would suggest a common origin for a group of objects; i.e., the Uranian moons, most probably, have formed independently from each other.

Neptune has 6 irregulars, among which 3 are prograde and 3 retrograde (see Table 5.5), with semimajor axes 0.05–0.42$R_{\rm H}$, where Neptune's Hill radius $R_{\rm H} = 116$ mln km $= 0.78$ AU. Neptune's most famous (due to its record eccentricity $e \approx 0.75$) irregular moon N2 Nereid is prograde. Goldreich et al. (1989) suggested that Nereid's high eccentricity is due to perturbations of formerly captured Triton. While migrating, Triton might have also disrupted orbits of other satellites of Neptune, if they have ever existed.

The orbital distributions of the Uranian and Neptunian moons (except two Neptunian moons N9 Halimede and N11 Sao) are consistent with the broad gap in the compiled inclination distribution[4] of the known irregulars in the Jovian and Saturnian systems: no object has inclination in the range between $\approx 50°$ and $\approx 140°$. Again, a plausible explanation is that most orbits with $i \sim 90°$ are unstable due to the LKE (Carruba et al. 2002; Nesvorný et al. 2003).

[4] With respect to the ecliptic plane.

Vashkovyak and Teslenko (2008b) integrated numerically the orbits of all irregulars of Uranus and Neptune, known up to 2008, and inferred that U23 Margaret and N11 Sao satisfied the Lidov-Kozai resonance conditions $c_1 < 3/5$ and $c_2 < 0$. In the diagrams "i–ω" and "i–e" (Fig. 5.3), the ω-librators are identified. N13 Neso is apparently close to ω-libration. In Tables 5.4 and 5.5, those Uranian and Neptunian satellites that are observed to be in ω-libration, or close to this state, are distinguished in bold font.

Finally, note that if an additional perturbation dominates over the LK-term in the Hamiltonian of the motion, then the LKE may be quenched, as discussed above in Sect. 3.3. Such a suppression explains, e.g., the stable existence of *regular* satellites of Uranus (Lidov 1963b). The regular Uranian moons move in orbits close to the planet's equatorial plane, which is inclined by 98° with respect to the orbital plane. The LKE driven by Solar perturbations would enforce the satellites to fall onto the planet, but this does not occur because the frequencies of orbital precession (caused by the planet's oblateness and mutual perturbations between the moons) are large enough to suppress the LKE.

Chapter 6
Sungrazing Comets

. . . fatal phare
Des vols migrateurs des plaintifs Icares!

Jules Laforgue, *Clair de Lune*

The importance of the LKE in the cometary dynamics was first studied by Kozai (1979, 1980). In the following years, the theme was thoroughly developed, in particular, in works of Quinn et al. (1990), Bailey et al. (1992), and Thomas and Morbidelli (1996). Perhaps, the most spectacular LKE consequence that was revealed is that the LKE may make comets collide with the Sun; just in the same manner as it forced *Luna*-3 (see Chap. 1) to collide with the Earth.

The phenomenon of comets colliding with the Sun is directly observed: in fact, many such collisions have been monitored by the *SOHO* spacecraft. These collisions take place because many highly-eccentric comets, in the course of their secular orbital evolution, become *sungrazing*, i.e., their pericentric distances become close to the radius of the Sun. Most of the observed sungrazers are extremely-eccentric long-period comets. For instance, the spectacular comet 1965 VIII Ikeya–Seki (Great Comet of 1965, which, due to its close approach to Sun, reached the visual magnitude of minus ten and was visible in daytime) is, in fact, a sungrazer.

In the course of an LK-cycle, the eccentricity of a comet, moving under the perturbation of Jupiter and other giant planets, can be boosted, while the semimajor axis stays constant. Thus, the perihelion distance radically decreases, and the comet becomes sungrazing. Bailey et al. (1992), using the Kozai diagram techniques (discussed further on), established that the LKE can effectively produce a lot of sungrazing comets.

Tantalizingly, the reservoir for the long-period comets, the Oort cloud, was formed (billions years ago) most probably also by an LK-mechanism (Duncan et al. 1987): planetesimals were scattered by giant planets to distances of thousands astronomical units from the Sun, where they suffered perturbations by the so-called *Galactic tide*, operating due to the Galactic-plane matter concentration. The corresponding LKE acted to decrease their eccentricities, thus forming the cloud.

I. I. Shevchenko, *The Lidov-Kozai Effect – Applications in Exoplanet Research and Dynamical Astronomy*, Astrophysics and Space Science Library 441,
DOI 10.1007/978-3-319-43522-0_6

Yet another point is that the LK-mechanism due to the Galactic tide also acts to "borrow" comets from the Oort cloud, thus delivering matter to the inner Solar system, where the comets may become sungrazers and be disrupted by the Sun in its vicinities; and their matter is dispersed in the interplanetary space. Thus, the LK-mechanism worked and works independently *thrice* (forming the Oort cloud, borrowing comets from the Oort cloud, producing sungrazers from the borrowed comets), in sum realizing the delivery of the primordial matter to the inner Solar system.

In this chapter we show how simple analytic considerations of the LK-dynamics provide understanding for the origin of the cometary sungrazers and their pre-impact secular evolution.

6.1 Cometary Dynamics Subject to LKE

Before we consider the cometary motion subject to the LKE, it is instructive to recall some relevant properties of the motion in the non-averaged restricted three-body problem, namely, the properties concerning the Jacobi integral and Tisserand relation.

6.1.1 The Jacobi Integral and Tisserand Relation

In the restricted three-body problem (R3BP), a massless particle moves in the gravitational field of two bodies ("primaries") with masses $m_0 \geq m_1$. In the *circular* R3BP, the orbits of the primaries around their center of masses are circular.

Due to the zero mass of the particle, neither energy nor angular momentum is conserved in the restricted problem[1]; but in the circular R3BP there exists a constant of motion, the *Jacobi integral*, or *Jacobi constant*, which is a combination of these two entities.

Hereafter, we adopt the mass unit such that $\mathcal{G}(m_0 + m_1) = 1$ (where $\mathcal{G}$ is the gravitational constant), and define the mass parameter $\mu = m_1/(m_0 + m_1)$. The unit of length is such that the (constant) distance between the primaries is unity. Therefore, the mean motion of each primary $n_{\rm prim} \equiv n_0 = n_1 = 1$.

Let us denote the inertial (*siderial*) orthogonal barycentric frame (ξ, η, ζ): at the initial epoch ($t = 0$), the ξ axis is directed from body m_0 to body m_1, the η axis is in the orbital plane of the primaries and perpendicular to the ξ axis, the ζ axis is normal to the orbital plane of the primaries and co-directed with the angular momentum vector. The primaries' coordinates are (ξ_0, η_0, ζ_0) and (ξ_1, η_1, ζ_1), those of the particle (ξ, η, ζ) are not indexed.

[1] For a discussion of this non-conservation see Szebehely (1967).

The equations of motion of a test particle in the gravitational field of two bodies (e.g., the Sun and Jupiter) are given by

$$\ddot{\xi} = (1-\mu)\frac{\xi_0 - \xi}{r_{0\mathrm{p}}^3} + \mu\frac{\xi_1 - \xi}{r_{1\mathrm{p}}^3}, \tag{6.1}$$

$$\ddot{\eta} = (1-\mu)\frac{\eta_0 - \eta}{r_{0\mathrm{p}}^3} + \mu\frac{\eta_1 - \eta}{r_{1\mathrm{p}}^3}, \tag{6.2}$$

$$\ddot{\zeta} = (1-\mu)\frac{\zeta_0 - \zeta}{r_{0\mathrm{p}}^3} + \mu\frac{\zeta_1 - \zeta}{r_{1\mathrm{p}}^3}, \tag{6.3}$$

where

$$r_{0\mathrm{p}}^2 = (\xi_0 - \xi)^2 + (\eta_0 - \eta)^2 + (\zeta_0 - \zeta)^2, \tag{6.4}$$

$$r_{1\mathrm{p}}^2 = (\xi_1 - \xi)^2 + (\eta_1 - \eta)^2 + (\zeta_1 - \zeta)^2 \tag{6.5}$$

are the squares of the distances "Sun–particle" and "Jupiter–particle", respectively.

Now consider the non-inertial rotating barycentric frame (x, y, z) in which the primaries stand still, i.e., the frame's angular velocity is n_{prim}. This is the so-called *synodic* frame. The x axis is directed from m_0 to m_1; thus, the primaries' coordinates are $(x_0, y_0, z_0) = (-\mu, 0, 0)$ and $(x_1, y_1, z_1) = [(1-\mu), 0, 0]$. The particle's coordinates are (x, y, z).

Rewriting the equations of motion in the synodic system (see, e.g. Murray and Dermott 1999), one obtains

$$\ddot{x} - 2n_{\mathrm{prim}}\dot{y} - n_{\mathrm{prim}}^2 x = -\left[(1-\mu)\frac{x+\mu}{r_{0\mathrm{p}}^3} + \mu\frac{x-1+\mu}{r_{1\mathrm{p}}^3}\right], \tag{6.6}$$

$$\ddot{y} + 2n_{\mathrm{prim}}\dot{x} - n_{\mathrm{prim}}^2 y = -\left[\frac{1-\mu}{r_{0\mathrm{p}}^3} + \frac{\mu}{r_{1\mathrm{p}}^3}\right] y, \tag{6.7}$$

$$\ddot{z} = -\left[\frac{1-\mu}{r_{0\mathrm{p}}^3} + \frac{\mu}{r_{1\mathrm{p}}^3}\right] z, \tag{6.8}$$

where

$$r_{0\mathrm{p}}^2 = (x+\mu)^2 + y^2 + z^2, \tag{6.9}$$

$$r_{1\mathrm{p}}^2 = [x-1+\mu]^2 + y^2 + z^2. \tag{6.10}$$

Introducing the *potential*

$$U(x,y,z) = \frac{n_{\text{prim}}^2}{2}\left(x^2+y^2\right) + \frac{1-\mu}{r_{0\text{p}}} + \frac{\mu}{r_{1\text{p}}}, \tag{6.11}$$

one can arrange the equations of motion in the form

$$\ddot{x} - 2n_{\text{prim}}\dot{y} = \frac{\partial U}{\partial x}, \tag{6.12}$$

$$\ddot{y} + 2n_{\text{prim}}\dot{x} = \frac{\partial U}{\partial y}, \tag{6.13}$$

$$\ddot{z} = \frac{\partial U}{\partial z}. \tag{6.14}$$

Multiplying Equations (6.12), (6.13), and (6.14) by $\dot{x}$, $\dot{y}$, and $\dot{z}$, respectively, and combining, one has

$$\dot{x}\ddot{x} + \dot{y}\ddot{y} + \dot{z}\ddot{z} = \frac{\partial U}{\partial x}\dot{x} + \frac{\partial U}{\partial y}\dot{y} + \frac{\partial U}{\partial z}\dot{z} = \frac{\mathrm{d}U}{\mathrm{d}t} \tag{6.15}$$

and, after integration,

$$\dot{x}^2 + \dot{y}^2 + \dot{z}^2 = 2U - C_{\text{J}}, \tag{6.16}$$

where C_{J} is the integration constant, called the *Jacobi integral*, or *Jacobi constant*.

Transforming the synodic coordinates x, y, z to the siderial ones ξ, η, ζ (see, e.g. Murray and Dermott 1999; Szebehely 1967), one obtains an expression for C_{J} in the inertial frame:

$$C_{\text{J}} = 2\left[\frac{1-\mu}{r_{0\text{p}}} + \frac{\mu}{r_{1\text{p}}}\right] + 2n_{\text{prim}}(\xi\dot{\eta} - \eta\dot{\xi}) - \dot{\xi}^2 - \dot{\eta}^2 - \dot{\zeta}^2, \tag{6.17}$$

representing a combination of the energy and the vertical component of the angular momentum, any of which is not conserved separately.

Since the work by Tisserand (1896), the Jacobi constant formalism has important applications in cometary dynamics.

Let a comet suffer a distant encounter with Jupiter. Before the encounter, its semimajor axis, eccentricity, and inclination are designated by a, e, and i, and after the encounter by $\tilde{a}$, $\tilde{e}$, and $\tilde{i}$. In the siderial frame, the Jacobi constant C_{J} is given by Equation (6.17), where $r_{0\text{p}}$ and $r_{1\text{p}}$ are the distances "comet–Sun" and "comet–Jupiter", respectively. In our unit system, the distance "Sun–Jupiter" is unity, $n_{\text{prim}} = 1$, and $\mathcal{G}\left(m_{\text{Sun}} + m_{\text{Jupiter}}\right) = 1$. Jupiter's eccentricity is set to zero. The barycentric position and velocity vectors of the comet are $\boldsymbol{\rho} \equiv (\xi, \eta, \zeta)$ and $\dot{\boldsymbol{\rho}} \equiv (\dot{\xi}, \dot{\eta}, \dot{\zeta})$.

Since $m_{\text{Jupiter}} \ll m_{\text{Sun}}$, one can use, in approximation, the energy integral of the two-body problem "Sun–comet"

$$\dot{\xi}^2 + \dot{\eta}^2 + \dot{\zeta}^2 \approx \frac{2}{\rho} - \frac{1}{a}, \tag{6.18}$$

where the "comet–barycenter" distance ρ $(= \|\boldsymbol{\rho}\|)$ is approximately equal to the heliocentric "comet–Sun" distance $r_{0\text{p}}$. The angular momentum (per unit mass) $\mathbf{h}$ of the comet is equal to the vector product $\boldsymbol{\rho} \times \dot{\boldsymbol{\rho}}$, and its vertical component is given by

$$\xi\dot{\eta} - \eta\dot{\xi} = h\cos i, \tag{6.19}$$

where $h = \|\boldsymbol{\rho} \times \dot{\boldsymbol{\rho}}\| = \left[(1-e^2)a\right]^{1/2}$ and i is the inclination with respect to Jupiter's orbital plane. Then Equation (6.17) for the Jacobi constant gives:

$$\frac{1}{a} + 2\left[(1-e^2)a\right]^{1/2}\cos i = 2\mu\left(\frac{1}{\rho} - \frac{1}{r_{1\text{p}}}\right) + C_{\text{J}}. \tag{6.20}$$

Ignoring the terms with μ and also assuming that the "comet–Jupiter" distance $r_{1\text{p}}$ does not acquire too small values (i.e., the encounter is not too close), one has

$$\frac{1}{2a} + \left[(1-e^2)a\right]^{1/2}\cos i \approx \text{const}. \tag{6.21}$$

Therefore,

$$\frac{1}{2a} + \left[(1-e^2)a\right]^{1/2}\cos i \approx \frac{1}{2\tilde{a}} + \left[(1-\tilde{e}^2)\tilde{a}\right]^{1/2}\cos\tilde{i} \tag{6.22}$$

before and after the encounter.

Equation (6.22) is called the *Tisserand relation*. It was proposed by Tisserand (1896) to provide an easy instrument for the observational identification of comets: due to an encounter, the orbital elements of a comet may change considerably, but the Tisserand relation allows one to certify that the old and new elements correspond to one and the same object.

The Tisserand parameter

$$C_{\text{T}} \equiv \frac{1}{2a} + \left[(1-e^2)a\right]^{1/2}\cos i \tag{6.23}$$

is approximately conserved also if the perturber's eccentricity is moderately non-zero. This fact is illustrated in the graph of C_{T} as a function of time, in Fig. 6.1, constructed by Murray and Dermott (1999) by numerical integration of the equations of motion for the case of Jupiter's zero eccentricity (the lower curve in the Figure) and for the case of Jupiter's current eccentricity $e_{\text{Jupiter}} = 0.048$ (the upper

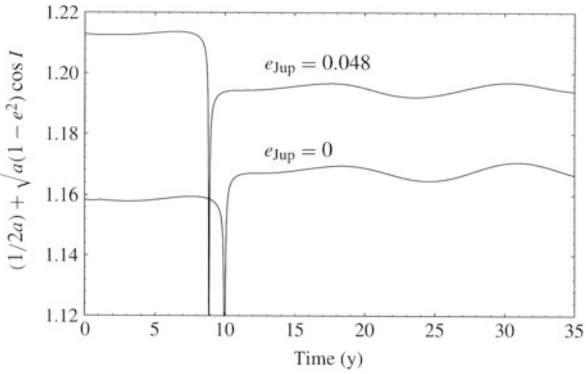

Fig. 6.1 The time dependence of the Tisserand "constant" $C_{\rm T}$ in two cases of the perturber's eccentricity ($e_{\rm Jupiter} = 0$ and 0.048) (Figure 3.4 from Murray and Dermott 1999. With permission from Cambridge University Press)

curve in the Figure). Except for a short time interval at the close approach, the net variation of $C_{\rm T}$ due to the encounter is less than 1 % and 2 % in the first and second cases, respectively.

In the planar ($i = 0$) circular restricted three-body problem, relation (6.21) takes the form

$$\frac{1}{2a} + \left[(1-e^2)a\right]^{1/2} \approx \text{const.} \tag{6.24}$$

Recall that a is measured in units of the perturber's semimajor axis. If $a \gg 1$ and $e \sim 1$, one has

$$\frac{1}{2a} + \left[(1+e)q\right]^{1/2} \approx 2^{1/2} q^{1/2} \approx \text{const.} \tag{6.25}$$

Therefore, q is approximately conserved for a highly eccentric particle orbiting a small inner binary, if the orbits of the particle and the binary are coplanar (Shevchenko 2015). In other words, the angular momentum is approximately conserved (the relative variations are small), whereas the energy may substantially vary (the relative variations may be large). This circumstance forms the basis for construction of the so-called *Kepler map*, which is an analogue of the *separatrix map*: while the latter describes the motion in the vicinity of the separatrix of a perturbed non-linear pendulum (and, generally, a perturbed non-linear resonance; see Chirikov 1979; Shevchenko 2000), the former describes the perturbed motion in the vicinity of the parabolic orbit, which is the separatrix between the bound and unbound states of the particle's motion (Shevchenko 2011b).

Note that the conservation of q for a highly-eccentric circumbinary particle in the hierarchical planar problem is different from what is known to take place in the secular planetary problem (where eccentricities are small) and in the LKE (where inclinations are high): there, on the contrary, the semimajor axis is secularly conserved, while the total angular momentum may vary.

Apart from the limiting cases, the elements a, e, and i may all vary substantially, being subject only to the Jacobi integral conservation. The Jacobi integral formalism is valid on the both orbital and secular timescales, because it does not imply any averaging. It follows from expression (6.23) for the Tisserand parameter, that, if the particle's semimajor axis a is conserved on the secular timescale, then the vertical component of the angular momentum is also conserved, and one has the LK integral c_1 (see formula (3.23) or (5.4)). Thus, the averaging acts to decouple the variations in the energy and in the vertical component of the angular momentum, "splitting" the Jacobi integral into two new ones: the semimajor axis a and the LK integral c_1.

6.1.2 Comets in Highly Inclined Orbits

It follows from the LK integral c_1, given by formula (3.23), that over a half LK-cycle the eccentricity of a comet, moving in an inclined orbit under the perturbation of Jupiter (and other giant planets), can be substantially pumped, while the semimajor axis stays constant. Thus, the perihelion distance of the comet may radically decrease, and the comet may become sungrazing.

That the LKE may invoke such a kind of collisions was, in fact, revealed as early as in 1961 by Lidov in his pioneer paper (Lidov 1961), in the beginning of which he described the orbital behaviour of the space probe *Luna*-3, launched to an orbit highly-inclined with respect to the ecliptic plane. *Luna*-3 became an "Earth-grazer" in eleven orbital revolutions. Thus, the "planet-grazing" phenomenon is known to be a spectacular consequence of the LKE since 1961.

On the other hand, Kozai as early as in 1962 (Kozai 1962) demonstrated how changes of the eccentricity and inclination of a minor body in the gravitational field of the Sun and Jupiter are secularly correlated due to conservation of an integral of motion (which is called now the Lidov-Kozai integral, see formula (3.23) or (5.4)). He found out that the variations of the eccentricity might be huge, and, due to the secular conservation of the semimajor axis, might lead to huge changes of the body's pericentric and apocentric distances (the eccentricity e being maximum when the inclination i is minimum, and vice versa).

The ω-libration, which takes place at the test particle's high enough inclinations, is often interpreted as a kind of secular resonance, called the *Lidov-Kozai resonance* (see, e.g. Morbidelli 2002; Murray and Dermott 1999). However, it does not concern any eugenfrequency of the Solar system, as other well-known secular resonances do, as discussed in the next section. The LK-resonance means that the averaged $\dot{\omega}$ is zero, i.e., $\dot{\varpi} = \dot{\Omega}$, where ϖ and Ω are, respectively, the longitude of pericenter and the longitude of ascending node of the test body. This condition can be fulfilled merely for the orbits inclined enough. In fact, an asteroid or a comet with small eccentricity and inclination has $\dot{\varpi} \approx -\dot{\Omega}$ (see, e.g. Murray and Dermott 1999, p. 316).

Table 6.1 Data on prominent comets

Comet	τ	q (AU)	e	i (°)
1P/Halley	1986 Feb 05.9	0.5860	0.9671	162.26
8P/Tuttle	2008 Jan 27.0	1.0271	0.8198	54.98
67P/Churyumov–Gerasimenko	2015 Aug 13.1	1.2432	0.6410	7.04
96P/Machholz 1	2012 Jul 14.8	0.1237	0.9592	58.31
109P/Swift–Tuttle	1992 Dec 12.0	0.9595	0.9632	113.45
C/1843 D1 Great March comet	1843 Feb 27.9	0.005527	0.999914	144.35
C/1965 S1-A Ikeya–Seki	1965 Oct 21.2	0.007786	0.999915	141.86
C/1965 S1-B Ikeya–Seki	1965 Oct 21.2	0.007778	0.999925	141.86
C/1969 Y1 Bennett	1970 Mar 20.0	0.5376	0.9962	90.04
C/1973 D1 Kohoutek	1973 Jun 07.2	1.3820	0.9987	121.60
C/1973 E1 Kohoutek	1973 Dec 28.4	0.1424	1.0000	14.30
C/1975 V1-A West	1976 Feb 25.2	0.1966	0.99997	43.07
C/1995 O1 Hale–Bopp	1997 Apr 01.1	0.9141	0.99508	89.43
C/1996 B2 Hyakutake	1996 May 01.4	0.2302	0.99990	124.92
C/2006 P1 McNaught	2007 Jan 12	0.17075	1.00002	77.83
C/2011 W3 Lovejoy	2011 Dec 16	0.00555	0.99993	134.36
C/2012 S1 ISON	2013 Nov 28.8	0.01245	1.0002	62.40

Notes: τ is the time of perihelion transit, q is the perihelion distance (AU), e eccentricity, i inclination. The Table is compiled based on data given in the JPL Small-Body Database (http://ssd.jpl.nasa.gov/). The Kreutz sungrazers are distinguished in bold font

Some representative examples of well-known comets are listed in Table 6.1. In this Table, the time of last perihelion transit τ, perihelion distance q (AU), eccentricity e, and inclination i are given for each listed object. Already from this short list it is clear that the LKE manifestations can be ubiquitous for comets. Some of the comets have perihelia values quite close to the Solar radius $R_{\rm Sun} \approx 0.005$ AU. This means that they are either sungrazers, or close to the sungrazing state. Among the comets presented in the Table, the Great March comet, comet Ikeya–Seki, and comet Lovejoy are believed to be *Kreutz sungrazers*, belonging to a group of comets of common origin—a result of a breakup of a larger body, as it was originally supposed and argued by Kreutz (1888). In Table 6.1, the Kreutz sungrazers are distinguished in bold font.

The sungrazing behaviour is observed not only for comets, but as well for asteroids in the inner Solar system, mostly for NEAs. For them, a number of resonant mechanisms (in particular, interaction of secular and mean motion resonances) for transportation to the Sun, apart from the LKE, were proposed (Farinella et al. 1994). However, the LKE is one of the most efficient, as it was demonstrated by Farinella et al. (1994) for asteroid (5731) Zeus (see Table 7.1), which exhibits enormous secular changes in the orbital inclination, due to the LKE.

6.2 Origin of Sungrazers

The LK-mechanism might be responsible for both (1) the formation of the reservoir for the long-period comets and (2) the delivery of the comets from the Oort cloud to the inner Solar system. Finally, by means of the LKE again, (3) the delivered comets can become sungrazers; and the Sun disperses their primordial matter inside the Solar system.

Bailey et al. (1992) established that the LKE is able to produce a lot of sungrazing comets, emerging from long-period comets.[2] They were the first to reveal that a high-amplitude libration around the points at $\omega = 90°$ and 270°, prominent in the Kozai diagrams (on the diagrams, see Sect. 3.2.4), can be responsible for the emergence of sungrazing phenomena in the secular evolution of long-period comets with extremely high eccentricities.

Such high eccentricities can be achieved when a half of a libration cycle around any of these two points is completed, see Fig. 6.2. This figure, constructed by Thomas and Morbidelli (1996), demonstrates the orbital behaviour of one the most illustrious comets ever observed, C/1965 S1 Ikeya–Seki, superimposed on the theoretical Kozai diagram for this comet. To construct this Figure, Thomas and Morbidelli used a refined numerical-experimental model, containing all four

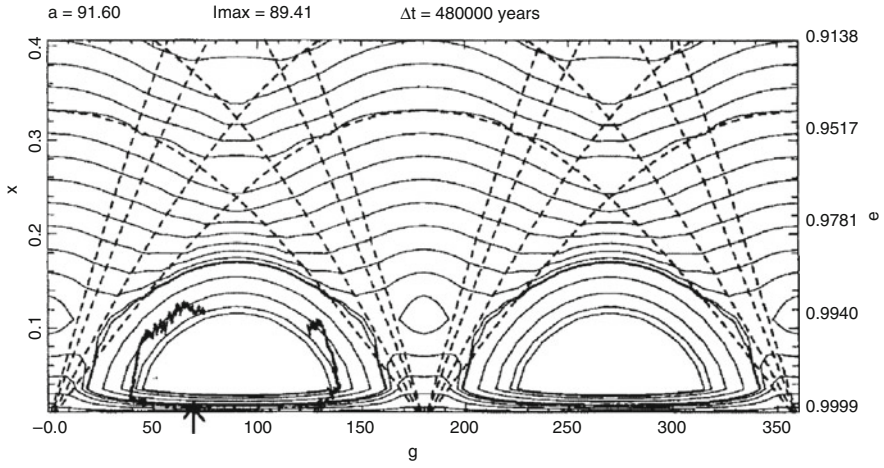

Fig. 6.2 The Kozai diagram ($g = \omega$, $X = (1 - e^2)^{1/2}$) constructed for the Ikeya–Seki comet (the current orbital elements $a = 91.6$ AU, $e = 0.9999$, $i = 141.86°$, $g = 69.05°$). The *superimposed bold curve* shows the evolution of the Ikeya–Seki comet position on the diagram during a time interval of 480,000 years. The *curve* is obtained by a direct numerical integration in the full setting of the dynamical problem. The present position of the comet is marked by *an arrow* (Figure 8 from Thomas and Morbidelli (1996). With permission from Springer International Publishing AG)

[2] A long-period comet is the comet with the orbital period greater than 200 years.

giant planets as the perturbers. One can see that the evolutionary track obtained by the direct numerical integration in the full dynamical problem follows the theoretical level curves of the Hamiltonian of the averaged problem rather roughly, because the short-period oscillations were not averaged in the integration and also because the planetary eccentricities and inclinations were not taken into account in the Hamiltonian. However, the qualitative agreement is obvious. Figure 6.2 clearly demonstrates how sungrazers can emerge, in both theoretical and numerical-experimental aspects.

Note that, to construct this graph, Thomas and Morbidelli (1996) employed a technical trick, well-known since the works of Lidov (1963b) and Gordeeva (1968): they used not the usual coordinates g and e, but g and $X = (1 - e^2)^{1/2}$. This trick allows one to zoom the domain of high eccentricities, thus making regular islands at extreme eccentricities detectable.

Thomas and Morbidelli (1996) considered the secular dynamics of 49 long-period comets, in a realistic model with perturbations from all four giant planets taken into account. For each of the comets, they computed the value of the vertical component H of the angular momentum, constructed the contour plot of the Kozai Hamiltonian[3] in the "argument of perihelion—eccentricity" plane for the given value of H, and identified the location of the comet in the diagram. It turned out, quite unexpectedly, that more than a half of the studied comets were located inside the islands of ω-libration, and all other close to these islands. Among the ω-librators some famous sungrazers (in particular, Great Comet of 1965) were recognized. The inference of Bailey et al. (1992) on the LKE as an effective mechanism for producing sungrazing comets was thus confirmed.

6.3 The Oort Cloud and Cometary Transport

Oort (1950) put forward a hypothesis that long-period comets are "injected", due to some occasional perturbations, into the Solar system from a huge unobserved outer spherical reservoir of primordial objects. Now this reservoir is called the *Oort cloud*. The Oort cometary cloud could have been formed as an outcome of close encounters of planetesimals with major planets during early epochs of the Solar system history (Fernández 1997). Now the Oort cloud extends radially from $\sim 10^3$ to $\sim 10^5$ AU. The outer border is approximately delimited by the Hill sphere of the Sun in the Galactic gravitational field.[4]

Oort (1950) supposed that the cometary injection was due to occasional external perturbations. The Galactic field stars (or giant molecular clouds), passing close to the Oort cloud, perturb it. Therefore, the perihelion distances of some objects of the

[3] The numerical technique for construction of the Kozai diagrams is described in detail further on, in Sect. 7.1.

[4] The Hill sphere of the Sun is defined in Sect. 9.4.

Oort cloud may sharply diminish, and the orbits of such objects may start to cross the inner Solar system, reaching heliocentric distances $r < 5$ AU; some objects may become even observable at perihelia.

In 1980s, a new mechanism for the transport of objects from the Oort cloud was proposed (Duncan et al. 1987; Heisler and Tremaine 1986; Matese and Whitman 1989; Higuchi et al. 2007), based essentially on the LKE due to the Galactic perturbation. Matese and Whitman (1992) and other authors demonstrated that the Galactic latitudes of perihelia of the observed comets were distributed according to the effect of the Galactic disk tide.[5] The new mechanism turned out to be theoretically efficient for producing the observable comets, probably even more efficient than the effect of stellar passages. Now the Galactic tide and the stellar passages are both considered to be active in providing the transport of comets from the parent reservoir (Fouchard et al. 2011; Matese and Lissauer 2002).

Exploring the Galactic tide effect on the motion of comets, Brasser (2001) averaged the perturbing potential over the mean anomaly and the longitude of the ascending node, thus reducing the system's number of degrees of freedom to one. Though the perturbing potential was different from that in the three-body problem case considered by Lidov and Kozai, the resulting secular behaviour turned out to have much in common with the classical LKE. The argument of perihelion was shown to librate if $i \geq 26.57°$. Using a direct numerical integration of the non-averaged system, Brasser (2001) identified a *chaotic behaviour* near the separatrix between the libration and circulations of the argument of perihelion. This chaos is due to the presence of periodic perturbations, absent in the analytical treatment, where they were averaged out. At $\omega = 26.56°$ (a critical value), the chaotic orbits were found to exist at $40° \leq i \leq 140°$, independent from the eccentricity.

[5]The disk tide is the tidal force arising due to the change of the Galactic gravitational potential with distance from the Galactic midplane.

Chapter 7
Asteroids and Kuiper Belt Objects in Inclined Orbits

Ô Loi du rythme sans appel,
Le moindre astre te certifie,
Par son humble chorégraphie!

Jules Laforgue, *Le Concile féerique*

In the asteroid belt, the asteroids move in the orbits inner to those of the main perturbers (Jupiter and other giant planets), whereas in the Kuiper belt the situation is opposite. Therefore, the settings for the analytical treatment are different in these two cases; and, indeed, the LK-dynamics are different. The common feature is that the LKE plays an important role in sculpting both the asteroid belt and the Kuiper belt.

In the asteroid belt, the LKE pumps the eccentricity of highly-inclined asteroids to values at which they become planet-crossing, and this leads to close encounters of the asteroids with the planets. Thus, the LKE causes the asteroid belt depletion at high inclinations. In the Kuiper belt, on the contrary, quite a number of objects are observed to be at high inclinations. This is because the LK-mechanism in this region does not pump eccentricities to planet-crossing values, if the initial eccentricities are small or moderate, at any inclinations (Thomas and Morbidelli 1996). Therefore, the inclined close-to-circular and moderately elongated orbits are not destabilized by encounters with planets.

In the both belts, the interaction of the LK-resonance with mean motion and secular resonances is an important dynamical factor, defining the structure of the belts and the dynamics of individual objects (Morbidelli 2002). Inside the Jovian 2/1 mean motion resonance in the main belt, at large eccentricities, the LK-resonance interacts with the secular ν_5 and ν_6 resonances at any inclination, and this gives rise to dynamical chaos, due to which the asteroidal eccentricity can diffuse to unity. Thus, the LK-resonance contributes to the depletion of the 2/1 mean motion resonance zone in the asteroid belt. Similar effects are observed in other major mean motion resonances, such as 3/1. In the Kuiper belt, the LK-resonance affects the secular dynamics inside the 2/3 mean motion resonance with Neptune. Enough to say, Pluto is simultaneously in the 2/3 resonance and in the LK-resonance (Malhotra

I. I. Shevchenko, *The Lidov-Kozai Effect – Applications in Exoplanet Research and Dynamical Astronomy*, Astrophysics and Space Science Library 441,
DOI 10.1007/978-3-319-43522-0_7

and Williams 1997; Williams and Benson 1971). However, most of Plutinos[1] do not have their arguments of perihelia librating.

In this chapter, various multi-resonant phenomena in the motion of asteroids and trans-Neptunian objects (TNOs) are considered. In particular, a peculiar multi-resonant "dance" of the asteroid 2335 James is discussed, illustrating the interaction of the LK-resonance and ordinary secular resonances. As follows from results of long-term numerical integrations by Froeschlé et al. (1991), 2335 James intermittently resides in the LK-resonance and in the ν_5 and ν_{16} secular resonances, sometimes escaping some of them, sometimes returning. The alternation of the ω-libration and ω-circulation regimes in the behaviour of 2335 James was earlier revealed by Vashkovyak (1986), who performed a study of orbital evolution of several asteroids, using an analytical-numerical approach.

Data on relevant asteroids, Centaurs, and TNOs (with a number of bodies subject to the LKE, among them) are given in Tables 7.1, 7.2, and 7.3.

7.1 The Kozai Hamiltonian and Diagrams

The averaged truncated Hamiltonian of the motion of a massless test body (asteroid) in the gravitational field of a planetary system, when expressed through the modified Delaunay variables (defined by Equations (2.17)), can be rendered the form (Morbidelli 2002):

$$\mathcal{H}_{\rm sec} = \epsilon \mathcal{H}_1(P, Q, p, q, e_j, \varpi_j, i_j, \Omega_j), \tag{7.1}$$

where e_j, ϖ_j, i_j, and Ω_j are, respectively, the eccentricity, longitude of perihelion, inclination, and longitude of ascending node of planet j; Λ and λ, P and p, Q and q are the pairs of the modified Delaunay variables of the test body; ϵ is the mass of the largest planet in units of the mass of the host star.

In formula (7.1), the terms depending on Λ and Λ_j are omitted, because they are constant, and the term $\epsilon\mathcal{H}_1$ includes all the terms of the first and higher orders in ϵ. The planetary elements e_j, ϖ_j, i_j, and Ω_j change with time, albeit slowly; this slow evolution can be described by the Lagrange–Laplace solution (see, e.g. Morbidelli 2002; Murray and Dermott 1999).

One can transform Hamiltonian (7.1) to an autonomous form:

$$\mathcal{H}_{\rm sec} = \sum_k (g_k \Gamma_k + s_k \Sigma_k) + \epsilon \mathcal{H}_1(P, Q, p, q, e_j, \varpi_j, i_j, \Omega_j), \tag{7.2}$$

[1] Plutinos are the trans-Neptunian objects that reside in the 2/3 mean motion resonance with Neptune, as Pluto does.

Table 7.1 Data on relevant asteroids

Asteroid	a (AU)	e	i (°)	Object type
(2) Pallas	2.7716	0.2313	34.84	Main-belt asteroid
(292) Ludovica	2.5296	0.0342	14.90	Main-belt asteroid, res. 3/1
(329) Svea	2.4763	0.0254	15.88	Main-belt asteroid, res. 3/1
(617) Patroclus	5.2176	0.1393	22.05	Jupiter Trojan
(1036) Ganymed	2.6633	0.5340	26.69	Amor (NEO)
(1362) Griqua	3.2145	0.3715	24.23	Outer main-belt asteroid
(1373) Cincinnati	3.4216	0.3144	38.93	Outer main-belt asteroid
(1379) Lomonosowa	2.5244	0.0920	15.61	Main-belt asteroid, res. 3/1
(1566) Icarus	1.0779	0.8270	22.83	Apollo (NEO)
(1866) Sisyphus	1.8937	0.5385	41.19	Apollo (NEO)
(1915) Quetzalcoatl	2.5449	0.5705	20.40	Amor (NEO)
(1981) Midas	1.7761	0.6500	39.83	Apollo (NEO), res. ν_{16}
(2102) Tantalus	1.2901	0.2991	64.01	Apollo (NEO)
(2335) James	2.1233	0.3602	36.32	Mars-crossing asteroid, res. ν_5, ν_{16}
(3040) Kozai	1.8407	0.2003	46.64	Mars-crossing asteroid
(3200) Phaethon	1.2712	0.8898	22.24	Apollo (NEO)
(3752) Camillo	1.4134	0.3017	55.56	Apollo (NEO)
(3789) Zhongguo	3.2859	0.1848	2.75	Outer main-belt asteroid
(4034) Vishnu	1.0597	0.4439	11.17	Apollo (NEO)
(4236) Lidov	3.4427	0.0315	7.29	Outer main-belt asteroid
(4660) Nereus	1.4887	0.3600	1.43	Apollo (NEO)
(5496) 1973NA	2.4353	0.6359	67.99	Apollo (NEO)
(5731) Zeus	2.2630	0.6537	11.43	Apollo (NEO), sungrazer

Notes: a is the semimajor axis, e eccentricity, i inclination. The Table is compiled based on data given in the JPL Small-Body Database (http://ssd.jpl.nasa.gov/). The orbital elements correspond to epoch 2016 Jan 13.0, except that for (2), (617), (1362), (1566), (1915), (3200), (3789), (4034), and (4236) the epoch is 2014 Dec 09.0, for (4034) the epoch is 2011 Jan 26.0. The inclination is referred to heliocentric ecliptic J2000. The ω-librators are distinguished in bold font

where the *new angles* $\varpi_j = g_j t + \beta_j$, $\Omega_j = s_j t + \delta_j$, and Γ_j and Σ_j are the respective conjugate actions. Here g_j and s_j are the planetary frequencies, β_j and δ_j are the planetary angular phases (see, e.g., Laskar 1990). Then, a truncated expansion of Hamiltonian (7.2) in a power series of e_j and $\sin(i_j/2)$ is given by

$$\mathcal{H}_{\rm sec} = \sum_k (g_k \Gamma_k + s_k \Sigma_k) + \sum_{n \geq 0} \mathcal{K}_n(P, Q, p, q, \varpi_j, \Omega_j) \tag{7.3}$$

(Morbidelli 2002; Williams 1969), where $\mathcal{K}_n$ is the quantity of order n in e_j and $\sin(i_j/2)$; $n = 0, 1, \ldots$. Hamiltonian (7.3) provides an approximation suitable for a body in a highly inclined and/or eccentric orbit.

The leading term $\mathcal{K}_0$ does not contain planetary eccentricities or inclinations. Due to the D'Alembert rules, it does not depend on the planetary angles ϖ_j and Ω_j.

Table 7.2 Data on relevant trans-Neptunian objects

TNO	a (AU)	e	i (°)
1995 GJ	42.9031	0.0908	22.93
1996 RQ20	43.8978	0.1003	31.71
1996 TL66	84.0015	0.5826	23.99
1997 CW29	39.3753	0.0788	18.98
2008 KV42	41.4076	0.4899	103.48
2012 VP113	263.12	0.6940	24.02
(15883) 1997 CR29	47.3544	0.2144	19.11
(90377) Sedna	524.43	0.8549	11.93
(118228) 1996 TQ66	39.4924	0.1228	14.68
(134340) Pluto	39.4451	0.2502	17.09
(136108) Haumea	43.2175	0.1913	28.19
(136199) Eris	67.7807	0.4407	44.04

Notes: a is the semimajor axis, e eccentricity, i inclination. The Table is compiled based on data given in the JPL Small-Body Database (http://ssd.jpl.nasa.gov/). The orbital elements of the given TNOs correspond to epoch 2014 Dec 09.0, except 1995 GJ (epoch 1995 Apr 04.0), 1997 CW29 (epoch 1997 Feb 21.0), and Pluto (epoch 2006 Sep 22.0). The inclination is referred to heliocentric ecliptic J2000. The ω-librators are distinguished in bold font

Table 7.3 Data on relevant Centaurs

Centaur	a (AU)	e	i (°)
(944) Hidalgo	5.7365	0.6616	42.52
(5145) Pholus	20.3384	0.5736	24.73
(7066) Nessus	24.4744	0.5195	15.66
(8405) Asbolus	18.0147	0.6190	17.63
(10199) Chariklo	15.7647	0.1720	23.41

Notes: a is the semimajor axis, e eccentricity, i inclination. The Table is compiled based on data given in the JPL Small-Body Database (http://ssd.jpl.nasa.gov/). The orbital elements correspond to epoch 2014 Dec 09.0. The inclination is referred to heliocentric ecliptic J2000. The ω-librator (Hidalgo) is distinguished in bold font

It depends only on one angle: the argument of perihelion $g = q - p$ (recall that $p = -g - h = -\varpi$ and $q = -h = -\Omega$). Therefore, $\mathcal{K}_0$ is integrable.

Expressed through the Delaunay variables G, H, g, and h, given by formulas (2.15), the Hamiltonian

$$\mathcal{H}_{\rm int} = \sum_k (g_k \Gamma_k + s_k \Sigma_k) + \mathcal{K}_0(G, H, g) \tag{7.4}$$

can serve as an integrable approximation of the secular Hamiltonian (7.2). Following Thomas and Morbidelli (1996), $\mathcal{K}_0$ is called the *Kozai Hamiltonian*, honouring Kozai, who was the first to study the asteroidal dynamics in this approximation (Kozai 1962, 1979, 1980).

Since angle h is absent in $\mathcal{K}_0$, its conjugate action $H = [a(1-e^2)]^{1/2}\cos i$ is a constant of motion. The semimajor axis a is also constant; therefore, the mean elements e and i are related by the Lidov-Kozai integral (3.23).

To study the asteroidal secular dynamics, it is helpful to construct level curves of $\mathcal{K}_0(G, H, g)$, parameterized by the value of H. These level curves represent plots of functions $G(g)$ or $e(g)$. Families of these level curves are called the *Kozai diagrams*, again in honour of Kozai, who invented this global graphical representation of the asteroidal secular dynamics (Kozai 1962, 1979).

The Kozai diagrams can be constructed either analytically (in relatively simple models, such as R3BP) or numerically (in realistic problem settings, say, when perturbations from all planets are taken into account).

A numerical procedure for construction of the Kozai diagrams of asteroidal dynamics is described in Morbidelli (2002). In brief, it is as follows. An average of the original system Hamiltonian over the mean anomalies l and l_j of the test body and the planets is given by

$$\mathcal{H}_{\rm sec} = -\frac{\mathcal{G}}{4\pi^2}\sum_{j=1}^{N} m_j \int_0^{2\pi}\int_0^{2\pi}\left(\frac{1}{\|\mathbf{r}-\mathbf{r}_j\|} - \frac{\mathbf{r}\cdot\mathbf{r}_j}{\|\mathbf{r}_j\|^3}\right) \mathrm{d}l\,\mathrm{d}l_j \tag{7.5}$$

(Morbidelli 2002; Thomas and Morbidelli 1996), where $\mathbf{r}$ and $\mathbf{r}_j$ are the heliocentric radial vectors of the test body and jth planet, respectively; all the vectors' components are implied to be expressed through the orbital elements. Note that, as shown in Subbotin (1968),

$$\int_0^{2\pi}\int_0^{2\pi} \frac{\mathbf{r}\cdot\mathbf{r}_j}{\|\mathbf{r}_j\|^3}\,\mathrm{d}l\,\mathrm{d}l_j \equiv 0. \tag{7.6}$$

If one sets inclinations i_j and eccentricities e_j for all j (i.e., all planets) equal to zero, expression (7.5) to the accuracy of the first order in ϵ coincides with the Kozai Hamiltonian $\mathcal{K}_0$. It is independent of angle h, and depends merely on e, i, g, and the secular constants a and a_j. Besides, on a surface defined by $H = [a(1-e^2)]^{1/2}\cos i$= const ($H$ is a conserved reduced Delaunay momentum, see Sect. 3.2.1) one has $i = \arccos\left\{H\left[a(1-e^2)\right]^{-1/2}\right\}$. Therefore, the numerically computed values of $\mathcal{K}_0$ are determined merely by e and g. Therefore, one can construct contour plots in the (g, e) plane.

Setting $i_j = 0$ and $e_j = 0$, the integral over l_j in formula (7.5) can be expressed analytically through elliptic integrals of the first kind; namely, one has

$$\int_0^{2\pi} \left(\frac{1}{\|\mathbf{r} - \mathbf{r}_j\|} - \frac{\mathbf{r} \cdot \mathbf{r}_j}{\|\mathbf{r}_j\|^3} \right) \mathrm{d}l_j = \frac{4}{(r^2 + a_j^2)^{1/2}} \left(1 - \frac{m}{2}\right)^{1/2} K(m), \tag{7.7}$$

where

$$m = \frac{4a_j(x^2 + y^2)^{1/2}}{r^2 + a_j^2 + 2a_j(x^2 + y^2)^{1/2}}, \tag{7.8}$$

$r = \|\mathbf{r}\|$, x and y are the coordinates of $\mathbf{r}$ projected onto the orbital plane of the planets (Bailey et al. 1992; Morbidelli 2002; Williams 1969). On the other hand, the integral over l in expression (7.5) can be taken only numerically.

Thus, the Kozai diagrams (contour plots of $\mathcal{K}_0$) can be constructed in such a way: one computes values of $\mathcal{H}_{\mathrm{sec}}$, given by expression (7.5) on a fine grid of the (g, e) values at $H = \mathrm{const}$, and then plots the level curves. This numerical procedure was extensively employed by Thomas and Morbidelli (1996) and Thomas (1998).

As soon as a minor body may move around the Sun either in the orbits inner to the main perturbers (as in the main belt of asteroids), or in the orbits outer to the main perturbers (as in the Kuiper belt), two types of the restricted problem, approximating these dynamical situations, can be considered: the *inner* problem and the *outer* problem, in which the massless test particle is a member of the inner or outer binary, respectively. Accordingly, there are two types of the LKE: the inner LKE and the outer LKE. It is mostly the inner LKE that was theoretically studied since the works of Lidov (1961) and Kozai (1962). The outer LKE, corresponding to the outer problem, is not less important than the inner one; its analytical treatment was performed first by Ziglin (1975). The secular outer R3BP in the quadrupole approximation was analyzed by Farago and Laskar (2010). They provided a complete classification of possible motions and derived analytical expressions for the secular periods.

In the Solar system dynamics, the inner LKE case can be called the asteroidal case, because the main-belt asteroids move inside the orbits of the main perturbers; and the outer LKE case can be called the TNO case (the case of trans-Neptunian objects), because the TNOs move outside the orbits of the main perturbers. These two cases are the subjects of the following two sections.

7.2 Inclined Asteroids: Inside Perturber's Orbit

Let us consider typical patterns of the secular evolution of asteroids in the main belt subject to planetary perturbations. The secular dynamics of asteroids presents a rich variety of behaviours, resulting in formation of various asteroidal populations. Several examples of relevant asteroids of the main belt (including those subject to the LKE) are given in Table 7.1.

The LKE importance in the dynamics of short-period comets and similar highly-eccentric objects, such as Centaurs, was first pointed out by Kozai (1979). The secular evolution of numbered asteroids, short-period comets and Halley-type comets (all such objects known up to 1979) was explored by him by means of numerical integrations taking into account four giant planets as perturbers. The averaging was also performed numerically.

For (944) Hidalgo, (1373) Cincinnati, (1866) Sisyphus, and (1981) Midas, the arguments of perihelion were found to be in libration. It was shown for the first time that the LKE can serve as a mechanism protecting a minor body from encounters with planets: due to ω-libration, (1373) Cincinnati avoids close encounters with Jupiter, and (1866) Sisyphus and Midas (1981) avoid close encounters with Mars.

None of the studied short-period comets were found to be in ω-libration, though the libration islands exist in the phase space of motion. In what concerns the Halley-type comets, 15 objects were identified to be in ω-libration, the Halley comet itself among them. However, their eccentricities do not change much, contrary to the case of the asteroids in ω-libration. Though the secular motion of the Halley comet is close to the separatrix of the LK-resonance, its eccentricity varies only weakly. The range of variation of e is 0.89–0.97; this is rather moderate, compared, e.g., to the case of (944) Hidalgo, for which the eccentricity varies between 0.52 and 0.82.

In 1980, Kozai found four more asteroids to be in ω-libration: (2102) Tantalus, (2335) James, (3040) Kozai, and (5496) 1973NA (Kozai 1980). The secular theory at that time had not yet been generalized to deal with resonant objects (the objects that reside in mean motion resonances), that is why the identified LK-asteroids were all non-resonant. In 1985, Kozai developed a semi-analytical approach to deal with the secular dynamics of asteroids in mean motion resonances (Kozai 1985). For the sake of analytical simplicity, he assumed that an asteroid is in *exact* mean motion resonance: the amplitude of resonant libration is zero, in other words, the object is in the resonance center. In this way, a survey of resonant main-belt asteroids was accomplished on the subject of possible LK-oscillations. The asteroids known to reside in the 1/1, 4/3, 3/2, 2/1, and 3/1 mean motion resonances with Jupiter were analyzed. However, a few objects were found to be subject to ω-libration. In particular, no Jovian Trojan (1/1 resonance), though they are numerous and highly-inclined, was found to librate. ω-librators were identified only in the 3/1 resonance; these were (292) Ludovica, (329) Svea, and (1379) Lomonosowa.

Though the survey was generally restricted to main-belt asteroids, Kozai (1985) considered also Pluto, which is in resonance 2/3 with Neptune, and discovered that it was subject to the LKE with the argument of perihelion librating around 90°.

In the works by Quinn et al. (1990) (on the quasi-parabolic comets arriving from the Oort cloud), Bailey et al. (1992) (on the LKE-maintained production of most of the sungrazing comets), and Thomas and Morbidelli (1996) (on the long-period comets) the basic inferences of Kozai (1979, 1980) were confirmed and the numerical-experimental technique was developed to a new level.

Of especial (even practical) interest the LKE is for the case of near-Earth asteroids (NEA) and, more generally, near-Earth objects (NEO). Michel and Thomas (1996) analyzed secular dynamics of near-Earth asteroids; for this purpose, they

integrated orbits of all asteroids with semimajor axes less than 2 AU. Four objects subject to the LKE were identified: (1981) Midas, (3752) Camillo, (4034) Vishnu, and (4660) Nereus (see Table 7.1 for orbital data). The arguments of pericenters of two of them, (4034) Vishnu and (4660) Nereus, librate not around 90° or 270°, as one would expect, but around 180°. This is due to a modification of the secular phase space in presence of inner planets intersecting the orbits of the asteroids. Thus, Michel and Thomas (1996) showed that the LKE is possible even at low inclinations ($i < 14°$, see Table 7.1) and ω librating around 0° or 180°, when perturbers with orbits intersecting that of a test body are present. In the both libration cases (around 90° and 270° or around 0° and 180°), the LKE serves as a mechanism of the temporary protection from close encounters of an asteroid subject to LKE with a perturbing planet.

As found out by Michel and Thomas (1996), the LKE can make a NEA *metastable*. If an asteroid's semimajor axis is close to that of a planet, encounters are potentially possible. However, if the inclination is low and the eccentricity is high, and ω librates around 0° or 180°, the node crossings take place near the asteroid's perihelia and aphelia, i.e., far from all possible positions of the perturbing planet moving in a close-to-circular orbit.

Yet another LKE-based protecting mechanism can work both for NEAs and main-belt asteroids. If an asteroid may approach a planetary orbit, but the inclination is high and ω librates around 90° or 270°, the dynamical consequences of an encounter is minimum, because it occurs at a high relative velocity; thus, the asteroid's orbit can be modified only slightly. The both protecting mechanisms are discussed in detail in Michel and Thomas (1996).

As already discussed above, if one sets all i_j and e_j equal to zero, the secular Hamiltonian $\mathcal{H}_{\rm sec}$, given by Equation (7.5), coincides with the Kozai Hamiltonian $\mathcal{K}_0$ (to the accuracy of the first order in ϵ). As soon as $\mathcal{K}_0$ is independent of angle h, the action $H = [a(1-e^2)]^{1/2} \cos i = \text{const}$. In Fig. 7.1, constructed by Thomas (1998), the LK-evolution of eccentricity e and argument of pericenter g is graphically presented for six representative constant values of H. The asteroid's semimajor axis is set to $a = 3$ AU, i.e., the asteroid moves in an orbit located between the 5/2 and 2/1 mean motion resonances with Jupiter. Thus, the diagrams feature a typical asteroid of the main belt. The perturbations from all four giant planets are taken into account.

Any chosen value of $H = \text{const}$ sets a maximum value of the inclination that is achieved at $e = 0$:

$$i_{\max} = \arccos\left(Ha^{-1/2}\right). \tag{7.9}$$

At each panel of Fig. 7.1, this maximum value is indicated. In all panels, the diagram boundary circle corresponds to the maximum possible (at the given value of H) eccentricity

$$e_{\max} = \left(1 - \frac{H^2}{a}\right)^{1/2}. \tag{7.10}$$

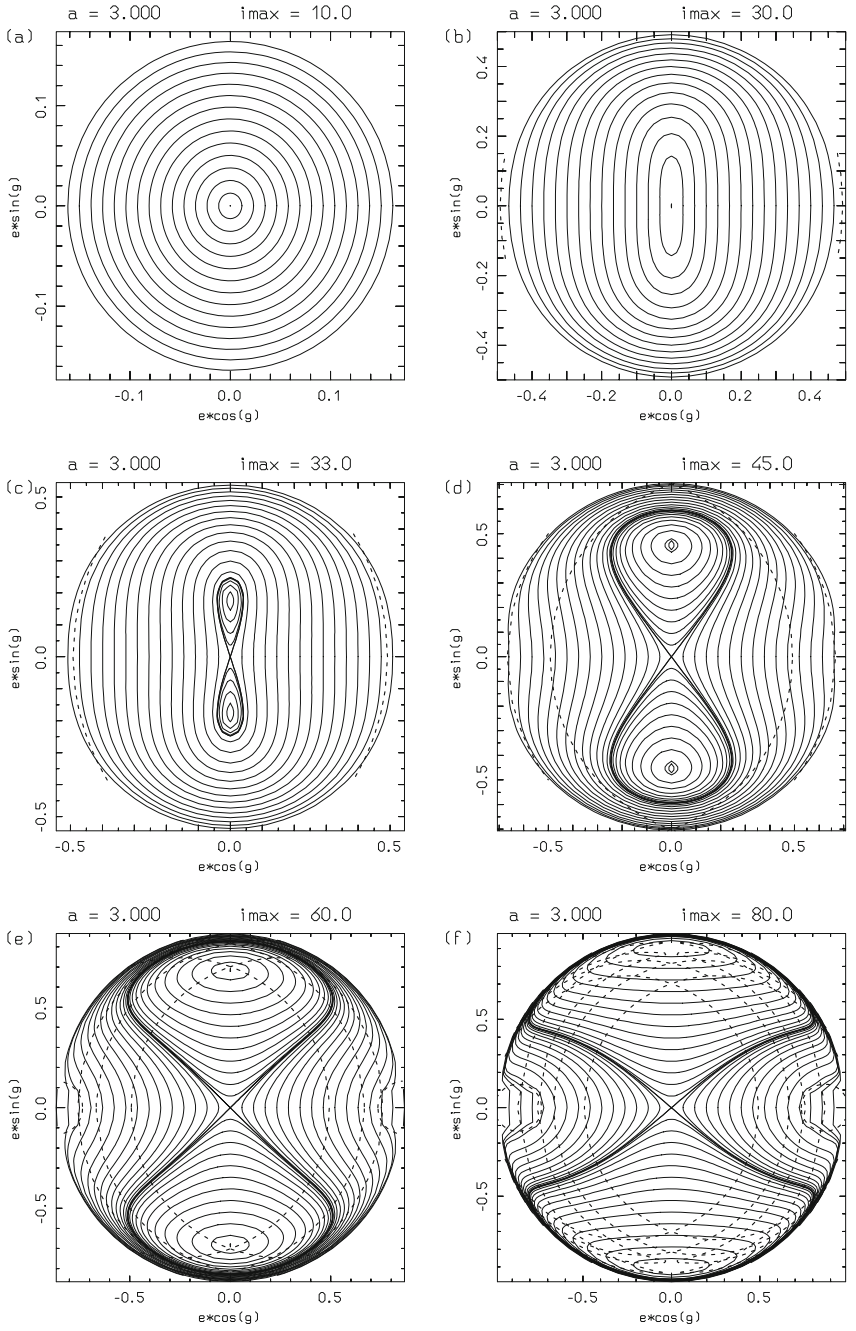

Fig. 7.1 Secular behaviour of a typical main-belt asteroid (the semimajor axis $a = 3$ AU) in the polar coordinates (with angular variable $g \equiv \omega$ and radial variable e). At each panel, the maximum inclination $i_{\max}$, achieved at $e = 0$, is indicated, and the dashed curves correspond to the node-crossings of planetary orbits (Figure 8.1 from Morbidelli 2002. With permission from Academic Books)

An analysis of the Kozai diagrams was accomplished by Thomas and Morbidelli (1996), Thomas (1998), and Morbidelli (2002). The main inferences are as follows. At small $i_{\max}$ (see Fig. 7.1a, where $i_{\max} = 10°$), the level curves are close-to-circular: as the argument of perihelion circulates from 0° to 360°, the eccentricity and inclination remain approximately constant. At a greater value of $i_{\max}$ (Fig. 7.1b, $i_{\max} = 30°$), the eccentricity and inclination start to oscillate (the (e, g) oval level curves elongate), though the amplitude is yet low. At $g = 90°$ and 270°, the eccentricity and inclination are, respectively, maximum and minimum, the level curves spread along the vertical axis. The LK-dynamics radically changes at $i_{\max}$ greater than a threshold value (see Fig. 7.1c, where $i_{\max} = 33°$); the threshold value resides somewhere between 30° and 33°. At this threshold, the point at the frame origin $e = 0$ transforms into an unstable equilibrium; a separatrix, emanating from this unstable equilibrium, divides the phase space in three domains: two domains of ω-libration at $g = 90°$ and 270°, and the domain where g circulates. Such a dynamical pattern with a separatrix formally corresponds to a nonlinear resonance, that is why the ω-libration is frequently called the *Lidov-Kozai resonance*, as discussed in detail above in Sect. 4.6.

Panels (d), (e), and (f) of Fig. 7.1 illustrate the LK-dynamics at greater values of $i_{\max}$, namely, at $i_{\max} = 45°$, 60°, and 80°, respectively. The libration domains apparently enlarge. The point at $e = 0$ is still always an unstable equilibrium; any initially close-to-circular (starting at $e \ll 1$) orbit of the test body reaches maximum eccentricities (including extreme ones $e \sim 1$) at $g = 90°$ and 270°.

In panels (b), (c), (d), (e), and (f) of Fig. 7.1, the so-called *curves of node-crossings* of planetary orbits are shown dashed. What do these curves indicate? Let us define the *heliocentric nodal distance* $r^{\pm}_{\text{nodal}}$, as the "Sun–test body" distance at the moment of time when the test body crosses the reference plane:

$$r^{\pm}_{\text{nodal}} = \frac{a(1-e^2)}{1 \pm e\cos g} \tag{7.11}$$

(Morbidelli 2002; Thomas and Morbidelli 1996). Here, superscripts "+" and "−" designate the ascending and descending nodes, respectively. As follows from formula (7.11), if the test body achieves a high orbital eccentricity, the quantity $r^{\pm}_{\text{nodal}}$ becomes small. Thus, the asteroid may start to cross the orbits of inner planets: in panels (a) and (b), it is the orbit of Mars that is crossed; and in panel (f) the curves of node-crossings for Jupiter and all four inner planets, including Mercury, are present. (The curves are produced simply by equating the right-hand side of Equation (7.11) to the semimajor axis of a planetary orbit.) A node-crossing of a planetary orbit by an asteroid may result, sooner or later, in a close asteroid–planet encounter, drastically transforming the asteroid's orbit. Thus, the LKE explains the depletion of the main belt at high inclinations.

As shown by Kozai (1962), the threshold $i_{\max}$ value, at which the LK-resonance emerges, depends on a/a_{pert}, where a and a_{pert} are the semimajor axes of the test particle and perturber, respectively. However, as shown in Thomas (1998), at any value $0 \lesssim a/a_{\text{pert}} \lesssim 1$ the LK-dynamics is qualitatively similar to that shown in Fig. 7.1.

As noted by Morbidelli (2002), the relative perturbation strength (ϵ in Equation (7.1)) in the R3BP affects merely the timescale of LK-oscillations, but not their amplitude, due to the two-body problem degeneracy. In other words, the perturber's mass and its distance from the test body do not influence the amplitude of the LK-oscillations, but affect merely the time needed to reach the maxima.

The LKE, however, can be suppressed, if any additional perturbation causes a rapid enough precession of the argument of perihelion, as we have already discussed thoroughly in Sect. 3.3. Indeed, in such a case, the secular Hamiltonian, to the lowest order, is given by

$$\mathcal{H}_{\rm sec} = \alpha G + \mathcal{K}_0(G, H, g), \tag{7.12}$$

where the coefficient α is the frequency of the forced (due to the additional perturbation) precession of the angle g, and $\mathcal{K}_0$ is the basic Kozai Hamiltonian. If the term αG dominates over $\mathcal{K}_0$, then the LK-resonance disappears whatever the inclination might be.

7.3 Inclined TNOs: Outside Perturber's Orbit

In this section, we consider the LK-dynamics in the Kuiper belt. We shall see that it differs substantially from that in the main belt of asteroids. Several examples of relevant trans-Neptunian objects (TNO), including those subject to the LKE, are given in Table 7.2.

Diagrams, representing the global secular dynamics in the outer Solar system, were constructed by Thomas and Morbidelli (1996). The method of construction is the same as described in Sect. 7.1 and used in the case of the inner Solar system in Sect. 7.2.

The Kozai diagrams for the outer Solar system are reproduced in Fig. 7.2. They illustrate the LK-dynamics of a test particle with semimajor axis $a = 45$ AU, typical for a TNO. Such a test body moves in an orbit mostly exterior with respect to the main perturbers (the four giant planets).

An analysis of the diagrams was accomplished by Thomas and Morbidelli (1996) and Morbidelli (2002). The main inferences are as follows. At each panel of Fig. 7.2, the maximum inclination $i_{\rm max}$, achieved at $e = 0$, is indicated, so that one can follow how the level curves deform and transform with increasing $i_{\rm max}$. In panel (a) ($i_{\rm max} = 10°$), the level curves of $\mathcal{K}_0$ are close-to-circular and the eccentricity is almost constant with time, as in the case of a main-belt asteroid at comparable values of $i_{\rm max}$. Beginning with panel (b) ($i_{\rm max} = 30°$), the dashed curves represent the curves of node-crossings of planetary orbits. In panel (b), they correspond to the node-crossings with the orbit of Neptune. The objects in the orbits with low enough eccentricities are protected from encounters with Neptune, whereas those in the orbits with high enough eccentricities are forced, due to ω-circulation, to cross, sooner or later, the orbit of this planet. On increasing $i_{\rm max}$, two points

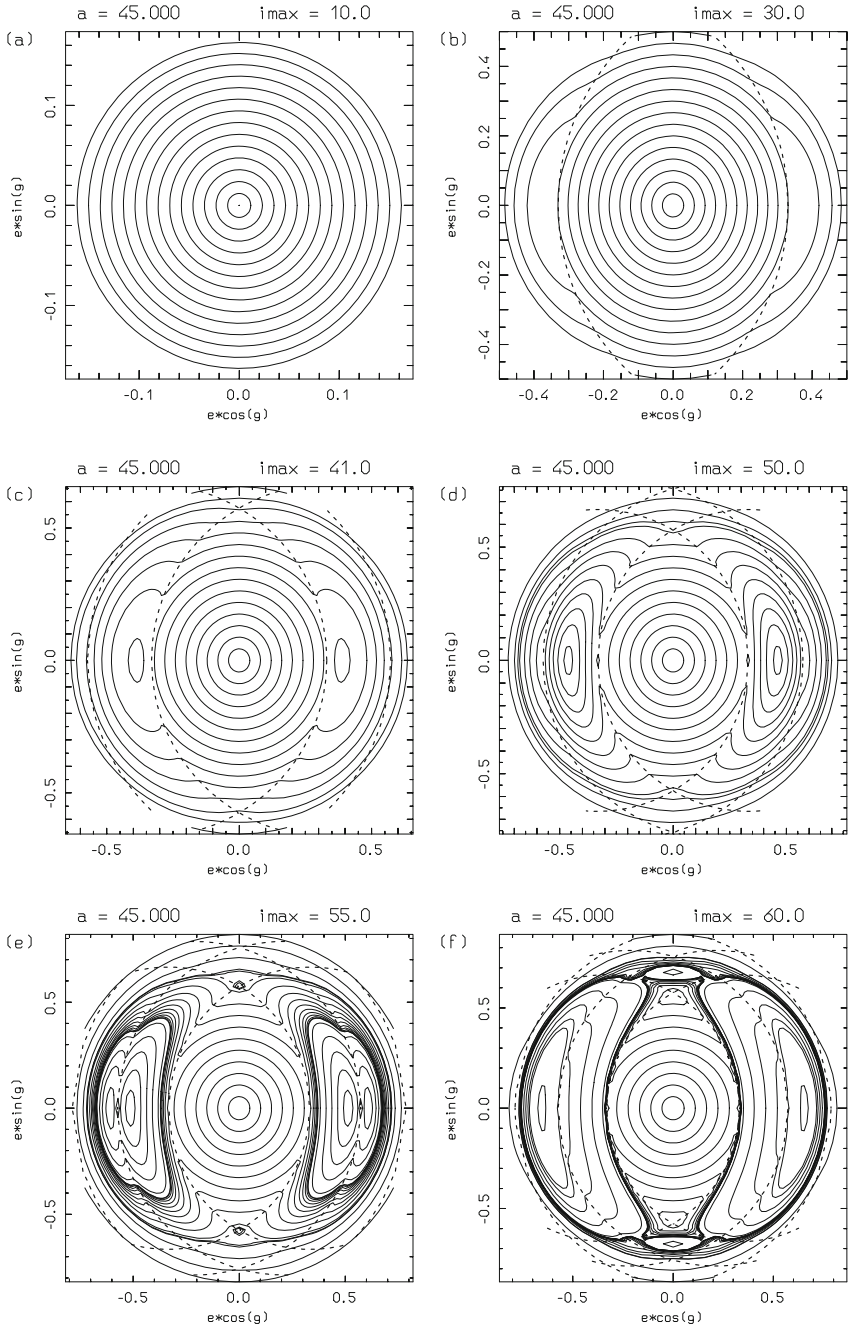

Fig. 7.2 The same as Fig. 7.1, but for a test particle with semimajor axis $a = 45$ AU, typical for the Kuiper belt. At each panel, the maximum inclination $i_{\max}$, achieved at $e = 0$, is indicated. The *dashed curves* correspond to the node-crossings of the orbits of Neptune (panels (**b**)–(**f**)), Uranus (panels (**c**)–(**f**)), and Saturn (panels (**e**)–(**f**)) (Figure 8.2 from Morbidelli 2002. With permission from Academic Books)

of stable equilibria at $g = 0°$ and $g = 180°$ appear (Fig. 7.2c, $i_{\max} = 41°$). They are the centers of regular islands of orbits with the argument of perihelion librating; amongst the highly-eccentric orbits, merely these ones are protected from encounters with Neptune. Besides, new dashed curves appear, tracing the node-crossings with Uranus; consequently, at extreme eccentricities, encounters with Uranus become possible. With increasing $i_{\max}$ further on, the libration islands swell (Fig. 7.2d, $i_{\max} = 50°$); therefore, the orbits with high amplitudes of libration are enforced to cross the orbit of Uranus. In Fig. 7.2e ($i_{\max} = 55°$), the curves of node-crossings of the orbit of Uranus divide each libration island in two halves; thus, four smaller encounter-protected libration islands are born. At extreme eccentricities, additional dashed curves correspond to encounters with Saturn. In the last panel (Fig. 7.2f, $i_{\max} = 60°$) two new small islands appear at $g = 90°$ and 270°, bounded by the curves of node-crossings with the orbits of Neptune and Uranus; and two islands remain (at $g = 0°$ and 180°) in the exterior of the curve of node-crossings with the orbit of Uranus.

From Fig. 7.2 it is clear that, at all $i_{\max}$, the LKE in the Kuiper belt does not pump initially small eccentricities up to high values; therefore, the objects with initially small enough eccentricities are permanently preserved from encounters with planets. Conversely, in the main belt of asteroids, such a pumping is prominent, as discussed in the previous section. This is a major dynamical difference between the two belts. It explains why there exist objects in the Kuiper belt that have much higher inclinations in comparison with the main-belt population.

To represent graphically the LK-dynamics at extreme eccentricities, Thomas and Morbidelli (1996) constructed the level curves of the Kozai Hamiltonian using the coordinates g and $X = (1-e^2)^{1/2}$, instead of g and e; see Fig. 7.3. Thus, the domain of high eccentricities is effectively zoomed, due to the specific non-linearity of X in e (see discussion in Sect. 6.2). This allows one to identify regular islands, protected from encounters with planets, at extreme eccentricities. Therefore, the constructed graphs can be used to characterize the secular evolution of extremely-eccentric objects.

Thomas and Morbidelli (1996) accomplished an analysis of these Kozai diagrams; their main inferences are as follows. In panel (a) of Fig. 7.3 ($i_{\max} = 60°$), the same diagram is depicted as in panel (f) of Fig. 7.2, but in different coordinates, namely, g and $X = (1 - e^2)^{1/2}$, instead of g and e. In panel (b) ($i_{\max} = 68°$), the curves of node-crossings of the orbits of Jupiter and Saturn split both regular islands at $g = 0°$ and 180°, each into three encounter-protected sub-islands. In panel (c) ($i_{\max} = 76°$), the upper islands at $g = 0°$ and 180° disappear. In comparison with panel (b), merely the island located under the curves of node-crossings with the orbit of Jupiter is still present, but its size diminishes, because the curves of node-crossings with the orbits of Neptune and Uranus become closer to each other. Another island appears, also under the curves of node-crossings of the orbit of Jupiter, but at $g = 90°$ and 270°. It swells with increasing $i_{\max}$; in panel (d) ($i_{\max} = 86°$), it dominates the phase space, whereas the island at $g = 0°$ and 180° is almost absent.

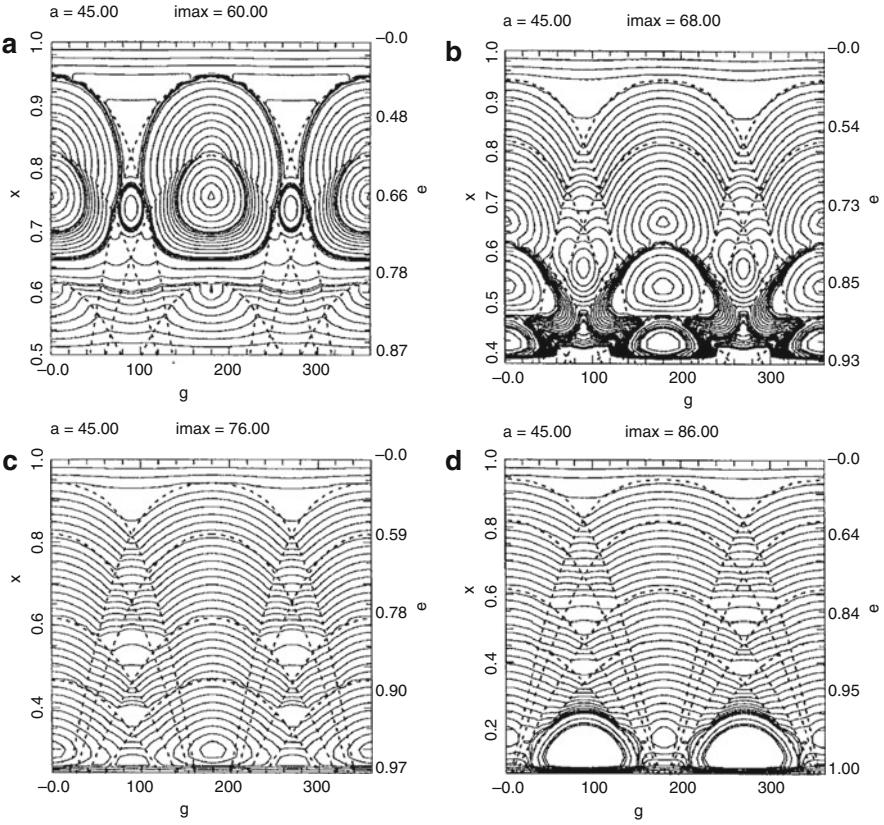

Fig. 7.3 The LKE at extreme eccentricities and inclinations in the Kuiper belt. At the vertical axis, the coordinate $X = (1 - e^2)^{1/2}$ is used instead of e, in order to "zoom" the domain of high eccentricities (Figure 5 from Thomas and Morbidelli 1996. With permission from Springer International Publishing AG)

The LK-dynamics, as shown in Figs. 7.2 and 7.3, is typical for the outer Solar system: at larger semimajor axes, the dynamical picture simply repeats itself, but at a greater eccentricity and the same inclination, i.e., at a greater value of $i_{\max}$. The reason is that the location, emergence and death of the libration islands are governed by the behaviour of the curves of node-crossings of the orbits of planets.

A particular "extreme" population of the Solar system bodies is formed by the so-called *extreme trans-Neptunian objects* (ETNO). Formally, they are defined as the objects with perihelion distances greater than 30 AU and semimajor axes greater than 150 AU. The observed ETNOs are nothing but inner objects of the Oort cloud (on the Oort cloud, see Sect. 6.3). It is very likely that they are "LK-shepherded" by a distant, yet unobserved, massive planet (Trujillo and Sheppard 2014): all such bodies, discovered up to now, concentrate heavily near the zero value of the argument of perihelion, $\omega \approx 0°$; see Fig. 7.4. In particular, the argument of

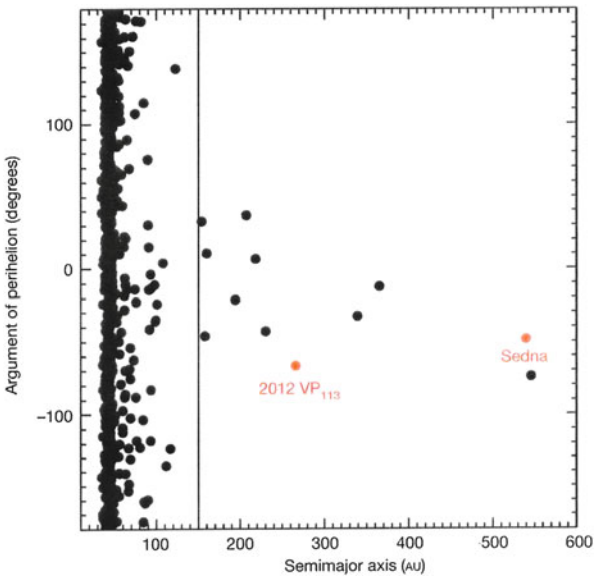

Fig. 7.4 The distribution of TNOs in the "semimajor axis–argument of perihelion" plane. ETNOs concentrate near $\omega \approx 0^\circ$ (Figure 3 from Trujillo and Sheppard 2014. With permission from Nature Publishing Group)

perihelion of ETNO 2012 VP113, which has the largest pericentric distance amongst all known Solar system bodies (see Table 7.2), is close to zero.

In numerical experiments accomplished in the framework of the circular R3BP, Trujillo and Sheppard (2014) demonstrated that a super-Earth (a planet by an order of magnitude more massive than our planet) in an orbit with the semimajor axis $\sim$250 AU is able to produce the observed zero-ω concentration of ETNOs, enforcing the ω-libration of these objects. Thus, the LKE theory acts here for the first time as an "agent" allowing one to predict the existence of a planet yet undiscovered; this is reminiscent of the glorious times of Celestial Mechanics, when Neptune was predicted in 1846; though the theoretical approach is different.

de la Fuente Marcos and de la Fuente Marcos (2014) explored possible observational selection effects that may affect the ω-distribution and concluded that the observed concentration of objects near $\omega = 0$ is real. What is more, they argued that there might exist even two trans-Plutonian massive planets, "shepherding" the ETNOs via the LK-mechanism.

Centaurs are the objects intermediate in their orbital characteristics between the main belt and Kuiper belt bodies[2]; therefore, they may have secular dynamics of intermediate type. Gronchi and Milani (1999) identified regular islands of ω-libration for such objects; the islands, as always, are defined by the curves of node-crossings of the planetary orbits and serve to protect the bodies from encounters with the outer planets of the Solar system.

[2]The Centaurs have intermediate values of orbital semimajor axes, between 5 and 30 AU; see examples in Table 7.3.

The secular dynamics, qualitatively similar to that in the Kuiper belt, can be also observed in the inner Solar system, if a body moves in a moderately inclined orbit slightly exterior to the orbit of Venus or the Earth (Michel and Thomas 1996). If the body's inclination is not high enough, then the perturbations from Venus or the Earth dominate over the Jovian perturbations, and, therefore, the LK-dynamics is similar to that in the Kuiper belt (the case of an inner perturber); conversely, at high enough inclinations, the Jovian perturbations dominate over the perturbations from Venus and the Earth, and the LK-dynamics is similar to that in the main belt (the case of an outer perturber).

7.4 Inclined Asteroids and TNOs in Mean Motion Resonances

In the both belts of minor bodies in the Solar system (the main belt and the Kuiper belt), the interaction of the LK-resonance with mean motion and secular resonances is an important dynamical factor, defining the secular dynamics of individual objects, as well as the global dynamical structure of the belts.

Considering the LKE in various applications, it is usually assumed that the system is not subject to mean motion resonances. When resonant contributions to the perturbing functions are considered (for the first time this was accomplished by Kozai 1985), it may concern the case of the *LK-resonance within a mean motion resonance*. The LK-resonance within mean motion resonances in the main belt of asteroids and in the Kuiper belt was analyzed in a number of works, including the monograph by Morbidelli (2002), articles by Gallardo (2006), Wan and Huang (2007), and Gallardo et al. (2012).

7.4.1 Mean Motion Resonances

Inside the 2/1 mean motion resonance of an asteroid with Jupiter, the LK-resonance may interact (at large asteroidal eccentricities) with the secular ν_5 and ν_6 resonances, and this may give rise to dynamical chaos, due to which the asteroidal eccentricity can diffuse to unity. In this way, the LK-resonance contributes to the depletion of the 2/1 mean motion resonance zone in the main belt (Moons et al. 1998). Similar secular resonant interactions are observed inside other major mean motion resonances, such as the 3/1 resonance (Farinella et al. 1993; Moons and Morbidelli 1995).

In the Kuiper belt, the LK-resonance affects the secular dynamics inside the 2/3 mean motion resonance with Neptune (Morbidelli 2002). Enough to say, Pluto is simultaneously in the 2/3 resonance and in the LK-resonance (Malhotra and Williams 1997; Williams and Benson 1971, see also Section 4.2).

In the framework of the circular R3BP, Krasinsky (1972) showed that the critical inclination in the case of the inner perturber (with the orbital semimajor axis much smaller than that of the perturbed particle) is $\approx 63°$, i.e., much greater than that in the case of the outer perturber, where it is $\approx 39°$. Pluto has a moderate inclination, $i \approx 17°$ (see Table 7.2), but it is nevertheless subject to ω-libration, due to perturbation from the inner perturber (Neptune). The reason is that inside a mean motion resonance the conditions for emergence of the LK-resonance are different; besides, the problem is far from being strongly hierarchical (see, e.g., Gallardo et al. 2012).

LK-plutinos is a natural designation for those objects that reside both in the LK-resonance and in the 2/3 mean motion resonance with Neptune. The LK-plutinos have their orbital pericenters out of the ecliptic plane, due to ω-libration around 90° or 270°. This introduces a selection effect, preventing from discovering LK-plutinos in observational ecliptic surveys. Cosmogonical scenarios of the primordial migration of the giant planets predict the LK-plutino fraction in the total plutino population to be in the range 10–30 %; however, the fraction deduced from observational surveys is substantially lower (8–25 %), perhaps due to observational biases (see Lawler and Gladman 2013, and references therein).

The 2/3 resonance with Neptune, in concert with the LK-resonance, serves as a protection mechanism for plutinos: the LK-plutinos avoid close encounters with Neptune. However, most of the total plutino population does not have the arguments of perihelia librating; Nesvorný et al. (2000) attribute this to a destabilization of their orbits due to perturbations from Pluto.

As shown by Wan and Huang (2007) in massive numerical experiments on the dynamics of TNOs, the LK-resonance with centers at $\omega = 90°$ or 270° can persist in the dynamics of plutinos both inside and outside the 2/3 mean motion resonance with Neptune.

7.4.2 Secular Resonances

The LK-resonance is often regarded as a kind of a *secular resonance*. Therefore, let us briefly discuss the major secular resonances in the Solar system, and consider their properties, as well as interactions with the LK-resonance.

An ordinary secular resonance takes place if a resonant combination of frequencies is formed by the frequency of the proper[3] longitude of pericenter $\dot{\varpi}_{\text{proper}}$ or the proper longitude of ascending node $\dot{\Omega}_{\text{proper}}$ of a test body and one of the eugenfrequencies of a system of perturbers. The classical secular planetary theory

[3]By a *free* or *proper* orbital element one denotes the element's value after removal of any contributions due to perturbations from other bodies. Thus, the proper eccentricity or inclination reflects the "inherent" properties of the orbit. For rigourous definitions and procedures of calculation see section 7.10 in Murray and Dermott (1999).

for the Solar system is based on the Lagrange planetary equations of the lowest order in the eccentricities and inclinations. Its solution splits in two sub-solutions: one in the elements (e, ϖ) and one in the elements (i, Ω), independent from each other (see, e.g. Murray and Dermott 1999). This allows one to identify analytically the locations of the main secular resonances in the space of the proper elements. When higher-order terms in the eccentricity and inclination and/or the second order terms in the mass parameter are taken into account, the (e, ϖ) and (i, Ω) solutions are no more decoupled, and the theory is much more complicated; for reviews on the subject see Froeschlé and Morbidelli (1994) and Knežević and Milani (1994). The secular-resonant relations, due to this nonlinear coupling, describe specific two-dimensional surfaces in the three-dimensional space of proper elements (a, e, i).

For a minor body in the Solar system, a secular resonance takes place, in particular, if any of the proper frequencies of the orbital precession of the body equals any of the proper frequencies of our planetary system. For the asteroids in the main belt, there exist three such prominent resonances, a pair at ∼2 AU and one at ∼2.6 AU. Williams (1969) and Williams and Faulkner (1981) computed locations of the principal secular resonances in the main belt; these were the *linear* secular resonances, now called the ν_5, ν_6, and ν_{16} resonances; for them, $\dot{\varpi}_{\text{proper}} - g_5 = 0$, $\dot{\varpi}_{\text{proper}} - g_6 = 0$, and $\dot{\Omega}_{\text{proper}} - s_6 = 0$, respectively, where g_k and s_k are the planetary frequencies, $k = 1, 2, \ldots, 8$. The subscript in the designations indicates the ordinal number of the relevant planetary frequency: $\nu_1 = g_1, \ldots, \nu_{10} = g_{10}, \nu_{11} = s_1, \ldots, \nu_{18} = s_8$. In Fig. 7.5, the sets of points corresponding to the linear secular resonances generate curves in the "proper semimajor axis–proper inclination" plane; the curves are presented for $e_{\text{proper}} = 0.1$ (Milani and Knežević 1990). They are superimposed on the distribution of the main-belt asteroids. Note that the apparent depletion of the main-belt population at ∼2.5 and ∼3.3 AU is due to the mean motion resonances 3/1 and 2/1 with Jupiter.

From Fig. 7.5, it is clear that the inner edge of the main belt is formed mostly by the secular resonance ν_6, whereas the outer edge is formed by the 2/1 mean motion resonance. The "vertical" structure (i.e., the distribution of the asteroids in the inclination) of the main belt at moderate inclinations (namely, at $i < 30°$) is formed by secular resonances ν_6, ν_{16}, and ν_5.

The apparent deficit of asteroids in the ν_5 resonance is mostly due to the LKE. Generally, the LKE is responsible for the overall depletion of the main belt at high inclinations, due to the eccentricity pumping up to values, corresponding to crossings of planetary orbits. The ν_5 resonance itself plays a subordinate role in forming this depletion, because the amplitude of the eccentricity variations, caused by this resonance, is small (∼0.05), as the amplitude of its harmonic in the Hamiltonian is small, in the semimajor axis range of the main belt (Morbidelli 2002; Morbidelli and Henrard 1991a,b).

The ν_{16} resonance in the main belt exists not only inside the LK-resonance, but outside it as well. Nakai and Kinoshita (1985) showed that the ν_{16} amplitude outside the LK-resonance can be greater than 15°, significantly exceeding the ν_{16} amplitude inside the LK-resonance. Besides, outside the LK-resonance, the libration center of

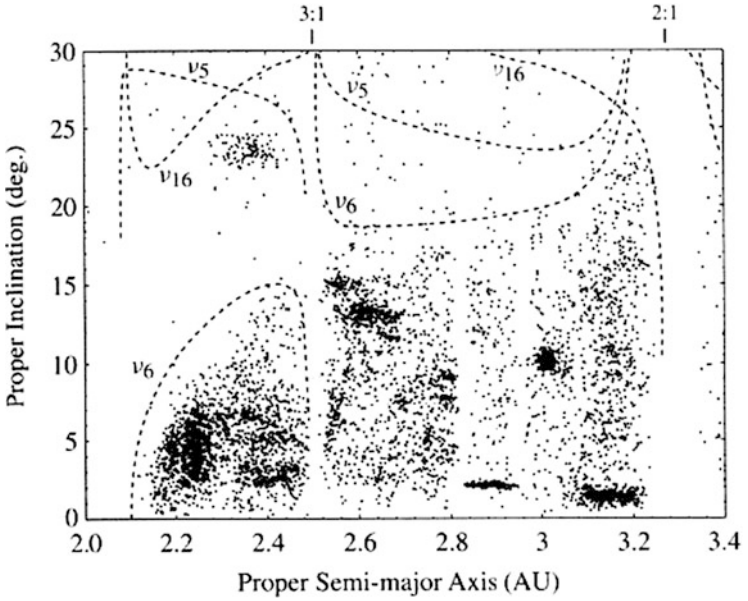

Fig. 7.5 Linear secular resonances ν_5, ν_6, and ν_{16} in the "proper semimajor axis–proper inclination" space. The *curves* are computed for $e_{\text{proper}} = 0.1$. The distribution of asteroids is represented by *dots* (Figure 7.19 from Murray and Dermott 1999. With permission from Cambridge University Press)

the ν_{16} resonance is situated at $\sigma_{16} = 180°$, i.e., it is shifted by 180° in comparison with its position when the asteroid is inside the LK-resonance. An illustration of a secular asteroidal motion residing simultaneously in the LK-resonance and in the ν_{16} resonance will be given further on in Sect. 7.5 and Fig. 7.6.

The so-called *nonlinear*[4] secular resonances correspond to the terms of higher order in the eccentricities and inclinations in the expansion of the perturbing function in power series. Of course, their set is restricted by the condition that the D'Alembert rules must be obeyed. In particular, the following nonlinear secular resonances are operational in the main belt (Knežević and Milani 1994): $\dot{\varpi}_{\text{proper}} + \dot{\Omega}_{\text{proper}} - g_5 - s_6$, $\dot{\varpi}_{\text{proper}} + \dot{\Omega}_{\text{proper}} - g_6 - s_6$, $\dot{\varpi}_{\text{proper}} + \dot{\Omega}_{\text{proper}} - g_5 - s_7$, $\dot{\varpi}_{\text{proper}} - 2g_6 + g_5$, $\dot{\varpi}_{\text{proper}} - 2g_6 + g_7$, $\dot{\varpi}_{\text{proper}} - 3g_6 + 2g_5$, $\dot{\Omega}_{\text{proper}} - s_6 - g_5 + g_6$, $2\dot{\varpi}_{\text{proper}} + \dot{\Omega}_{\text{proper}} - 2g_6 - s_6$, and $3\dot{\varpi}_{\text{proper}} + \dot{\Omega}_{\text{proper}} - 3g_6 - s_6$.

[4]The term "nonlinear resonance" here has a meaning different from that adopted generally in the Hamiltonian dynamics. In the latter case, the "nonlinear resonance" is such a resonance that has the frequency of libration on resonance dependent on the libration amplitude; conversely, in the case of "linear resonance", this frequency is constant with the amplitude (see Chirikov 1979; Lichtenberg and Lieberman 1992).

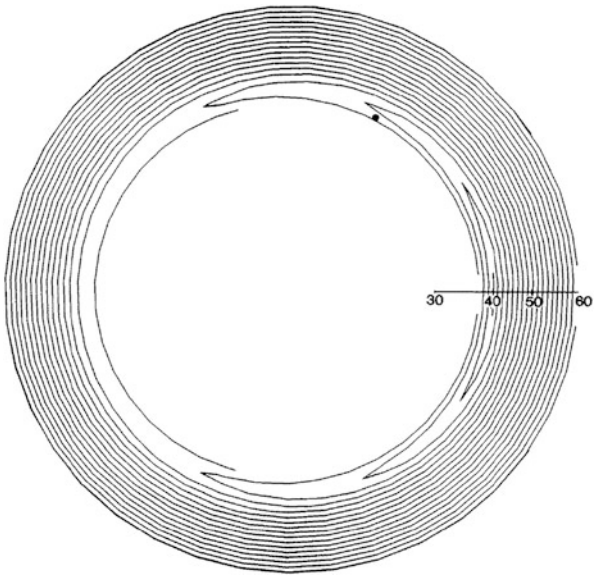

Fig. 7.6 The ν_{16} secular resonance inside the LK-resonance. The diagram is computed for the values of semiproper action variables corresponding to asteroid 2335 James. The radial coordinate is the semiproper inclination i_{sp} defined as the minimum value of the inclination during the LK-libration cycle, and the angular coordinate is the resonant angle of the ν_{16} resonance. The current position of the asteroid is shown by a *dot* (Figure 5 from Morbidelli 1993. With permission from Elsevier Inc)

7.5 A Resonant "Dance" of 2335 James

A prominent example of an asteroid, exhibiting an outstanding multi-resonant secular dynamics, including transitions between secular resonances, is given by asteroid 2335 James.[5]

Froeschlé et al. (1991) found out that asteroid 2335 James (orbiting at $a \sim 2.12$ AU) is a chaotic object with a peculiar long-term behaviour: a direct numerical integration of its orbit showed that it entered and leaved the LK-resonance sporadically. When outside the LK-resonance, 2335 James moves simultaneously inside two secular resonances ν_5 and ν_{16} (resonant angles σ_5 and σ_{16} both librate). When inside the LK-resonance, the asteroid is outside the ν_5 resonance, but is still inside ν_{16}. The resonant angle σ_{16} librates around 0° or 180°, when the asteroid is respectively inside or outside the LK-resonance. The separatrix of the LK-resonance is crossed by the asteroid sporadically due to strong oscillations caused by the ν_{16} resonance in its inclination.

As noted already, the alternation of the ω-libration and ω-circulation regimes in the behaviour of 2335 James was earlier revealed by Vashkovyak (1986), using an analytical-numerical approach. Due to the chaotic character of the orbital evolution, the regimes alternate (the LK-separatrix is crossed) at unpredictable time moments, that is why in the works of Vashkovyak (1986) and Froeschlé et al. (1991) these moments are different.

[5]The asteroid is named after James Williams, who contributed much to the modern understanding of the secular dynamics of asteroids.

In Fig. 7.6, the secular dynamics of 2335 James in resonance ν_{16} inside the LK-resonance is illustrated. In this diagram, constructed by Morbidelli (1993), the dynamics is presented in polar coordinates: the radial one is the semiproper inclination i_{sp} defined as the minimum value of the inclination during the LK-libration cycle, and the angular one is the resonant angle of the ν_{16} resonance. The current location of the asteroid in these coordinates is marked by a dot. The level curves of the Hamiltonian of the secular resonance are presented only for the domain of libration of the argument of perihelion; on crossing the Kozai separatrix they are discontinued. Asteroid 2335 James librates around $\sigma_{16} = 0$, and its semiproper inclination varies in the interval between $\sim 37°$ and $\sim 42°$. The libration curve apparently crosses the Kozai separatrix (at the point with the coordinates $\sigma_{16} = 0$ and $i_{sp} \sim 37°$). This means that the asteroid may leave the LK-resonance (Morbidelli 1993, 2002); on leaving the resonance, the asteroid would have the argument of perihelion circulating.

Chapter 8
The Role in Sculpting Exoplanetary Systems

With the count of known exoplanetary systems rising (now exceeding two thousands, among which many are observed to be multiplanet,[1] and many belong to binary stars), the LK-mechanism has been invoked to explain several characteristic features of their dynamics. As early as in 1997, it was employed to explain a highly-eccentric orbit of an exoplanet (Holman et al. 1997).

The LKE might act in many observed multiplanet systems and in planetary systems of binary stars (with planets in inclined orbits), or acted in previous epochs, imprinting modern orbital configurations. The discovery of a qualitative multitude of orbital behaviours in exoplanetary systems has boosted celestial-mechanical studies of their secular dynamics (see, e.g. Ferraz-Mello et al. 2005; Greenberg and Van Laerhoven 2012; Lee and Peale 2003, and references therein), based on earlier theoretical works on secular dynamics of triple stars (e.g., Ford et al. 2000; Marchal 1990). As an important constituent of the new exoplanetary studies, the LKE theory has been extended and refined (e.g., Libert and Henrard 2007; Naoz et al. 2011).

Due to the LKE, the eccentricities and inclinations of planets may suffer large oscillations. Highly-eccentric circumstellar orbits are observed in planetary systems of some stellar binaries, in particular, in the 16 Cyg and γ Cep systems; this can be explained in the LKE framework (Haghighipour et al. 2010; Holman et al. 1997; Innanen et al. 1997; Mazeh et al. 1997; Takeda and Rasio 2005).

As a rule, exoplanetary systems are not at all similar to our own Solar system. Many exoplanets have large orbital eccentricities; what is more, giant exoplanets are usually observed to have orbits very close to their parent stars; these objects are called *hot Jupiters* (or *hot Neptunes* in case of smaller masses). Orbital periods of a few days and even less are observed. The origin of hot Jupiters since their discovery was most enigmatic, though they are abundant.

[1] A planetary system is called multiplanet if it contains more than one planet.

I. I. Shevchenko, *The Lidov-Kozai Effect – Applications in Exoplanet Research and Dynamical Astronomy*, Astrophysics and Space Science Library 441,
DOI 10.1007/978-3-319-43522-0_8

A theoretical problem with hot Jupiters is that a giant planet can form only at large enough distance from its parent star, that is why a delivery process of the planet to its current close-to-star location is needed. This process is called *migration*. Indeed, a significant presence of gas and dust in the disk where the planets form leads to a slow radial shifting (migration) of the planetary orbit. The migration can be directed either inwards (to the parent star), or outwards. The phenomenon of hot Jupiters might be also a result of the so-called *Lidov-Kozai migration*, discussed further on in this chapter.

Another problem concerns a mechanism of the migration stalling close to the parent star. Though, their might be no stalling at all, and the hot Jupiters are sooner or later absorbed by the star. Tidal effects are, of course, vital in such close-to-star vicinities (Batygin et al. 2009; Correia et al. 2013; Lovis et al. 2011; Van Laerhoven and Greenberg 2012).

Free-floating planets (FFP), sometimes also called *rogue planets* or *orphan planets*, are the planets that do not belong to any planetary system of a star, i.e., they travel freely in the interstellar space. Originally, such objects were discovered in a stellar cluster in the Orion nebula (Zapatero et al. 2000). They may appear due to escaping from planetary systems, in particular, from planetary systems of binary stars. Such an escaping is a dynamical process familiar from many studies in celestial mechanics. For example, it is known that Mercury can chaotically escape from our Solar system, though on a very long timescale, about billion years (Laskar 1994). A significant fraction of the planets formed in systems of binary stars can be ejected (Zinnecker 2001). A possible mechanism of the FFP production might include the LKE, because it is able to push planets to extreme apocentric distances, thus providing a condition for a planetary escape.

Based on the quoted inferences, in this chapter we consider the LKE in multi-planet systems and in planetary systems of binary stars. We discuss the phenomenon of the Lidov-Kozai migration, explaining the production of hot Jupiters and even (hypothetically) the origin of planets observed to be in retrograde orbits.

8.1 Secular Dynamics of Exoplanetary Systems

In view of the current rapid observational progress in exoplanetary studies, the term *planet* itself requires a rigourous definition, distinguishing the planets from other populations of celestial bodies. In application to the Solar system, the 26th General Assembly of the International Astronomical Union (Prague, 2006) adopted the following definition: the *planet* is a celestial body that (1) orbits around the Sun; (2) has mass large enough for the self-gravity to dominate over the rigid-body forces, so that the body acquires a hydrostatic-equilibrium (nearly spherical) figure; (3) has purged a neighborhood of its orbit, so that no planetesimal material is left in this neighborhood. This definition is a result of a thorough scientific debate (see Soter 2006; Stern and Levison 2002, and references therein); in particular, it is based on criteria of the stability of the close-to-coorbital motion. Apparently, its

field of applicability is restricted to the Solar system realm. A generalization for the exoplanetary systems requires limiting the planetary mass from above. Such a limit is given by the minimum mass of a brown dwarf star, which equals ∼17 Jupiter masses.

The discoveries of new exoplanets grow in number like an avalanche, due to the invention of new effective observational instruments and techniques (mostly space-based). To the beginning of 2016, more than 3400 exoplanets have been discovered (and much more await confirmation),[2] belonging to ∼2600 exoplanetary systems; about 23 % of these systems are observed to be *multiplanet*, i.e., they are observed to contain more than one planet. The distances to known exoplanets span the range from 4 light years (a planet in the α Centauri system, see Dumusque et al. 2012) to ∼30,000 light years (SWEEPS-04 and SWEEPS-11, see Sahu et al. 2006), i.e., four orders of magnitude!

Before we proceed to the LKE phenomena in exoplanetary systems, let us consider the secular theory in the planar restricted three-body problem (in a hierarchical setting, relevant for further exoplanetary applications). The LKE is absent in the planar problem; however, an analysis of the planar case is helpful before considering the general spatial case.

In the framework of the coplanar elliptic restricted three-body problem, Heppenheimer (1978) derived a secular perturbation theory, providing analytical formulas for the forced eccentricity e and the longitude of periastron ϖ of a test particle initially in a circular orbit around one of the components of a stellar binary. Thus, this secular theory corresponded to the circumstellar (circumprimary or circumsecondary) variant of the hierarchical elliptic R3BP. It was aimed for an analytical description of circumstellar planetesimal disks in binary stellar systems. In Whitmire et al. (1998) and Thébault et al. (2006), it was used to analytically describe how the circumstellar disk of a young star was stirred by a companion star. Conversely, the circumbinary variant (in which the test particle orbits around both components of the binary) was considered by Moriwaki and Nakagawa (2004). They presented equations of the secular circumbinary motion; see the Appendix in Moriwaki and Nakagawa (2004). In Demidova and Shevchenko (2015), the approaches of Heppenheimer (1978) and Moriwaki and Nakagawa (2004) were combined to derive the explicit analytical formulas for the secular evolution of the particle's eccentricity and longitude of pericenter in both circumbinary and circumstellar variants of the problem.

Consider first the planar R3BP "binary–particle" in the hierarchical circumbinary setting, i.e., assume that the distance of the particle from the binary barycenter is much greater than the size of the binary. In fact, it is superfluous to consider a non-hierarchical circumbinary case because a large central chaotic circumbinary zone exists at all eccentricities of the particle if $\mu \gtrsim 0.05$ (Shevchenko 2015), where $\mu = m_1/(m_0 + m_1)$ is the mass parameter of the binary ($m_0 \geq m_1$). This relative

[2]This rapid growth has been mostly due to the success of the *Kepler* space observatory mission.

mass threshold has an important physical meaning (Shevchenko 2015): above the threshold, the particle can diffuse, even starting from small eccentricities, following the sequence of the overlapping integer p:1 mean motion resonances between the binary and the particle, up to ejection from the system; close encounters with other bodies are not required for the escape. Note that, on the other hand, in the circumstellar case stable orbits always exist inside the Hill spheres of the binary components.

Let us adopt the barycentric frame; $m_0 \geq m_1$ are the masses of the binary components, a_b is the binary semimajor axis, e_b is the binary eccentricity, a is the semimajor axis of the particle's orbit. The masses are measured in Solar units, distances in astronomical units (AU), and time in years. Thus, the gravitational constant $\mathcal{G}$ is equal to $4\pi^2$.

The averaged perturbing function for the circumbinary case is given in Moriwaki and Nakagawa (2004). It is presented in the form of a truncated power-law expansion in the ratio of the binary and particle semimajor axes and in the eccentricities. In Demidova and Shevchenko (2015), the corresponding equations of secular motion (see Equations (A7) in Moriwaki and Nakagawa 2004) were integrated analytically, and thus the formulas for the secular time evolution of the eccentricity e and the longitude of periastron ϖ of the circumbinary particle were straightforwardly derived. They turned out to be very similar to those in the circumstellar case, presented in Heppenheimer (1978). They are given by

$$e = e_{\max} \left| \sin \frac{ut}{2} \right|, \tag{8.1}$$

$$\tan \varpi = -\frac{\sin ut}{1 - \cos ut}, \tag{8.2}$$

where t is time,

$$u = \frac{3\pi}{2} \frac{m_0 m_1}{(m_0 + m_1)^{3/2}} \frac{a_\mathrm{b}^2}{a^{7/2}} \left(1 + \frac{3}{2} e_\mathrm{b}^2\right), \tag{8.3}$$

and $e_{\max} = 2e_\mathrm{f}$, where e_f is the so-called forced eccentricity

$$e_\mathrm{f} = \frac{5}{4} \frac{(m_0 - m_1)}{(m_0 + m_1)} \frac{a_\mathrm{b}}{a} e_\mathrm{b} \frac{\left(1 + \frac{3}{4} e_\mathrm{b}^2\right)}{\left(1 + \frac{3}{2} e_\mathrm{b}^2\right)}. \tag{8.4}$$

Using a new variable, namely, $y = ut/2$, Equation (8.2) can be rewritten in the form

$$\text{if } y \geq -\pi \text{ and } y \leq -\frac{\pi}{2}, \text{ then } \varpi = y + 5\frac{\pi}{2};$$

$$\text{if } y \geq -\frac{\pi}{2} \text{ and } y \leq 0, \text{ then } \varpi = y + \frac{\pi}{2};$$

$$\text{if } y \geq 0 \text{ and } y \leq \frac{\pi}{2}, \text{ then } \varpi = y + 3\frac{\pi}{2};$$
$$\text{if } y \geq \frac{\pi}{2} \text{ and } y \leq \pi, \text{ then } \varpi = y - \frac{\pi}{2}. \tag{8.5}$$

Thus, u can be regarded as a "precession rate" (though in a modified fashion) of an individual orbit.

Numerical simulations of the dynamical stirring of planetesimal disks on secular timescales were performed in Moriwaki and Nakagawa (2004), Meschiari (2012a,b), and Paardekooper et al. (2012) in various problem settings. In particular, graphs of the eccentricity and longitude of periastron of a circumbinary particle as a function of its semimajor axis were constructed numerically. Such graphs can also be constructed analytically using the described above secular theory (see Demidova and Shevchenko 2015).

In the hierarchical circumstellar case, the expressions for the secular eccentricity and longitude of periastron as functions of time are virtually the same as in the hierarchical circumbinary case and are given by Equations (8.1), (8.2), and (8.5), but the formulas for the u and $e_{\rm f}$ parameters, entering these expressions, are different. They are given in Heppenheimer (1978), Whitmire et al. (1998), and Thébault et al. (2006). In our notation, they are given by

$$u = \frac{3\pi}{2}\frac{m_1}{m_0^{1/2}}\frac{a^{3/2}}{a_{\rm b}^3}\left(1-e_{\rm b}^2\right)^{-3/2}, \tag{8.6}$$

$$e_{\rm f} = \frac{5}{4}\frac{a}{a_{\rm b}}\frac{e_{\rm b}}{\left(1-e_{\rm b}^2\right)}. \tag{8.7}$$

Here m_0 is the primary mass (around which the particle orbits) and m_1 the perturbing mass; $m_0 > m_1$. Note that in the treatment by Heppenheimer (1978), the secular perturbing function is not expanded in the eccentricities, but merely in the ratio of the particle and binary semimajor axes (up to the third order inclusive).

Thus, the secular dynamics in the planar circumstellar case is described analytically by Equations (8.1), (8.2), (8.5), (8.6), and (8.7).

8.2 LKE in Multiplanet Systems

About a third of all newly discovered exoplanets belongs to multiplanet systems, i.e., the systems containing more than one planet (Rein 2012). In application to the multiplanet systems, the LKE theory was extended and refined in Libert and Henrard (2007), Naoz et al. (2011), and other works reviewed below. The LKE might act in many observed multiplanet systems and in planetary systems of binary stars (with planets in highly inclined orbits), or has acted in previous epochs, imprinting the modern orbital architecture of these systems.

In Chap. 7 we have already seen, in the example of the motion of asteroids in the main belt and TNOs in the Kuiper belt, how the LKE operates in the presence of several perturbers. Of course, when the perturber is not single, the analytical approach is much more complicated, and the main tool to study the LKE in such circumstances consists in numerical experiment.

Already in the 1990s, Innanen et al. (1997) showed that, in the presence of a distant inclined stellar companion, the LKE-induced variations of the eccentricity and inclination of an exoplanet may lead to planet-planet scattering. An outer planet orbiting one of the binary components may attain, via the LKE, the eccentricity high enough for encounters with inner planets. Consequently, the outer planetary system of the component can be disrupted. In a cluster of young stars, the newly-born planets can thus be "torn away" from their parent stars (Malmberg et al. 2007); thus, these bodies enter the population of *free-floating* planets. The same mechanism may work in multiplanet systems of single stars.

The LKE manifestations were studied also in the cases of quadruple stars (Beust and Dutrey 2006) and triple stars with a planet (Marzari and Barbieri 2007), where the LKE role can be even more pronounced.

The LKE might be active in configuring *binary planets* in exoplanetary systems. Indeed, there exists an analogy with objects in our Solar system: Perets and Naoz (2009) and Fang and Margot (2012) showed that the LKE is important for the dynamics of binary minor planets in the Solar system. In this case, the "inner binary" is the binary minor planet, and the outer perturber is the Sun. In the Solar system, the mutual orbits of binary minor planets (asteroids and TNOs) secularly evolve due to encounters with other bodies, mutual tides and the Sun-induced LKE; this evolution has resulted in an almost isotropic distribution of the inclinations of the mutual orbits of the binaries with respect to the planes of their orbits around the Sun; in particular, the inclinations are typically high (Naoz et al. 2010). For tight binaries, the LKE in concert with the tidal friction may produce circularized short-period binaries and even lead to coalescence of binary companions (Perets and Naoz 2009). In what concerns the possible role of the LKE, these inferences on the binary asteroids, after rescaling, might be applicable to assess the statistics of orbital properties of binary planets in exosystems.

As we have already thoroughly discussed in Chaps. 3 and 4, in the spatial case of the three-body problem, if the system is in LK-resonance, the secular variations in the eccentricity e and inclination i are coupled: they are in antiphase, if $i < \pi/2$, and in phase, if $i > \pi/2$. The maximum eccentricity is achieved at $i = 0$, and the maximum inclination at $e = 0$. If the initial inclination i_0 is greater than the critical inclination, then the maximum eccentricity achieved by the inner binary during the LK-cycle is insensitive to e_0 (if $e_0 \lesssim 0.1$) and is given by

$$e_{\max} \approx \left(1 - \frac{5}{3}\cos^2 i_0\right)^{1/2}, \tag{8.8}$$

where i_0 is the initial inclination of the inner binary with respect to the outer perturber's orbital plane (Holman et al. 1997; Innanen et al. 1997). This result is

valid in the quadrupole order approximation of the Hamiltonian. If the amplitude of ω-libration is not too high (the system is not close to the separatrix of the LK-resonance), the libration period, according to formula (4.44), is given by

$$P_{\rm LK} \approx P_1 \frac{(m_0 + m_1)}{m_{\rm pert}} \left(\frac{a_{\rm pert}}{a_1} \right)^3 (1 - e_{\rm pert}^2)^{3/2}, \tag{8.9}$$

where P_1, m_0, m_1, and a_1 are, respectively, the orbital period, masses and semimajor axis of the inner binary (which is subject to the LKE induced by an outer perturber orbiting the binary). The quantities $P_{\rm pert}$, $m_{\rm pert}$, and $e_{\rm pert}$ are, respectively, the orbital period, mass, and eccentricity of the outer perturber.

In a slightly different version this approximate formula was given by Kiseleva et al. (1998):

$$P_{\rm LK} \approx \frac{2}{3\pi} \frac{P_{\rm pert}^2}{P_1} \frac{(m_0 + m_1 + m_{\rm pert})}{m_{\rm pert}} (1 - e_{\rm pert}^2)^{3/2}. \tag{8.10}$$

As follows from formulas (8.9) or (8.10), during a main-sequence star lifetime, the number of LK-librations of the inner binary may exceed hundreds or even thousands, if generic conditions allowing the LKE are fulfilled (Ford et al. 2000; Kiseleva et al. 1998).

8.3 LKE in Planetary Systems of Binary Stars

More than a half of the main-sequence stars in our Galaxy belongs to multiple (including binary) stellar systems (Duquennoy and Mayor 1991; Mathieu et al. 2000). At present, planets are known to exist in $\sim$100 multiple (mostly binary, of course) stellar systems; recall that more than 2000 exosystems are known in total. The majority of planets, discovered to be present in binary systems, are the so-called *S-type* planets (orbiting one component of a binary, i.e., *satellite-type*), and others are *P-type* planets (moving in an orbit around both components of a binary, i.e., *planet-type*). The S-type planets are also called inner or circumstellar planets, and the P-type planets are also called outer or circumbinary planets.

Until the launch of the *Kepler* space observatory mission, a few circumbinary planetary systems had been known to exist (belonging to binary stars HW Vir, NN Ser, UZ For, DP Leo, FS Aur, SZ Her, among others). However, none of them belonged to a main-sequence star. Due to the *Kepler* mission, several circumbinary planetary systems of main-sequence stars were discovered. The first among them were *Kepler*-16, 34, 35, 38, and 47 (Doyle et al. 2011; Orosz et al. 2012; Welsh et al. 2012). Among them, the *Kepler*-47 system is multiplanet: it includes two circumbinary planets. The planets in the *Kepler* circumbinary systems are all co-planar with the parent binaries, but this does not say anything on the real inclination statistics, because the planets were discovered using the transit method, implying

the coplanarity of the orbits of the eclipsing stellar binary and the transiting planet. In the discovered circumbinary systems, the LKE does not play role because the inclinations are small.

Theoretical studies of the stability of hypothetical planetary systems in binary stellar systems were initiated already in the 1960s of the twentieth century (Huang 1960), long before the observational discovery of planets belonging to binary stars. Subsequently, the theory was thoroughly developed in the 1980s, in application to some binary stars in the Solar neighbourhood (Benest 1988a,b, 1989). At present, the formation scenarios and the observed dynamics of planets (often at the "brink of stability") of binary stars present a number of theoretical challenges, especially concerning the circumbinary planets (Meschiari 2012a,b, 2014; Paardekooper et al. 2012). To analyze the dynamical stability and the possibility of formation of such systems, especial criteria of stability are developed (Moriwaki and Nakagawa 2004; Shevchenko 2015).

In young binary stars that contain planetesimal disks around one of the companions, the LKE may excite the orbital eccentricities of the planetesimals. Thus, the planet formation can be hindered, if the orbit of the perturbing companion is inclined enough with respect to the disk (Fragner et al. 2011; Marzari and Barbieri 2007). The LKE can be suppressed, though in a way different from that discussed in Chap. 3: here, the gas drag in the disk and/or the disk self-gravity can significantly hinder the angular momentum transfer, suppressing the LKE; this makes the planetary formation possible (Batygin et al. 2011; Xie et al. 2011).

As follows from formula (8.9) or (8.10), the Lidov-Kozai libration period sharply rises with increasing the relative size of the outer perturber orbit (i.e., with decreasing α); therefore, the S-planetary LKE in wide stellar binaries is much less impressive than the LKE in compact binaries. However, even in wide binaries, the LKE oscillation timescale, though enormous (up to Gigayears), can be nevertheless sufficient for the LKE to make a planetary orbit highly eccentric.

As early as in 1997, the LKE was invoked to explain a highly-eccentric orbit of an exoplanet (namely, a planet of 16 Cyg B), subject to perturbations from a distant companion of the planet's parent star (Holman et al. 1997). The planet orbiting 16 Cyg B has the eccentricity $\approx$0.67. Highly-eccentric circumstellar orbits of planets are observed in several stellar binaries, in particular, in 16 Cyg and γ Cep; this might be understood in the LKE framework (Haghighipour et al. 2010; Holman et al. 1997; Innanen et al. 1997; Mazeh et al. 1997; Takeda and Rasio 2005). That the LKE is active here is confirmed by the fact that the planets with such extreme eccentricities are mostly contained in planetary systems with an outer stellar companion (Wright et al. 2011).

The 16 Cyg AB system is a binary consisting of two solar-type stars, separated from each other by $\sim 10^3$ AU. Radial-velocity measurements showed that the binary component 16 Cyg B has a Jovian-mass planet, designated 16 Cyg Bb; its orbit around 16 Cyg B has semimajor axis $a \approx 1.7$ AU, period $P \approx 2.2$ years, eccentricity $e \approx 0.67$ (Cochran et al. 1997). Such a large eccentricity looks rather unexpected for a giant planet, because the planets form in protoplanetary disks in which the planetesimal motions are circularized. Holman et al. (1997) and Mazeh et al. (1997)

put forward a hypothesis that the large eccentricity could be boosted by an inclined outer stellar perturber, due to the LKE. In this system, the perturber is 16 Cyg A. However, as pointed out by Holman et al. (1997), general relativity may play a role in this system to suppress the LKE (see Sect. 3.3), because the relativistic advance of the planet's pericenter may have the period as low as 70 million years; for the suppression to happen the inequality $a_2 q_2 \lesssim 3 \cdot 10^5$ (where the stellar binary's semimajor axis a_2 and pericentric distance q_2 are measured in AU) must hold. This inequality follows from comparison of analytical expressions for the LK and relativistic timescales. Holman et al. (1997) showed that, given a small initial eccentricity and an initial inclination in the range 45°–135°, the planet may suffer eccentricity changes up to 0.8 (see Fig. 3.3), being in the high-eccentricity ($e > 0.6$) state up to 35 % of its lifetime. The amplitudes of changes in the eccentricity and inclination are independent of the binary's a_2 and q_2; these two quantities only affect the timescale of the LK-oscillations.

In Fig. 8.1, a comparison is given of various characteristic secular timescales of this system: $P_{\mathrm{A,\,Low-i}}$ and $P_{\mathrm{A,\,High-i}}$ are the periods (in quadrupole approximation) of LK-oscillations due to influence of 16 Cyg A in a low-inclined ($i < 40°$) and highly-inclined ($\sin i \sim 1$) orbits, P_{GR} is the period of the relativistic apsidal precession; P_{Bc} is the period of LK-oscillations due to influence of a hypothetical second planet, 16 Cyg Bc, of a Jovian mass in a circular orbit coplanar with 16 Cyg Bb; τ_{ms} is the age of the star 16 Cyg B. All time quantities are given in years. The periods $P_{\mathrm{A,\,High-i}}$ and $P_{\mathrm{A,\,Low-i}}$ correspond to a range of orbital solutions due to Hauser and Marcy (1999). The quantities $P_{\mathrm{A,\,Low-i}}$, $P_{\mathrm{A,\,High-i}}$, and P_{GR} are plotted as a function of the inner binary's semimajor axis, and P_{Bc} as a function of the semimajor axis of the hypothetical 16 Cyg Bc.

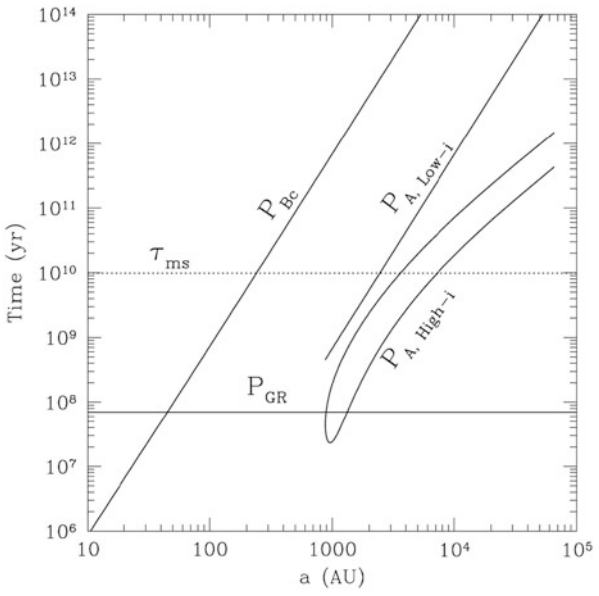

Fig. 8.1 The precession timescales for the longitude of pericenter of a planet orbiting 16 Cyg B. See text for details (Figure 16 from Ford et al. 2000. Copyright AAS. Reproduced with permission)

One can see that, unexpectedly enough, only in a rather small range of the perturber's orbit size the LKE may dominate over the general relativity effect. Ford et al. (2000) find that only one quarter of orbital solutions due to Hauser and Marcy (1999) allow for the LK-period shorter than the relativistic one. However, they note that, as soon as the mass ratio of the planet and the perturber is small, and the planet's eccentricity is large, the ratio $C_3/C_2 \sim 1$ (see formulas (4.28) and (4.29)), and, thus, the octupole term is essential in the long-term dynamics of the planet and it should be taken into account. Besides, as follows from the plot, the hypothetical 16 Cyg Bc may well induce the required LKE, if its orbit is small enough.

Holman et al. (1997) hypothesized that the motion of 16 Cyg Bb might be chaotic (see Fig. 3.3), because the amplitude of ω-libration is large; however, as Melnikov (2016) showed by means of massive computations of Lyapunov exponents on representative sets of initial values of orbital elements, this is unlikely because a too close proximity to the separatrix of the LK-resonance is required for the dynamical chaos to emerge.

8.4 The Lidov-Kozai Migration and the Origin of "hot Jupiters"

In our Solar system, the giant planets (Jupiter, Saturn, Uranus, and Neptune) have orbital radii from 5 to 30 AU. In contrast to this fact, the observed exoplanetary systems frequently contain giant planets with orbital radii hundreds times smaller. Such planets, orbiting within $\sim$0.1 AU of the parent star, are called *hot Jupiters*, on apparent reasons. The orbital periods of hot Jupiters can be as small as a few days. Of course, there exists a selection bias: massive planets in tight orbits are most easy to discover, if one uses usual methods, such as the *transit method* (analysis of a lightcurve of a star, subject to eclipses by a planet) or the *RV-method* (analysis of spectroscopic measurements of the radial velocity variations of a star).[3] In fact, due to this bias, the first exoplanet found to orbit a main-sequence star turned out to be a hot jupiter. It is planet 51 Peg b, discovered by Mayor and Queloz (1995).

A problem with hot Jupiters is that they cannot form in situ, because the planet-forming accretion of matter cannot take place in such close vicinities to the parent star (Bodenheimer et al. 2000). Therefore, they are transported to their observed location, either due to a slow radial inward *migration* in a thick protoplanetary disk, or due to some other dynamical mechanism provided by perturbing bodies, such as a stellar companion of the parent star and/or other massive planets. In the latter case, the LKE may be a decisive component of any dynamical route for the hot Jupiters' formation.

[3]For a description of methods for the discovery of exoplanets, see, e.g., Ferraz-Mello et al. 2005.

The dissipative effects and the LKE may operate in concert. The LKE in the presence of dissipation due to tides causes the so-called *Lidov-Kozai migration* (Lithwick and Naoz 2011; Naoz et al. 2011). The Lidov-Kozai migration can be regarded as a modification of the LKE in the presence of the star-planet tidal phenomena; together they act to decrease the semimajor axis of a planet extremely (Wu and Murray 2003). The role of the tidal dissipation in the secular orbital evolution has been intensely explored (e.g., Batygin et al. 2009; Correia et al. 2013; Lovis et al. 2011).

In total, there are at least five possible scenarios for the formation of hot Jupiters, involving dynamical interactions with distant perturbers (Davies et al. 2014). They include: (1) the secular orbital evolution of a planet perturbed by an inclined stellar companion of the parent star; (2) the same as (1) except the main perturber is an inclined planet; (3) the gravitational scattering of planets during an early stage of the evolution of a tightly-packed planetary system; (4) the secular orbital evolution of a planar planetary system (without the LKE); (5) a significant variability of the inclination of the protoplanetary disk due to perturbations from neighboring stars in a cluster, or due to the gravitational influence of a stellar companion (in a binary system).

In any of these scenarios, the planet is born at a typical orbital distance $\sim$10 AU from the parent star. These scenarios differ in the routes that bring the orbital pericenter of the planet to the vicinities of the star, where the tidal forces come into play. In particular, such a route can be provided by the LKE due to a stellar companion or an additional giant planet. Originally, the LKE was invoked by Wu and Murray (2003) to explain how hot Jupiters may emerge in a binary stellar system with a single planet orbiting one of the stellar companions. The tidal friction makes the orbit tighter and tighter and circularizes it (Fabrycky and Tremaine 2007; Nagasawa et al. 2008; Wu and Murray 2003; Wu et al. 2007).

For the typical Jupiter-like planets orbiting Solar-type stars, Wu and Murray (2003) estimate the circularization radius of the planetary orbit (the semimajor axis at which the orbit becomes circular) as $a_{\rm circ} \sim 3R_{\rm Sun}$, where $R_{\rm Sun}$ is the Solar radius. When a planet is close to the parent star, the tides are raised on both of them. The tides on the star are responsible mostly for decreasing the planetary orbital semimajor axis, whereas the tides on the planet are responsible mostly for decreasing the planetary eccentricity. The tidal processes are very effective in the orbital evolution of hot Jupiters (for details see, e.g., Ivanov and Papaloizou 2004, 2011). They are as well effective in the orbital evolution of components of triple stars, if the pericenter of a perturbed star approaches the primary closely enough (Mazeh and Shaham 1979).

From the observational viewpoint, the LKE is a likely (though not the only possible) mechanism to operate in typical exoplanetary systems containing hot Jupiters, because a significant fraction of hot Jupiters are observed to move in the orbits that are radically misaligned with respect to the equatorial planes of the parent

stars, or even in the orbits retrograde with respect to the rotation of the parent star. This evidence is provided by observations of the *Rossiter–McLaughlin effect*[4] (see, e.g., Winn et al. 2010, 2009).

In Chap. 3, we have seen that the LKE in the motion of a body can be suppressed if additional dynamical perturbations, causing the body's orbit to precess, dominate. The LKE in the motion of planets, analogously, can be suppressed in at least three ways, due to (1) the rotational oblateness of a planet, causing its orbital precession; (2) tides raised on the planet,—they also cause the orbital precession; (3) the general-relativistic precession of the planetary orbits whose pericenters are close to compact primaries, especially if the orbits are highly eccentric.

In Sect. 3.3 on the LKE-preventing phenomena, we have already thoroughly discussed orbital precession phenomena arising due to a number of physical causes. The formulas for the precession rates can be rendered the following convenient form (Wu and Murray 2003):

$$\frac{\dot{\varpi}_{\rm rot}}{n_{\rm p}} = \frac{m_{\rm star}}{m_{\rm p}}\frac{k_2^{(\rm p)}}{2(1-e_{\rm p}^2)^2}\left(\frac{\Omega_{\rm p}}{n_{\rm p}}\right)^2\left(\frac{R_{\rm p}}{a_{\rm p}}\right)^5, \tag{8.11}$$

$$\frac{\dot{\varpi}_{\rm tidal}}{n_{\rm p}} = \frac{15}{2}\frac{m_{\rm star}}{m_{\rm p}}k_2^{(\rm p)}\frac{\left(1+\frac{3}{2}e_{\rm p}^2+\frac{1}{8}e_{\rm p}^4\right)}{(1-e_{\rm p}^2)^5}\left(\frac{R_{\rm p}}{a_{\rm p}}\right)^5, \tag{8.12}$$

$$\frac{\dot{\varpi}_{\rm GR}}{n_{\rm p}} = 3\frac{\mathcal{G}m_{\rm star}}{a_{\rm p}c^2(1-e_{\rm p}^2)}. \tag{8.13}$$

Note that all ratios in the formulas are unitless. The formulas correspond, respectively, to the effects of rotational oblateness, tides on the planet, and general relativity. Here, $n_{\rm p}$, $a_{\rm p}$, $e_{\rm p}$, $m_{\rm p}$, $R_{\rm p}$, $k_2^{(\rm p)}$, and $\Omega_{\rm p}$ are, respectively, the planet's mean motion, semimajor axis, eccentricity, mass, radius, Love tidal number, and rotation frequency; $m_{\rm star}$ is the mass of the parent star; $\mathcal{G}$ and c are the gravitational constant and the speed of light. Formulas (8.11), (8.12), and (8.13) allow one to judge on the relative importance of a planetary system's parameters for enforcing the orbital precession of any origin. If one of the frequencies (8.11), (8.12), and (8.13), calculated independently from each other, exceeds $\dot{\omega}_{\rm LK} \propto P_{\rm LK}^{-1}$ (see formula (8.9)), then the LKE is most likely suppressed. For typical values of parameters in (8.11), (8.12), and (8.13), this may occur if the pericenter distance $q_{\rm p} = a_{\rm p}(1-e_{\rm p}) \lesssim 1$ AU.

The Rossiter–McLaughlin observations reveal the existence of strongly misaligned, close-to-polar, and even *retrograde* planetary configurations with hot

[4]The essence of the Rossiter–McLaughlin effect is as follows. A planet transiting a rotating star affects the measured radial velocity of the star differently at different phases of the transit, because the eclipsed disk on the star's disk corresponds to different local radial velocities of the star's surface. The Rossiter–McLaughlin effect allows one to estimate the angle between the star's equatorial plane (the plane orthogonal to the rotation axis of the star) and the planet's orbital plane.

Jupiters. The classical LKE (the LKE in the circular R3BP) is unable to produce retrograde configurations. However, they might be produced by the LK-oscillations of the particle in the elliptic three-body problem (Katz et al. 2011; Lithwick and Naoz 2011). This theoretical possibility is discussed in the next section.

The existence of strongly misaligned and retrograde orbits testify that the origin of hot Jupiters cannot be explained in the scenario of *planar* migration in a gas-dust disk. On the other hand, a scenario with the eccentricity excitation due to the LKE, complemented with a tidal shrinking and circularization of planetary orbits, produces tight misaligned configurations quite naturally (see, e.g., Nagasawa et al. 2008). What is more, transit observations from the *Kepler* space observatory provide a definite evidence that hot Jupiters are solitary, i.e., they do not form any close-to-star groups (Steffen et al. 2012). This is natural in scenarios involving the LKE and tides, but not in scenarios based on the planar migration in disks.

According to modern independent estimates (Naoz et al. 2012; Wu et al. 2007), the LK-migration scenario might be responsible for the origin of 10–30 % of the whole hot-jupiter population. The remaining fraction is due to scattering events followed by the tidal circularization. At least two mechanisms involving the LKE are able to explain the formation of hot Jupiters: (1) a combined scenario of the mutual scattering, LKE, and tidal circularization in multiplanet systems (e.g. Nagasawa et al. 2008), and (2) the LK-evolution (induced by a stellar or giant-planet companion) in a single-planet system (e.g. Fabrycky and Tremaine 2007).

8.5 Producing Retrograde Orbits?

Observations of the Rossiter–McLaughlin effect provide data on the obliquities of planetary orbits with respect to the equatorial planes of parent stars. They indicate that only about a half of all hot Jupiters (that were explored on this subject) has their orbital planes approximately aligned with the equatorial planes of the parent stars, whereas $\sim$30 % move in strongly misaligned prograde orbits and $\sim$20 % move in retrograde orbits (Albrecht et al. 2012).

Lithwick and Naoz (2011) and Katz et al. (2011) (in the framework of the restricted three-body problem, where the planet is massless), and Naoz et al. (2011) (in the framework of the general three-body problem, where the planet's mass is non-zero) showed that the planetary orbits subject to perturbations from a highly-inclined eccentric outer orbiter may exhibit transitions from prograde to retrograde modes of orbital motion and vice versa (the so-called *flips*). This was demonstrated by means of a theoretical analysis of the octupole-order expansion of the three-body Hamiltonian of the problem; the analysis was complemented by numerical-experimental examples of the flips.

The role of the octupole terms can be estimated by the value of the parameter

$$\epsilon_{\rm oct} = \frac{(m_0 - m_1)}{(m_0 + m_1)} \cdot \frac{a_1}{a_{\rm pert}} \cdot \frac{e_{\rm pert}}{(1 - e_{\rm pert}^2)}, \tag{8.14}$$

where $m_0 > m_1$ are the masses of the central binary (a star and a planet), a_1 is the semimajor axis of the planetary orbit, $a_{\rm pert}$ and $e_{\rm pert}$ are the semimajor axis and eccentricity of the perturber's orbit (Shappee and Thompson 2013). In the restricted problem, this formula reduces to formula (4.55). At a flip epoch, when the planet's inclination reaches the value of 90°, the planet's eccentricity strongly oscillates and can reach extreme values very close to unity.

Figure 8.2 illustrates the flip phenomenon in the general three-body problem (the planet's mass is non-zero). In panel (a), the planet's inclination is plotted versus

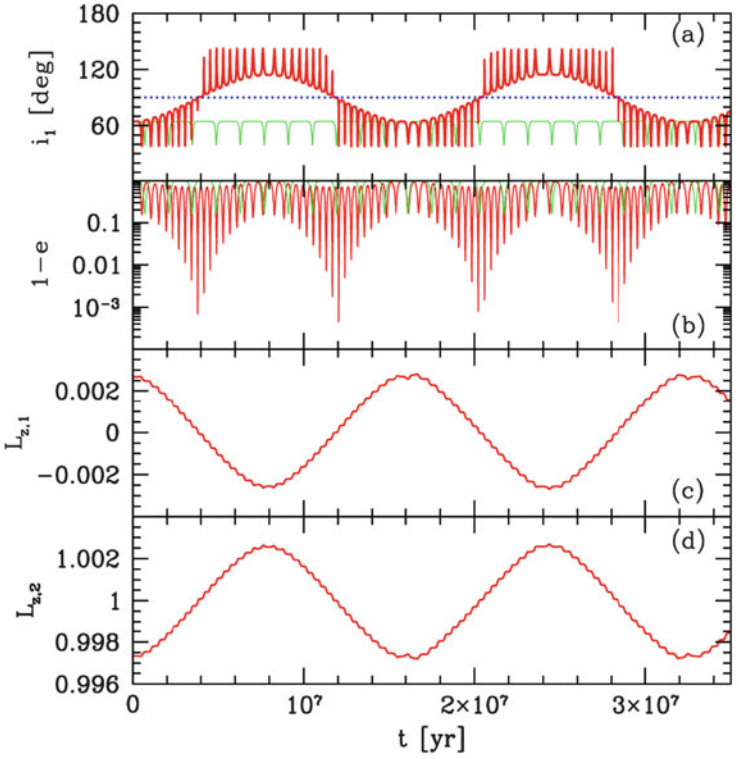

Fig. 8.2 Flips in the general three-body problem. Panel (**a**): the inclination versus time. Panel (**b**): the quantity $(1-e)$ (in logarithmic scale, e is the eccentricity) versus time. The *upper curve* in panel (**a**) and the *lower curve* in panel (**b**) (both in *red*) represent the refined theory using the perturbing function truncated to octupole order; the *lower curve* in panel (**a**) and the *upper curve* in panel (**b**) (both in *green*) represent the theory using the perturbing function truncated to quadrupole order. Panels (**c**) and (**d**): normalized vertical angular momenta of the inner and outer orbits, respectively, versus time (Figure 1 from Naoz et al. 2011. With permission from Nature Publishing Group)

time; in panel (b), the quantity $(1 - e)$, where e is the eccentricity, is plotted (in logarithmic scale) versus time. The masses of the inner binary are $m_0 = 1M_{\rm Sun}$ and $m_1 = 1M_{\rm J}$. Initially, $a_1 = 6\,{\rm AU}$ and $e_1 = 0.001$. The outer body has mass $m_{\rm pert} = 40M_{\rm J}$ (a brown dwarf), and its orbit around the central binary has initial semimajor axis $a_{\rm pert} = 100\,{\rm AU}$ and initial eccentricity $e_{\rm pert} = 0.6$. The inclination flips, occurring periodically every $\sim 10^7$ years, are apparent. They are accompanied by increases of the maximum eccentricity of the planet to extreme values.

From Fig. 8.2, one can see that the flips are present merely when the refined (octupole-order) theory is used. In panels (c) and (d), the normalized vertical angular momenta of the inner and outer orbits are plotted, demonstrating their anti-phase variations.

The flip phenomenon is possible both in the eccentric restricted three-body problem and in the general three-body problem with an initially eccentric orbit of the perturber. However, it disappears in the limit $m_1 \to m_0$ (the case of a symmetric inner binary), as apparent from formula (8.14). The dynamical reason is that the terms of odd order in the multipole expansion of the Hamiltonian average to zero in this case (see formula (4.10)). Shappee and Thompson (2013) used octupole-order numerical experiments to show that the flips become ubiquitous at $m_1 \lesssim 0.5m_0$.

In the framework of the hierarchical R3BP (the planet is massless), Katz et al. (2011) averaged the secular equations of motion[5] over the Lidov-Kozai cycle and found a new constant of the motion; this allowed them to derive an analytical condition for the flips to occur. The timescales of the eccentric LK-mechanism have been considered above in Sect. 4.5.2.

As we have already noted, the role of the octupole terms can be estimated by the value of the parameter, given by formula (8.14). In the restricted limit of the three-body problem ($m_0 \gg m_1$), the formula reduces to formula (4.55), i.e.,

$$\epsilon_{\rm oct} = \frac{a_1}{a_{\rm pert}} \cdot \frac{e_{\rm pert}}{(1 - e_{\rm pert}^2)}. \tag{8.15}$$

According to Katz et al. (2011), if the initial inclination of the particle $i_0 \gtrsim 60^\circ$ and its initial eccentricity $e_0 \ll 1$, then the flip takes place if $\epsilon_{\rm oct}$ exceeds a critical value, given by

$$\epsilon_{\rm crit} = \frac{16 \cdot 3^{1/2}}{\pi} \int_{\frac{3-3y}{3+2y}}^{1} \frac{K(x) - 2E(x)}{(41x - 21)(2x + 3)^{1/2}} {\rm d}x, \tag{8.16}$$

where $y = \frac{1}{2}\cos^2 i_0$; $K(m)$ and $E(m)$ are the complete elliptic integrals of the first and second kind, respectively.

[5]Note that this is a *third* averaging of the original equations of motion, because the secular equations are derived by double averaging of the original equations (over the orbital periods of the particle and the perturber).

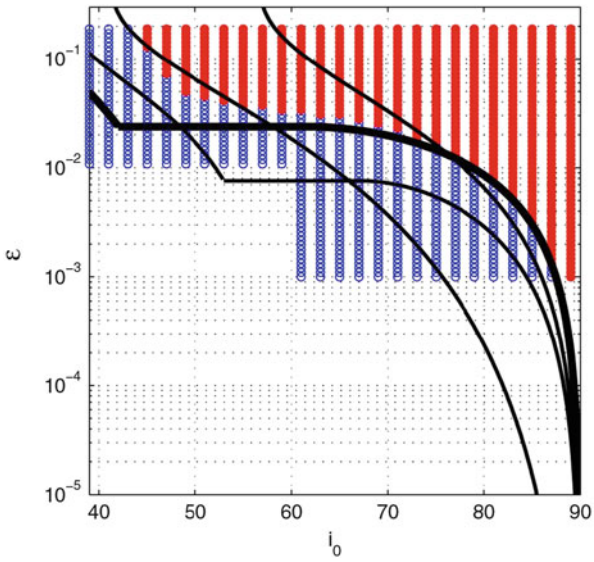

Fig. 8.3 The analytical threshold for a flip (the *thick curve*), given by formula (8.16); $\varepsilon \equiv \epsilon_{\rm crit}$. The *circles* denote the results of direct numerical integrations: the *filled circles* (in *red*) represent the cases with a flip, and the *non-filled circles* (in *blue*) represent the cases without a flip. The *thin curves* are described in text (Reprinted figure 4 with permission from Katz et al. 2011. Copyright (2011) by the American Physical Society)

The threshold for the flips is represented graphically in Fig. 8.3, where it is analyzed as a function of the initial inclination. Katz et al. (2011) checked the performance of the criterion by accomplishing numerical integrations of the secular equations of motion on a representative set of initial conditions. In Fig. 8.3, the integration results are shown as circles. The integrations were performed setting $e_0 = 0.001 \ll 1$. The thick curve is given by formula (8.16). The thin curves correspond to theoretical thresholds for moderate and large values of the initial eccentricity e_0 (from 0.2 to 0.5); a formula suitable for such values of e_0 is much more complicated than expression (8.16).

Katz et al. (2011) estimate that criterion (8.16) is in accord with the results of the numerical experiment to better than 10 % at $i_0 > 80°$ and better than 20 % at $i_0 > 70°$. At $i_0 < 50°$, the deviation is greater than twice and sharply increases with i_0 increasing. This is conceivable, since the analytical criterion was derived assuming a high enough initial inclination.

Criterion (8.16) is valid at high enough starting inclinations of the particle, as already mentioned. The reason is that, to derive the criterion, Katz et al. (2011) used the approximation of a small value of the vertical angular momentum (at the time moment of the flip, it is strictly zero). Li et al. (2014a) derived a criterion valid in another domain of initial conditions, namely, at the low inclinations and high eccentricities of the test particle. In this situation, the eccentricity grows *monotonically* until the epoch when the flip may occur (depending on initial conditions). This follows from an analysis of the octupole secular equations of motion in the almost coplanar setting of the hierarchical three-body problem, in the test particle approximation (see Li et al. 2014a). No next-level averaging of the

secular equations is needed to derive the criterion. It has the form

$$\epsilon_{\rm oct} > \epsilon_{\rm crit} = \frac{8(1-e_1^2)}{5\left[7-e_1(4+3e_1^2)\cos\varpi_1\right]}, \tag{8.17}$$

where $\epsilon_{\rm oct}$ is still given by formula (8.15), e_1 and ϖ_1 are the initial values of the eccentricity and the longitude of pericenter of the planetary orbit, respectively ($\varpi = \omega + \Omega$, where ω and Ω are the argument of pericenter and the longitude of ascending node of the planetary orbit, respectively).

The performance of criterion (8.17) is illustrated in Fig. 8.4, constructed by Li et al. (2014a). The performance of the criterion is checked by comparing the analytical curve with results of a numerical experiment: Li et al. (2014a) accomplished numerical integrations of the octupole secular equations of motion,

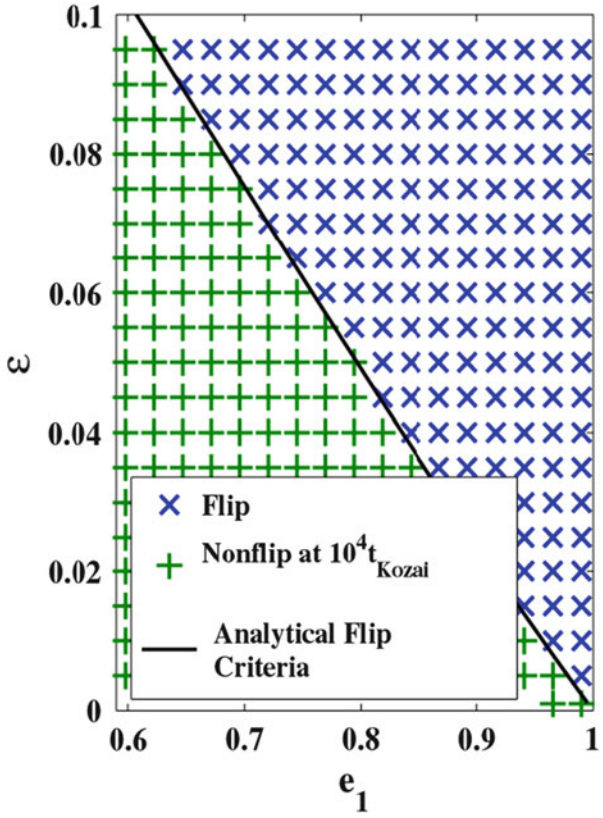

Fig. 8.4 The analytical threshold for a flip (the *thick curve*, $\varepsilon \equiv \epsilon_{\rm crit}$, given by formula (8.17)) and results of a numerical experiment: the *crosses* (in *blue*) represent the cases with a flip, and the *pluses* (in *green*) represent the cases without a flip (Figure 5 from Li et al. 2014a. Copyright AAS. Reproduced with permission)

setting $m_0 = 1M_{\rm Sun}$, $m_{\rm pert} = 0.1M_{\rm Sun}$, $a_2 = 1$ AU, $a_{\rm pert} = 45.7$ AU, and setting the initial conditions $\omega_1 = 0$, $\Omega_1 = 180°$, and, especially, $i_1 = 5°$, i.e., the initial system is almost coplanar. The trajectories were integrated on the time span of $10^4 T_{\rm LK}$, where $T_{\rm LK}$ is the duration of the Lidov-Kozai cycle. As it is clear from the diagram, the performance of the analytical criterion at the given values of the parameters and initial conditions is excellent.

The importance of this so-called "low inclination—high eccentricity" (the initial values are meant here) case of the eccentric LKE is that it may account for the production of hot Jupiters moving in *low-inclined* retrograde orbits, as Li et al. (2014a) argue. The existence of such objects is implied by results of massive observations of the obliquities of hot Jupiters with respect to the spin vectors of host stars (see Albrecht et al. 2012).

8.6 LKE and Dynamical Chaos

In this section, we explore interrelations between the concepts of resonances, dynamical chaos, and the LKE, in application to the dynamics of exoplanetary systems.

8.6.1 Dynamical Chaos Due to Resonance Overlap

The motion in a vicinity of the perturbed separatrices of nonlinear resonances is chaotic. For weakly perturbed systems the *chaotic layer* concept is convenient to apply for description of the chaotic component. The chaotic layer is a zone in a vicinity of the separatrices in the phase space where the dynamical system moves chaotically. The chaotic layer theory has applications in various areas of physics, mechanics and, in particular, in celestial mechanics (Chirikov 1979; Shevchenko 2000, 2007).

For dynamical chaos to emerge, three basic conditions must be satisfied (Devaney 1986; Meiss 1992): (1) Sensitive dependence on initial conditions, implying that nearby trajectories in the phase space diverge in time exponentially. (2) The boundedness of the motion, implying that the exponential divergence is not just a smooth infinite expansion. (3) The set of trajectories with such behaviour must have non-zero measure.

The rate of divergence of close trajectories (in the phase space and in the logarithmic scale of distances) is characterized by the *maximum Lyapunov exponent*. A distinction of the maximum Lyapunov exponent from zero testifies that the motion is chaotic (Chirikov 1979; Lichtenberg and Lieberman 1992). The inverse of this quantity, $T_{\rm L} \equiv L^{-1}$, is the *Lyapunov time*. It represents the characteristic time of predictable dynamics. The importance of this timescale for celestial mechanics is provided by the fact that any exact theory of the motion of any celestial-mechanical system cannot be constructed on any times much greater than its Lyapunov time.

The art of calculation of the Lyapunov exponents on computers has more than a thirty-year history and during this time it has become an extensive part of applied mathematics; see reviews in (Froeschlé 1984; Lichtenberg and Lieberman 1992). Modern numerical methods provide calculation of the Lyapunov exponents which is effective and precise. On the other hand, methods of analytical estimating the Lyapunov exponents appeared only recently (Holman and Murray 1996; Murray and Holman 1997; Shevchenko 2002, 2011a, 2014). A method of estimating the maximum Lyapunov exponent (Shevchenko 2002, 2011a, 2014), based on the theory of separatrix maps, allows one to obtain analytical estimates of the Lyapunov exponents (in accord with the numerical-experimental ones) in a number of problems on dynamics of the Solar system bodies; see a review by Shevchenko (2007). Generally, estimating the Lyapunov exponents is one of the most important tools in the study of chaotic motion (Lichtenberg and Lieberman 1992), in particular in celestial mechanics.

Resonances and chaos are ubiquitous phenomena in the motion of bodies (in particular, planets) of the Solar system. The approximate orbital commensurabilities Jupiter–Saturn (the ratio of mean motions $\approx$5/2), Saturn-Uranus ($\approx$3/1), Uranus–Neptune ($\approx$2/1), and the Neptune–Pluto resonance (3/2) are well known. At the end of the eighties Sussman and Wisdom and, independently, Laskar in complicated numerical experiments obtained the first estimates of the Lyapunov time of the Solar system (Laskar 1989; Sussman and Wisdom 1988). It turned out that it is not at all infinite, i.e., the motion of the Solar system is not regular. Moreover, the Lyapunov time is rather small: it is three orders of magnitude less than the age of the Solar system. According to Sussman and Wisdom's calculations, the Lyapunov time of the outer Solar system (that from Jupiter to Pluto) is equal to $\approx$10 million years. And for the system of all planets, either with Pluto or without it, $T_{\mathrm{L}} \approx 5$ million years.

At a first glance it might seem that the basic contribution to chaos must be brought by the planets with relatively small masses, i.e., the planets of terrestrial group, as well as Pluto ranked as a planet until recently. However, if the calculations were limited only to four giant planets, then, as it was found out in 1992 by Sussman and Wisdom and confirmed in 1999 by Murray and Holman, chaos remains and, moreover, the Lyapunov time practically does not change: $T_{\mathrm{L}} \approx 5$–7 million years (Murray and Holman 1999; Sussman and Wisdom 1992).

Murray and Holman (1999) found that chaos could be due to a multiplet of subresonances associated with a particular three-body resonance Jupiter–Saturn–Uranus. This conclusion, however, has a preliminary character, because no full agreement of the analytical model with the numerical experiments has been achieved up to now. If it is true, the degree of chaoticity of the Solar system has, in some sense, an arbitrary character: if the semimajor axis of the orbit of Uranus differed from the present value by only several diameters of Uranus, the chaoticity would sharply decrease, if not at all practically disappear. Recent numerical-experimental studies by Hayes and co-workers (Hayes 2007, 2008; Hayes et al. 2010) show that the spatial interplay of chaos and order may be present even on much finer scales. In the future researches, if the guiding three-body resonance is accurately identified, then analytical estimation of the Lyapunov time T_{L} will be possible to accomplish using the separatrix map theory (Shevchenko 2014).

8.6.2 Chaos in the Planetary Motion Subject to LKE

The double-averaged Hamiltonian of the eccentric restricted three-body problem can be written explicitly in terms of canonical variables. Namely, the expansion of the Hamiltonian in a power series of $a_1/a_{\rm pert}$ up to the second (quadrupole) and third (octupole) orders is given by

$$\mathcal{H} = \mathcal{H}_{\rm quad} + \epsilon_{\rm oct}\mathcal{H}_{\rm oct}, \tag{8.18}$$

where

$$\mathcal{H}_{\rm quad} = \frac{1}{2}(1-J^2) - \frac{J_z^2}{J^2} - \frac{3(1-J^2)J_z^2}{2J^2} - \frac{5}{2}\frac{(1-J^2)J^2}{(J^2-J_z^2)}\cos 2\omega, \tag{8.19}$$

$$\begin{aligned}\mathcal{H}_{\rm oct} = &-\frac{5}{16}\left[(1-J^2)^{1/2} + \frac{3}{4}(1-J^2)^{3/2}\right] \\ &\times\left[\left(1 - \frac{11J_z}{J} - \frac{5J_z^2}{J^2} + \frac{15J_z^3}{J^3}\right)\cos(\omega-\Omega)\right. \\ &\left.+\left(1 + \frac{11J_z}{J} - \frac{5J_z^2}{J^2} - \frac{15J_z^3}{J^3}\right)\cos(\omega+\Omega)\right] \\ &+\frac{175}{64}(1-J^2)^{3/2}\times\left[\left(1 - \frac{J_z}{J} - \frac{J_z^2}{J^2} + \frac{J_z^3}{J^3}\right)\cos(3\omega-\Omega)\right. \\ &\left.+\left(1 + \frac{J_z}{J} - \frac{J_z^2}{J^2} - \frac{J_z^3}{J^3}\right)\cos(3\omega+\Omega)\right]\end{aligned} \tag{8.20}$$

(Li et al. 2014b; see also Lithwick and Naoz 2011 and Li et al. 2014a). Here (J, ω) and (J_z, Ω) are pairs of the canonically conjugate variables, $J = (1-e_1^2)^{1/2}$ is the unitless (scaled) angular momentum of the inner orbit, $J_z = (1-e_1^2)^{1/2}\cos i_1$ is the vertical component of the angular momentum (e_1 and i_1 are the eccentricity and inclination of the inner orbit), ω and Ω are, respectively, the argument of pericenter and the longitude of ascending node of the inner orbit; $\epsilon_{\rm oct}$ is defined by formula (8.15). The time in the equations of motion is made unitless by scaling (dividing) it by the constant

$$t_{\rm LK} = \frac{8}{3}\cdot\frac{m_0}{m_{\rm pert}}\left(\frac{a_{\rm pert}}{a_1}\right)^3\cdot(1-e_{\rm pert}^2)^{3/2}, \tag{8.21}$$

where m_0 and $m_{\rm pert}$ are the masses of the star and perturber, respectively. Hamiltonian (8.20) is scaled accordingly.

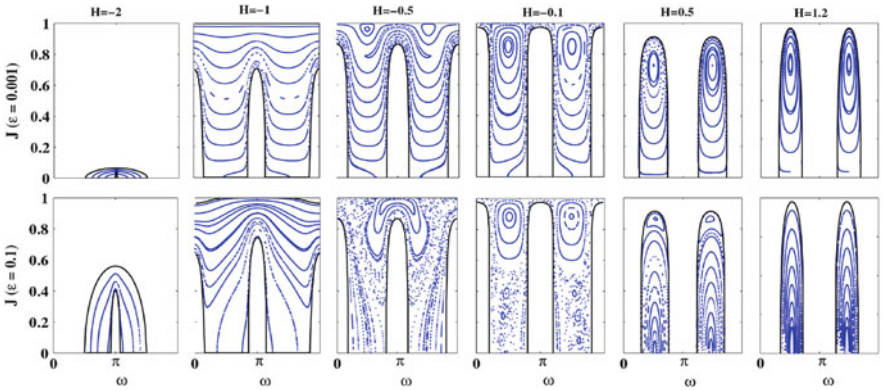

Fig. 8.5 The (ω, J) phase space sections for $\epsilon_{\rm oct} = 0.001$ (*upper panels*) and $\epsilon_{\rm oct} = 0.1$ (*lower panels*) (Figure 3 from Li et al. 2014b. Copyright AAS. Reproduced with permission)

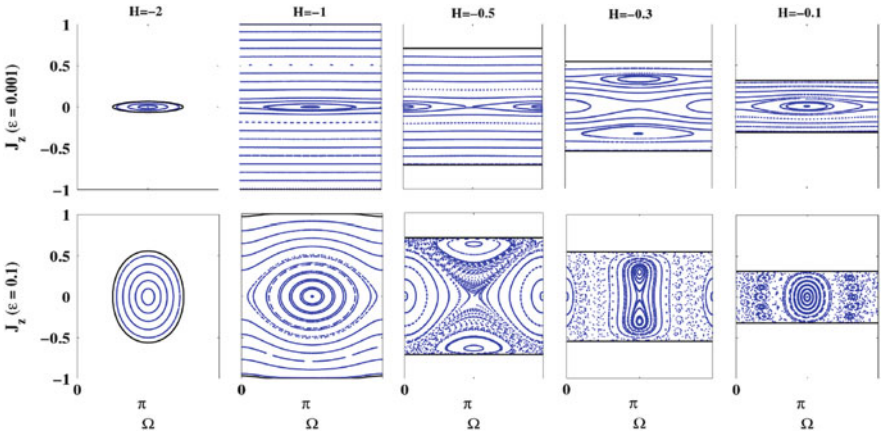

Fig. 8.6 The (Ω, J_z) phase space sections for the same values of $\epsilon_{\rm oct}$ as in Fig. 8.5 (Figure 4 from Li et al. 2014b. Copyright AAS. Reproduced with permission)

Sections of the phase space of Hamiltonian (8.18) at various values of $\mathcal{H}$ and $\epsilon_{\rm oct}$ were massively computed by Li et al. (2014b). These phase space sections are reproduced here in Figs. 8.5 and 8.6. The chaotic layers around the separatrices of resonances are clearly recognizable in both graphs, in the panels corresponding to $-0.5 \leq \mathcal{H} \leq -0.1$. An analytical description of the chaos properties, such as the Lyapunov and diffusion timescales, width of such chaotic layers, is a problem for future studies.

Chapter 9
Applications in Stellar Dynamics

And with a tilt most dangerous,
Most frightful, anyway,
To other worlds and systems
Is turned the Milky Way.

Boris Pasternak, *Night* (1956)[1]

Studies in secular dynamics of multiple stars, and, first of all, triples, is one of the fundamental themes of modern stellar dynamics. An analytical description of secular dynamics is possible for *hierarchical triple stars*, for which the orbit of the "outer binary" (formed by the outer body and the barycenter of the two inner bodies) is much greater than the size of the inner binary (Ford et al. 2000; Harrington 1968, 1969; Marchal 1990).

The planes of stellar orbits in multiple stars are mostly not aligned, and that is why the LKE is important. The LKE may control the secular evolution of the inner binary and, combined with the tidal friction, may produce a close binary of only a few stellar radii in size or even contact (Fabrycky and Tremaine 2007; Harrington 1969; Kiseleva et al. 1998). This mechanism may generate most of tight binaries. Moreover, of especial astrophysical interest is that it may lead to a merger of the binary components. Not only multiple Solar-type stars were studied on this subject; it was found out that the LKE might explain "white dwarf–white dwarf", "neutron star–neutron star", and "black hole–black hole" mergers (Perets and Fabrycky 2009; Prodan et al. 2013; Seto 2013; Thompson 2011).

The formation and evolution mechanisms of binaries are very important to understand because the majority of stars are double or multiple; in fact, according to Duquennoy and Mayor (1991), almost 70 % of stars in the Solar neighborhood belong to binary systems.

On the reason that the LKE in triples can produce stellar mergers, it was invoked to model the statistics of type Ia supernovae, which appear through mergers of white dwarfs when the Chandrasekhar limit is exceeded (Prodan et al. 2013; Thompson 2011). What is more, as shown by Perets and Fabrycky (2009), LKE-generated

[1]Translated from Russian by I. I. Shevchenko.

I. I. Shevchenko, *The Lidov-Kozai Effect – Applications in Exoplanet Research and Dynamical Astronomy*, Astrophysics and Space Science Library 441,
DOI 10.1007/978-3-319-43522-0_9

mergers of Solar-type stars can produce *blue stragglers*, i.e., blue massive stars, anomalously young in comparison with other stars in their environments in star clusters; they cannot be produced by the ordinary stellar evolution.

Many stars in the Galactic center vicinities are observed to move in highly eccentric orbits around the center. This was explained by Löckmann et al. (2008) as due to the LKE induced by massive central stellar disks. However, this is still controversial. Chang (2009) showed that the effectiveness of the LK-mechanism due to the stellar disks might be suppressed by the spherical stellar bulge. The LKE may nevertheless be induced by a flattened stellar bulge or other non-sphericities of the potential.

Among other applications in the Galactic astronomy, the LKE was invoked to describe the production, evolution, and mergers of black holes in globular clusters (Miller and Hamilton 2002b; Wen 2003), formation of dark matter complexes around supermassive black holes (Naoz and Silk 2014). In the gravitational-wave astronomy, it was studied as a possible mechanism for mergers generating specific gravitational wave signals (Antonini et al. 2014; Miller and Hamilton 2002a; Seto 2013).

Finally, perhaps the most grandiose manifestations of the LKE are related to the so-called *Galactic tide*, i.e., the tidal force due to the Galactic gravitational field. The LKE induced by the Galactic tide is considered in the last section of this book.

9.1 LKE in Triples: Formation of Tight Binaries

Beginning with the works of Harrington (1968, 1969), the LKE was studied to understand the secular evolution of triple stars. Perhaps the most intriguing implication of the LKE concerns the formation of tight binaries due to secular perturbations from outer components of the triples. Tokovinin et al. (2006) and Fabrycky and Tremaine (2007) explained the ubiquity of tight (those having orbital periods $\lesssim$3d) binaries of solar-type stars belonging to triples as due to the triple-affecting LKE, in concert with the tidal friction, at an evolutionary stage when the pericentric distances in the binaries become small. Indeed, as revealed by Tokovinin et al. (2006), almost all observed tight binaries possess outer stellar companions.

In the framework of the hierarchical general three-body problem (in which the components of a triple may have comparable masses), Naoz et al. (2011) showed that the inner binary, subject to perturbations from a highly-inclined eccentric distant outer orbiter, may suffer transitions from prograde to retrograde modes and vice versa. Thus, the orbit of the less massive component of the inner binary "flips": its inclination exhibits transitions through the value $i = 90^\circ$ in both directions, lingering intermittently in each mode.

The possibility of the flips in the general three-body problem can be demonstrated by analyzing the double-averaged expansion of the three-body Hamiltonian in the octupole order. As already discussed in Chaps. 4 and 8, the dynamical role of the octupole term can be assessed by using formulas (4.55) and (8.14), namely, by estimating the quantity

$$\epsilon_{\rm oct} = \frac{(m_0 - m_1)}{(m_0 + m_1)} \cdot \frac{a_2}{a_{\rm pert}} \cdot \frac{e_{\rm pert}}{(1 - e_{\rm pert}^2)}. \tag{9.1}$$

Here $m_0 > m_1$ are the masses of the perturbed binary, a_2 is the semimajor axis of its less massive component, $a_{\rm pert}$ and $e_{\rm pert}$ are the semimajor axis and eccentricity of the perturber's orbit.

Thus, $\epsilon_{\rm oct}$ is directly proportional to the mass difference $(m_0 - m_1)$ of the perturbed binary; i.e., if the masses are equal, than the flipping phenomenon is absent. As emphasized by Shappee and Thompson (2013), this has important consequences for the evolution of triples whose inner binaries consist of solar-type stars. Indeed, such binaries usually have mass ratios $\sim$1 (Mazeh et al. 1992; Raghavan et al. 2010); there even exists a preference for *twin stars* (Pinsonneault and Stanek 2006). For the twins, $\epsilon_{\rm oct} \ll 1$ and the flips are impossible. However, if one of the primaries, in the course of the stellar evolution, explodes and becomes a white dwarf or a neutron star, the mass ratio changes and the LK-mechanism comes into play, and, if the perturber is eccentric, the flips may emerge. Besides, a general route opens, due to the LKE, to the tidal circularization and shrinking of the primaries' orbits (see, e.g. Eggleton and Kiseleva-Eggleton 2001; Kiseleva et al. 1998). Combined with the tidal friction, the LKE operating in a multiple star can produce a tight binary, which can be even contact (Fabrycky and Tremaine 2007; Harrington 1968; Kiseleva et al. 1998).

Shappee and Thompson (2013) considered evolving triples with mass loss and made a number of estimates concerning percentages of systems with typical final states. The hierarchical triple solar-type stars are mostly (in the generic ranges of initial conditions) not prone to the LKE, but the situation changes, when one of the members of the central binary becomes a compact object. If the outer perturber is sufficiently eccentric, the LKE may even lead to orbital flips of the perturbed body. Shappee and Thompson (2013) call this scenario the *mass-loss-induced eccentric* LK-mechanism (the mass-loss-induced ELKM). However, most (about one third) of the evolving triples seem to suffer tidal-collisional interactions already at an earlier stage of evolution, mostly due to the ordinary LKE, when one of the primaries becomes a red giant with a diameter of several astronomical units. Only about 2 % of the evolving triples suffer tidal-collisional interactions at the "compact-object" stage, due to the mass-loss-induced ELKM. Summing up, most or even all tight binaries could have been formed out from wider ones.

9.2 LKE in Triples: A Progenitor for Supernovae, "blue stragglers", etc.

Of especial astrophysical interest is that the LKE in a stellar triple can lead to a merger of the inner binary components. The LKE might explain "white dwarf–white dwarf", "neutron star–neutron star", and "black hole–black hole" mergers (Perets and Fabrycky 2009; Prodan et al. 2013; Seto 2013; Thompson 2011). The LKE-induced merger phenomenon was invoked to model the rates of type Ia supernovae, appearing due to mergers of white dwarfs (which result in exceeding the Chandrasekhar limit; see Prodan et al. 2013; Thompson 2011). The LKE might be also relevant to the secular dynamics of binary millisecond pulsars (Gopakumar et al. 2009).

On the other hand, Iben and Tutukov (1984) and Webbink (1984) suggested that the type Ia supernovae can be also generated by mergers of white dwarfs in binaries, as a binary shrinks due to the gravitational wave radiation (GWR). However, the pure GWR effect can produce a merger on a timescale less than the age of the Universe ($\sim 10^{10}$ years) only in the binaries that are tight enough, and this makes the predicted GWR-conditioned merger frequency much less than the observed frequency of the type Ia supernovae events. The situation changes if one considers binaries inside triples. A companion in an inclined orbit around a binary may trigger LK-oscillations of the inner orbit's eccentricity, pumping huge eccentricities and generating small pericentric distances in the inner binary; leading, consequently, to stellar mergers. The GWR and tidal timescales decrease dramatically with diminishing the pericentric distances. Therefore, the merger timescale also decreases, and, correspondingly, the merger frequency rises. Quantitative estimates of the resulting rates allow one to assess the described scenario as plausible for explaining the type Ia supernovae events (Blaes et al. 2002; Miller and Hamilton 2002a).

Therefore, in hierarchical triples, the merger frequency, maintained by the LKE–GWR (the LKE in concert with the energy loss due to the GWR), is substantially enhanced in comparison with the merger rate in isolated binaries. Thompson (2011) showed this process to be effective in the evolution of "white dwarf–white dwarf", "white dwarf–neutron star" and "neutron star–neutron star" pairs. Such mergers might be responsible not only for the Ia supernovae events, but also for observed γ-ray bursts.

Prodan et al. (2013) explored the tidal effects in concert with the LKE in compact triples with characteristics typical for the Galactic field and globular clusters (namely, the triple size $\sim$1 AU and the size of the inner binary $\sim$0.05 AU). At high enough mutual inclinations, the LKE triggers the GWR timescale and the tidal timescale to decrease substantially. At appropriate initial inclination values, the inner binary may even merge straightforwardly (i.e., GWR and tides are not necessary), due to shrinking pericentric distances (Kushnir et al. 2013).

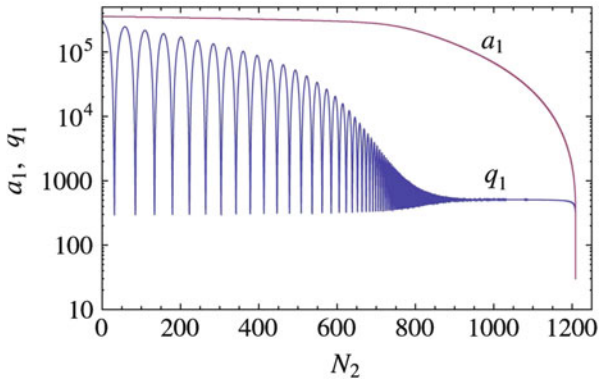

Fig. 9.1 The time dependence (as given by the secular theory) of the semimajor axis a_1 and pericentric distance q_1 of a compact twin (equal-mass) binary, perturbed by a distant companion; time N_2 is in units of the orbital period of the perturber. The binary merges at $N_2 \approx 1200$. (Reprinted figure 1 with permission from Seto 2013. Copyright (2013) by the American Physical Society)

In Fig. 9.1, the time evolution of the semimajor axis a_1 and pericentric distance q_1 of a neutron-star binary (perturbed by a distant stellar companion) is illustrated, as given by the secular theory (Seto 2013), for a representative initial orbital configuration and masses of the triple. The initial mutual inclination is 91°. Time N_2 is measured in units of the perturber's orbital period. Initially, the LK-oscillations with the decaying amplitude of the eccentricity are observed, while the minimum q_1 is constant. (The amplitude decays due to "detuning" of the LKE by the general-relativistic precession of the neutron-star binary. The detuning takes place on the timescale of the precession period; for details see Thompson 2011. When the precession period becomes much less than the LKE timescale, the LKE is suppressed altogether; see Sect. 3.3.) Thus, the maximum apocentric distance decays, and, eventually (at $N_2 \sim 800$ in this example), the neutron-star binary's orbit is circularized at a small value of its size $a_1 \approx q_1$. Further on, a_1 shrinks due to the energy loss by GRW, until the merger happens (at $N_2 \sim 1200$ in this example). Note that the GRW itself without the LKE (i.e., in the absence of the inclined perturber) would cause the merger on a considerably greater (in this example, $10^7 - 10^8$ times greater) timescale. What is more, as demonstrated by Seto (2013), the secular theory predicts too high minima for the pericentric distances of a compact binary in a hierarchical triple, as the short-period oscillations are averaged out. Therefore, in reality, the merger timescale is much less, as the effectiveness of the energy loss by GRW depends drastically on q_1. In the given typical example of evolution obtained in the secular theory, the merger time $N_2 \sim 1000$, whereas in the corresponding numerical simulation it is by an order of magnitude less.

Another vivid example of a potential effectiveness of the LKE in triple stars is given by the phenomenon of *blue stragglers*—the blue massive stars, anomalously young in comparison with other stars in their environments in stellar clusters. They are observed to exist in globular clusters. They cannot be a product of the ordinary

stellar evolution of single stars. In a cluster's colour-magnitude diagram, they appear bluer and more luminous than the stars at the main-sequence turn-off (Sandage 1953). Blue stragglers are supposed to be an evolutionary product of either (1) normal main-sequence stars subject to the Roche-lobe overflow of fresh hydrogen from evolved close companions (McCrea 1964), or (2) mergers of companions in binaries (see, e.g., Leigh et al. 2013). In the both cases, the tight binary generating the blue straggler might have appeared due to the LKE. Perets and Fabrycky (2009) explain the formation of blue stragglers in globular clusters as due to the LKE in concert with the tidal friction, acting in triples in the clusters.

9.3 Highly Eccentric Stars in the Galactic Center

The center of our Milky Way Galaxy is identified with the radio source Sgr A*. It is believed that the radio emission is due to a standard mechanism of the galactic nuclei activity, associated with the disk accretion onto a supermassive black hole (SMBH). This accretion is accompanied by the powerful radio emission from plasma jets orthogonal to the accretion disk (e.g. Begelman et al. 1980).

The stellar population surrounding the central SMBH has an intricate kinematical structure (e.g. Chang 2009). So-called *S-stars* and *S0-stars* move within central 0.04 pc in highly eccentric orbits distributed isotropically in inclination. On the contrary, a larger (up to 0.4 pc) stellar subsystem of young massive stars is not isotropic (Lu et al. 2006; Paumard et al. 2006): it is organized in a single disk, or a pair of disks, mutually almost orthogonal. For a review on possible origins of these central stellar populations see Alexander (2005).

Šubr et al. (2004) and Šubr and Karas (2005) demonstrated a possible relevance of the LKE (driven by a circumnuclear massive disk) for pumping the eccentricities the stars in the SMBH neighbourhood; they also outlined conditions needed for the SMBH-driven relativistic precession to suppress the LKE. Furthermore, the high eccentricities ($e \approx 1$) of the S-stars might be pumped by the LKE induced by a pair of large stellar disks, as suggested by Löckmann et al. (2008). In this scenario, the S-stars are generated by tidal disruption of binaries (explored in Gould and Quillen 2003), when, in the course of the LK-evolution, they come close enough to the SMBH. The inflow of binaries is supplied by the outer disks. The LKE, in its turn, generates a highly-eccentric and isotropic population. The evolved orbital semimajor axes of the former components of the binaries are by an order of magnitude smaller than their initial values (Gould and Quillen 2003); this explains the relatively small size of the S-stellar subsystem.

The typical timescales of the LK-oscillations in the vicinity of the Galactic center are illustrated in Fig. 9.2, where a numerical-experimental example of a pure (i.e., with other effects absent) LK-oscillation induced by a stellar disk of mass 2000 M_{Sun}

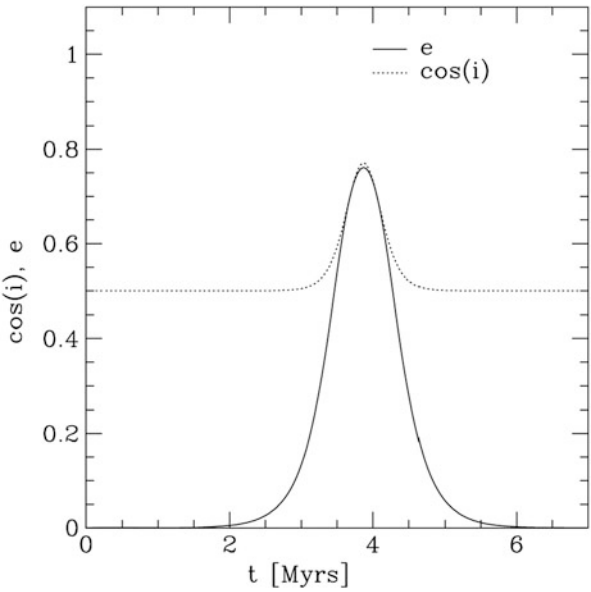

Fig. 9.2 A pure LK-oscillation induced by a stellar disk of mass 2000 $M_{\rm Sun}$ in the Galactic center. The initial inclination of a star's orbit with respect to the disk plane is 60°, the star's semimajor axis is 0.1 pc (Figure 1 from Chang 2009. With permission from Oxford University Press)

is given for a star orbiting the central SMBH.[2] However, note that the effectiveness of the disk-driven LK-mechanism in the Galactic center is still controversial. Chang (2009) showed that the LKE due to the stellar disks might be suppressed by the spherical stellar bulge. On the other hand, the presence of a non-suppressed LKE of another origin (induced by a flattened stellar bulge or other non-sphericities of the potential) is not ruled out.

According to Chang (2009), an LK-mechanism of a similar kind may be active in our neighbour galaxy M31, which has a much more massive (relative to the mass of the central SMBH) central stellar disk (∼10 % of the SMBH mass).

Generally speaking, the LKE may act in the nuclei of many galaxies other than ours, producing various dynamical and astrophysical phenomena. Analogously to the situation in our Galaxy, the most massive galaxies are believed to contain single, binary, or even multiple SMBHs in their centers. The central SMBH multiplicity might be an outcome of a merger of parent galaxies (e.g. Begelman et al. 1980). As argued by Blaes et al. (2002), the LKE induced by the galactic disk or a third SMBH may produce pericentric distances in the inner binary small enough for the energy loss through the GWR become substantial to lead to a merger of the binary components; such mergers may have outstanding observational consequences.

[2]The massive black hole in the center of our Galaxy is estimated to have mass equal to (3–4)·10^6 Solar masses; it is one of the least massive nuclear black holes known at present in galaxies (Alexander 2005).

9.4 The Galactic Tide

Perhaps the most grandiose manifestations of the LKE are related to the *Galactic tide*, the tidal force due to the Galactic gravitational field. The term "Galactic tide" is also used to refer generally to any perturbative influence of the Galactic gravitational field on the motion of objects inside stellar and planetary systems of the Galaxy.

The notion of the Hill radius (defined previously in Chap. 5, see formula (5.1)) is straightforwardly generalizable to the case of a body orbiting in the Galactic gravitational field. The Hill radius of a star or any other object (say, a globular cluster) subject to the Galactic tide can be rendered the form

$$R_{\rm H} \approx 1.7 \cdot 10^5 {\rm AU} \left(\frac{m}{m_{\rm Sun}} \right)^{1/3} \left(\frac{\rho_{\rm G}}{0.15 m_{\rm Sun} {\rm pc}^{-3}} \right)^{-1/3}, \tag{9.2}$$

where m is the mass of the object, $m_{\rm Sun}$ is the Solar mass, and $\rho_{\rm G}$ is the local Galactic density (e.g. Veras et al. 2009). Planets or minor bodies (planetesimals, comets, etc.) whose orbital apocenters exceed $R_{\rm H}$ are expected to escape from the host star, due to the Galactic perturbation.

The formula for the period of LK-oscillations (see Sect. 3.4) is also straightforwardly generalizable. Namely, the timescale of LK-oscillations due to the Galactic tide is given by

$$T_{\rm LK} \approx 5.0 \left(\frac{0.1 m_{\rm Sun} {\rm pc}^{-3}}{\rho_{\rm G}} \right) \left(\frac{10^4 {\rm AU}}{a} \right)^{3/2} {\rm Gyr}, \tag{9.3}$$

where a is the orbital semimajor axis of a massless particle orbiting a star (Brasser et al. 2010).

Inside the Hill radius of a star, a star-orbiting body may be subject, depending on initial conditions, to the LKE due to the Galactic tide; thus, the body may reach high apocentric distances and escape. However, the LK-period (given by formula (9.3)) is small enough (less than the age of the Solar system) on a rather large spatial scale, defined by the semimajor axis a in formula (9.3): the value of a should be greater than $\sim 10^4$–10^5 AU, for the Galactic-tidal LKE to be effective. By the order of magnitude, this scale is close to the Solar $R_{\rm H}$, given by formula (9.2).

More precisely, the LKE starts be effective for orbital sizes exceeding $\sim$5000 AU; at such radial distance from the Sun the Oort cloud starts to be more or less isotropic with respect to the Sun (because the Galactic tide starts to be able to perturb the cloud); at smaller radii, the planetesimal distribution remains concentrated to the ecliptic plane (Duncan et al. 1987).

As discussed already in Sect. 6.2, the Oort cloud itself is formed most probably thanks to an LK-mechanism (Duncan et al. 1987): the minor bodies scattered by the planets to large enough distances from the Sun suffer perturbations by the Galactic tide, and the Galactic-tidal LKE acts to decrease their eccentricities, thus forming the cloud. What is more, the Galactic-tidal LKE also acts to "borrow" comets from the Oort cloud and deliver them to the inner Solar system.

Finally, what is the effect of the Galactic tide on the planets of our Solar system? May the LKE be present in their motion, due to the mutual inclination of the Galactic and Solar system planes? The planetary orbits in our Solar system are subject to long-term perturbations due to the Galactic tide. Being inclined by $\sim 60°$ with respect to the Galactic plane, the Solar system might seem to be subject to destabilization by the LKE. However, if an additional perturbation dominates the LK-term in the Hamiltonian of the motion, then the LKE disappears, as discussed in detail in Sect. 3.3. And indeed, the LKE in the motion of planets is completely suppressed by their orbital precession arising due to their mutual perturbations (Matese and Whitman 1992; Morbidelli 2002); besides, the LKE timescale for the Solar system size is $\sim 10^3$ times greater than the age of the Solar system, as follows from formula (9.3).

If the orbits of the planets were large enough, the Galactic tide would be important in perturbing their dynamics; but for the known planets of the Solar system the effect is absent. However, the Galactic tide can well produce the LKE in exoplanetary systems (Veras and Evans 2013). The reason is that planets and brown dwarfs orbiting stars may have orbits far larger (by two orders of magnitude) than the size of our Solar system: the orbital semimajor axes of known objects reach values up to 2500 AU (Kalas et al. 2005; Gladman et al. 2010; Kuzuhara et al. 2011; Luhman et al. 2012).

In wide binaries in the Galactic field, the Galactic tide induces variations of the orbit of the stellar perturber, and this may explain why the exoplanets observed in them possess on the average greater eccentricities than the planets of single stars (Kaib et al. 2013).

Appendix A
Basic Notations

In this Appendix, the basic notations for the mathematical operators and astronomical and physical quantities used throughout the book are given. Note that only the most frequently used quantities are mentioned; besides, overlapping symbol definitions and deviations from the basically adopted notations are possible, when appropriate.

Mathematical Quantities and Operators

$\|\mathbf{x}\|$ is the length (norm) of vector $\mathbf{x}$
$\mathbf{x} \cdot \mathbf{y}$ is the scalar product of vectors $\mathbf{x}$ and $\mathbf{y}$
$\nabla_{\mathbf{r}}$ is the gradient operator in the direction of vector $\mathbf{r}$
$\{f, g\}$ is the Poisson bracket of functions f and g
$K(m)$ or $K(k)$ (where $m = k^2$) is the complete elliptic integral of the first kind with modulus k
$E(m)$ or $E(k)$ is the complete elliptic integral of the second kind
$F(\alpha, m)$ is the incomplete elliptic integral of the first kind
$E(\alpha, m)$ is the incomplete elliptic integral of the second kind
Λ_0 is Heuman's Lambda function
P_i is the Legendre polynomial of degree i
x_0 is the initial value of a variable x

Coordinates and Frames

x, y, z are the Cartesian (orthogonal) coordinates
r, ϕ, α are the spherical coordinates (radial distance, longitude, and latitude)

I. I. Shevchenko, *The Lidov-Kozai Effect – Applications in Exoplanet Research and Dynamical Astronomy*, Astrophysics and Space Science Library 441,
DOI 10.1007/978-3-319-43522-0

In the three-body problem:
$\mathbf{r_1}$ is the position vector of body 1 relative to body 0
$\mathbf{r_2}$ is the position vector of body 2 relative to the center of mass of the inner binary
Φ is the angle between vectors $\mathbf{r}_1$ and $\mathbf{r}_2$
In the many-body problem:
$\mathbf{r}$ and $\mathbf{r}_i$ $(i = 1, \ldots, N)$ are the primary-centric positions of a particle and N gravitating perturbers (with masses m_i)
$\mathbf{r}_{i0}$ is the position vector of body i relative to body 0
$\mathbf{r}_{ij}$ the position vector of body i relative to body j

Orbital Elements and Corresponding Quantities

a, e, i, ω, ϖ, Ω, M, l are, respectively the semimajor axis, eccentricity, inclination, argument of pericenter, longitude of pericenter, longitude of ascending node, mean anomaly, mean longitude of a massless test particle or a massive test body
$q = a(1 - e)$ is the pericentric distance
$Q = a(1 + e)$ is the apocentric distance
$a_{\rm pert}$, $e_{\rm pert}$, $i_{\rm pert}$, $\omega_{\rm pert}$, $\varpi_{\rm pert}$, $\Omega_{\rm pert}$, $M_{\rm pert}$, $l_{\rm pert}$ are, respectively the semimajor axis, eccentricity, inclination, argument of pericenter, longitude of pericenter, longitude of ascending node, mean anomaly, mean longitude of a perturber's orbit
$a_{\rm p}$, $e_{\rm p}$ are, respectively the semimajor axis and eccentricity of a planetary orbit
$a_{\rm b}$, $e_{\rm b}$ are, respectively the semimajor axis and eccentricity of a binary
a_1, a_2 are the semimajor axes of the inner and outer binaries, respectively
e_1, e_2 are the eccentricities of the inner and outer binaries, respectively
$\alpha = a_1/a_2$ is the ratio of semimajor axes of the inner and outer binaries
$e_{\rm f}$ is the forced eccentricity
$i_{\rm E}$ is the inclination to the ecliptic plane
e_i, ϖ_i, i_i, and Ω_i are, respectively, the eccentricity, longitude of pericenter, inclination, and longitude of ascending node of planet i
n is the mean motion of a test body
$n_{\rm pert}$ is the mean motion of a perturber
P_1 is the orbital period of the inner binary
P_2 is the orbital period of the outer binary
τ is the time of the pericenter transit

Dynamical Definitions

n is the number of degrees of freedom
$\mathcal{R}$ is the perturbing function
$\mathcal{H}$ is a Hamiltonian
$\mathcal{K}$ is a normalized Hamiltonian

q is the vector of canonical coordinates
p is the vector of conjugate canonical momenta
l, g, h are the Delaunay canonical angles, corresponding to the mean anomaly M, argument of pericenter ω, and longitude of ascending node Ω, respectively
L, G, H are the Delaunay canonical momenta, conjugate to the Delaunay canonical angles
Λ and λ, P and p, Q and q are the pairs of the modified Delaunay variables of the test body
$\omega \equiv \varpi - \Omega$ is the argument of pericenter, the critical angle of the LK-resonance
α is the frequency of the forced (due to a perturbation) precession of ω
$T_{\rm LK}$ is the period of LK-oscillations
$\epsilon_{\rm oct}$ is a constant parameter characterizing the role of octupole terms
β_k and δ_k are the planetary angular phases, $k = 1, 2, \ldots, 8$
g_k and s_k are the planetary frequencies, $k = 1, 2, \ldots, 8$
ν_5 is a secular resonance
ν_6 is a secular resonance
ν_{16} is a secular resonance

Masses and Mass Parameters

m_0 is the mass of the "central" body (the primary, usually the most massive in a system)
m is the mass of a test body (e.g., an asteroid, a planet)
$m_{\rm pert}$ is the mass of a perturber
$\mu = m_1/(m_0 + m_1)$ is the mass parameter of a binary
$m_{\rm star}$ is the mass of the parent star in a system
$M_{\rm Sun}$ is the mass of the Sun
$m_{\rm pl}$ is the mass of a planet
ϵ is the mass of the largest planet in a system in units of the mass of the host star

Other Physical Quantities

$\mathcal{G}$ is the gravitational constant
c is the speed of light
$R_{\rm p}$ is the mean radius of a planet
$R_{\rm Sun}$ is the radius of the Sun
$R_{\rm Earth}$ is the radius of the Earth
$R_{\rm Moon}$ is the radius of the Moon
$R_{\rm H}$ is the Hill radius
J_2 is the second zonal harmonic coefficient of a planet
k_2 is the Love number

G is the module of the angular momentum
H is the angular momentum vector's vertical component
ϕ is the angle of the pendulum deviation from the vertical
m is the mass of a pendulum
l is the length of a pendulum
φ is the angle of a pendulum, or a resonance phase angle
p is the momentum of a pendulum
Ω is the perturbation frequency
τ is the phase angle of perturbation
L is the maximum Lyapunov exponent
$T_{\mathrm{L}} \equiv L^{-1}$ is the Lyapunov time
ω_0 is the frequency of the pendulum small-amplitude oscillations
J is the unitless (scaled) angular momentum of the inner orbit
J_z is the vertical component of the angular momentum
G_1 and G_2 are the angular momenta of the inner and outer binaries, respectively
C_{J} is the Jacobi integral, also called the Jacobi constant

Appendix B
Astronomical Constants and Parameters

The astronomical constants and parameters given in Table B.1 are merely those that are necessary to make numerical estimates throughout the book. The values of astronomical constants are those adopted by the 16th General Assembly of the International Astronomical Union in 1976.

Table B.1 Astronomical constants and parameters

Constant	Value
Speed of light c	$2.997925 \cdot 10^{10}$ cm/s
Gravitational constant $\mathcal{G}$	$6.672 \cdot 10^{-8}$ g^{-1}cm^{3}s^{-2}
Solar mass $M_{\rm Sun}$	$1.989 \cdot 10^{33}$ g
Solar radius $R_{\rm Sun}$	$6.960 \cdot 10^{10}$ cm
Mass of the Earth $M_{\rm Earth}$	$5.977 \cdot 10^{27}$ g
Equatorial radius of the Earth $R_{\rm Earth}$	$6.378140 \cdot 10^{8}$ cm
Mean radius of the Earth $\langle R_{\rm Earth}\rangle$	$6.371032 \cdot 10^{8}$ cm
Mean distance "Earth–Moon" $a_{\rm EM}$	$3.84401 \cdot 10^{10}$ cm
Mass of Jupiter $M_{\rm J}$	$1.898 \cdot 10^{30}$ g
Semimajor axis of Jupiter's orbit	5.20337 AU
Semimajor axis of Neptune's orbit	30.058 AU
Semimajor axis of Pluto's orbit	39.46 AU
Astronomical unit (AU)	$1.49600 \cdot 10^{13}$ cm
Parsec	$3.0857 \cdot 10^{18}$ cm = 206265 AU
Ecliptic-to-equator obliquity (epoch 2000)	$23^\circ 26' 21''$
Ratio of masses of the Earth and Moon	81.30
Ratio of masses of the Sun and Earth	332958
Oblateness of the Earth ellipsoid $(a-b)/a$	$1/298.257$

I. I. Shevchenko, *The Lidov-Kozai Effect – Applications in Exoplanet Research and Dynamical Astronomy*, Astrophysics and Space Science Library 441,
DOI 10.1007/978-3-319-43522-0

References

Abramowitz, M., & Stegun, I. A. (1970) *Handbook of Mathematical Functions* (Dover, New York)

Aksenov, E. P. (1979a) "The doubly averaged, elliptical, restricted, three-body problem." Sov. Astron., **23**, 236–239

Aksenov, E. P. (1979b) "Trajectories in the doubly-averaged elliptical restricted three-body problem." Sov. Astron., **23**, 351–354

Alexander, T. (2005) "Stellar processes near the massive black hole in the Galactic center." Phys. Rep., **419**, 65–142

Antognini, J. M. O. (2015) "Timescales of Kozai–Lidov oscillations at quadrupole and octupole order in the test particle limit." Mon. Not. R. Astron. Soc., **452**, 3610–3619

Antonini, F., Murray, N., & Mikkola, S. (2014) "Black hole triple dynamics: a breakdown of the orbit average approximation and implications for gravitational wave detections." Astrophys. J., **781**, 45 (13pp)

Albrecht, S., Winn, J. N., Johnson, J. A., Howard, A. W., Marcy, G. W., Butler, R. P., *et al.* (2012) "Obliquities of hot jupiter host stars: evidence for tidal interactions and primordial misalignments." Astrophys. J., **757**, 18 (25pp)

Arnold, V. I., Kozlov, V. V., & Neishtadt, A. I. (2002) *Mathematical Aspects of Classical and Celestial Mechanics* (Editorial URSS, Moscow) (in Russian)

Arnold, V. I., Kozlov, V. V., & Neishtadt, A. I. (2006) *Mathematical Aspects of Classical and Celestial Mechanics*, 3rd Edition (Springer, New York)

Bailey, M. E., Chambers, J. E., & Hahn, G. (1992) "Origin of sungrazers: a frequent cometary end-state." Astron. Astrophys., **257**, 315–322

Batygin, K., Laughlin, G., Meschiari, S., Rivera, E., Vogt, S., & Butler, P. (2009) "A quasi-stationary solution to Gliese 436b's eccentricity." Astrophys. J., **699**, 23–30

Batygin, K., Morbidelli, A., & Tsiganis, K. (2011) "Formation and evolution of planetary systems in presence of highly inclined stellar perturbers." Astron. Astrophys., **533**, A7 (8pp)

Belbruno, E. A. (2004) *Capture Dynamics and Chaotic Motions in Celestial Mechanics* (Princeton University Press, Princeton)

Beletsky, V. V. (1972) *Essays on the Motion of Cosmic Bodies* (Nauka Publishers, Moscow) (in Russian)

Begelman, M. C., Blandford, R. D., & Rees, M. J. (1980) "Massive black hole binaries in active galactic nuclei." Nature, **287**, 307–309

I. I. Shevchenko, *The Lidov-Kozai Effect – Applications in Exoplanet Research and Dynamical Astronomy*, Astrophysics and Space Science Library 441,
DOI 10.1007/978-3-319-43522-0

Benest, D. (1988a) "Planetary orbits in the elliptic restricted problem I. The α Centauri system." Astron. Astrophys., **206**, 143–146

Benest, D. (1988b) "Stable planetary orbits around one component in nearby binary stars." Celest. Mech., **43**, 47–53

Benest, D. (1989) "Planetary orbits in the elliptic restricted problem II. The Sirius system." Astron. Astrophys., **223**, 361–364

Beust, H., & Dutrey, A. (2006) "Dynamics of the young multiple system GG Tauri. II. Relation between the stellar system and the circumbinary disk." Astron. Astrophys., **446**, 137–154

Blaes, O., Lee, M. H., & Socrates, A. (2002) "The Kozai mechanism and the evolution of binary supermassive black holes." Astrophys. J., **578**, 775–786

Bodenheimer, P., Hubickyj, O., & Lissauer, J. J. (2000) "Models of the in situ formation of detected extrasolar giant planets." Icarus, **143**, 2–14

Brasser, R. (2001) "Some properties of a two-body system under the influence of the Galactic tidal field." Mon. Not. R. Astron. Soc., **324**, 1109–1116

Brasser, R., Higuchi, A., & Kaib, N. (2010) "Oort cloud formation at various Galactic distances." Astron. Astrophys., **516**, A72 (12 pp)

Breiter, S. (2003) "Extended fundamental model of resonance." Celest. Mech. Dyn. Astron., **85**, 209–218

Broucke, R. A. (2003) "Long-term third-body effects via double averaging." Journal of Guidance, Control, and Dynamics, **26**, No. 1, 27–32

Brouwer, D., & Clemence, G. M. (1961) *Methods of Celestial Mechanics* (Academic, New York)

Brown, E. W. (1936) "The stellar problem of three bodies. III. The motions of the apse and node with applications to the Moon." Mon. Not. R. Astron. Soc., **97**, 116–126

Burns, J. A. (1986) "Some background on satellites." In: *Satellites*, ed. by Burns, J. A., & Matthews, M. S. (Univ. of Arizona Press, Tucson) pp. 1–38

Carruba, V., Burns, J. A., Nicholson, P. D., & Gladman, B. J. (2002) "On the inclination distribution of the Jovian irregular satellites." Icarus, **158**, 434–449

Carruba, V., Burns, J. A., Nicholson, P. D., & Gladman, B. J. (2003) Erratum to "On the inclination distribution of the Jovian irregular satellites." Icarus, **162**, 230–231

Chang, Ph. (2009) "The effectiveness of the Kozai mechanism in the Galactic Centre." Mon. Not. R. Astron. Soc., **393**, 224–228

Chenciner, A., & Montgomery, R. (2000) "A remarkable periodic solution of the three-body problem in the case of equal masses." Annals of Mathematics – Second Series, **152**, 881–901

Chirikov, B. V. (1959) "Resonance processes in magnetic traps." Atomnaya Energiya, **6**, 630–638 (in Russian) [Chirikov, B. V. (1960) "Resonance processes in magnetic traps." J. Nucl. Energy, Part C: Plasma Physics, **1**, 253–260]

Chirikov, B. V. (1979) "A universal instability of many-dimensional oscillator systems." Phys. Rep., **52**, 263–379

Chirikov, B.V. (1982) "Nonlinear resonances and dynamical stochasticity." Priroda, No. 7, 15–25 (in Russian)

Claret, A. (1995) "Stellar models for a wide range of initial chemical compositions until helium burning. I. From $X = 0.60$ to $X = 0.80$ for $Z = 0.02$." Astron. Astrophys. Suppl., **109**, 441–446

Clemence, G. (1947) "The relativity effect in planetary motions." Rev. Mod. Phys., **19**, 361–364

Cochran, W. D., Hatzes, A., Butler, R. P., & Marcy, G. W. (1997) "The discovery of a planetary companion to 16 Cygni B." Astrophys. J., **483**, 457–463

Colombo, G., & Franklin, F. A. (1971) "On the formation of the outer satellite groups of Jupiter." Icarus, **15**, 186–189

Correia, A. C. M., Boué, G., Laskar, J., & Morais, M. H. M. (2013) "Tidal damping of the mutual inclination in hierarchical systems." Astron. Astrophys., **553**, A39 (15pp)

Danby, J. (1962) *Fundamentals of Celestial Mechanics* (Macmillan, New York)

Davies, M. B., Adams, F. C., Armitage, P., Chambers, J., Ford, E., Morbidelli, A., Raymond, S. N., & Veras, D. (2014) "The long-term dynamical evolution of planetary systems." In: *Protostars*

and Planets VI, ed. by Beuther, H., Klessen, R. S., Dullemond, C. P., & Henning, T. (University of Arizona Press, Tucson) pp. 787–808

de la Fuente Marcos, C., & de la Fuente Marcos, R. (2014) "Extreme trans-Neptunian objects and the Kozai mechanism: signalling the presence of trans-Plutonian planets." Mon. Not. R. Astron. Soc., **443**, L59–L63

Demidova, T. V., & Shevchenko, I. I. (2015) "Spiral patterns in planetesimal circumbinary disks." Astrophys. J., **805**, 38 (8pp)

Deprit, A. (1969) "Canonical transformations depending on a small parameter." Celest. Mech., **1**, 12–30

Devaney, R. (1986) *An Introduction to Chaotic Dynamical Systems* (Benjamin/Cummings, Menlo Park)

Doyle, L. R., Carter, J. A., Fabrycky, D. C., *et al.* (2011) "Kepler-16: a transiting circumbinary planet." Science, **333**, 1602–1606

Duncan, M. J., Quinn, T., & Tremaine, S. (1987) "The formation and extent of the solar system comet cloud." Astron. J., **94**, 1330–1338

Dumusque, X., Pepe, F., Lovis, C., *et al.* (2012) "An Earth-mass planet orbiting α Centauri B." Nature, **491**, 207–211

Duquennoy, A., & Mayor, M. (1991) "Multiplicity among solar-type stars in the solar neighbourhood. II — Distribution of the orbital elements in an unbiased sample." Astron. Astrophys., **248**, 485–524

Eggleton, P. P., & Kiseleva-Eggleton, L. (2001) "Orbital evolution in binary and triple stars, with an application to SS Lacertae." Astrophys. J., **562**, 1012–1030

Emelyanov, N. V., & Vashkovyak, M. A. (2012) "Evolution of orbits and encounters of distant planetary satellites. Study tools and examples." Sol. Sys. Res., **46**, 423–435

Fabrycky, D., & Tremaine, S. (2007) "Shrinking binary and planetary orbits by Kozai cycles with tidal friction." Astrophys. J., **669**, 1298–1315

Fang, J., & Margot, J.-L. (2012) "The role of Kozai cycles in near-Earth binary asteroids." Astron. J., **143**, 59 (8pp)

Farago, F., & Laskar, J. (2010) "High-inclination orbits in the secular quadrupolar three-body problem." Mon. Not. R. Astron. Soc., **401**, 1189–1198

Farinella, P., Froeschlé, Ch., & Gonczi, R. (1993) "Meteorites from the asteroid 6 Hebe." Celest. Mech., **56**, 287–305

Farinella, P., Froeschlé, Ch., Froeschlé, C., Gonczi, R., Hahn, G., Morbidelli, A., & Valsecchi, G. B. (1994) "Asteroids falling onto the Sun." Nature, **371**, 314–317

Fernández, J. A. (1997) "The formation of the Oort cloud and the primitive galactic environment." Icarus, **129**, 106–119

Ferraz-Mello, S. (2007) *Canonical Perturbation Theories. Degenerate Systems and Resonance* (Springer, New York)

Ferraz-Mello, S., Michtchenko, T., Beaugé, C., & Callegari, N. Jr. (2005) "Extrasolar planetary systems." In: *Chaos and Stability in Planetary Systems*, ed. by Dvorak, R., Freistetter, F., & Kurths, J. (Lect. Notes Phys., v. 683) (Springer, Heidelberg) pp. 219–271

Ferrer, S., & Osácar, C. (1994) "Harrington's Hamiltonian in the stellar problem of three bodies: reductions, relative equilibria and bifurcations." Celest. Mech. Dyn. Astron., **58**, 245–275

Ford, E. B., Kozinsky, B., & Rasio, F. A. (2000) "Secular evolution of hierarchical triple star systems." Astrophys. J., **535**, 385–401

Fouchard, M., Froeschlé, Ch., Rickman, H., & Valsecchi, G. B. (2011) "The key role of massive stars in Oort cloud comet dynamics." Icarus, **214**, 334–347

Fragner, M. M., Nelson, R. P., & Kley, W. (2011) "On the dynamics and collisional growth of planetesimals in misaligned binary systems." Astron. Astrophys., **528**, A40 (21pp)

Froeschlé, Cl. (1984) "The Lyapunov characteristic exponents — applications to celestial mechanics." Celest. Mech., **34**, 95–115

Froeschlé, Ch., & Morbidelli, A. (1994) "The secular resonances in the solar system." In: *Asteroids, Comets, Meteors 1993*, ed. by Milani, A., di Martino, M., & Cellino, A. (Kluwer, Dordrecht) pp. 189–204

Froeschlé, Ch., Morbidelli, A., & Scholl, H. (1991) "Complex dynamical behaviour of the asteroid 2335 James associated with the secular resonances ν_5 and ν_{16}: numerical studies and theoretical interpretation." Astron. Astrophys., **249**, 553–562

Gallardo, T. (2006) "The occurrence of high-order resonances and Kozai mechanism in the scattered disk." Icarus, **181**, 205–217

Gallardo, T., Hugo, G., & Pais, P. (2012) "Survey of Kozai dynamics beyond Neptune." Icarus, **220**, 392–403

Giacaglia, G. E. O. (1968) "Secular motion of resonant asteroids." Smithsonian Astrophysical Observatory, Special Report No. 278. 70 pp.

Giacaglia, G. E. O. (1969) "Resonance in the restricted problem of three bodies." Astron. J, **74**, 1254–1261

Giacaglia, G. E. O. (1972) *Perturbation Methods in Non-Linear Systems* (Springer, New York)

Gladman, B., Kavelaars, J. J., Holman, M., Nicholson, P. D., Burns, J. A., Hergenrother, C., Petit, J.-M., Marsden, B. G., Jacobson, R., Gray, W., & Grav, T. (2001) "Orbital clustering for twelve newly discovered Saturnian satellites: Evidence for collisional families." Nature, **412**, 163–166

Goldman, B., Marsat, S., Henning, T., Clemens, C., & Greiner, J. (2010) "A new benchmark T8-9 brown dwarf and a couple of new mid-T dwarfs from the UKIDSS DR5+ LAS." Mon. Not. R. Astron. Soc., **405**, 1140–1152

Goldreich, P. (1966) "History of the Lunar orbit." Review of Geophysics and Space Physics, **4**, 411–439

Goldreich, P., Murray, N., Longaretti, P. Y., & Banfield, D. (1989) "Neptune's story." Science, **245**, 500–504

Gopakumar, A., Bagchi, M., & Ray, A. (2009) "Ruling out Kozai resonance in highly eccentric galactic binary millisecond pulsar PSR J1903+0327." Mon. Not. R. Astron. Soc., **399**, L123–L127

Gordeeva, Yu. F. (1968) "The time dependence of elements in the long-period oscillations in the restricted three-body problem." Cosmic Research, **6**, 450–453

Gould, A., & Quillen, A. C. (2003) "Sagittarius A* companion S0-2: a probe of very high mass star formation." Astrophys. J., **592**, 935–940

Greenberg, R., & Van Laerhoven, C. (2012) "Aligned major axes in a planetary system without tidal evolution: The 61 Virginis example." Mon. Not. R. Astron. Soc., **419**, 429–435

Gronchi, G. F., & Milani, A. (1998) "Averaging on Earth-crossing orbits." Celest. Mech., **71**, 109–136

Gronchi, G. F., & Milani, A. (1999) "The stable Kozai state for asteroids and comets, with arbitrary semimajor axis and inclination." Astron. Astrophys., **341**, 928–935

Haghighipour, N., Dvorak, R., & Pilat-Lohinger, E. (2010) "Planetary dynamics and habitable planet formation in binary star systems." In: *Planets in Binary Star Systems*, ed. by Haghighipour, N. (Springer, Dordrecht) pp. 285–327

Hagihara, Y. (1972) *Celestial Mechanics* Vol. 2, Part 2 (MIT Press, Cambridge)

Hamilton, D. P., & Burns, J. A. (1992) "Orbital stability zones about asteroids. II. The destabilizing effects of eccentric orbits and of solar radiation." Icarus, **96**, 43–64

Harrington, R. S. (1968) "Dynamical evolution of triple stars." Astron. J., **73**, 190–194

Harrington, R. S. (1969) "The stellar three-body problem." Celest. Mech., **1**, 200–209

Hauser, H. M., & Marcy, G. W. (1999) "The orbit of 16 Cygni AB." Publ. Astron. Soc. Pacific, **111**, 321–334

Hayes, W. B. (2007) "Is the outer Solar System chaotic?" Nature Phys., **3**, 689–691

Hayes, W. B. (2008) "Surfing on the edge: chaos versus near-integrability in the system of Jovian planets." Mon. Not. R. Astron. Soc., **386**, 295–306

Hayes, W. B., Malykh, A. V., & Danforth, C. M. (2010) "The interplay of chaos between the terrestrial and giant planets." Mon. Not. R. Astron. Soc., **407**, 1859–1865

Heisler, J., & Tremaine, S. (1986) "The influence of the galactic tidal field on the Oort comet cloud." Icarus, **65**, 13–26

Henrard, J., & Lemaître, A. (1983) "A second fundamental model for resonance." Celest. Mech., **30**, 197–218

Heppenheimer, T. A., & Porco, C. C. (1977) "New contributions to the problem of capture." Icarus, **30**, 385–401

Heppenheimer, T. A. (1978) "On the formation of planets in binary star systems." Astron. Astrophys., **65**, 421–426

Higuchi, A., Kokubo, E., Kinoshita, H., & Mukai, T. (2007) "Orbital evolution of planetesimals due to the Galactic tide: formation of the comet cloud." Astron. J., **134**, 1693–1706

Holman, M. J., & Murray, N. W. (1996) "Chaos in high-order mean motion resonances in the outer asteroid belt." Astron. J., **112**, 1278–1293

Holman, M., Touma, J., & Tremaine, S. (1997) "Chaotic variations in the eccentricity of the planet orbiting 16 Cygni B." Nature, **386**, 254–256

Hori, G. I. (1966) "General perturbations theory with unspecified canonical variables." Publ. Astron. Soc. Japan, **18**, 287–296

Huang, S.-S. (1960) "Life-supporting regions in the vicinity of binary systems." Publ. Astron. Soc. Pacific, **72**, 106–114

Iben, I., Jr., & Tutukov, A. V. (1984) "Supernovae of type I as end products of the evolution of binaries with components of moderate initial mass ($M \lesssim 9M_{\odot}$)." Astrophys. J. Suppl., **54**, 335–372

Innanen, K. A., Zheng, J. Q., Mikkola, S., & Valtonen, M. J. (1997) "The Kozai mechanism and the stability of planetary orbits in binary star systems." Astron. J., **113**, 1915–1919

Ivanov, P. B., & Papaloizou, J. C. B. (2004) "On the tidal interaction of massive extra solar planets on highly eccentric orbits." Mon. Not. R. Astron. Soc., **347**, 437–453

Ivanov, P. B., & Papaloizou, J. C. B. (2011) "Close encounters of a rotating star with planets in parabolic orbits of varying inclination and the formation of hot Jupiters." Celest. Mech. Dyn. Astron., **111**, 51–82

Jefferys, W. H., & Moser, J. (1966) "Quasi-periodic solutions for the three-body problem." Astron. J., **71**, 568–578

Kaib, N. A., Raymond, S. N., & Duncan, M. (2013) "Planetary system disruption by Galactic perturbations to wide binary stars." Nature, **493**, 381–384

Kalas, P., Graham, J. R., & Clampin, M. (2005) "A planetary system as the origin of structure in Fomalhaut's dust belt." Nature, **435**, 1067–1070

Katz, B., Dong, S., & Malhotra, R. (2011) "Long-term cycling of Kozai–Lidov cycles: Extreme eccentricities and inclinations excited by a distant eccentric perturber." Phys. Rev. Lett., **107**, 181101 (5pp)

Kholshevnikov, K. V. (1985) *Asymptotic methods of celestial mechanics* (Leningrad State Univ., Leningrad) (in Russian)

Kholshevnikov, K. V. (1997) "D'Alembertian functions in celestial mechanics." Astron. Rep., **41**, 135–142

Kholshevnikov, K. V. (2001) "The Hamiltonian in the planetary or satellite problem as a D'Alembertian function." Astron. Rep., **41**, 135–142, **45**, 577–579

Kinoshita, H., & Nakai, H. (1999) "Analytical solution of the Kozai resonance and its application." Celest. Mech. Dyn. Astron., **75**, 125–147

Kinoshita, H., & Nakai, H. (2007) "General solution of the Kozai mechanism." Celest. Mech. Dyn. Astron., **98**, 67–74

Kirkwood, D. (1867) *Meteoric Astronomy* (Lippincott, Philadelphia)

Kiseleva, L. G., Eggleton, P. P., & Mikkola, S. (1998) "Tidal friction in triple stars." Mon. Not. R. Astron. Soc., **300**, 292–392

Knežević, Z., & Milani, A. (1994) "Asteroid proper elements: the big picture." In: *Asteroids, Comets, Meteors 1993*, ed. by Milani, A., di Martino, M., & Cellino, A. (Kluwer, Dordrecht) pp. 143–158

Kolomensky, A. A., & Lebedev, A. N. (1966) *Theory of Cyclic Accelerators* (Wiley, New York)

Kozai, Y. (1962) "Secular perturbations of asteroids with high inclination and eccentricity." Astron. J., **67**, 591–598

Kozai, Y. (1979) "Secular perturbations of asteroids and comets." In: *Dynamics of the Solar System*, ed. by Duncombe, R. L. (Reidel, Dordrecht) pp. 231–237

Kozai, Y. (1980) “Asteroids with large secular orbital variations.” Icarus, **41**, 89–95
Kozai, Y. (1985) “Secular perturbations of resonant asteroids.” Celest. Mech., **36**, 47–69
Kozai, Y. (2012) “Kozai mechanism.” In: *Asteroids, Comets, Meteors 2012*, Proceedings of the conference held May 16–20, 2012 in Niigata, Japan. LPI Contribution No. 1667, id. 6195
Krasinsky, G. A. (1972) “Critical inclinations in planetary problems.” Celest. Mech., **6**, 60–83
Krasinsky, G. A. (1974) “Stationary solutions of the averaged three-body problem and some problems of planet motion stability.” In: *The Stability of the Solar System and of Small Stellar Systems* (IAU Symp. No. 62), ed. by Kozai, Y. (Springer, Berlin) pp. 95–116
Kreutz, H. C. F. (1888) “Untersuchungen uber das cometensystem 1843 I, 1880 I und 1882 II.” (Druck von C. Schaidt, Kiel)
Krymolowski, Y., & Mazeh, T. (1999) “Studies of multiple stellar systems – II. Second-order averaged Hamiltonian to follow long-term orbital modulations of hierarchical triple systems.” Mon. Not. R. Astron. Soc., **304**, 720–732
Kushnir, D., Katz, B., Dong, S., Livne, E., & Fernández, R. (2013) “Head-on collisions of white dwarfs in triple systems could explain Type Ia supernova.” Astrophys. J., **778**, L37 (6pp)
Kuzuhara, M., Tamura, M., Ishii, M., Kudo, T., Nishiyama, S., & Kandori, R. (2011) “The widest-separation substellar companion candidate to a binary T Tauri star.” Astron. J., **141**, 119 (10pp)
Laplace, P. S. (1805) *Mécanique Céleste*, V. 4 (Courcier, Paris)
Laskar, J. (1989) “A numerical experiment on the chaotic behaviour of the Solar system.” Nature, **338**, 237–238
Laskar, J. (1990) “The chaotic motion of the solar system: a numerical estimate of the size of the chaotic zones.” Icarus, **88**, 266–291
Laskar, J. (1994) “Large-scale chaos in the solar system.” Astron. Astrophys., **287**, L9–L12
Lawler, S. M., & Gladman, B. (2013) “Plutino detection biases, including the Kozai resonance.” Astronomical Journal, **146**, 6 (13pp)
Lee, M. H., & Peale, S. (2003) “Secular evolution of hierarchical planetary systems.” Astrophys. J., **592**, 1201–1216 [Erratum: (2003) Astrophys. J., **597**, 644 (1p)]
Leigh, N., Knigge, Ch., Sills, A., Perets, H. B., Sarejedini, A., & Glebbeek, E. (2013) “The origins of blue stragglers and binarity in globular clusters.” Mon. Not. R. Astron. Soc., **428**, 897–905
Lemaître, A. (1984) “High-order resonances in the restricted three-body problem.” Celest. Mech. Dyn. Astron., **32**, 109–126
Li, G., Naoz, S., Kocsis, B., & Loeb, A. (2014a) “Eccentricity growth and orbit flip in near-coplanar hierarchical three-body systems.” Astrophys. J., **785**, 116 (8pp)
Li, G., Naoz, S., Holman, M., & Loeb, A. (2014b) “Chaos in the test particle eccentric Kozai–Lidov mechanism.” Astrophys. J., **791**, 86 (10pp) [Erratum: (2015) Astrophys. J., **802**, 71 (1p)]
Li, G., Naoz, S., Kocsis, B., & Loeb, A. (2015) “Implications of the eccentric Kozai–Lidov mechanism for stars surrounding supermassive black hole binaries.” Mon. Not. R. Astron. Soc., **451**, 1341–1349
Libert, A.-S., & Henrard, J. (2007) “Exoplanetary systems: The role of an equilibrium at high mutual inclination in shaping the global behavior of the 3-D secular planetary three-body problem.” Icarus, **191**, 469–485
Lichtenberg, A. J., & Lieberman, M. A. (1992) *Regular and Chaotic Dynamics.* 2nd edition (Springer-Verlag, New York)
Lidov, M. L. (1961) “Evolution of artificial planetary satellites under the action of gravitational perturbations due to external bodies.” Iskusstviennye Sputniki Zemli (Artificial Satellites of the Earth), **8**, 5–45 (in Russian)
Lidov, M. L. (1962) “The evolution of orbits of artificial satellites of planets under the action of gravitational perturbations of external bodies.” Planet. Space Sci., **9**, 719–759 (An English translation of Lidov’s (1961) article.)
Lidov, M. L. (1963a) “Evolution of the orbits of artificial satellites of planets as affected by gravitational perturbation from external bodies.” AIAA Journal, **1**, 1985–2002 (An English translation of Lidov’s (1961) article.)
Lidov, M. L. (1963b) “On the approximate analysis of the evolution of orbits of artificial satellites.” In: *Problems of the Motion of Artificial Celestial Bodies.* (Reports at the Conference on general

and applied problems of theoretical astronomy. Moscow, November 20–25, 1961.) (Publishers of the USSR Academy of Sciences, Moscow) pp. 119–134 (in Russian) [Available at NASA ADS: 1963pmac.book..119L, including incomplete English translation.]

Lidov, M. L. (1963c) "On the approximated analysis of the orbit evolution of artificial satellites." In: *Dynamics of Satellites* (IUTAM Symp.), ed. by Roy, M. (Springer, Berlin) pp. 168–179

Lidov, M. L. (2010) *A Course of Lectures on Theoretical Mechanics* 2nd edition (FIZMATLIT, Moscow) (in Russian)

Lidov, M. L., & Ziglin, S. L. (1974) "The analysis of the restricted circular twice-averaged three body problem in the case of close orbit." Celest. Mech., **9**, 151–173

Lidov, M. L., & Ziglin, S. L. (1976) "Non-restricted double-averaged three body problem in Hill's case." Celest. Mech., **13**, 471–481

Lithwick, Y., & Naoz, S. (2011) "The eccentric Kozai mechanism for a test particle." Astrophys. J., **742**, 94 (8pp)

Löckmann, U., Baumgardt, H., & Kroupa, P. (2008) "Origin of the S stars in the Galactic center." Astrophys. J., **683**, L151–L154

Lovis, C., Ségransan, D., Mayor, M., Udry, S., Benz, W., Bertaux, J.-L., Bouchy, F., Correia, A. C. M., Laskar, J., Lo Curto, G., Mordasini, C., Pepe, F., Queloz, D., & Santos, N. C. (2011) "The HARPS search for southern extra-solar planets. XXVIII. Up to seven planets orbiting HD 10180: probing the architecture of low-mass planetary systems." Astron. Astrophys., **528**, A112 (16pp)

Lu, J. R., Ghez, A. M., Hornstein, S. D., Morris, M., Matthews, K., Thompson D. J., & Becklin E. E. (2006) "Galactic center youth: orbits and origins of the young stars in the central parsec." Journal of Physics Conference Series, **54**, 279–287

Luhman, K. L., Burgasser, A. J., Labbé, I., Saumon, D., Marley, M. S., Bochanski, J. J., Monson, A. J., & Persson, S. E. (2012) "Confirmation of one of the coldest known brown dwarfs." Astrophys. J., **744**, 135 (8pp)

Malhotra, R. (1998) "Orbital resonances and chaos in the Solar system." In: *Solar System Formation and Evolution* (ASP Conf. Ser. 149), ed. by Lazzaro, D., Vieira Martins, R., Ferraz-Mello, S., Fernández, J., & Beaugé, C. (Astron. Soc. of the Pacific, San Francisco) pp. 37–63

Malhotra, R., & Williams, J. G. (1997) "Pluto's heliocentric orbit." In: *Pluto and Charon*, ed. by Stern, S. A., & Tholen, D. (Univ. of Arizona Press, Tucson) pp. 127–157

Malhotra, R. (2012) "Orbital resonances in planetary systems." In: *Encyclopedia of Life Support Systems by UNESCO*. Volume 6.119.55 *Celestial Mechanics*. 31 pp.

Malmberg, D., Davies, M. B., & Chambers, J. E. (2007) "The instability of planetary systems in binaries: how the Kozai mechanism leads to strong planet-planet interactions." Mon. Not. R. Astron. Soc., **377**, L1–L4

Marchal, C. (1990) *The Three-Body Problem* (Elsevier, Amsterdam)

Mardling, R. A., & Aarseth, S. J. (2001) "Tidal interactions in star cluster simulations." Mon. Not. R. Astron. Soc., **321**, 398–420

Markeev, A. P. (1990) *Theoretical Mechanics* (Nauka Publishers, Moscow) (in Russian)

Marzari, F., & Barbieri, M. (2007) "Planet dispersal in binary systems during transient multiple star phases." Astron. Astrophys., **472**, 643–647

Matese, J. J., & Lissauer, J. J. (2002) "Characteristics and frequency of weak stellar impulses of the Oort cloud." Icarus, **157**, 228–240

Matese, J. J., & Whitman, P. G. (1989) "The galactic disk tidal field and the nonrandom distribution of observed Oort cloud comets." Icarus, **82**, 389–401

Matese, J. J., & Whitman, P. G. (1992) "A model of the Galactic tidal interaction with the Oort comet cloud." Celest. Mech. Dyn. Astron., **54**, 13–35

Mathieu, R. D., Ghez, A. M., Jensen, E. L. N., & Simon, M. (2000) "Young binary stars and associated disks." In: *Protostars and Planets IV* (Univ. Arizona Press, Tucson) pp. 703–730

Mayor, M., & Queloz, D. (1995) "A Jupiter-mass companion to a solar-type star." Nature, **378**, 355–359

Mazeh, T., & Shaham, J. (1979) "The orbital evolution of close triple systems — the binary eccentricity." Astron. Astrophys., **77**, 145–151

Mazeh, T., Goldberg, D., Duquennoy, A., & Mayor, M. (1992) "On the mass-ratio distribution of spectroscopic binaries with solar-type primaries." Astrophys. J., **401**, 265–268
Mazeh, T., Krymolowski, Y., & Rosenfeld, G. (1997) "The high eccentricity of the planet orbiting 16 Cygni B." Astrophys. J., **477**, L103–L106
McCrea, W. H. (1964) "Extended main-sequence of some stellar clusters." Mon. Not. R. Astron. Soc., **128**, 147–155
McMillan, S., Hut, P., & Makino, J. (1991) "Star cluster evolution with primordial binaries. II – Detailed analysis." Astrophys. J., **372**, 111–124
Meiss, J.D. (1992) "Symplectic maps, variational principles, and transport." Rev. Mod. Phys., **64**, 795–848
Melnikov, A. V. (2016) "On the chaotic orbital dynamics of the planet in the system 16 Cyg." Astron. Lett., **42**, 115–125
Meschiari, S. (2012a) "Circumbinary planet formation in the Kepler-16 system. I. N-body simulations." Astrophys. J., **752**, 71 (6pp)
Meschiari, S. (2012b) "Planet formation in circumbinary configurations: Turbulence inhibits planetesimal accretion." Astrophys. J., **761**, L7 (5pp)
Meschiari, S. (2014) "Circumbinary planet formation in the Kepler-16 system. II. A toy model for in-situ planet formation within a debris belt." Astrophys. J., **790**, 41 (14pp)
Michaely, E., Perets, H. B., & Grishin, E. (2015) "On the existence of regular and irregular outer moons orbiting the Pluto–Charon system." ArXiv: 1506.08818 [astro-ph.EP] (20pp)
Michel, P., & Thomas, F. (1996) "The Kozai resonance for near-Earth asteroids with semimajor axes smaller than 2 AU." Astron. Astrophys., **307**, 310–318
Milani, A., & Knežević, Z. (1990) "Secular perturbation theory and computation of asteroid proper elements." Celest. Mech., **49**, 347–411
Miller, M. C., & Hamilton, D. P. (2002a) "Four-body effects in globular cluster black hole coalescence." Astrophys. J., **576**, 894–898
Miller, M. C., & Hamilton, D. P. (2002b) "Production of intermediate-mass black holes in globular clusters." Mon. Not. R. Astron. Soc., **330**, 232–240
Moiseev, N. D. (1945a) "On some basic simplified schemes of celestial mechanics obtained by means of averaging the restricted circular three-body problem. Part 1." Publications of the Sternberg State Astronomical Institute (Moscow State Univ.), **15**, issue 1, pp. 75–99 (in Russian, the issue was typeset in 1941)
Moiseev, N. D. (1945b) "On some basic simplified schemes of celestial mechanics obtained by means of averaging the restricted circular three-body problem. Part 2." Publications of the Sternberg State Astronomical Institute (Moscow State Univ.), **15**, issue 1, pp. 100–117 (in Russian, the issue was typeset in 1941)
Moons, M., & Morbidelli, A. (1995) "Secular resonances inside mean-motion commensurabilities: the 4/1, 3/1, 5/2 and 7/3 cases." Icarus, **114**, 33–50
Moons, M., Morbidelli, A., & Migliorini, F. (1998) "Dynamical structure of the 2/1 commensurability and the origin of the resonant asteroids." Icarus, **135**, 458–468
Morbidelli, A. (1993) "Asteroid secular resonant proper elements." Icarus, **105**, 48–66
Morbidelli, A. (2002) *Modern Celestial Mechanics* (Taylor and Francis, London)
Morbidelli, A., & Henrard J. (1991a) "Secular resonances in the asteroid belt: theoretical perturbation approach and the problem of their location." Celest. Mech., **51**, 131–167
Morbidelli, A., & Henrard J. (1991b) "The main secular resonances ν_6, ν_5 and ν_{16} in the asteroid belt." Celest. Mech., **51**, 169–197
Moriwaki, K., & Nakagawa, Y. (2004) "A planetesimal accretion zone in a circumbinary disk." Astrophys. J., **609**, 1065–1070
Murray, C. D., & Dermott, S. F. (1999) *Solar System Dynamics* (Cambridge Univ. Press, Cambridge)
Murray, N. W., & Holman, M. J. (1997) "Diffusive chaos in the outer asteroid belt." Astron. J., **114**, 1246–1259
Murray, N., & Holman, M. (1999) "The origin of chaos in the outer Solar system." Science, **283**, 1877–1881

Nagasawa, M., Ida, S., & Bessho, T. (2008) "Formation of hot planets by a combination of planet scattering, tidal circularization, and the Kozai mechanism." Astrophys. J., **678**, 498–508

Nakai, H., & Kinoshita, H. (1985) "Secular perturbations of asteroids in secular resonances." Celest. Mech., **36**, 391–407

Naoz, S., Farr, W. M., & Rasio, F. A. (2012) "On the formation of hot Jupiters in stellar binaries." Astrophys. J., **754**, L36 (6pp)

Naoz, S., Perets, H. B., & Ragozzine, D. (2010) "The observed orbital properties of binary minor planets." Astrophys. J., **719**, 1775–1783

Naoz, S., Farr, W. M., Lithwick, Y., Rasio, F. A., & Teyssandier, J. (2011) "Hot Jupiters from secular planet-planet interactions." Nature, **473**, 187–189

Naoz, S., Farr, W. M., Lithwick, Y., Rasio, F. A., & Teyssandier, J. (2013a) "Secular dynamics in hierarchical three-body systems." Mon. Not. R. Astron. Soc., **431**, 2155–2171

Naoz, S., Kocsis, B., Loeb, A., & Yunes, N. (2013b) "Resonant post-newtonian eccentricity excitation in hierarchical three-body systems." Astrophys. J., **773**, 187 (16pp)

Naoz, S., & Silk, J. (2014) "Formation of dark matter tori around supermassive black holes via the eccentric Kozai–Lidov mechanism." Astrophys. J., **795**, 102 (11pp)

Nesvorný, D., Roig, F., & Ferraz-Mello, S. (2000) "Close approaches of trans-Neptunian objects to Pluto have left observable signatures on their orbital distribution." Astron. J., **119**, 953–969

Nesvorný, D., Alvarellos, J. L. A., Dones, L., & Levison, H. F. (2003) "Orbital and collisional evolution of the irregular satellites." Astron. J., **126**, 398–429

Oort, J. H. (1950) "The structure of the cloud of comets surrounding the Solar System and a hypothesis concerning its origin." Bull. Astron. Inst. Neth., **11**, 91–110

Orosz, J. A., Welsh, W. F., Carter, J. A., Fabrycky, D. C., Cochran, W. D., *et al.* (2012) "Kepler-47: a transiting circumbinary multiplanet system." Science, **337**, 1511–1514

Paardekooper, S.-J., Leinhardt, Z. M., Thébault, T., & Baruteau, C. (2012) "How not to build Tatooine: the difficulty of in situ formation of circumbinary planets Kepler 16b, Kepler 34b, and Kepler 35b." Astrophys. J., **754**, L16 (5pp)

Paumard, T., Genzel, R., Martins, F., Nayakshin, S., Beloborodov, A. M., Levin, Y., Trippe, S., Eisenhauer, F., Ott, T., Gillessen, S., Abuter, R., Cuadra, J., Alexander, T., & Sternberg, A. (2006) "The two young star disks in the central parsec of the Galaxy: properties, dynamics, and formation." Astrophys. J., **643**, 1011–1035

Perets, H. B., & Fabrycky, D. C. (2009) "On the triple origin of blue stragglers." Astrophys. J., **697**, 1048–1056

Perets, H. B., & Naoz, S. (2009) "Kozai cycles, tidal friction, and the dynamical evolution of binary minor planets." Astrophys. J., **699**, L17–L21

Pinsonneault, M. H., & Stanek, K. Z. (2006) "Binaries like to be twins: implications for doubly degenerate binaries, the type Ia Supernova rate, and other interacting binaries." Astrophys. J., **639**, L67–L70

Poincaré, H. (1899) *Les Méthodes Nouvelles de la Mécanique Céleste III* (Gauthier–Villars, Paris)

Poincaré, H. (1905) *Leçons de Mécanique Céleste* (Gauthier–Villars, Paris)

Pollack, J. B., Burns, J. A., & Tauber, M. E. (1979) "Gas drag in primordial circumplanetary envelopes: A mechanism for satellite capture." Icarus, **37**, 587–611

Pollack, J. B., Lunine, J. I., & Tittemore, W. C. (1991) "Origin of the Uranian satellites." In: *Uranus*, ed. by Bergstrahl, J. T., Miner, E. D., & Matthews, M. S. (Univ. Arizona Press, Tucson) pp. 469–512

Prodan, S., Murray, N., & Thompson, T. A. (2013) "On WD–WD mergers in triple systems: the role of Kozai resonance with tidal friction." ArXiv: 1305.2191 [astro-ph.SR] (8pp)

Prokhorenko, V. I. (2002a) "Investigation of periods of evolution for elliptical orbits in the double-averaged Hill problem." Cosmic Research, **40**, 48–54

Prokhorenko, V. I. (2002b) "Investigation of the time of ballistic existence for elliptic orbits evolving under the influence of gravitational perturbations of external bodies" Cosmic Research, **40**, 264–273

Prokhorenko, V. I. (2015) "On the application of qualitative methods of perturbation theory in solving practical problems of selection and correction of the orbits of the satellites of the planets

given the secular and long-period components of the evolution under the influence of external gravitational perturbations." In: *Space Ballistics — from its Origin to the Future.* (Institute of Space Research, Russian Academy of Sciences, Moscow) pp. 130–161 (in Russian)

Quinn, T., Tremaine, S., & Duncan, M. (1990) "Planetary perturbations and the origin of short-period comets." Astrophys. J., **355**, 667–679

Raghavan, D., McAlister, H. A., Henry, T. J., *et al.* (2010) "A survey of stellar families: multiplicity of Solar-type stars." Astrophys. J. Suppl., **190**, 1–42

Ragozzine, D., & Wolf, A. S. (2009) "Probing the interiors of very hot Jupiters using transit light curves." Astrophys. J., **698**, 1778–1794

Raushenbakh, B. V., & Ovchinnikov, M. Yu. (1997) *Lectures on Dynamics of Spaceflight* (Moscow Physics–Technical Institute, Moscow) (in Russian)

Riddle, R. L., Tokovinin, A., Mason, B. D., *et al.* (2015) "A survey of the high order multiplicity of nearby Solar-type binary stars with Robo–AO." Astrophys. J., **799**, 4 (21pp)

Rein, H. (2012) "Period ratios in multiplanetary systems discovered by Kepler are consistent with planet migration." Mon. Not. R. Astron. Soc., **427**, L21–L24

Roy, A. E. (1988) *Orbital Motion* (Adam Hilger, Bristol)

Saha, P., & Tremaine, S. (1993) "The orbits of the retrograde jovian satellites." Icarus, **106**, 549–562

Sahu, K. C., Casertano, S., Bond, H. E., *et al.* (2006) "Transiting extrasolar planetary candidates in the Galactic bulge." Nature, **443**, 534–540

Sandage, A. R. (1953) "The color-magnitude diagram for the globular cluster M 3." Astron. J., **58**, 61–75

Seto, N. (2013) "Highly eccentric Kozai mechanism and gravitational-wave observation for neutron-star binaries." Phys. Rev. Lett., **111**, 061106 (5pp)

Shappee, B. J., & Thompson, T. A. (2013) "The mass-loss-induced eccentric Kozai mechanism: a new channel for the production of close compact object–stellar binaries." Astrophys. J., **766**, 64 (12pp)

Shevchenko, I. I. (2000) "Geometry of a chaotic layer." J. Exp. Theor. Phys., **91**, 615–625

Shevchenko, I. I. (2002) "On the maximum Lyapunov exponents of the chaotic rotation of natural planetary satellites." Cosmic Research, **40**, 296

Shevchenko, I. I. (2007) "On the Lyapunov exponents of the asteroidal motion subject to resonances and encounters." In: *Near Earth Objects, our Celestial Neighbors: Opportunity and Risk* (Proc. IAU Symp. 236), ed. by Milani, A., Valsecchi, G. B., & Vokrouhlický, D. (Cambridge Univ. Press, Cambridge) pp. 15–29

Shevchenko, I. I. (2011a) "Lyapunov and diffusion timescales in the solar neighborhood." Astrophys. J., **733**, 39 (8pp)

Shevchenko, I. I. (2011b) "The Kepler map in the three-body problem." New Astronomy, **16**, 94–99

Shevchenko, I. I. (2014) "Lyapunov exponents in resonance multiplets." Phys. Lett. A, **378**, 34–42

Shevchenko, I. I. (2015) "Chaotic zones around gravitating binaries." Astrophys. J., **799**, 8 (7pp)

Shinkin, V. N. (1995) "The integrable cases of the general spatial three-body problem at third-order resonance." Celest. Mech. Dyn. Astron., **62**, 323–334

Söderhjelm, S. (1984) "Third-order and tidal effects in the stellar three-body problem." Astron. Astrophys., **141**, 232–240

Soter, S. (2006) "What is a planet?" Astron. J., **132**, 2513–2519

Stern, S. A., & Levison, H. F. (2002) "Regarding the criteria for planethood and proposed planetary classification schemes." Highlights of Astronomy, **12**, 205–213

Sterne, T. E. (1939) "Apsidal motion in binary stars." Mon. Not. R. Astron. Soc., **99**, 451–462

Steffen, J. H., *et al.* (2012) "Kepler constraints on planets near hot Jupiters." Proceedings of the National Academy of Science, **109**, 7982–7987

Stevenson, D. J., Harris, A. W., & Lunine, J. I. (1986) "Origins of satellites." In: *Satellites*, ed. by Burns, J. A., & Matthews, M. S. (Univ. Arizona Press, Tucson) 39–88

Subbotin, M. F. (1968) *An Introduction to Theoretical Astronomy* (Nauka Publishers, Moscow) (in Russian)

Šubr, L., & Karas, V. (2005) "On highly eccentric stellar trajectories interacting with a self-gravitating disc in Sgr A*." Astron. Astrophys., **433**, 405–413
Šubr, L., Karas, V., & Huré, J.-M. (2004) "Star-disc interactions in a galactic centre and oblateness of the inner stellar cluster." Mon. Not. R. Astron. Soc., **354**, 1177–1188
Sussman, G.J., & Wisdom, J. (1988) "Numerical evidence that Pluto is chaotic." Science, **241**, 433–437
Sussman, G. J., & Wisdom, J. (1992) "Chaotic evolution of the solar system." Science, **257**, 56–62
Šuvakov, M., & Dmitrašinović, V. (2013) "Three classes of Newtonian three-body planar periodic orbits." Phys. Rev. Lett., **110**, 114301 (4pp)
Szebehely, V. (1967) *The Theory of Orbits* (Academic Press, New York)
Takeda, G., & Rasio, F. A. (2005) "High orbital eccentricities of extrasolar planets induced by the Kozai mechanism." Astrophys. J., **627**, 1001–1010
Tamayo, D., Burns, J. A., Hamilton, D. P., & Nicholson, P. D. (2013) "Dynamical instabilities in high-obliquity systems." Astron. J., **145**, 54 (12pp)
Thébault, P., Marzari, F., Scholl, H. (2006) "Relative velocities among accreting planetesimals in binary systems: The circumprimary case." Icarus, **183**, 193–206
Thomas, F. (1998) "La dynamique résonnante dans le système solaire. Application au mouvement des objets transneptuniens." Ph. D. thesis (Obs. de Paris, Paris)
Thomas, F., & Morbidelli, A. (1996) "The Kozai resonance in the outer solar system and the dynamics of long-period comets." Celest. Mech. Dyn. Astron., **64**, 209–229
Thompson, T. A. (2011) "Accelerating compact object mergers in triple systems with the Kozai resonance: a mechanism for "prompt" type Ia supernovae, gamma-ray bursts, and other exotica." Astrophys. J., **741**, 82 (14pp)
Tisserand, F.-F. (1896) *Traité de Mécanique Céleste IV* (Gauthier-Villars, Paris)
Tokovinin, A. A. (1997) "On the multiplicity of spectroscopic binary stars." Astron. Lett., **23**, 727–730
Tokovinin, A. (2014) "From binaries to multiples. II. Hierarchical multiplicity of F and G dwarfs." Astron. J., **147**, 87 (14pp)
Tokovinin, A., Thomas, S., Sterzik, M., & Udry, S. (2006) "Tertiary companions to close spectroscopic binaries." Astron. Astrophys., **450**, 681–693
Tremaine, S., Touma, J., & Namouni, F. (2009) "Satellite dynamics on the Laplace surface." Astron. J., **137**, 3706–3717
Trujillo, C. A., & Sheppard, S. S. (2014) "A Sedna-like body with a perihelion of 80 astronomical units." Nature, **507**, 471–474
Van Laerhoven, C., & Greenberg, R. (2012) "Characterizing multi-planet systems with classical secular theory." Celest. Mech. Dyn. Astron., **113**, 215–234
Vashkovyak, M. A. (1981a) "Evolution of orbits in the restricted circular twice-averaged three-body problem. I — Qualitative investigations." Cosmic Research, **19**, 1–10
Vashkovyak, M. A. (1981b) "Evolution of orbits of asteroids not belonging to the main belt." Cosmic Research, **19**, 357–365
Vashkovyak, M. A. (1982) "Evolution of orbits in the two-dimensional restricted elliptic twice-averaged three-body problem." Cosmic Research, **20**, 236–244
Vashkovyak, M. A. (1984) "Integrable cases of the restricted twice-averaged three-body problem." Cosmic Research, **22**, 260–267
Vashkovyak, M. A. (1986) "An investigation of the evolution of some asteroid orbits." Cosmic Research, **23**, 255–267
Vashkovyak, M. A. (1999) "Evolution of the orbits of distant satellites of Uranus." Astron. Lett., **25**, 476–481
Vashkovyak, M. A. (2001) "Orbital evolution of Saturn's new outer satellites and their classification." Astron. Lett., **27**, 455–463
Vashkovyak, M. A. (2003) "Orbital evolution of new distant Neptunian satellites and ω-librators in the satellite systems of Saturn and Jupiter." Astron. Lett., **29**, 695–703
Vashkovyak, M. A. (2005) "Particular solutions of the singly averaged Hill problem." Astron. Lett., **31**, 487–493

Vashkovyak, M. A., & Teslenko, N. M. (2008a) "Evolution characteristics of Jupiter's outer satellites." Sol. Sys. Res., **42**, 281–295 [Erratum: Sol. Sys. Res., **43**, 463]

Vashkovyak, M. A., & Teslenko, N. M. (2008b) "Evolutionary characteristics of the orbits of outer Saturnian, Uranian, and Neptunian satellites." Solar Sys. Res., **42**, 488–504 [Erratum: Sol. Sys. Res., **43**, 464]

Veras, D., & Evans, N. W. (2013) "Exoplanets beyond the Solar neighbourhood: Galactic tidal perturbations." Mon. Not. R. Astron. Soc., **430**, 403–415

Veras, D., Crepp, J. R., & Ford, E. B. (2009) "Formation, survival, and detectability of planets beyond 100 AU." Astrophys. J., **696**, 1600–1611

von Zeipel, H. (1916) "Recherches sur le mouvement des petites planètes." Ark. för Mat., Astr. och Fys., **B. II**, H. 1, 1–58

Wan, X.-S., & Huang, T.-Y. (2007) "An exploration of the Kozai resonance in the Kuiper Belt." Mon. Not. R. Astron. Soc., **377**, 133–141

Webbink, R. F. (1984) "Double white dwarfs as progenitors of R Coronae Borealis stars and Type I supernovae." Astrophys. J., **277**, 355–360

Welsh, W. F., Orosz, J. A., Carter, J. A., Fabrycky, D. C., Ford, E. B., *et al.* (2012) "Transiting circumbinary planets Kepler-34b and Kepler-35b." Nature, **481**, 475–479

Wen, L. (2003) "On the eccentricity distribution of coalescing black hole binaries driven by the Kozai mechanism in globular clusters." Astrophys. J., **598**, 419–430

Whitmire, D., Matese, J., Criswell, L., & Mikkola, S. (1998) "Habitable planet formation in binary star systems." Icarus, **132**, 196–203

Williams, J. G. (1969) "Secular perturbations in the solar system." Ph. D. thesis (Univ. of California, Los Angeles)

Williams, J. G., & Benson, G. S. (1971) "Resonances in the Neptune–Pluto system." Astron. J., **76**, 167–177

Williams, J. G., & Faulkner, J. (1981) "The positions of secular resonance surfaces." *Icarus*, **46**, 390–399

Winn, J. N., Fabrycky, D., Albrecht, S., & Johnson, J. A. (2010) "Hot stars with hot Jupiters have high obliquities." Astrophys. J., **718**, L145–L149

Winn, J. N., Johnson, J. A., Albrecht, S., Howard, A. W., Marcy, G. W., Crossfield, I. J., *et al.* (2009) "HAT-P-7: a retrograde or polar orbit, and a third body." Astrophys. J., **703**, L99–L103

Wright, J. T., Fakhouri, O., Marcy, G. W., Han, E., Feng, Y., Johnson, J. A., Howard, A. W., Fischer, D. A., Valenti, J. A., Anderson, J., & Piskunov, N. (2011) "The exoplanet orbit database." Publ. Astron. Soc. Pacific, **123**, 412–422

Wu, Y., & Murray, N. (2003) "Planet migration and binary companions: The case of HD 80606b." Astrophys. J., **589**, 605–614

Wu, Y., Murray, N. W., & Ramsahai, J. M. (2007) "Hot Jupiters in binary star systems." Astrophys. J., **670**, 820–825

Xie, J.-W., Payne, M. J., Thébault, P., Zhou, J.-L., & Ge, J. (2011) "Planet formation in highly inclined binary systems. I. Planetesimals jump inward and pile up." Astrophys. J., **735**, 10 (18pp)

Zapatero Osorio, M. R., Béjar, V. J. S., Martín, E. L., Rebolo, R., Barrado y Navascués, D., Bailer-Jones, C. A. L., & Mundt, R. (2000) "Discovery of young, isolated planetary mass objects in the σ Orionis star cluster." Science, **290**, 103–107

Zhuravlev, V. F., & Klimov, D. M. (1988) *Applied Methods in the Theory of Oscillations* (Nauka Publishers, Moscow) (in Russian)

Ziglin, S. L. (1975) "Secular evolution of the orbit of a planet in a binary-star system." Sov. Astron. Lett., **1**, 194–195

Zinnecker, H. (2001) "A free-floating planet population in the Galaxy?" In: ASP Conf. Series, **239**, 223–228

Index

I. I. Shevchenko, *The Lidov-Kozai Effect – Applications in Exoplanet Research and Dynamical Astronomy*, Astrophysics and Space Science Library 441,
DOI 10.1007/978-3-319-43522-0